

**Molecular and functional characterization of
potential pathogenicity related genes from
*Verticillium longisporum***

**Molekulare und funktionelle Charakterisierung von
potenziell pathogenitätsrelevanten Genen aus
*Verticillium longisporum***

Dissertation
zur Erlangung des Doktorgrades
der Fakultät für Agrarwissenschaften
der Georg-August-Universität Göttingen

vorgelegt von Malte Beinhoff
geboren in Hannover

Göttingen, im Juni 2011

D 7

1. Referent : Prof. Petr Karlovsky

2. Referent : Prof. Andrea Polle

Tag der mündlichen Prüfung: 21. Juli 2011

<u>Aim of this project</u>	1
<u>REFERENCES</u>	2
<u>Chapter 1: General background</u>	4
<u><i>Verticillium</i> spp.</u>	4
<u><i>Verticillium longisporum</i></u>	6
<u>Life cycle of <i>V. longisporum</i></u>	7
<u>Plant-Pathogen interactions</u>	9
<u>Necrosis- and ethylene-inducing peptides (NEPs)</u>	11
<u>Polyketide synthases (PKSs)</u>	11
<u>REFERENCES</u>	12
<u>Chapter 2: Gene silencing in <i>Verticillium longisporum</i>: evaluation and establishment of a method for post-transcriptional downregulation of genes</u>	23
<u>ABSTRACT</u>	23
<u>INTRODUCTION</u>	24
<u>MATERIALS AND METHODS</u>	27
<u>Bacterial and fungal stains</u>	27
<u>Plasmids and enzymes</u>	27
<u>Alkaline agarose gel electrophoresis</u>	29
<u>Extraction of genomic DNA (gDNA) and total RNA from fungal mycelium</u>	30
<u>Southern hybridization</u>	30
<u>Transformation of <i>V. longisporum</i></u>	31
<u>qRT-PCR</u>	32
<u>Primer design</u>	32
<u>RESULTS AND DISCUSSION</u>	35
<u>Construction of HP fragments using OE-PCR</u>	36
<u>Construction of HP fragments using conventional cloning steps</u>	48
<u>CONCLUSIONS</u>	54
<u>ACKNOWLEDGMENTS</u>	56
<u>REFERENCES</u>	57
<u>APPENDIX</u>	61

<u>Chapter 3: Characterization of NEP-like proteins of <i>Verticillium longisporum</i> according to their relevance for pathogenicity in <i>Brassica napus</i></u>	63
<u>ABSTRACT</u>	63
<u>INTRODUCTION</u>	64
<u>MATERIALS AND METHODS</u>	66
<u>Fungal and bacterial strains</u>	66
<u>Preparation of spore suspensions</u>	67
<u>Plant material</u>	67
<u>Plasmids</u>	68
<u>Enzymes</u>	68
<u>Genomic library of <i>V. longisporum</i></u>	69
<u>VI-NEP-1 gene silencing</u>	69
<u>Transformation of <i>V. longisporum</i></u>	69
<u>Southern hybridization</u>	70
<u>Plant pathogenicity assay using VI-NEP-1 silencing mutants</u>	70
<u>Extraction of gDNA and total RNA</u>	71
<u>qRT-PCR</u>	71
<u>qPCR</u>	71
<u>Measurement of ethylene (C₂H₄)-production of <i>V. longisporum</i></u>	72
<u>High-performance liquid chromatography-mass spectrometry (HPLC-MS)</u>	72
<u>Confocal laser scanning microscopy (CLSM)</u>	72
<u>Purification of VI-NEP-1 protein using pET21 system</u>	73
<u>Sodium dodecyl sulfate poly acrylamide gel electrophoresis (SDS page)</u>	74
<u>Leaf-infiltration assay with VI-NEP-1 protein</u>	74
<u>Seedling growth and root development assay</u>	74
<u>Western hybridization</u>	75
<u>Immunofluorescence microscopy</u>	75
<u>Statistical analysis</u>	77
<u>RESULTS AND DISCUSSION</u>	77
<u>NLP orthologs of <i>V. longisporum</i></u>	77
<u>Expression of VI-NEP orthologs</u>	84

<u>Gene silencing of VI-NEP-1</u>	85
<u>Plant pathogenicity assay using VI-NEP-1 silencing mutants</u>	88
<u>Effects on phytohormone level</u>	94
<u>Overexpression and purification of VI-NEP-1 protein and subsequent experiments</u> ..	102
<u>CONCLUSIONS</u>	110
<u>ACKNOWLEDGMENTS</u>	113
<u>REFERENCES</u>	114
<u>APPENDIX</u>	122
<u>Chapter 4: Detection and functional analysis of a polyketide synthase gene of</u>	
<u><i>Verticillium longisporum</i></u>	
<u>ABSTRACT</u>	131
<u>INTRODUCTION</u>	131
<u>MATERIALS AND METHODS</u>	133
<u>Fungal and bacterial strains</u>	133
<u>Preparation of spore suspensions</u>	134
<u>Plant material</u>	134
<u>Plasmids</u>	135
<u>Enzymes</u>	135
<u>Primer walking</u>	135
<u>VI-PKS-1 gene silencing</u>	136
<u>Transformation of <i>V. longisporum</i></u>	136
<u>Southern hybridization</u>	136
<u>Plant pathogenicity assay using VI-PKS-1 silencing mutants</u>	136
<u>Extraction of gDNA and total RNA</u>	137
<u>qRT-PCR</u>	137
<u>Fungal interaction assay</u>	137
<u>Statistical analysis</u>	137
<u>RESULTS AND DISCUSSION</u>	138
<u>CONCLUSIONS</u>	149
<u>ACKNOWLEDGMENTS</u>	151
<u>REFERENCES</u>	152

APPENDIX	155
Chapter 5: Final discussion	157
Gene silencing in <i>V. longisporum</i>	158
The impact of VI-NEP-1 on the pathogenicity to <i>B. napus</i>	159
The role of VI-PKS-1 in the life cycle of <i>V. longisporum</i>	160
Outlook	162
REFERENCES	163
Danksagung	167
Curriculum Vitae	169
Eidesstattliche Erklärung	171

Aim of the project

This thesis was realized during participation in the research unit FOR 546 (“Signalling between the soil-borne fungus *Verticillium longisporum* and its host plants”) funded by the Deutsche Forschungsgemeinschaft (DFG). The research unit consists of nine different laboratories working in the fields of plant pathology, biochemistry, cell biology, molecular genetics, plant physiology and microbiology, mainly located at the Georg-August University of Göttingen. The major research objectives (1) of this *Verticillium* unit are:

- The identification of signals of plant and fungal origin that shape the interaction between the pathogen and host plants.
- The elucidation of the response of the plant to the fungus, including signal transduction processes and functional analysis of the elicited responses.
- The elucidation of the response of the fungus to the plant, including signal transduction processes as well as functional analysis of the elicited response for its pathogenicity.

As a member of the “Molecular phytopathology and mycotoxin research” laboratory headed by Prof. Petr Karlovsky we were working on the detection and characterization of fungal genes, putatively involved in the interaction of *V. longisporum* and its host plant *Brassica napus*. The molecular basis of the adaption of *V. longisporum* on *Brassicaceae* and the physiological processes in the mycelium during infection are mostly unknown. Therefore, molecular studies on pathogenicity-related genes provides the opportunity for a better understanding of the disease caused by *V. longisporum* and thereby help in finding new strategies for the prevention or the control of infection.

This thesis mainly focuses on the results of analysis of two genes detected in the genome of *V. longisporum* putatively involved in the pathogenic life-cycle of the fungus, and the establishment of a method to trigger post-transcriptional gene silencing in *V. longisporum*. The first gene belongs to a relatively newly described group of proteins, mostly expressed from phytopathogens, called necrosis- and ethylene-inducing peptides (NEP). We detected and sequenced five NEP orthologs in the *V. longisporum* genome, designated as VI-NEP-1 to -5, using primers of homologous gene sequences derived from *V. dahliae* published by “The

Broad Institute *Verticillium* database” (2). VI-NEP-1 was chosen for further investigation (see Chapter 3). VI-NEP-1 is a gene with high homology to other fungal NEP-1 genes, which are known to elicit plant responses and symptom development in different plant systems (3, 4, 5).

The second gene codes for a polyketide synthase (PKS). This class of enzymes catalyzes the series of small carboxylic acid residues into polyketides (6). Polyketides belong to a large group of secondary metabolites, known to play a role as pathogenicity or virulence factors in phytopathogenic fungi (7). Using degenerate primers for conserved regions of fungal PKS genes, we identified a gene designated as VI-PKS-1 (8) with high homology to other fungal PKS genes coding for L-ketoacylsynthases that are believed to be involved in the biosynthesis of melanin (9). The role of VI-PKS-1 for the life cycle of *V. longisporum* should be clarified during this thesis (see Chapter 4).

To check the relevance of these genes for the pathogenic life-cycle of *V. longisporum* and whether they act as virulence or pathogenicity factors we have tried to establish a method for the construction of silencing vectors to trigger post-transcriptional gene silencing of candidate genes in *V. longisporum* (see Chapter 2).

REFERENCES

1. **Research Unit DFG 546** homepage (<http://www.ubpb.gwdg.de/~forschergruppe/index.html>).
2. **The Broad Institute** homepage *Verticillium* group database (<http://www.broad.mit.edu/annotation/genome/verticilliumdahliae/MultiHome.html>).
3. **Wang J., Cai Y., Gou J., Mao Y., Xu Y., Jiang W., Chen X.** (2004). VdNEP, an elicitor from *Verticillium dahliae*, induces cotton plant wilting. *Appl. Environ. Microbiol.* 70:4989-4995.
4. **Bailey B.A., Apel-Birkhold P.C., Luster D.G.** (2002). Expression of NEP1 by *Fusarium oxysporum* f.sp. *erythroxyli* after gene replacement and overexpression using polyethylene glycol-mediated transformation. *Genet. Resistance* 92:833-841.

5. **Qutob D., Kemmerling B., Brunner F., Kűfner I., Engelhardt S., Gust A.A., Lacombe Luberacki B., Seitz H.U., Stahl D., Rauhut T., Glawischnig E., Schween G., B., Watanabe N., Lam E., Schlichting R., Scheel D., Nau K., Dodt G., Hubert D., Gijzen M., Nűrnberger T. (2002).** Phytotoxicity and innate immune responses induced by Nep1-like proteins. *Plant Cell* 18:3721-3744.
6. **Hopwood A. (1997).** Genetic Contributions to Understanding Polyketide Synthases. *Chem. Rev.* 97: 2465-2497.
7. **Huang J.-S. (2001).** *Plant Pathogenesis and Resistance.* Dordrecht/Boston/London
8. **Hiegl W. (2006).** Untersuchung der Biosynthese von Phytohormonen bei *Verticillium longisporum*. Diplomarbeit, Georg-August Universitat Gottingen.
9. **Takano Y., Kubo Y., Shimizu K., Mise K., Okuno T., Furusawa I. (1995).** Structural analysis of PKS1, a polyketide synthase gene involved in melanin biosynthesis in *Colletotrichum lagenarium*. *Mol. Gen. Genet.* 249:162-167.

Chapter 1: General background

***Verticillium* spp.**

Fungi of the genus *Verticillium* belong to one of the most widespread groups of plant pathogens in the world and are present in both temperate and subtropical regions (1). *Verticillium* species are soil-borne fungi, and are part of the division ascomycota which comprises the most abundant class of fungal species (45,000 known species, 65 % of all fungal species). Most of the *Verticillium* species belong to the artificial described class of deuteromycetes (*Fungi imperfecti*) which is characterized by the lack of any sexual teleomorph (2). Serious economic losses have been recorded caused by the infection of host plants by plant pathogenic *Verticillium* species (3). The host range of the fungi is considered to be very diverse. *Verticillium* species has been detected in over 200 plant species (4). At the moment, six plant pathogenic *Verticillium* species are commonly accepted by plant pathologists (5). The acceptance of a seventh species, named *V. longisporum* (6), which is the subject of this thesis, is a controversial issue that is still under discussion.

***Verticillium* Nees (1817)**

- *V. albo-atrum* Reinke & Berthold (1879)
 - *V. albo-atrum* var. *caespitosum* Wollenweber (1929)
 - *V. albo-atrum* var. *caespitosum* f. *pallens* Wollenweber (1929)
 - *V. albo-atrum* var. *tuberosum* Rudolph (1931)
- *V. dahliae* Klebahn (1913)
 - *V. dahliae* var. *longisporum* Stark (1961)
 - *V. albo-atrum* var. *medium* Wollenweber (1929)
 - *V. albo-atrum* auct. *pro parte*
 - *V. ovatum* Berkeley & Jackson (1926)
- *V. nigrescens* Pethybridge (1919)
- *V. nubilum* Pethybridge (1919)
- *V. theobromae* (Turconi) Mason & Hughes (1951)
- *V. tricorpus* Isaac (1953)
- ***V. longisporum* Karapapa & Stark (1997)**

In contrast to *V. nigrescens*, *V. nubilum*, *V. theobromae* and *V. tricorpus*, which have a relatively small influence on agricultural breeding, *V. dahliae* and *V. albo-atrum* cause high economic yield losses and are therefore the focus of scientific research. Host plants of *V. dahliae* include tomato, pepper, watermelon, mint, muskmelon, lettuce, potato, cotton and strawberry (12). On the other hand *V. albo-atrum* particularly infects alfalfa, hop, tomato and potato (13). Symptoms caused by *Verticillium* species are very diverse, depending on the host plant (14). The typical symptom of a *Verticillium* infection is wilting of the host-plant (1). Additionally, stunting of infected plants and also chlorotic and necrotic lesions on leaves may be observed. Inside infected plants, a brown discoloration of the vascular system is shown, which is probably due to an accumulation of phenolic substances (15). Because of the large variety of symptoms caused by *Verticillium* ssp., clear differentiation of symptoms from those caused by other plant pathogens in the field is very difficult. Only at a late stage of infection and due to the visible formation of microsclerotia in the dying tissues of affected plants, is it possible to differentiate by eye whether symptoms are caused by *Verticillium* species or other plant pathogenic organisms. Therefore, molecular techniques are often used to make a clear assignment to other plant pathogens in the field (16). Despite the possibility of early detection of *Verticillium* infection, no fungicides are available which can stop the spread of the fungus in the plant (17, 18, 19). Because plant pathogenic *Verticillium* ssp. are soil-borne and the infection of plants is carried out by microsclerotia germination and penetration of the roots, it is difficult to prevent *Verticillium* infection by the use of common fungicides. The search for resistant varieties of host plants is therefore of great importance. A promising approach is the production of re-synthesized oilseed rapeseed lines (20, 21, 22). In 2006, the complete genome of *V. dahliae* was published (23) which allows a more detailed phylogenetic study on the taxonomy of the *Verticillium* species (24, 25, 26, 27). In 2004, an extensive genome sequencing project for *V. dahliae* and *V. albo-atrum* was founded by the “NSF/USD Microbial Genome Sequencing Program” and the “Broad Institute”. As a result of this project, 2600 expressed sequence tags (ESTs) were received from the *V. dahliae* transcriptome. The data was obtained by two independent approaches (28, 29) and is available through the NCBI GenBank database. Because of the variety of investigations on the pathosystem *Verticillium*/host plants, the fungus is on the way to becoming a model system for studying diseases caused by plant pathogenic fungi.

Verticillium longisporum

In 1961, Stark described an isolate derived from horseradish with an unusual length of conidia. He named this isolate with elongated conidia as *V. dahliae* var. *longisporum* (30). In addition to the almost twice as long conidia, *V. longisporum* has an almost twice as large DNA content (1.78 x) compared to *V. dahliae* or *V. albo-atrum* and is described as "near-diploid" (31, 32). In addition to this, it was demonstrated that the isolate has even more differences in the molecular characteristics compared to *V. dahliae* and *V. albo-atrum* (e.g. 33, 34, 35, 36, 37, 38, 39, 40, 41, 42). Consequently, Karapapa postulated in 1997 that the species *V. dahliae* var. *longisporum* should be classified as a separate species (6). The taxonomical discussion is still not completed and the classification of *V. longisporum* as a unique species has not been unanimously agreed by plant pathologists.

The first reports about a disease of oilseed rape due to *V. longisporum* infestation occurred 50 years ago in Sweden. Until *Verticillium*-infected plants were found in the area of the former East Germany (43), symptoms on oilseed rape plants resulting from *Verticillium* ssp. were considered to represent a problem only in Scandinavian countries (44). The increasing economic importance of rape and the resulting increase in acreage has also been accompanied by a rising occurrence of plant pathogens such as *V. longisporum* (45). In 2006/2007, the rape-growing area was extended to about 6.2 million hectares. Besides wheat and barley, oilseed rape is the crop with the largest agricultural area in Germany at present. Data concerning yield losses caused by *Verticillium* infection reports losses as about 10- 50% (46). The host range of *V. longisporum* is limited to the family of *Brassicaceae* (6). Study of plant/pathogen interaction is impaired by the relatively long life cycle of rape crops used in the field. Consequently, in the 80s, a *Brassica* species was bred which had a shorter life cycle compared to field crops lasting up to two years (47). This species, referred as "rapid-cycling rape plants", requires 25 days on average to flower and 55 days to reach seed maturity, and has found an application in many research laboratories dealing with diseases of oilseed rape (48). *V. longisporum* induces stunting, chlorosis and anthocyanin accumulation, affects the flowering time, and triggers early onset of senescence on host plants (49).

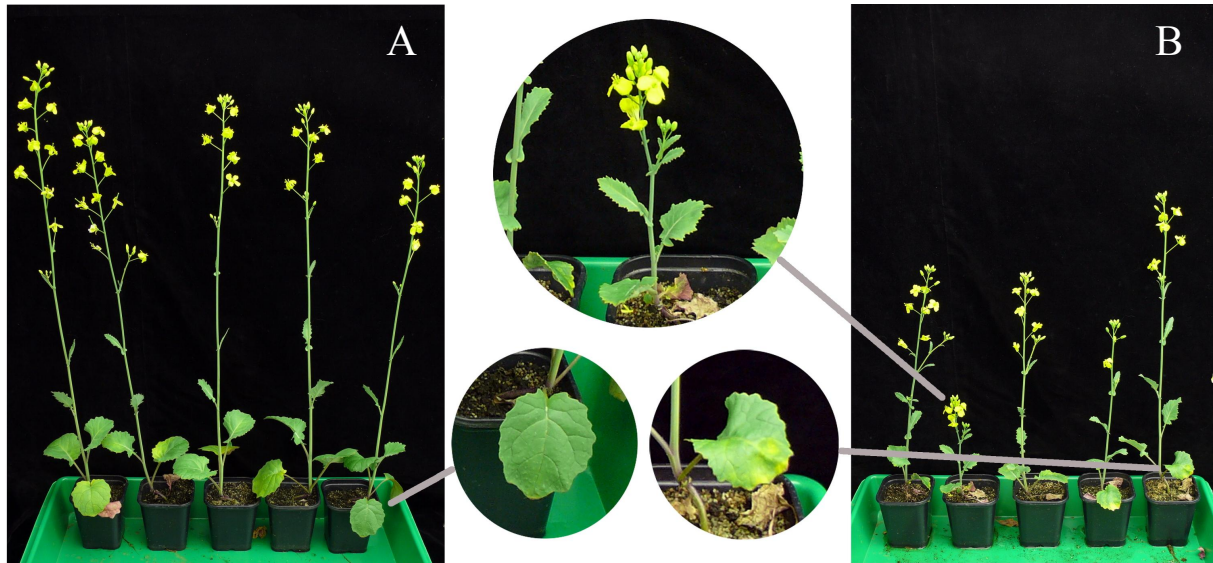


Figure 1: Symptom-development of *V. longisporum*-infected *B. napus* plants under climate chamber conditions (stunting and chlorosis)

A. water inoculated (28 dpi) B. wild type inoculated (28 dpi)

The typical symptom after *Verticillium* infection is wilting of the host plant (50). In field trials with oilseed rape infected with *V. longisporum*, wilting and also typical stunting effects on plant height (51, 52, 53, 54) could not be observed. Artificially *V. longisporum* inoculated oilseed rape plants show clear stunting of infected plants under greenhouse conditions, but again, no wilting. Compared to other *Verticillium* species, the control of diseases caused by *V. longisporum* is known to be difficult. The use of chemical fungicides is hampered because of the soil-borne life cycle and the microsclerotia contamination of the soil. The use of any commercially available fungicide shows no effects on crop yield (55, 56). Also, biological control with antagonistic microorganisms has not led to any practicable results (57, 58). The search for oilseed rape varieties that show resistance to *V. longisporum* infection is therefore in the foreground of current scientific research. Experiments with various rape cultivars show promising differences in the disease severity during infection with *V. longisporum* in the greenhouse (59, 60, 61, 62, 63, 64) and in the field (65, 66, 67).

Life cycle of *V. longisporum*

The life cycle of *V. longisporum* is nearly equal to that of other plant pathogenic *Verticillium* species and can be divided into three vegetative stages referred to as the dormant, the parasitic, and the saprophytic phases (see Figure 2).

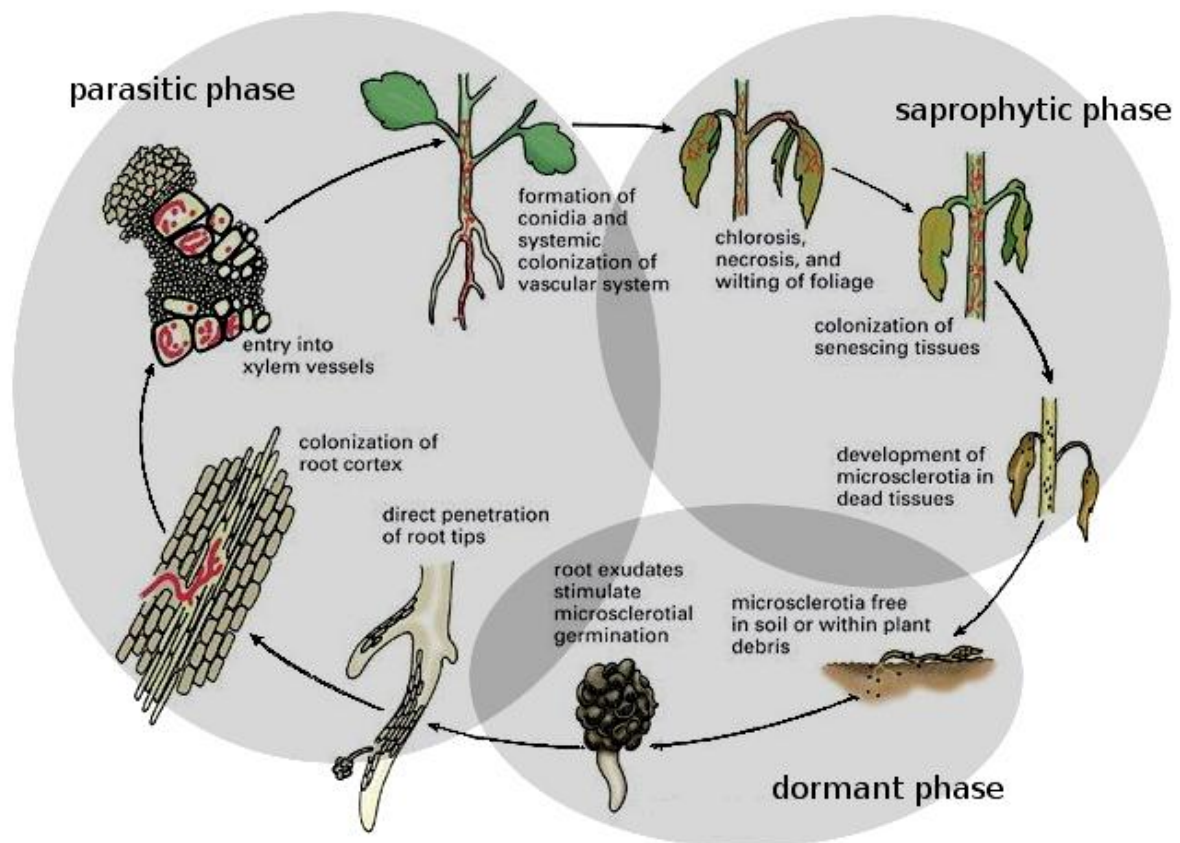


Figure 2: Life cycle of *Verticillium* spp.

(modified picture, drawn by Vickie Brewster, coloured by Jesse Ewing)

Resting structures of *V. longisporum* are melanized aggregates formed from enlarged hyphal cells which are capable of remaining in the soil for many years (68, 69). In contrast to the compact and nodular formed microsclerotia of *V. dahliae*, these so-called microsclerotia are elongated and arranged in irregular fashion in the soil (6, 70). In the dormant phase of the *V. longisporum* life cycle, the fungus rests in the soil until the environmental conditions allow it to pass into the next phase. In the following parasitic phase, microsclerotia starts to germinate under the effect of root exudates released from plants into the rhizosphere (71). Grown hyphae are able to travel short distances to reach the host plant and directly penetrate the epidermal cells of the root cortex (72) where they grow in inter and intracellular fashion until they penetrate the vessel system (73). The fungus colonizes the vascular system where it mostly stays during the biotrophic stage of the plant colonization. Spores are transported with the transpiration stream from the root vessels into the shoot to infest the whole plant. It is most likely that the fungus must derive nutrition from the xylem sap to survive and spread in

the plant but recent reports about xylem sap composition of *B. napus* after *V. longisporum* infection show no limitation of nutrients compared to that of non-infected plants (74) which concludes that *V. longisporum*-induced stunting of oilseed rape is not caused by nutrient limitations. The same study showed that also a putative reduced water supply or a suppression of the photosynthesis is not involved in the symptom development caused by the fungus. It is unknown how the fungus responds to environmental changes to prevent recognition by the plant, thus allowing the biotrophic growth. In later stages of the infection, the fungus enters the saprophytic phase and metabolises nutrients released by dead plant tissue. The life cycle is completed by the formation of microsclerotia that are released to the soil. This change of a biotroph and a necrotrophic stage in the life cycle during plant colonization is characteristic a hemibiotrophic plant pathogen. The molecular processes in *V. longisporum* during infection of the host plant are largely unknown but some virulence factors of *Verticillium* species are known to set off infection of the plant.

Plant-Pathogen interactions

Understanding how certain plant pathogens cause disease in one host plant and not in another has long been a concern of modern plant pathologists. Plant-pathogen interaction can be defined as the interplay of plant pathogenic organisms trying to invade the plant, and the recognition by the plant and the attempt to counteract this invasion. Plants have developed various mechanisms to react against an attack of pathogens. One of the most effective defence reactions of plants is the recognition of pathogen-related molecules and the binding of these through receptors which are expressed in response to infection. These receptors are expressed by so-called resistance genes (R genes) to bind elicitors such as proteins, polysaccharide or lipids derived from the cell walls of pathogens. If a plant is susceptible to the attack of a pathogen, the interaction is referred to as a 'compatible reaction'. In this case the pathogen is known to be virulent to the plant. If a plant is able to overcome the pathogen infestation the reaction is called 'incompatible' and the pathogen is avirulent. The question of why a pathogen infects a certain plant can probably be answered by the interplay between specific proteins expressed by avirulence genes (*avr* genes) from the pathogen, and the products expressed by the R genes from the plant. In a compatible reaction, the plant cannot recognize the *avr* gene product and the pathogen can infect the plant. Conversely, if the plant can recognize the gene product which is expressed by the fungi a diverse pattern of defence genes

are expressed by the plant to reduce the disease severity (75). As a result of the incompatible reaction, the plant often responds by killing cells at and around the site of infection to generate a physical barrier and to limit the nutrient supply for the pathogen (76, 77). This programmed cell death is also termed the ‘hypersensitive response’ (HR). The HR is accompanied by the induction of several anti-microbial defence molecules such as pathogenesis-related (PR) proteins, glucanases, chitinases and phytoalexins. In addition to local responses, plants can also counteract pathogens through systemic-acquired resistance (SAR), which means that the plant gains the ability to act against pathogens in other areas apart from directly affected plant parts. The SAR is generally evolved within several days after the first infection with the pathogen (78) and is effective against a broad spectrum of pathogens. Many proteins are needed for the SAR, including hydrolytic PR-proteins (79, 80, 81) and the signal molecule salicylic acid (SA) (82). On the other side, plant pathogenic organisms need the factors of virulence and pathogenicity to overcome the plant defences. Pathogenicity factors are described as compounds which trigger the disease but have no influence on disease severity. Conversely, virulence factors are compounds with an impact on the intensity of the pathogen-propagation. As mentioned previously, the molecular processes of plant-infestation in *V. longisporum* are largely unknown. The biotrophic growth of the fungus inside the plant requires a compatible reaction. In the early stages of the fungal infestation no defence reactions of the plant could be observed. The supply of carbon, which is essential for the fungal growth, is limited by the fact that *V. longisporum* is strictly localized in the xylem vessels of host plants during the biotrophic phase. Therefore, it is most likely that the fungus secretes cell wall-degrading enzymes such as pectin lyases that destabilize the xylem-vessel to release nutrients from the plant tissue (83, 84, 85). Pectinase-deficient mutants of *V. longisporum* show interfered symptom development in the plant but finally no change in the degree of colonization compared to wild type infected plants. Accordingly, pectinases have been classified as virulence factors and not as pathogenicity factors (86, 87). In general, little is known about phytotoxic metabolites of *Verticillium* spp., but recently a family of small phytotoxic peptides have been described. These so-called necrosis and ethylene-inducing peptides (NEPs) were detected in various organisms, causing wilting and chlorosis in leaves that had been infiltrated by the protein. Several NEPs were tested in different plant systems to discover if any plant responses were triggered. Mostly HR-like symptoms were observed but the mechanisms of initiation remain unclear (89, 90, 91).

Necrosis- and ethylene-inducing peptides (NEPs)

The class of necrosis- and ethylene-inducing peptides (NEPs) belong to a family of relatively small secreted proteins (24-35 kDa) supposed to be involved in plant pathogenic processes. Fifteen years ago, Bailey described a protein from *Fusarium oxysporum* which triggers cell death in plants (89). This was the first representative of what is currently known in literature as NEP, NIP (necrosis-inducing peptides) or NPP (necrosis-inducing *Phytophthora* proteins) as designated by different authors (91, 92, 93, 94). Since this time NEPs have been found in many other organisms including bacteria, oomycetes and fungi. Most of the species are known to be plant pathogenic. In fungi and oomycetes, NEPs are dominantly present in species with a hemibiotrophic or a necrotrophic life cycle (94). All NEPs share a highly conserved hepta-peptide motif in the central area of the protein and two to four cysteine residues downstream at the N-terminus (91, 95, 96) which are supposed to be relevant for peptide activity (93). These conserved cysteines are used to classify NEPs into two groups referred to as Group I (proteins including two cysteines) and Group II (proteins including four cysteines) (97). Only dicotyledonous plants are affected by NEP-treatment; all tested monocotyledonous plants are insensitive so far (96, 98, 99). Sensitive plants respond with different modes of action such as H₂O₂ accumulation, production of nitric oxide, release of phytoalexins, expression of PR-genes, and also with the formation of necrotic lesions on affected plant tissue (93, 99, 100). In 2004, Wang produced the first report on an NEP found in a *Verticillium* species (88). This protein from *V. dahliae*, designated as VdNEP, triggers the formation of necrotic lesions in cotton and *A. thaliana* after leaf-infiltration with the protein. Less is known about NEPs from *V. longisporum*. For this, we want to detect NEP-like proteins (NLPs) in the fungus to elucidate their putative role in the pathogenic life-cycle.

Polyketide synthases (PKSs)

Polyketides (PKs) are secondary metabolites from bacteria, plants, animals and fungi, including natural products with manifold biological activities. In pharmacology, PKs are often used to kill or inhibit the growth of bacteria, fungi or animals through their toxic abilities. Polyketide synthases (PKS) catalyze the series of small carboxylic acids into PKs and can be distinguished into two classes according to their functionality. Type I-PKS are modular formed multifunctional enzymes with several domains, forming reduced PKs such as

erythromycin, which is produced by bacteria of the genus *Streptomyces*. In contrast, PKS from type II form mostly aromatic PKs such as tetracycline by the use of only a single domain. The biosynthesis of PKs in fungi is derived by large multifunctional type I-PKS, coded by single genes (101). Fungal PKs are scientifically well characterized, and are divided into two functional groups of secondary metabolites. Mould fungi produce a wide range of chemically diverse secreted PKs known as mycotoxins. These include zeralenone, fumonisin and aflatoxin (102, 103, 104). Mycotoxins have toxic abilities against endothermic animals but their ecological role in fungi is still not clear, for example whether they have an impact, through inhibitory effects, on the competition against other fungal species and microbes (105) or act as virulence factors, through poisonous effects, on plant tissue (103, 106). The second group of fungal PKs consist of non-secreted pigments such as melanin which is known to often play a role in plant pathology. A function of melanin in the appressoria-mediated penetration of plant cell walls was first shown in *Pyricularia oryzae* (102, 107). In *Colletotrichum lagenarium* PKS knock-down mutants change to an albino phenotype with non-melanized appressoria showing a reduced ability to penetrate the cell wall of host-plants (108). Regardless of the absence of appressoria-mediated colonization of plants by *V. longisporum*, we found an upregulated PKS-gene with high homology to the PKS-gene of *C. lagenarium*. This gene is involved in the biosynthesis of 1,8-dihydroxynaphthalene (DHN)-melanin. The function of this gene will be characterized in this thesis to determine its impact in the life cycle of *V. longisporum*.

REFERENCES

1. **Pegg, G.F., Brady, B.L.** (2002). *Verticillium* Wilts. Wallingford, UK: CAB Publishing.
2. **Schwantes, H.O.** (1996). *Biologie der Pilze*. Verlag Eugen Ulmer, Stuttgart. 6.
3. **Bhat RG, Subbarao KV** (1999). Host range specificity in *Verticillium dahliae*. *Phytopathology* 89: 1218-1225.
4. **Agrios G.N.** (1997). Plant diseases caused by fungi: *Verticillium* wilts. In Agrios G.N. (ed.): *Plant Pathology* 346, Academic Press, San Diego.

5. **Barbara, D. J. & Clewes, E.** (2003). Plant pathogenic *Verticillium* species: how many of them are there? *Molecular Plant Pathology* 4: 297-305.
6. **Karapapa et al.** (1997). *Advances in Verticillium research and disease management*. Tjamos, E.C., Rowe, R.C., Heale, J.B., Fravel, D.R. (eds.), St. Paul, Minnesota, APS Press, 196-203.
7. **Reinke, J.; Berthold, G.** (1879). Die Zersetzung der Kartoffel durch Pilze, *Unters. Bot. Lab. Univ. Göttingen. Heft I.* Berlin. 1879.
8. **Klebhahn H.** (1913). Beiträge zur Kenntnis der Fungi Imperfecti I. Eine *Verticillium* Krankheit auf *Dahliaen*. *Mycologisches Zentralblatt* 3: 49–66.
9. **Pethybridge G. H.** (1919). Notes on some saprophytic species associated with diseased potato plants and tubers. *Transactions of the British Mycological Society* 6: 104-120.
10. **Mason & Hughes in Hughes** (1951). Studies on microfungi, *Mycol. Pap.* 45: 27
11. **Isaac, I.** (1957). *Verticillium* wilt of Brussels sprout. *Annals of Applied Biology* 45: 276-283.
12. **Gordon, T.R., Kirkpatrick, S.C., Hansen, J., Shaw, D.V.** (2006). Response of strawberry genotypes to inoculation with isolates of *Verticillium dahliae* differing in host origin. *Plant Pathology* 55: 766-769.
13. **Heale, J.B.** (2000). Diversification and speciation in *Verticillium* – An overview. In: *Advances in Verticillium research and disease management*. Tjamos, E.C., Rowe, R.C., Heale, J.B., Fravel, D.R. (eds.), St. Paul, Minnesota, APS Press, 175-177.
14. **Fradin, E.F., Thomma, B.P.H.J.** (2006). Physiology and molecular aspects of *Verticillium* wilt diseases caused by *V. dahliae* and *V. albo-atrum*. *Molecular Plant Pathology* 7: 71-86.
15. **Pegg, G. F.** (1976). Response of ethylene-treated tomato plants to infection by *Verticillium albo atrum*. *Physiological Plant Pathology* 9: 215-226.
16. **Dunker S.** (2005). Untersuchungen zur Schadwirkung von *Sclerotinia sclerotiorum* (Lib. de Bary) und *Verticillium longisporum* (comb. nov. Karapapa) in Winterraps (*Brassica napus*). Dissertation, Georg-August Universität Göttingen.
17. **Nagtzaam M.P.M., Bollen G.J., Termorshuizen A.J.** (1998). Efficacy of *Talaromyces flavus* alone or in combination with other antagonists in controlling *Verticillium dahliae* in growth chamber experiments. *J. Phytopathol.* 146: 165-173.

18. **Tenuta M., Lazarovits G.** (2002). Ammonia and nitrous acid from nitrogenous amendments kill the microsclerotia of *Verticillium dahliae*. *Phytopathol.* 93: 255-264.
19. **Noble R., Coventry E.** (2005). Suppression of soil-borne plant diseases with composts: a review. *Biocontrol Sci. Technol.* 15: 3-20.
20. **Happstadius I., Ljunberg A., Kristiansson B., Dixelius C.** (2003). Identification of *Brassica oleracea* germplasm with improved resistance to *Verticillium* wilts. *Plant Breeding* 122: 30-34.
21. **Rygulla W., Snowdon R.J., Eynck C., Koopmann B., von Tiedemann A., Lühs W., Friedt W.** (2007). Broadening the genetic basis of *Verticillium longisporum* resistance in *Brassica napus* by interspecific hybridisation. *Plant Breeding* 126: 596-602.
22. **Rygulla W., Seyis F., Lühs W., Eynck C., von Tiedemann A., Friedt W., Snowdon R.J.** (2007). Combination of resistance to *Verticillium longisporum* from zero erucic acid *Brassica oleracea* and oilseed *Brassica rapa* genotypes in resynthesized rapeseed (*Brassica napus*) lines. *Phytopathology* 97: 1391-1396.
23. **Pantou M.P., Kouvelis V.N., Typas M.A.** (2006). The complete mitochondrial genome of the vascular wilt fungus *Verticillium dahliae*: a novel gene order for *Verticillium* and a diagnostic tool for species identification. *Curr. Genet.* 50:125-136.
24. **Zeise K., von Tiedemann A.** (2001). Morphological and Physiological Differentiation among Vegetative Compatibility Groups of *Verticillium dahliae* in Relation to *V. longisporum*. *J. Phytopathol.* 149: 469-475.
25. **Fahleson J., Lagercrantz U., Hu Q., Steventon L.A., Dixelius C.** (2003). Estimation of genetic variation among *Verticillium* isolates using AFLP analysis. *Eur. J. Plant Pathol.* 109: 361-371.
26. **Karapapa V.K., Typas M.A.** (2001). Molecular characterization of the host-adapted pathogen *Verticillium longisporum* on the basis of a group-I intron found in the nuclear SSU-rRNA gene. *Curr. Microbiol.* 42: 217-224.
27. **Kouvelis V.N., Sialakouma A., Typas M.A.** (2008). Mitochondrial gene sequences alone or combined with ITS region sequences provide firm molecular criteria for the classification of *Lecanillium* species. *Mycol. Res.* 112: 829-844.

28. **Wang J., Cai Y., Gou J., Mao Y., Xu Y., Jiang W., Chen X.** (2004). VdNEP, an elicitor from *Verticillium dahliae*, induces cotton plant wilting. *Appl. Environ. Microbiol.* 70: 4989-4995.
29. **Neumann M.J., Dobinson K.F.** (2003). Sequence tag analysis of gene expression during pathogenic growth and microsclerotia development in the vascular wilt pathogen *Verticillium dahliae*. *Fung. Genet. Biol.* 38: 54-62.
30. **Stark, C.** (1961). Das Auftreten der *Verticillium*-Tracheomykosen in Hamburger Gartenbau-Kulturen. *Gartenbauwissenschaft* 26: 493-528
31. **Typas, M. A., Heale, J. B.** (1977). Analysis of ploidy levels in strains of *Verticillium* using a Coulter counter. *Journal of General Microbiology* 101: 177-180.
32. **Typas, M. A., Heale, J. B.** (1980). DNA content of germination spores individual hyphal cells and resting structure cells of *Verticillium* spp. measured by microdensitometry. *Journal of General Microbiology* 121: 231-242.
33. **Koike, S.T., Subbarao, K.V., Davis, R.M., Gordon, T.R., Hubbard, J.C.** (1994). *Verticillium* wilt of cauliflower in California. *Plant Disease* 78: 1116-1121.
34. **Morton, A., Carder, J. H., Barbara, D. J.** (1995). Sequences of the internal transcribed spacers of the ribosomal RNA genes and relationships between isolates of *Verticillium alboatrum* and *V. dahliae*. *Plant Pathology* 44: 183-190.
35. **Subbarao, K.V., Chassot, A., Gordon, T.R., Hubbard, J.C., Bonello, P., Mulin, R., Okamoto, D., Davis, R.M., Koike, S.T.** (1995). Genetic relationships and cross pathogenicities of *Verticillium dahliae* isolates from cauliflower and other crops. *Phytopathology* 85: 1105-1112.
36. **Messner, R. Sweigkofler, W., Ibl, M., Berg, G., Prillinger, H.** (1996). Molecular characterization of the plant pathogen *Verticillium dahliae* Kleb. using RAPD-PCR and sequencing of the 18S rRNA-gene. *Journal of Phytopathology* 144: 347-354
37. **Karapapa, V. K., Typas, M. A.** (2001). Molecular characterization of the host-adapted pathogen *Verticillium longisporum* on the basis of a Group-I intron found in the nuclear SSU-rRNA gene. *Current Microbiology* 42: 217-224.
38. **Steventon, L.A., Fahleson, J., Hu, Q., Dixelius, C.** (2002). Identification of the causal agent of *Verticillium* wilt of winter oilseed rape in Sweden, *Verticillium longisporum*. *Mycological Research* 106: 570-578.

39. **Zeise K., von Tiedemann A.** (2002). Application of RAPD-PCR for Virulence Type Analysis within *Verticillium dahliae* and *Verticillium longisporum*. J. Phytopathol. 150: 557-563.
40. **Collins, A., Okoli, A.N., Morton, A., Parry, D., Edwards, S.G., Barbara, D.J.** (2003). Isolates of *Verticillium dahliae* pathogenic to crucifers are of at least three distinct molecular types. Phytopathology 93: 364-376.
41. **Fahleson, J., Lagercrantz, U., Hu, Q., Steventon, L. A. & Dixelius, C.** (2003). Estimation of genetic variation among *Verticillium* isolates using AFLP analysis. European Journal of Plant Pathology 109: 361-371.
42. **Collins A., Okoli C.A.N., Morton A., Parry D., Edwards S.G., Barbara D.J.** (2003). Isolates of *Verticillium dahliae* pathogenic to crucifers are of at least three distinct molecular types. Phytopathol. 93: 364-376.
43. **Daebeler F, Amelung D, Zeise K.** (1988). *Verticillium*-Welke an Winterraps-Auftreten und Bedeutung. Nachrichtenblatt Pflanzenschutzdienst DDR 42: 71-73.
44. **Svensson C., Lerenius C.** (1987). An investigation on the effect of *Verticillium* wilt (*Verticillium dahliae* Kleb.) on oilseed rape. Bulletin SROP 10: 30-34
45. **Krüger, W.** (1989)- Untersuchungen zur Verbreitung von *Verticillium dahliae* Kleb. und anderen Krankheits- und Schaderregern bei Raps in der Bundesrepublik Deutschland. Nachrichtenblatt des Deutschen Pflanzenschutzdienstes 41: 49-56.
46. **Dunker S, Keunecke H, Steinbach P, von Tiedemann A.** (2008). Impact of *Verticillium longisporum* on yield and morphology of winter oilseed rape (*Brassica napus*) in relation to systemic spread in the plant. Journal of Phytopathology, Published Online
47. **Williams, P. H. & Hill, C. B.** (1986). Rapid-cycling populations of *Brassica*. Science 232: 1385-1389.
48. **Musgrave, M. E.** (2000). Realizing the potential of rapid-cycling *Brassica* as a model system for use in plant biology research. Journal of Plant Growth Regulation 19: 314-325.
49. **Veronese, P., Narasimhan, M. L., Stevenson, R. A., Zhu, J. K., Weller, S. C., Subbarao, K. V. & D., Davis, R.M., Koike, S.T.** (1995). Genetic relationships and cross patho-genicities of *Verticillium dahliae* isolates from cauliflower and other crops. Phytopathology 85: 1105-1112.

50. **Niederleitner, S., Zinkernagel, V., Bartscherer, H.-C.** (1991). Untersuchungen zur Pathogenese von *Verticillium dahliae* an *Impatiens balsamina* und *Brassica napus*. Zeitschrift für Pflanzenkrankheiten und Pflanzenschutz 98: 484-489.
51. **Pullman, G. S., De Vay, J. E.** (1982). Epidemiology of *Verticillium* wilt of cotton: A relationship between inoculum density and disease progression. Phytopathology 72: 549-554.
52. **Koike M., Fujita M., Nagoa H., Ohshima S.** (1996): Random amplified polymorphic DNA analysis of Japanese isolates of *Verticillium dahliae* and *V. albo-atrum*. Plant Disease 80: 1224-1227.
53. **Xiao C. L., Subbaro K. V.** (1998). Relationship between *Verticillium dahliae* inoculum density and wilt incidence, severity, and growth of cauliflower. Phytopathology 88: 1108-1115.
54. **Debode, J., Claeys, D. & Höfte, M.** (2004). Control of *Verticillium* wilt of cauliflower with crop residues, lignin and microbial antagonists. IOBC WPRS Bull 27: 41–45.
55. **Wohlleben, S.** (2001). Epidemie- und Schadensdynamik von pilzlichen Krankheitserregern (*Leptosphaeria maculans*, *Sclerotinia sclerotiorum*, *Verticillium dahliae*) an Winterraps (*Brassica napus* L. var. *napus*) in Schleswig-Holstein. Dissertation, Christian-Albrechts-Universität Kiel.
56. **Keunecke H.** (2005). Einfluss von *Verticillium longisporum* auf die Wurzel- und Sprossentwicklung von Winterraps unter Berücksichtigung von Fungizidapplikationen. Masterarbeit, Georg-August-Universität Göttingen.
57. **Berg, G. & Ballin G.** (1994): Bacterial Antagonists to *Verticillium dahliae* Kleb. J. Phytopathology 141: 99-110.
58. **Alström, S.** (2000). Root-colonizing fungi from oilseed rape and their inhibition of *Verticillium dahliae*. J. Phytopathology 148: 417-423.
59. **Zeise, K.** (1992). Gewächshaustest zur Resistenzprüfung von Winterraps (*Brassica napus* L. var. *oleifera* Metzger) gegen den Erreger der Rapswelke *Verticillium dahliae* Kleb.. Nachrichtenbl. Deutsch. Pflanzenschutzd. 44: 125-128.
60. **Zeise, K. & A. v. Tiedemann** (2002). Host specialization among vegetative compatibility groups of *Verticillium dahliae* in relation to *Verticillium longisporum*. J. Phytopathology 150: 112-119.

61. **Steventon, L.A., Happstadius, I., Okori, P., Dixelius, C.** (2002) Development of a rapid technique for the evaluation of the response of *Brassica napus* to *Verticillium* wilt. *Plant Disease* 86: 854-858.
62. **Happstadius I., Ljunberg A., Kristiansson B., Dixelius C.** (2003). Identification of *Brassica oleracea* germplasm with improved resistance to *Verticillium* wilt. *Plant Breeding* 122: 30-34.
63. **Keunecke, H.** (2005). Einfluss von *Verticillium longisporum* auf die Wurzel- und Sprossentwicklung von Winterraps unter Berücksichtigung von Fungizidapplikationen. Masterarbeit, Georg-August Universität Göttingen.
64. **Eynck, C.** (2008). Identification of resistance sources and characterisation of resistance factors in *Brassica* species to *Verticillium longisporum*. Dissertation, Georg-August Universität Göttingen.
65. **Heppner, C. & Heitefuss R.** (1995). Untersuchungen zum Auftreten von *Verticillium dahliae* Kleb. und anderen pilzlichen Erregern am Erntegut von Winterraps (*Brassica napus* L. var. *oleifera* Metzger). *Nachrichtenbl. Deutsch. Pflanzenschutzd.* 47: 57-61.
66. **Zeise K., Steinbach P.** (2004). Schwarze Rapswurzeln und der Vormarsch der *Verticillium*-Rapswelke. *Raps* 22: 170-174
67. **Eynck C.** (2007). Identification of resistance sources and characterization of resistance factors in *Brassica* species to *Verticillium longisporum*. Dissertation, Georg-August Universität Göttingen.
68. **Schnathorst WC.** (1981). Life cycle and epidemiology of *Verticillium*. In: Mace ME, Bell AA, Beckmann CH (eds.) *Fungal Wilt Diseases of Plants*. Academic Press, New York, 81-111.
69. **Heale, J. B. & V. K. Karapapa,** (1999). The *Verticillium* threat to Canada's major oilseed crop canola. *Can. J. Plant. Pathol.* 21: 1-7.
70. **Zeise, K., von Tiedemann, A.** (2001). Morphological and physiological differentiation among vegetative compatibility groups of *Verticillium dahliae* in relation to *V. longisporum*. *Journal of Phytopathology* 149: 469-475.
71. **Heppner, C.,** (1995). Nachweis von *Verticillium dahliae* Kleb. im Boden mit Plattengussfahren und ELISA (enzyme-linked immunosorbent assay) sowie Untersuchungen zur Auswirkung des Inokulums auf den Befall von Winterraps

- (*Brassica napus* ssp. *Oleifera* Metzg.). Dissertation, Universität Göttingen, Cuvillier Verlag, Göttingen.
72. **Eynck, C., B. Koopmann, G. Grunewaldt-Stoecker, P. Karlovsky & A. von Tiedemann**, (2007). Differential interactions of *Verticillium longisporum* and *Verticillium dahliae* with *Brassica napus* detected with molecular and histological techniques. *Eur. J. Plant Pathol.* 118: 259-274.
73. **Beckmann C.H.** (1987). The nature of wilt disease of plants. St.Paul, MN, USA, APS Press.
74. **Floerl S, Druebert C, Majcherczyk A, Karlovsky P, Kües U, Polle A.** (2008). Defence reactions in the apoplastic proteome of oilseed rape (*Brassica napus* var. *napus*) attenuate *Verticillium longisporum* growth but not disease symptoms. *BMC Plant Biol.* 8: 129.
75. **Feys, B. J. & Parker, J. E.** (2000). Interplay of signaling pathways in plant disease resistance. *Trends in Genetics* 16: 449-455.
76. **Heath, M. C.** (1998). Apoptosis, programmed cell death and the hypersensitive response. *European Journal of Plant Pathology* 104: 117-124.
77. **Scheel, D.** (1998). Resistance response physiology and signal transduction. *Current Opinion in Plant Biology* 1: 305-310.
78. **Ryals, J. A., Neuenschwander, U. H., Willits, M. G., Molina, A., Steiner, H. Y. & Hunt, M. D.** (1996). Systemic acquired resistance. *Plant Cell* 8: 1809-1819.
79. **Schröder, M., Hahlbrock, K. & Kombrink, E.** (1992). Temporal and spatial patterns of 1,3- β -glucanase and chitinase induction in potato leaves infected by *Phytophthora infestans*. *Plant Journal* 2: 161-172.
80. **Hong, J. K., Jung, H. W., Kim, Y. J. & Hwang, B. K.** (2000). Pepper gene encoding a basic class II chitinase is inducible by pathogen and ethephon. *Plant Science* 159: 39-49.
81. **Jung, H. W. & Hwang, B. K.** (2000). Pepper gene encoding a basic β -1,3-glucanase is differentially expressed in pepper tissues upon pathogen infection and ethephon or methyl jasmonate treatment. *Plant Science* 159: 97-106.
82. **Ryals, J. A., Neuenschwander, U. H., Willits, M. G., Molina, A., Steiner, H. Y. & Hunt, M. D.** (1996). Systemic acquired resistance. *Plant Cell* 8: 1809-1819.

83. **Huang L.K., Mahoney R.R.** (1999). Purification and characterization of an endopolygalacturonase from *Verticillium albo-atrum*. *J. Appl. Microbiol.* 86: 145-156.
84. **Mussel H.W., Strause B.** (1972). Characterization of two polygalacturonases produced by *Verticillium albo-atrum*. *Can. J. Biochem.* 50: 625-632.
85. **Wang M.C., Keen N.T.** (1970). Purification and characterization of endopolygalacturonase from *Verticillium albo-atrum*. *Arch. Biochem. Biophys.* 141: 749-757.
86. **Durrands P.K., Cooper R.M.** (1988). Selection and characterization of pectinase deficient mutants of the vascular pathogen *Verticillium dahliae*. *Physiol. Mol. Plant Pathol.* 32: 343-362.
87. **Durrands P.K., Cooper R.M.** (1988). The role of pectinases in vascular wilt disease as determined by defined mutants of *Verticillium albo-atrum*. *Physiol. Mol. Plant Pathol.* 32: 363-371.
88. **Wang J., Cai Y., Gou J., Mao Y., Xu Y., Jiang W., Chen X.** (2004). VdNEP, an elicitor from *Verticillium dahliae*, induces cotton plant wilting. *Appl. Environ. Microbiol.* 70: 4989-4995.
89. **Bailey B.A.** (1995). Purification of a protein from cultures filtrates of *Fusarium oxysporum* that induces ethylene and necrosis in leaves of *Erythroxylum coca*. *Phytopathol.* 85: 1250-1255.
90. **Bailey, B.A., Jennings, J.C., and Anderson, J.D.** (1997). The 24-kDa protein from *Fusarium oxysporum* f.sp. *erythroxyli*: occurrence in related fungi and the effect of growth medium on its production. *Canadian Journal of Microbiology* 43: 45- 55.
91. **Pemberton C.L., Salmond G.P.C.** (2004). The Nep1-like proteins – a growing family of microbial elicitors of plant necrosis. *Mol. Plant Pathol.* 5: 353-359.
92. **Bailey B.A., Apel-Birkhold P.C., Luster D.G.** (2002). Expression of NEP1 by *Fusarium oxysporum* f.sp. *erythroxyli* after gene replacement and overexpression using polyethylene glycol-mediated transformation. *Genet. Resistance* 92: 833-841.
93. **Fellbrich G., Romanski A., Varet A., Blume B., Brunner F., Engelhardt S., Felix G., Kemmerling B., Krzymowska M., Nürnberger T.** (2002). NPP1, a *Phytophthora*-associated trigger of plant defense in parsley and *Arabidopsis*. *Plant J.* 32: 375-390.

94. **Qutob D., Kemmerling B., Brunner F., Kufner I., Engelhardt S., Gust A.A., Luberacki B., Seitz H.U., Stahl D., Rauhut T., Glawischnig E., Schween G., Lacombe B., Watanabe N., Lam E., Schlichting R., Scheel D., Nau K., Dodt G., Hubert D., Gijzen M., Nürnberger T.** (2002). Phytotoxicity and innate immune responses induced by Nep1-like proteins. *Plant Cell* 18: 3721-3744.
95. **Fradin E.F., Thomma B.P.H.J.** (2006). Physiology and molecular aspects of *Verticillium* wilt diseases caused by *V. dahliae* and *V. albo-atrum*. *Mol. Plant Pathol.* 7: 71-88.
96. **Staats M., van Baarlem P., Schouten A., van Kan J. A. L., Bakker F. T.** (2007). Positive selection in phytotoxic protein-encoding genes of *Botrytis* species. *Fung. Genet. Biol.* 44: 52-63.
97. **Gijzen, M. and Nürnberger, T.** (2006). Nep1-like proteins from plant pathogens: recruitment and diversification of the NPP1 domain across taxa. *Phytochemistry* 67(16): 1800-1807.
98. **Keates S.E., Kostman T.A., Anderson J.D., Bailey B.A.** (2003). Altered gene expression in three plant species in response to treatment with Nep1, a fungal protein that causes necrosis. *Plant Physiol.* 132: 1610-1622.
99. **Schouten, A., van Baarlen, P. and van Kan, J. A. L.** (2008). Phytotoxic Nep1-like proteins from the necrotrophic fungus *Botrytis cinerea* associate with membranes and the nucleus of plant cells. *New Phytologist* 177(2): 493-505.
100. **Bae, H., Bowers, J. H., Tooley, P. W. and Bailey, B. A.** (2005). NEP1 orthologs encoding necrosis and ethylene inducing proteins exist as a multigene family in *Phytophthora megakarya*, causal agent of black pod disease on cacao. *Mycological Research* 109: 1373-1385.
101. **Bingle, L.E.H., Simpson, T.J. & Lazarus, C.M.** (1999). Ketosynthase Domain Probes Identify Two Subclasses of Fungal Polyketide Synthase Genes. *Fungal Genetics and Biology* 26: 209-223.
102. **Kim Y.T., Lee Y.R., Jin J., Han K.H., Kim H., Kim J.C., Lee T., Yun S.H., Lee Y.W.** (2005). Two different polyketide synthase genes are required for zearalenone in *Gibberellazeae*. *Mol. Microbiol.* 58: 1102-1113.

103. **Proctor R.H., Desjardins A.E., Plattner R.D., Hohn T.M.** (1999). A polyketide synthase gene required for biosynthesis of fumonisin mycotoxins in *Gibberella fujikuroi* mating population A. *Fung. Genet. Biol.* 27: 100-112.
104. **Watanabe C.M., Wilson D., Linz J.E., Townsend C.A.** (1996). Demonstration of the catalytic roles and evidence for the physical association of type I fatty acid synthases and a polyketide synthase in the biosynthesis of aflatoxin B1. *Chem. Biol.* 3: 463-469.
105. **Greenberg J.T., Yao N.** (2004). The role and regulation of programmed cell death in plant-pathogen interactions. *Cell. Microbiol.* 6: 201-211.
106. **Gómez B.L., Nosanchuuk J.D.** (2003). Melanin and fungi. *Curr. Opin. Infect. Dis.* 16: 91-96.
107. **Howard R.J., Ferrari M.A., Roach D.H., Money N.P.** (1991). Penetration of hard substrates by a fungus employing enormous turgor pressures. *PNAS* 88: 11281-11284.
108. **Takano Y., Kubo Y., Shimizu K., Mise K., Okuno T., Furusawa I.** (1995). Structural analysis of PKS1, a polyketide synthase gene involved in melanin biosynthesis in *Colletotrichum lagenarium*. *Mol. Gen. Genet.* 249: 162-167.

Chapter 2: Gene silencing in *Verticillium longisporum*: evaluation and establishment of a method for post-transcriptional downregulation of genes

Malte Beinhoff, Arne Weiberg and Petr Karlovsky

Molecular Plant Pathology and Mycotoxin Research Unit, Department for Crop Sciences, Georg-August University of Goettingen, Grisebachstrasse 6, 37077 Goettingen, Germany.

ABSTRACT

The detection and characterization of fungal genes putatively involved in the interaction of *V. longisporum* and its host plants provide the opportunity for a better understanding of the disease caused by *V. longisporum*, and thereby help in finding new strategies for the prevention or the control of infection. *V. longisporum* is described to be near-diplod and it is therefore most likely that most of the fungal genes are present in two copies in the genome. Therefore, we employed a technique for downregulation of gene function by a process referred to as RNA-interference (RNAi) for analysing the gene function of putative pathogenicity-related genes. Gene silencing using RNAi was triggered by intracellular expression of hairpin (HP) RNA which was reported to be the most potent inductor for the degradation of cognate mRNA in a sequence-specific manner. For the construction of HP fragments, our main focus was on the establishment of a method that has been published recently relying on a technique referred to as overlap-extension polymerase chain reaction (OE-PCR). Problems encountered during establishment gave new insights into the applicability of OE-PCR for construction of HP fragments. Nevertheless, many candidate genes were efficiently silenced by intracellular expression of HP cassettes during this research, so that we obtained a reliable tool for the characterization of putative pathogenicity-related candidate genes of *V. longisporum*.

INTRODUCTION

The functional characterization of pathogenicity-related genes is of major interest in plant pathogenic research. One of the first steps in the characterization of up-regulated genes in plant-pathogen interactions is to turn off the gene function in order to get a clue to the role of the gene product in the pathogenic life cycle of plant pathogens. On the basis of knowledge about the central dogma of molecular biology (1), which is defined as the flow of information from gene to protein, three possible attachment sites can be considered to exert an influence on gene expression. Various methods are therefore described in modern research to negatively affect the gene-function of certain gene products by exerting an influence at the level of DNA, at the level of transcribed mRNA, or at the protein level. The inhibition of gene-function at protein level by the use of specific antibodies against the gene product of the candidate gene is known as immunodepletion (2). In contrast, gene targeting by homologous recombination is used as a technique to affect a gene of interest at DNA level. The possibility of knocking out or modifying the gene by insertion of nucleotide-sequences into the open reading frame (ORF) was first described in 1989 (3) and is mostly used in research into haploid organisms.

The plant pathogenic fungus *Verticillium longisporum* is described as an amphihaploid, interspecific hybrid of parental haploid *V. dahliae* and *V. albo-atrum* strains (4, 5). Therefore, *V. longisporum* often carries more than one copy of a gene and is described as near-diploid (5). Gene knockout of organisms with more than one gene-copy is laborious and requires the presence of more than one available marker for selection. However, single gene knockout is often insufficient to cause a phenotype because in the genome of haploid organisms a gene may have several homologs that have redundant functions. Therefore a novel technique which relies on the regulation of gene expression on the post-transcriptional level is often used to “silence” genes in organisms. Gene silencing triggered by an external influence was first demonstrated in 1998 (6) by injection of double-stranded RNA-molecules (dsRNA) into *Caenorhabditis elegans* and the causal downregulation of the expression of the corresponding protein by the degradation of the specific mRNA. In research to date, different intracellularly-expressed constructs have been tested showing the ability to trigger post-transcriptional downregulation of target-genes by the expression of sense-, antisense-, or HP- RNAs.

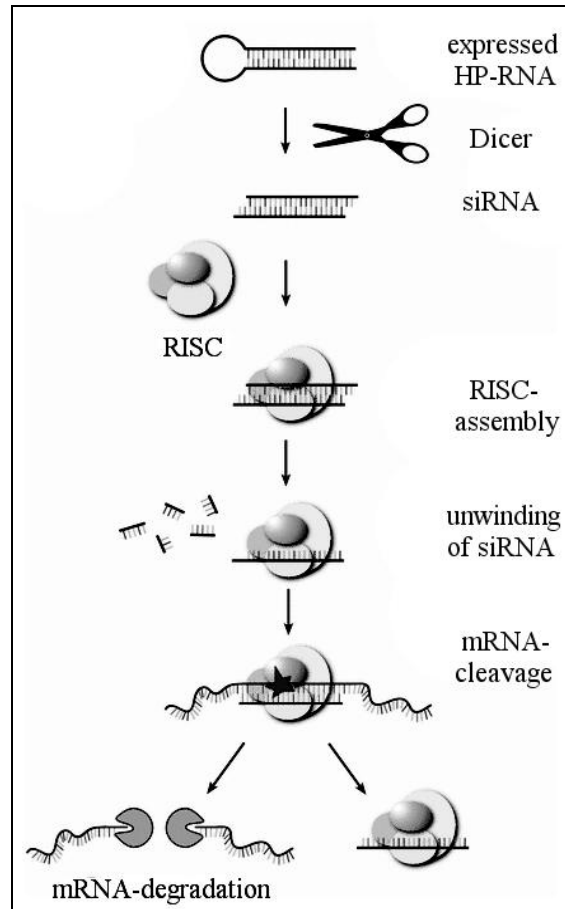


Figure 1: RNAi machinery triggered by intracellularly-expressed HP RNA (modified drawing, according to Cejka et al. 2006 (16))

DsRNA precursors derived from artificially introduced plasmids containing HP construct are cleaved by a dicer to create siRNA; siRNA is incorporated into RISC followed by unwinding of the ds-siRNA molecule by the helicase activity of the RISC; the antisense strand binds to the homologous region of candidate genes' mRNA, which is cleaved by RISC and subsequently degraded by cellular nucleases.

These methods are the basis of a process referred to as RNAi, which is important for the regulation of growth processes or defence against viruses (7) *in vivo*. Intracellularly-expressed dsRNA structures mostly occur during replication of viral RNA and induce the synthesis of an enzyme called Dicer, which cuts the dsRNA into small interfering RNA (siRNA)-fragments. These fragments provide a two base-pair overhang at the 3' end and a phosphate group at the 5' end which is recognized by an RNA-helicase, called Argonaute2, which separates the double strands into single strands (8). This strand is integrated into the RNA-induced silencing complex (RISC)-complex and serves as a recognition sequence for the binding and subsequent cleavage of complementary mRNA molecules by an endonucleolytically active

component of the RISC enzyme complex (9). Laboratory design of molecules triggering the intracellular expression of dsRNA is often carried out by the transformation of target-organisms with vectors carrying HP cassettes. HP cassettes consist of a promoter and terminator suitable for the expression of the intervening HP fragment, composed of candidate gene sequences in sense- and antisense-orientation with a spacer sequence forming the eponymous loop in between. In plants, HP RNA constructs with a spliceable intron as a spacer sequence had the highest efficiency, with 80 %- 100 % transformants showing silencing of target genes (10, 11). Currently, HP technology has become one of the most powerful tools for gene discovery and gene engineering in plants (12, 13, 14, 15).

Recently it was demonstrated that the mechanism of RNAi induced by the intracellular expression of HP constructs exists in *V. longisporum* (17). *V. longisporum* silencing-mutants of two isogenes of chorismate synthase *Vlaro2* constructed using the pSilent1-system showed a suppressed protein-expression of up to 94 % compared to wild type expression. Here we report our attempts to establish a method that have been published recently dealing with the construction of HP fragments by the use of an overlap-extension polymerase-chain reaction (OE-PCR). OE-PCR was first described in 1988 by Higuchi et al. (18) and was originally used to insert specific mutations in sequences during PCR. To utilize this method for the construction of HP fragments we followed the idea of producing polynucleotides from smaller DNA fragments with homologous sequences that can overlap during the annealing-step of PCR and that can be filled up with desoxyribonucleotide (dNTP) by a DNA polymerase during the elongation-step. The method relies on the ability of DNA polymerases to upfill DNA sequences by polymerization of dNTPs to only the 3' end of the newly-formed strand. This results in elongation of the new strand in a 5'-3' direction. Therefore, the ability to upfill overlapped ssDNA during OE-PCR is reduced to 50 % (see Figure 2).

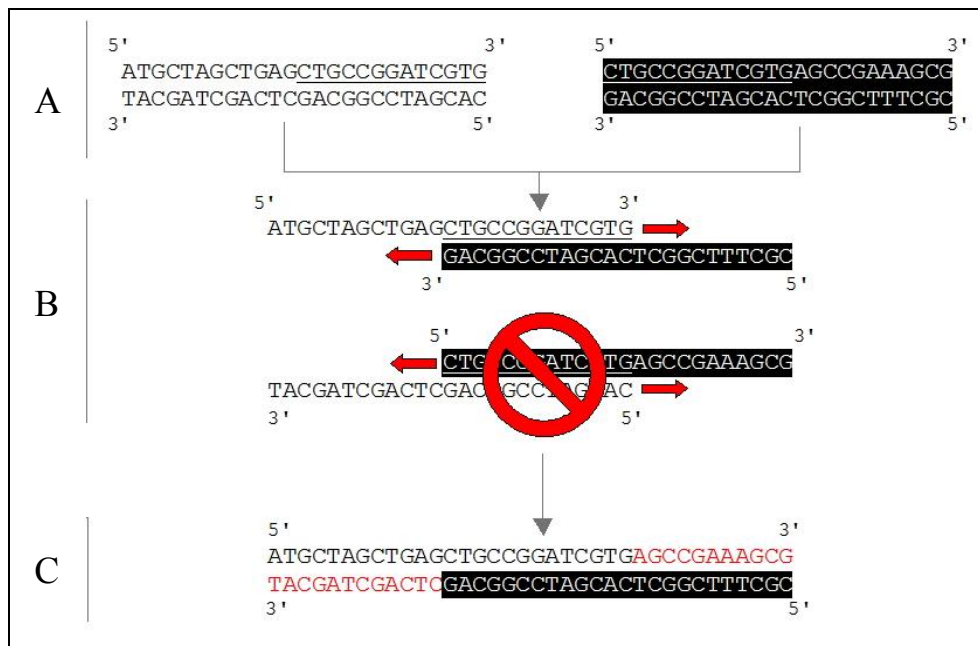


Figure 2: Scheme of OE-PCR

A = Two independent fragments (black and white bars) with homologous sequences (underlined) can overlap after the denaturation step of OE-PCR

B = 50 % of the overlapping fragments can be filled up by an DNA polymerase

C = The assembly is combined to a novel fragment by self-primed upfilling of annealed fragments during PCR

The results of this work provide new insights into the applicability of OE-PCR for the construction of HP fragments. Parallel to the establishment of the HP construction by the use of OE-PCR, we applied a construction method based on conventional cloning, including restriction and ligation steps. The efficiency of gene silencing caused by intracellularly-expressed HP cassettes transformed into *V. longisporum* compared to the effort needed for the construction should give us an effective and reliable tool for the characterization of putative pathogenicity-related candidate genes of the fungi.

MATERIALS AND METHODS

Bacterial and fungal stains

V. longisporum VL43 strain was provided by Prof. Andreas von Tiedemann, (General Plant Pathology and Crop Protection, Georg-August University Göttingen, Göttingen, Germany).

Agrobacterium tumefaciens strain AGL1 was provided by Dr. Susanne Frick (Leibniz Institute of Plant Biochemistry, Martin-Luther University Halle-Wittenberg, Halle/Saale, Germany) and was used for the transformation of *V. longisporum*.

Chemically competent *Escherichia coli* strain DH5 α and electrocompetent DH5 α and DH10 β strains (New England Biolabs, Ipswich, United Kingdom) were used for cloning purposes.

Plasmids and enzymes

For *A. tumefaciens*-mediated transformation (AMT) of *V. longisporum*, we used the binary vector pPK2 (12) including border sequences for the AMT and a hygromycin B-resistant cassette containing the hygromycin phosphotransferase gene from *E. coli* (hph) for selection of positive transformants. We cloned the *oliC* promoter from *Aspergillus nidulans* and the *tubA* terminator from *Botrytis cinerea* between the border sequences of the T-DNA providing the expression of intervening HP fragments.

Two different commercially available cloning vectors were used for subcloning of HP fragments derived from OE-PCR. The first was a modified vector (23) based on pBluescript SK⁻ (GenBank accession number X52330), containing a inserted 1620 bp spacer fragment in the multiple cloning side (MCS). Using the plasmid vector for ligation purposes, the prior preparation of insert-specific cutted vector-fragments from an agarose-gel is guaranteed due to the better separation of linerized vectors from non-sufficient cutted vector-fragments during agarose-gel electrophoresis. The resulting coherent elimination of any non-specific recirculated plasmid-vectors after ligation excludes any non-positive transformants. The second plasmid we used was the pBarn cloning vector (AppliChem GmbH, Darmstadt, Germany), including the toxic barnase gene expressing a small, highly active ribonuclease from *Bacillus amyloliquefaciens* (24). The disruption of the barnase gene by insertion of DNA fragments into the MCS prevents positive transformed *E. coli* cells being killed after transformation with the pBarn plasmid due to the toxic feature of the expressed ribonuclease.

Cloning of vectors containing HP cassettes was carried out by restriction enzymes, ‘T4-DNA Ligase’, ‘T4- Polynucleotide Kinase’ and affiliated buffers purchased from Fermentas Inc. (Fermentas, St. Leon-Rot, Germany).

Enzymes and reagents for first strand cDNA synthesis, including ‘Oligo(dT)18 Primer’, ‘RiboLock™ RNase Inhibitor’ and ‘M-MuLV Reverse Transcriptase’ were also purchased from Fermentas.

Different polymerases were used for the experiments in this chapter. ‘Biotaq™ DNA Polymerase’ (Bioline, Luckenwalde, Germany) was used for general amplification of fragments by PCR. ‘Pfu-Polymerase’ (Fermentas, St. Leon-Rot, Germany) was used for the amplification of blunt-end PCR-fragments, which in turn are intended to be used for OE-PCR and ligation purposes. High fidelity ‘Phusion®-Polymerase’ (Fisher Scientific GmbH, Schwerte, Germany) was used for sequencing purposes and also during the construction of HP fragments by OE-PCR. The ‘ABsolute Blue QPCR Fluorescein Mix’ (Fisher Scientific GmbH, Schwerte, Germany) was used for quantitative real-time PCR (qRT-PCR) to assess the silencing efficiency of *V. longisporum* mutants.

Alkaline agarose gel electrophoresis

Alkaline conditions were used for the separation and visualization of single-stranded DNA (ssDNA) fragments in agarose gels using gel electrophoresis. The run of DNA samples on agarose gels at a pH that is high enough to denature double-stranded DNA (dsDNA) prevents the accretion of homologous ssDNA-sequences to dsDNA fragments. For this purpose we followed a modified protocol of Sambrook et al. (26) for alkaline gel electrophoresis by adding NaOH to the agarose and buffers. Samples were heated up to 98 °C for 3 min prior to electrophoresis to ensure complete denaturation, of dsDNA into ssDNA. Samples were immediately mixed up with a loading buffer containing 200 mM NaOH to prevent the renaturation of ssDNA to dsDNA. The sample was loaded on an agarose gel flooded with an electrophoresis buffer containing 200 mM NaOH. We reduced the concentration of NaOH for the alkaline agarose gel electrophoresis from 300 mM, as suggested by Sambrook et al., to 200 mM to minimize the heating up of buffers and agarose because of to the higher hydroxide ionic level of the electrophoresis buffer, which leads to an improved electric flow during electrophoresis. Staining of ssDNA fragments with ethidium bromide is relatively poor in contrast to dsDNA because of the lower ability of the fluorescent agent to intercalate into the ssDNA. Additionally, the higher pH levels of the gel, due to the alkaline conditions, hamper the staining with ethidium bromide. Therefore, after gel electrophoresis, the gel was

transferred into a neutralization-puffer containing 1.5 M NaCl to compensate for the pH value. Also, the reduction of NaOH to 200 mM during the electrophoresis process leads to a more efficient staining and a better visualization of ssDNA fragments.

Extraction of genomic DNA (gDNA) and total RNA from fungal mycelium

Total RNA for qRT-PCR and gDNA for PCR and southern hybridization were extracted simultaneously using a modified protocol of Manitatis et al. (27). Approximately 1×10^5 spores of *V. longisporum* strain 43 were inoculated in 20 ml liquid potato-dextrose broth (PDB) media (Roth, Karlsruhe, Germany) and grown for approximately 10 days at 23 °C in the dark. Fungal mycelium was harvested and directly ground into a fine powder in a mortar in liquid nitrogen. The ground samples were stored at -80 °C or immediately used for extraction. To proceed with extraction, powdered mycelium was treated with a hot extraction buffer containing 0.1 M Tris-HCl, 0.1 M LiCl, 0.01 M EDTA and 1 % SDS. After phenol and chloroform/isoamylalcohol extraction, the RNA fraction was precipitated by incubating the samples overnight (ON) along with 1 vol. of a 4 M LiCl solution on ice. After centrifugation (6000 g, 15 min, 4 °C) to pellet the RNA, the gDNA was purified by transferring the supernatant from the LiCl-precipitation into a new reaction tube and was incubated along with 0.7 vol. NH₄Ac (7.5 M) and 2.5 vol. EtOH (96 % v/v) to precipitate the gDNA and pellet it by another centrifugation. Extracted RNAs were stored at -80 °C and gDNAs were stored in -20 °C freezers.

Southern hybridization

Southern hybridization was performed to check the number of copies of the genes to be silenced in the genome of near-diploid *V. longisporum* strain 43. Therefore, dioxygenin (DIG)-labelled fragments, specific for the gene of interest, were produced and used as a probe for hybridization with homologous sequences of digested gDNA from *V. longisporum* blotted on a membrane. The labelling of probes relies on the principles of PCR using DIG-tagged deoxyuridine triphosphates (DIG-dUTP) for the elongation of fragments instead of deoxythymidine triphosphate (dTTP). For this purpose the quantity of dTTP was substituted with DIG-dUTP in a proportion of 30 % (w/v) in a PCR run for 30 cycles using thermostable *Taq* polymerase. The probes were amplified using gDNA of *V. longisporum* as a target, and

specific oligonucleotides as primers. The efficiency of labelling of the probes was tested by dot-blot following the manufacturer's instructions (Roche Diagnostics GmbH, Penzberg, Germany). For the digestion of gDNA of *V. longisporum*, 10 µg was cut with *Bgl*III and *Hind*III. The gDNAs and a DIG labelled DNA molecular weight marker was subsequently separated on a 1 % agarose gel by gel electrophoresis at 2 V/cm for 4 hours. The agarose gel, containing the separated gDNA, was rinsed with 0.25 M HCl for a partial depurination of high molecular DNA fragments to ensure the transfer of the entire gDNA from the agarose gel to a nylon membrane by vacuum blot. Prior to vacuum blotting, the gel was also rinsed in 0.4 N NaOH for 20 min to ensure complete denaturation of the gDNA to allow the binding of probes to homologous regions of the DNA while hybridization. After vacuum blotting using a VacuGene XL blotting apparatus (Pharmacia, Freiburg, Germany), the gDNA was fixed on Hybond N+ nylon membrane (Amersham Biosciences Europe GmbH, Freiburg, Germany) using a UV-crosslinker (Vilber Lourmat, Torcy, France). Hybridization and detection of the DIG-labeled probe, using the DIG Easy Hyb hybridization solution, was performed following the manufacturer's instructions (Roche Diagnostics GmbH, Penzberg, Germany).

Transformation of *V. longisporum*

Agrobacterium tumefaciens-mediated transformation (AMT) of *V. longisporum* was performed following a protocol for the transformation of filamentous fungi published by Utermark in 2008 (28). Artificially initiated AMT consists of three consecutive steps: Firstly, the induction of the *A. tumefaciens* bacterial culture carrying the transformation-plasmid; Secondly the co-incubation of the bacterial culture with fresh fungal spores to apply the transformation process; and thirdly the selection of positive transformants by the use of a selection agent. The induction of the bacterial culture implies the expression of several *vir* genes, which are present on the pTiBo542ΔT plasmid of *A. tumefaciens* AGL1 cells, triggered by the addition of 200 mM acetosyringone to the induction medium. The expression of *vir* genes leads to the transfer of a particular DNA fragment, which was inserted between the left- and right-T-region border sequences, usually carrying the T-DNA of the tumour-inducing (Ti)-plasmid, into the fungal recipient. The replaced T-DNA sequence was thus incorporated into the nuclei of infected cells where it was then stably integrated into the host genome. Positive transformants were selected by the use of potato dextrose agar (PDA) plates containing 50 µg/ml hygromycin B (Carl Roth GmbH & Co. KG, Karlsruhe, Germany) and

200 mM cefotaxime (Carl Roth GmbH & Co. KG, Karlsruhe, Germany) to get rid of the bacteria from the selection media.

qRT-PCR

Total RNA extracted from silencing mutants and wild type *V. longisporum* was used for two-step qRT-PCR. For first strand cDNA synthesis, 50 pmol “Oligo(dT)18 primer” was used to reverse transcribe 400 ng of total RNA. For this purpose we incubated the RNA along with 1 mM dNTP mix, 20 U RiboLock RNase inhibitor and 40 U M-MuLV-reverse transcriptase for 60 min at 42 °C. The resulting cDNA was purified using “QIAquick PCR Purification Kit” (Qiagen, Hilden, Germany). Approximately 10 ng of total cDNA was used to measure the expression levels of candidate genes in fungal mycelium to assess the silencing efficiency of the transformed fungi compared to wild type gene-expression. Amplification of fragments and melting curve analysis was performed using the iCycler System (BioRad, San Diego, USA). The qRT-PCR protocol starts with a 15 min step at 95 °C to activate the polymerase included in the “The ABSolute Blue QPCR Fluorescin Mix” and is followed by 40 cycles including a denaturation step at 95 °C for 30 sec, an annealing step at 60 °C for 30 sec and a final elongation step at 72 °C for 30 sec. The detection of fluorescence was automatically carried out by the iCycler system during the elongation step of the PCR. The following melting curve analysis of the amplified fragments was carried out directly after the PCR run by heating the samples to 95°C for 1 min, cooling them to 55 °C for 1 min and then carrying out a stepwise increase of the temperature from 65 °C to 95 °C at the rate of 1 °C/min. The fluorescence was continuously measured by the cycler after each temperature increase. For normalization of fungal gene expression the two housekeeping genes β -tubulin and ribosomal protein S17 (29) were applied. Statistical analysis of three biological replicas was carried out with the REST-384© Version 1 (30) and efficiency normalization of PCR amplification was carried out by measuring cT values of a dilution series for each gene.

Primer design

Design and analysis of primer-sequences was carried out with the FastPCR software (25). Primers were synthesised and purchased from Invitrogen Inc. (Karlsruhe, Germany). We designed many primer-sets for the construction of HP fragments suitable for different

candidate genes of *V. longisporum*. All primer sets were designed in a comparable manner. Primer sets for one candidate gene named VI-12.1, which showed high homology to a zinc-finger transcription factor named ACE1, are described and listed subsequently.

The first two pairs of primers amplify a sense and antisense fragment of a candidate gene suitable for OE-PCR. These primers were designed by adding a homologous sequence to the spacer on the 3'-ends of the reverse primer to allow overlapping with the spacer during the annealing step of OE-PCR. The 5'-ends of the sense and antisense forward primers are associated with overhang sequences providing restriction sites for the directional ligation into a cloning vector. Primers for the amplification of a spacer (no. 5 and 6) were designed, amplifying a fragment comprising the sequence of a native intron from the *V. longisporum* hydrophobin gene *VIH1*, homologous to *VdH1* from *V. dahliae* (GenBank Accession No. DQ026260.1). Partial sequences of the resulting PCR fragments are shown in the flow chart for OE-PCR (see page 37).

no.	name	sequence (5' → 3')
1	sense- <i>SdaI</i> -F	TAGTGACCTGCAGGACATCGAGAGGATCGACGCCAGC
2	sense-OE-R	<u>ACAACGTACGGGTAGAGCAGTACATGT</u> CGCCGCGGAGCCTAC
3	antisense- <i>AscI</i> -F	GAGCTCGGCGCGCCACATCGAGAGGATCGACGCCAGC
4	antisense-OE-R	<u>CCAACAATAGCAAAGAGTGCCAGGACATGT</u> CGCCGCGGAGCCTAC
5	spacer-F	ACTGCTCTACCCGTACGTTG
6	spacer-R	CCTGGCACTCTTTGCTATTGTTGG
9	sense2- <i>SdaI</i> -F	TAGTGACCTGCAGGACATCGAGAGGATCGACGCCAGC
10	antis2- <i>AscI</i> -F	GAGCTCGGCGCGCCACATCGAGAGGATCGACGCCAGC

Table 1: Primer sequences for the amplification of fragments suitable for the construction of HP fragments using OE-PCR

Applies for all primer sequences in the following tables: restriction sites are marked in bold; primer sequences that could overlap with the spacer fragment during OE-PCR are underlined.

Primers for the amplification of sense (no.11 and 12) and antisense fragments (no. 13 and 14) for the construction of an HP fragment using conventional cloning steps were designed in a comparable manner to those designed for OE-PCR, with the difference that the homologous spacer sequences on the 3'-ends were replaced by restriction sites for the ligation with the spacer fragment. Therefore the primers (no. 15 and 16) for amplification of the spacer also contain analogue restriction sites for directional ligation with the flanking fragments.

no.	name	sequence (5' → 3')
11	sense- <i>SdaI</i> -F	TAGTGACCTGCAGGACATCGAGAGGATCGACGCCAGC
12	sense- <i>NdeI</i> -R	GATATGCATATGACATGTCGCCGCGCGAGCCTAC
13	antisense- <i>AscI</i> -F	GAGCTCGGCGCGCCACATCGAGAGGATCGACGCCAGC
14	antisense- <i>BglII</i> -R	GATATGAGATCTACATGTCGCCGCGCGAGCCTAC
15	spacer- <i>NdeI</i> -F	CTATACCATATGACTGCTCTACCCGTACGTTG
16	spacer- <i>BglII</i> -R	GATATGAGATCTCCTGGCACTCTTTGCTATTGTTGG

Table 2: Primer sequences for the amplification of fragments possess restriction sites suitable for the construction of an HP fragment using conventional cloning steps

Primers to amplify probes for southern hybridization (no. 19 and 20) were designed to detect the number of copies of candidate genes that are present in the genome of *V. longisporum*. Therefore, primer sequences were applied amplifying the same candidate gene sequence as we used for the construction of HP fragments, but primers lacked sequences for restriction sites.

no.	name	sequence (5' → 3')
19	SB-sense-F	ACATCGAGAGGATCGACGCCAGC
20	SB-sense-R	ACATGTCGCCGCGCGAGCCTAC

Table 3: Primer sequences for the amplification of probes for southern hybridization

To assess the silencing efficiency of *V. longisporum* mutants using qRT-PCR, we used primers (no. 21 and 22) to amplify fragments different to those used during construction of HP fragments. Otherwise, a mass of transcripts will be measured expressed by the inserted HP cassettes under the influence of the transient *oliC* promoter. For normalization of fungal gene expression, primers for the amplification of the two housekeeping genes β -tubulin (no. 23 and 24) and ribosomal protein S17 (no. 25 and 26) were applied.

no.	name	sequence (5' → 3')
21	RT-sense-F	AGCGTCCTGCAAACAGACC
22	RT-sense-R	TGTCAGTGGGAAAGCGATG
23	tubulin-F	GTTCATCTTCAGACCGGTCAGT
24	tubulin-R	CCAGACTGGCCGAAAACGAAGT
25	rps17-F	GCATCTGCGATGAGATCGCCA
26	rps17-R	TCGGAGTTCTGGGTAAAGTCGAGA

Table 4: Primer sequences to measure silencing efficiency when silencing mutants by qRT-PCR

RESULTS & DISCUSSION

Many candidate genes of *V. longisporum* were efficiently silenced by RNAi, triggered by the intracellular expression of HP cassettes, during the research reported in this thesis. To indicate the encountered problems during establishment of the construction for HP fragments by the use of OE-PCR and either conventional cloning steps, we give preference to one candidate gene. The following results demonstrate our procedures to construct transformation vectors, including HP cassettes to trigger post-transcriptional silencing for the *V. longisporum* candidate gene VI-12.1. This gene was displayed by a molecular fingerprinting method, known as cDNA-AFLP (amplified fragment-length polymorphism), as a gene putatively involved in the pathogenic life cycle of the fungus during the interaction with the natural host plant *B. napus* (38). The ORF of this gene comprises 2328 nucleotides and one intron. The translated mRNA is predicted to encode a protein which possesses 775 amino acids. Southern hybridization was performed, showing two gene copies in the genome of *V. longisporum*.

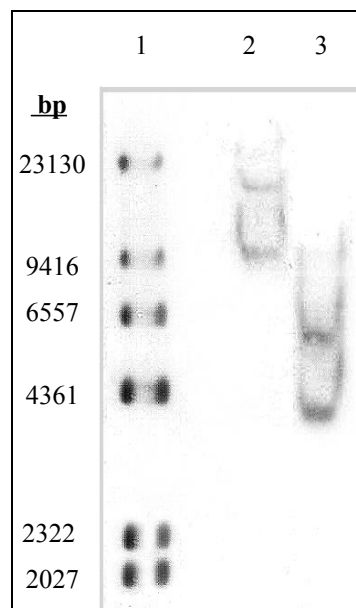


Figure 3: Southern hybridization for candidate gene VI-12.1

1 = self-made DNA ladder comprising incorporated DIG-dUTPs

2 = gDNA cut with *Bgl*III

3 = gDNA cut with *Xba*I

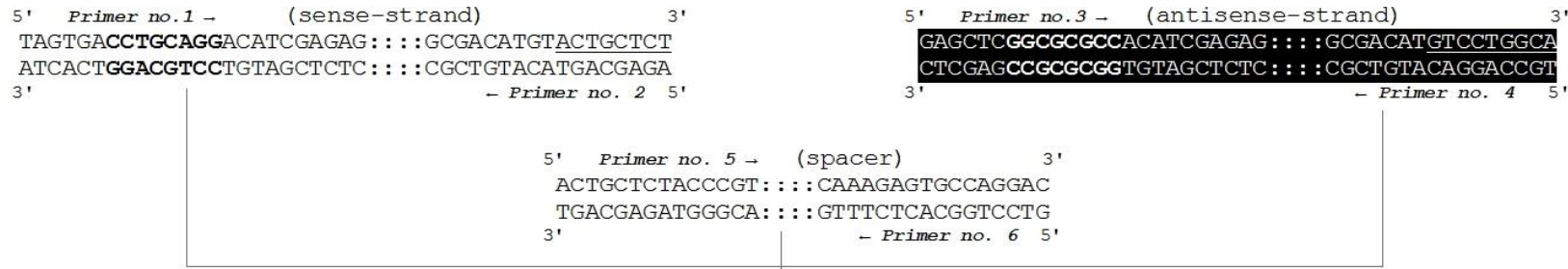
The design of the HP fragment for VI-12.1 provides two flanking 238 bp sense and antisense fragments and a 125 bp intervening spacer, forming the eponymous loop of the expressed HP RNA. The correctly assembled HP fragment comprises 601 bp.

Construction of HP fragments using OE-PCR

Expressing stem-loop HP RNAs were shown to efficiently silence homologous target gene expression in plants, animals and fungi (31). In regard to enabling the generation of HP RNA constructs, several vectors with a functional intervening intron spacer have been reported in literature (32, 33). However, these methods generally require amplification of target sequences and several rounds of restriction and ligation steps. The construction by the use of restriction enzyme-based cloning is laborious and there are inefficiencies in the assembly of some sequences to HP fragments (32). An alternative way to construct HP containing vectors takes advantage of “Gateway®” technology (Invitrogen, Karlsruhe, Germany) and facilitates easy cloning of DNA fragments but the reagents for this method are relatively expensive compared to the reagents for cloning with restriction enzymes. In this study, we tested different approaches published in recent years for the construction of HP fragments by PCR-based methods. All these methods utilize OE-PCR to assemble sense and antisense strands of a candidate gene with an intervening spacer, and do not depend on time-consuming restriction enzyme-based cloning steps or require costly consumables.

In 2005, Pawlowski et al. first reported their work on the construction of HP fragments by the use of OE-PCR (34). This method was referred to as “inverted-repeat PCR” and consisted of three consecutive PCR rounds (see flow chart on page 37, round 1= A; round 2= B to D; round 3= E). The first round of PCR was determined to amplify the three fragments which are intended to overlap and therefore build up the HP fragment during OE-PCR. Therefore, sense and antisense fragments of candidate genes were amplified with primers adding sequences to the 3'-ends homologous to the intervening spacer. This allowed overlapping during the annealing step of the following second round OE-PCR-step.

A



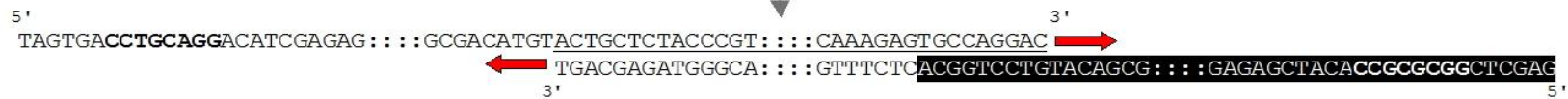
B



C



D



E



Flow chart showing the procedure for construction of hairpin-cassettes using OE-PCR

- Partial sequences are shown; restriction sites are marked in bold; homologous sequences to overlap with the spacer are underlined

A = round-one PCR: Sense/antisense- and spacer-fragments were amplified using primers shown in Table 1

B = round-two PCR (OE-PCR): Denaturation of fragments and annealing of homologous regions during OE-PCR

C = round-two PCR (OE-PCR): Self-primed strandfilling of sense/intron and antisense/intron during OE-PCR

D = round-two PCR (OE-PCR): Denaturation of fragments and annealing of homologous regions during OE-PCR

E = round-three PCR: Amplification of HP fragment with end terminal primer

In the protocol given by Pawlowski et al., the use of a thermostable DNA polymerase, named after the thermophilic bacterium *Thermus aquaticus* (*Taq*), was mentioned. *Taq*-polymerase makes DNA products that have adenine overhangs at their 3'-ends. Therefore, the addition of dNTPs to upfill the overlapping fragments during the elongation step of OE-PCR by a DNA polymerase should be inhibited if the following base of the linker cannot form a canonical Watson-Crick DNA base pairing with the adenine overhang of the *Taq*-derived fragment (see Figure 4).

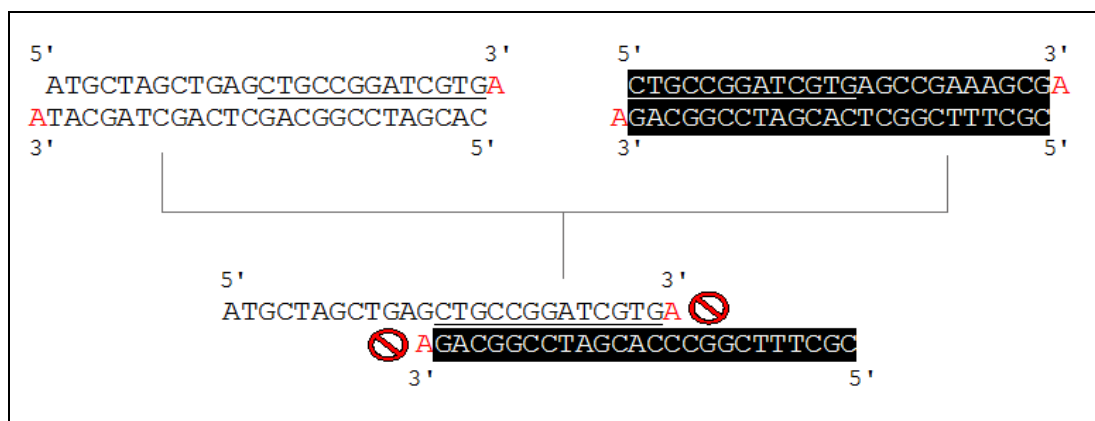


Figure 4: Inhibition of the addition of dNTPs during OE-PCR by the use of *Taq*-Polymerase

To provide the strand-filling of the overlapped fragments during OE-PCR we give preference to the use of a polymerase which generates blunt end fragments. The efficiency of HP assembling was tested by the use of *Taq*-polymerase and was then compared to high performance blunt end polymerases like *Pfu*, from *Pyrococcus furiosus*, or Phusion®, including a novel *Pyrococcus*-like enzyme with a processivity-enhancing dsDNA-binding domain. The error rate of Phusion® polymerase is 50 times lower than *Taq*-, and 6 times lower than *Pfu* polymerases (35). In our experiments, the use of both blunt end polymerases led to a higher assembly efficiency of single fragments to HP constructs than was achieved by the use of *Taq*-polymerase during OE-PCR (data not shown). Since the Phusion® polymerase was more expensive we decided to use a mixture of *Pfu*- and *Taq*-polymerase in a 1:10 ratio to benefit from the rapidity of *Taq*- (36) and also from the 3'- to 5'-end exonuclease proofreading activity and blunting property of *Pfu*-polymerase (37).

For the first round of PCR, approximately 1 ng of gDNA from *V. longisporum* was used to amplify the three fragments of the HP assembly. The PCR run was performed using 5 pmol of

each primer given in Table 1 (no. 1 to 6) with a starting denaturation step at 95 °C for 5 min followed by 35 PCR cycles including a denaturation step at 95 °C for 30 sec, an annealing step at 60 °C for 30 sec, and an elongation step at 72 °C for 30 sec. The PCR run finished with a final elongation step at 72 °C for 5 min. PCR products were run on a 1.7 % agarose gel to visualize the amplicons and to measure product amounts.

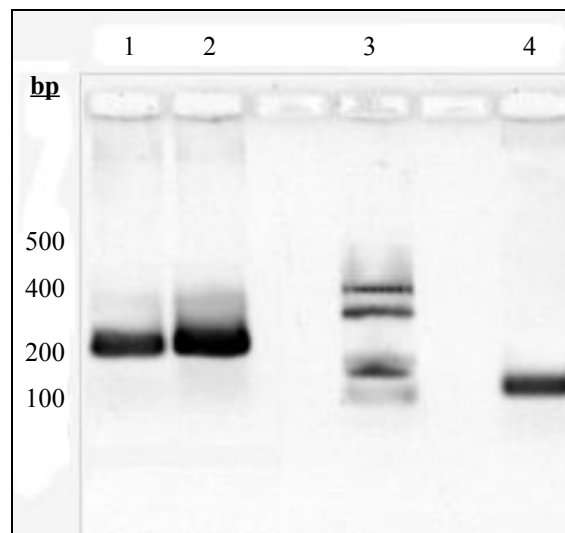


Figure 5: Agarose gel electrophoresis of the first round of PCR showing amplicons intended for OE-PCR

1= sense fragment of candidate gene amplified using primers 1 and 2 (Table 1)

2 = antisense fragment amplified with primers 3 and 4 (Table 1)

3 = self-made marker-fragments for agarose gel electrophoresis

4 = spacer amplified with primers 3 and 4 (Table 1)

Amplicons from round one PCR were purified from agarose gel using “QIAquick Gel Extraction Kit” (Qiagen, Hilden, Germany). For the second round of PCR, approximately 5 ng from the first round PCR-product was used in equal molar ratio for the three fragments. This round of PCR is what gives the name OE-PCR to this method and was performed according to the author’s recipe without the use of any primers to allow annealing of homologous overhangs of sense and antisense fragments to the spacer, and consequent self-primed strand-filling by the DNA polymerase. OE-PCR was initiated with a treatment of 95 °C for 5 min, then 8 PCR cycles (95 °C for 1 min, 52 °C for 1 min and 72 °C for 2 min), and finished with one cycle of 72 °C for 7 min. For the visualization of annealed HP fragments due to OE-PCR, we applied an identical OE-PCR run as above with an additional 27 cycles, and we pooled 6 PCR samples to gain sufficient numbers of annealed assemblies to show. To

demonstrate the ability of both flanking fragments to overlap with the spacer, we applied OE-PCR runs adding either sense and spacer fragment, antisense and spacer fragment or sense, antisense and spacer fragments to each individual PCR mixture. The samples were loaded after PCR on a 1.7 % agarose gel for electrophoresis.

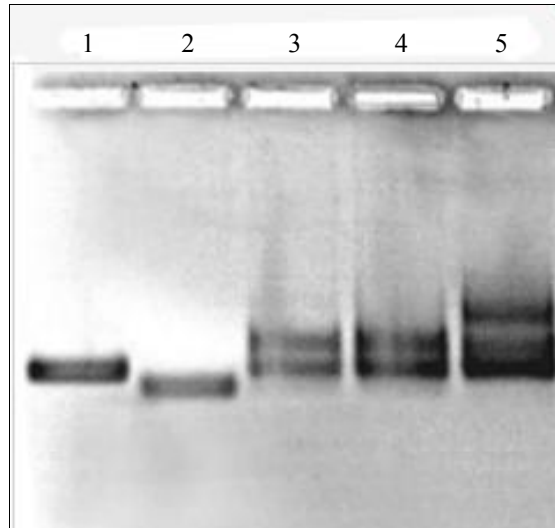


Figure 6: Agarose gel electrophoresis to show efficiency of OE-PCR to assemble HP fragments

1= sense fragment of candidate gene

2 = intron spacer

3 = assembly of sense fragment and intron spacer after OE-PCR

4 = assembly of antisense fragment and intron spacer after OE-PCR

5 = assembled HP fragment by adding sense/antisense fragment and intron spacer to the OE- PCR

As proposed by the author's recipe, we used an aliquot of 5 μ l from the 50 μ l PCR sample of round two PCR (analogue as with lane 5 shown in Figure 6) and added it to the third round of PCR (see Figure 4E) to increase the number of HP fragments by amplification using 25 pmol of end terminal primers (no. 1 and 3, Table 1) to the HP fragment. The mix was run at 95 $^{\circ}$ C for 5 min, then 30 PCR cycles including 1 min at 95 $^{\circ}$ C, 1 min at 55 $^{\circ}$ C and 2 min at 72 $^{\circ}$ C, and finished with one cycle for 5 min at 72 $^{\circ}$ C. The PCR sample was separated on a 1.7 % agarose gel by electrophoresis.

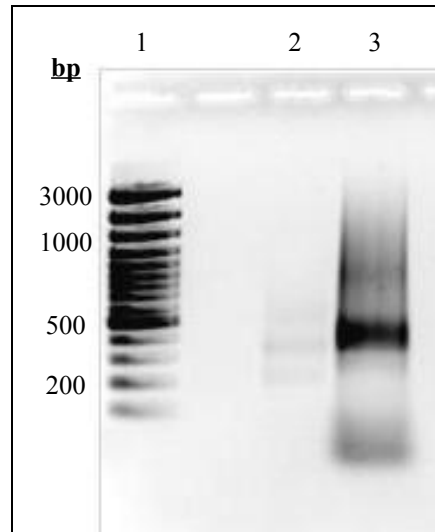


Figure 7: Agarose gel electrophoresis of amplicons from third round of PCR

1 = GeneRuler™ 100 bp Plus DNA Ladder (Fermentas, St. Leon-Rot, Germany)

2 = round two PCR sample (see Figure 6, lane 5)

3 = round three PCR sample, amplification of HP fragment with end terminal primers

For all tested candidate genes we were never able to amplify a PCR product with the calculated length for the correctly assembled HP fragments. The amplified fragments of the third PCR round were approximately as large as the fragments that emerged in the OE-PCR as a result of the overlapped sense or antisense fragments connected with the spacer. It is most likely that the homologous sequences of HP fragments, amplified during the third round of PCR, showed great affinity for annealing by pairing the sense and antisense sequences after each denaturation step of PCR and thus formed HP structures. Using this assumption, we suggest that the smaller fragment shown in lane 3 of Figure 7 may be the folded HP structure. We could show by a time course run of round three PCR, in which we removed a sample after each fifth PCR cycle, that an amplicon with the assumed length for the HP fragments appeared after 25 cycles of PCR and vanished within the next 5 cycles. PCR samples were examined by electrophoresis in a 1.7 % agarose gel.

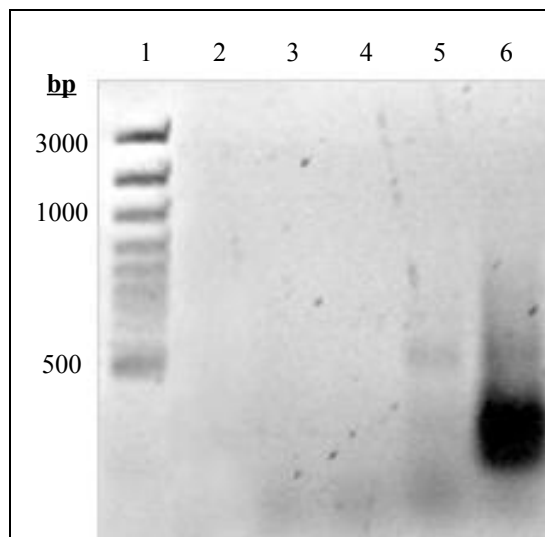


Figure 8: Agarose gel electrophoresis of amplified fragments from a time course PCR

1 = GeneRuler™ 100 bp Plus DNA Ladder

2 = round three PCR stopped after 10 cycles

3 = round three PCR stopped after 15 cycles

4 = round three PCR stopped after 20 cycles

5 = round three PCR stopped after 25 cycles, amplicon with assumed length for HP fragment appears

6 = round three PCR stopped after 30 cycles, previous amplicon vanishes and the smaller fragment emerges

We made a great effort to accomplish the amplification of the HP fragment during the third round of PCR by varying PCR conditions and by the use of extended primer sequences (Table 1, primer no. 7 and 8). Neither the use of increased primer concentration, nor changes in the PCR conditions, such as varying the $MgCl_2$ concentration or modification of incubation times for the different PCR steps, led to any improvement in the amplification of HP fragments. We proposed that the use of end terminal primers with extended sequences from the candidate gene would be more effective in binding to the homologous sequences of the HP fragments, and thus lead to an interfering apposition of HP fragments to HP structures and therefore allows amplification of the assembly. The PCR run with extended end terminal primers was done in the same way as the previous PCR run. The PCR sample was loaded in a 1.7 % agarose gel and the amplicons were separated by electrophoresis.

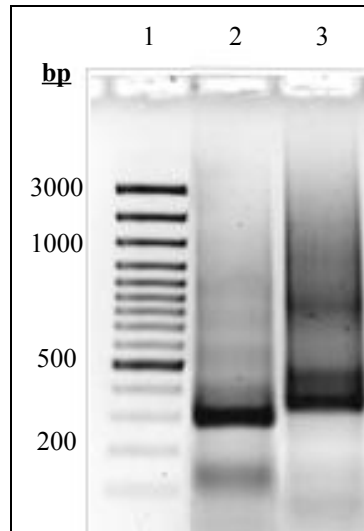


Figure 9: Agarose gel electrophoresis of round three PCR with extended primers

1= GeneRuler™ 100 bp Plus DNA Ladder

2 = round three PCR sample, amplification of HP fragment with end terminal primers (see Figure 7, lane 3)

3 = round three PCR sample, amplification of HP fragment with extended end terminal primers

Interestingly, the use of the extended end terminal primers for the third round of PCR led to an altered band pattern visualized on an agarose gel, but again not the expected amplicon for the HP fragment appears. Presumably, the larger size of the fragment that appeared after the third round PCR with extended primers was due to the fact that the end terminal primers can effectively bind in both PCR runs to the HP fragments but cannot prevent the folding of the HP structure, which consequently slows down the mobility of the fragment in passing through the agarose gel during electrophoresis, and results in the altered band pattern because of the larger extended primers used for PCR. To discover if the HP fragments were indeed amplified through the third round of PCR but instantly folded to HP structures, we applied agarose gel electrophoresis at a pH that was sufficiently high to denature dsDNA. This alkaline agarose gel electrophoresis can visualize ssDNAs by adding NaOH to agarose and buffers for electrophoresis. Therefore, we used both third round PCR samples for alkaline agarose gel electrophoresis and separated them at 1 V/cm for 2 h.

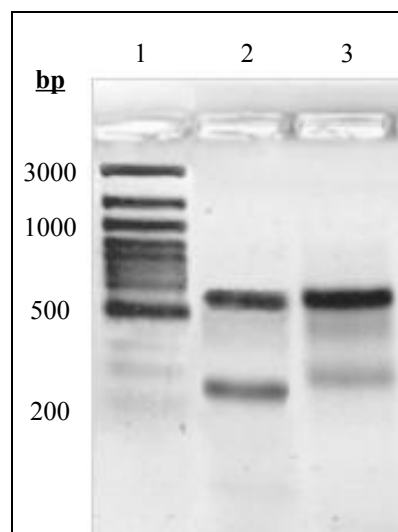


Figure 10: Alkaline agarose gel electrophoresis of samples from third round PCR

1 = GeneRuler™ 100 bp Plus DNA Ladder

2 = round three PCR sample using end terminal primers

3 = round three PCR sample using extended end terminal primers

For both PCR samples, using end terminal and extended end terminal primer sets, we could visualize a band with the calculated length for the HP fragment of candidate gene VI-12.1 by alkaline agarose gel-electrophoresis. Therefore, we propose that the folded HP structure that we suggested after the third round of PCR was separated into ssDNA HP fragments due to alkaline conditions. We were also able to reform the HP structure by heating the purified fragments from the alkaline agarose gel up to 60 °C for 5 min and then cooling them down before loading the samples on a normal agarose gel to separate them again by electrophoresis. The band pattern for both PCR samples was nearly identical to that shown in Figure 9 in lane 2. There was no band shift visible due to the PCR with extended primers as shown before. The primers to bind on the HP fragments were probably removed by gel extraction, thus both PCR samples of the third round PCR showed the folded HP without any bound primers. Unfortunately, no dsDNA of HP fragments, which could be used to proceed with ligation into a cloning vector, could be obtained due to reapposition of ssDNA to dsDNA. Attempts to use the assembly gained from round two PCR (see Figure 6, lane 5) for subcloning failed due to the insufficient amounts of DNA that could be obtained after purification and prior digestion of the insert to ligate into the vector. As mentioned in the introduction, the ability to upfill overlapping DNA strands during OE-PCR is reduced to 50 % (see Figure 2). The construction of an HP fragment requires two independent consecutive steps of OE-PCR to perform

successive upfilling of the overlapping sense or antisense fragment with the spacer, and subsequent upfilling of the overlapping sense/spacer with antisense/spacer assemblies to the HP fragment (see flow chart on page 37, B and D). This leads to a reduction of 75 % from the inserted DNA while OE-PCR to fulfil HP fragment assembly. Therefore, a third PCR round to enhance the HP fragment, and to gain sufficient amounts of insert suitable for subcloning, is inevitable.

To accomplish the amplification of HP fragments we made another attempt in compliance with a paper which was published in 2009 (39) performing an OE-PCR run by adding three pairs of primers in an asymmetric manner (see flow chart on page 46, A). The concept behind this method is to provide large numbers of fragments (see flow chart, B), amplified by all primers that have been previously utilized to amplify the three fragments in round one of PCR. This accomplishes HP fragment apposition due to assembling of fragments by base pairing of homologous sequences and consequent self-primed strandfilling. The authors suggested merging the second round with the third round of PCR by the use of primers for OE-PCR so that a third round of PCR with end terminal primers was no longer needed. As shown on page 46, end terminal primers were used for asymmetric OE-PCR in a concentration twenty times higher than the non-end terminal primers. On the one hand, this was done to ensure the amplification of HP fragments, as in the third round of PCR, by the use of large numbers of end terminal primers as we did before. On the other hand, it was also done to prevent the non-end terminal primers interfering with the binding of homologous sequences of the HP assembly by competing with the binding sites of the overlapping fragments. During asymmetric OE-PCR, the given primers are able to amplify various fragments, including sense, antisense, sense/spacer, antisense/spacer fragments that are intended to overlap and build up the HP fragments (see flow chart, C).

We tried to perform asymmetric OE-PCR by adding the three fragments from round one PCR and also, following a protocol published in 2010 (40), by adding gDNA from *V. longisporum*, as a template for primers during PCR. Thereby, the given primers in the PCR mixture should be able to amplify the fragments which are intended for assembling the HP fragments.

Primer ratio : 20

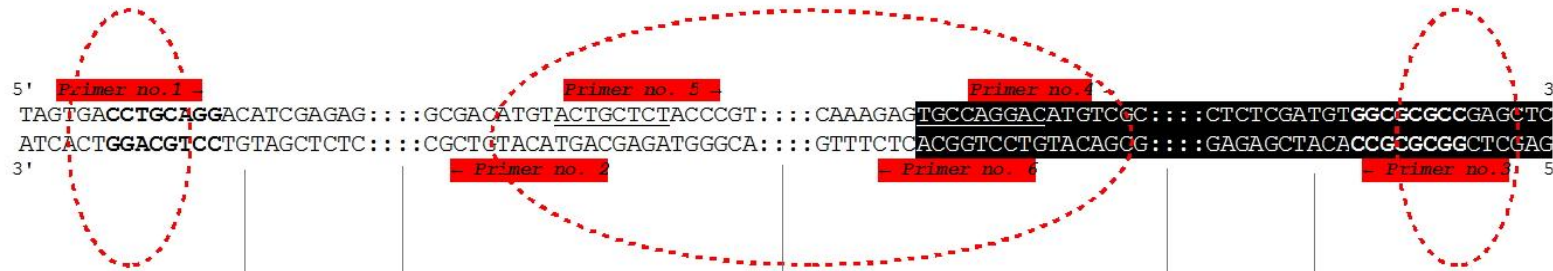
:

1

:

20

A



B



C



Flow-chart of asymmetric OE-PCR for the construction of hairpin-cassettes

Partial sequences are shown; restriction sites are marked in bold; homologous sequences to overlap with the spacer are underlined

A = asymmetric OE-PCR: along with the template for OE-PCR, primers shown in table 1 were used in a molar ratio of 20:1 as displayed to reach HP-fragment amplification

B = asymmetric OE-PCR: several amplified fragments thus can overlap with each other during annealing step of PCR and get filled up by a DNA-polymerase during elongation step

C = asymmetric OE-PCR: large amounts of HP-fragments should be obtained by asymmetric OR-PCR

Amplification of round one PCR fragments was performed according to the protocol given on page 37. For the asymmetric OE-PCR, 1 ng of the first round PCR products was used in equal molar ratio. For the amplification of HP fragments directly from gDNA, 10 ng from the gDNA of *V. longisporum* was used. Asymmetric OE-PCR was done using 25 pmol of end terminal primers and 1.25 pmol from the others in a 50 µl sample. The reaction started at 95 °C for 5 min, followed by 40 cycles of 95 °C for 30 sec., 55 °C for 30 sec. and 72 °C for 2 min. The PCR run finished with one cycle for 5 min at 72 °C. Both PCR samples were examined by electrophoresis on a 1.7 % agarose gel.

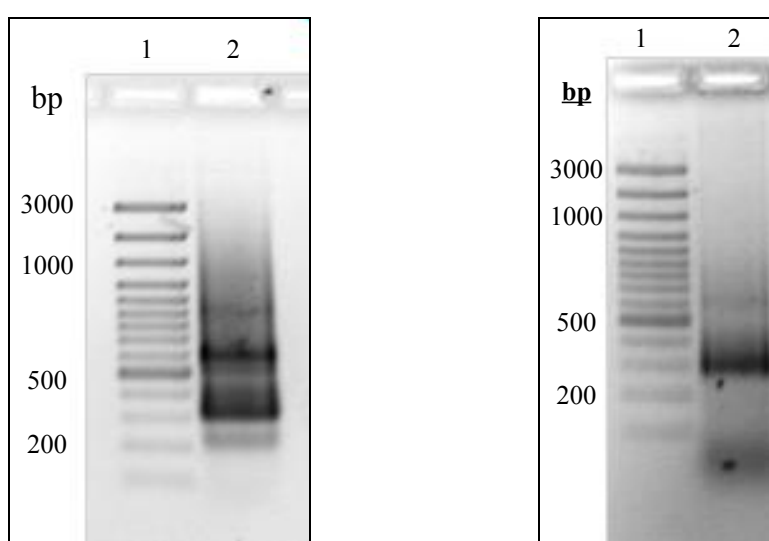


Figure 11-12: Agarose gel electrophoresis of asymmetric OE-PCR using round one PCR products (Figure 12: left side) or gDNA (Figure 13: right side)

1 = GeneRuler™ 100 bp Plus DNA Ladder

2 = PCR sample amplified by using PCR products from round one PCR or gDNA as template for asymmetric OE-PCR

For both samples of asymmetric OE-PCR, the band pattern of the stained agarose gels showed a fragment with the length to be assumed for HP fragments of the candidate gene VI-12.1. We could also observe that a more intense band was visualized which could probably be attributed to the formerly proposed folded HP structure as shown in Figure 7. Due to the larger amount of amplified HP fragments, we purified the distinct band for the calculated length of HP fragment from the agarose gel and used it for subcloning into a cloning vector.

Due to the amplification of HP fragments by a mixture of *Pfu*- and *Taq*-polymerase by OE-PCR, we were able to use the resulting blunt end amplicons directly for ligation into vectors,

which were linearized with restriction enzymes showing blunt end facilities. Linearized pBarn cloning vector was provided with removed phosphate groups of the *EcoRV* restriction sites to avoid recircularization of the vector while ligation. Therefore, we used a T4-polynucleotide kinase to perform 5'-phosphorylation of the insert to ensure proper ligation effectiveness. Besides the ligation into the pBarn cloning vector without any prior restriction of the insert, we also tried to ligate the purified fragment into the MCS of a modified vector base on pBluescript SK⁻ by cutting the vector and the insert by incubating the samples along with 10 U *SdaI* and 5 U *AscI* for 2 h at 37 °C prior to ligation. For both subcloning into pBarn and the modified pBluescript SK⁻, ligation was carried out using a 1:5 molar ratio of vector to insert. Approximately 50 ng of vector DNA was used for subcloning. The ligation was done in a total volume of 20 µl, containing 5 U of T4-DNA ligase and 2 µl of 50 % PEG 4000. Incubation was carried out at 37 °C for 16 h. 10 µl of the mixture was used for transformation of chemically competent *E. coli* cells and then plated on lysogeny broth (LB) agar media containing appropriate antibiotics for selection of positive transformants. Sequencing of transformants was carried out by “Eurofins MWG Operon” (Ebersberg, Germany).

Cloning of putative HP fragments turned out to be very difficult and resulted in a wide variety of non-positive transformants. Sequence analysis of assumed positive plasmids showed a mass of non-specific inserted fragments comprising repetitive sequences resulting from the apposition of parts of the three fragments that were intended to be assembled by OE-PCR. Out of more than 100 tested colonies, we only succeeded in subcloning one HP fragment into a modified pBluescript SK⁻ vector. Therefore, we decided to reject the construction of HP fragments by OE-PCR and establish a method using conventional cloning steps for the design of transformation vectors carrying HP fragments.

Construction of HP fragments using conventional cloning steps

To facilitate generation of HP constructs, several generic vectors with a functional intron have been reported (13, 16). The common approaches, which take advantage of the commercially available pHELLSGATE vector, utilizing Gateway® recombinational cloning (Invitrogen, Karlsruhe, Germany) for high throughput construction of HP vectors, are often too expensive to use in laboratories working in the molecular field. Normally, construction of transformation vectors containing HP fragments, following conventional cloning steps, is carried out in three

cloning steps of the desired stem loop structure, which ensures HP formation by the intracellular expression of the HP cassette.

Here we report our experimental procedure comprising two cloning steps for the construction of pPK2-vector containing HP fragment (pPK2-HP) for the *V. longisporum* candidate gene VI-12.1. An attempt to realize the construction of the HP fragment in one step with a three-parental ligation and the subsequent amplification of the assembly failed due to the formation of HP structure during amplification, as noted in the previous OE-PCR part. Transformation vectors were constructed using standard molecular techniques. Primers for PCR are listed in Table 2. The basis for the ligation with the HP fragment is the binary vector pPK2, which originates from the vector pPZP-201 (41) which was developed for the AMT of plants. Restriction sites for the ligation of fragments were available in the pPK2-vector due to further cloning of a fragment between *oliC* promoter and the *tubA* terminator comprising sequences that can be recognized by restriction enzymes (see Figure 13) suitable for assembly of the HP fragment in two cloning steps.

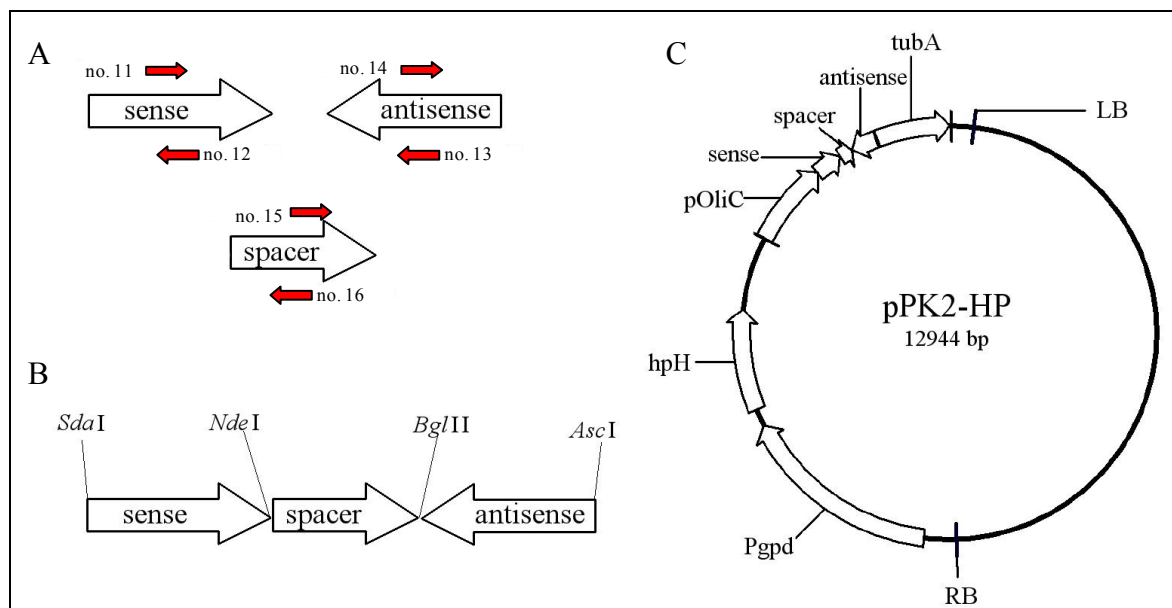


Figure 13: Designed HP fragment for the transformation into binary pPK2 vector

A = single amplicons for the construction of HP fragments are shown. Primers used for amplification by PCR are highlighted in red **B** = Assembled HP fragment showing restriction sites which were intended to be used for ligation of the single amplicons for building up the HP fragment **C** = pPK2-HP vector comprising left (LB) and right boarder (RB) for the AMT and a hygromycin B resistance cassette (hpH) under the control of constitutive promoter from *A. nidulans* (Pgpd) for the selection of transformants; included HP cassette comprises *oliC* promoter from *A. nidulans* and *tubA* terminator from *B. cinerea*

Cloning step one

Prior to the first cloning step, we amplified fragments comprising a 238 bp sequence of the VI-12.1 gene in the sense orientation and a 125 bp sequence covering the native intron from the *V. longisporum* hydrophobin gene *VlHI* by the use of Taq-polymerase. Primers were associated with overhang sequences providing restriction sites for the directional ligation of the fragments to the HP assembly and for the ligation into the binary vector pPK2. A PCR run was carried out following the method noted on page 36 for the amplification of fragments used for the construction of HP fragments by OE-PCR. 500 ng of each purified PCR product was incubated along with 5 U of *NdeI* for 2 h at 37 °C. Fragments were purified from agarose gel and used for ligation in equal molar ratio. The assembly of directionally ligated sense fragments of VI-12.1 associated with the *VlHI* intron spacer was used as a template for PCR to generate sufficient amounts of DNA for cloning into pPK2 vector. Amplification of the sense/intron assembly was done using primers no. 11 and 16 with approximately 1 ng of the DNA as a template. The resulting amplicon was purified and 500 ng were subsequently double-digested along with 1 µg of the pPK2-vector using 5 U of each of the *SdaI* and *BglII* restriction enzymes by incubation for 2 h at 37 °C. After digestion, both insert and vector were purified from agarose gel, and the amount of DNA was estimated by spectral measurement and quantification using a NanoDrop spectrophotometer (Thermo Scientific, Willmington, USA). Ligation of the sense-intron assembly with the linearized pPK2-vector was carried out using a 1:3 molar ratio of vector to insert. After ON incubation of the samples, along with 5 U of T4-DNA ligase, the mixture was directly used for electroporation into *E. coli* strain DH5α. Therefore, we used 1 µl from the 20 µl ligation mixture to mix with 50 µl of electrocompetent cells and electroporated it at 1700 V and 25 mF using the Gene Pulser II System (Biorad, Hercules, USA). Instantly, 800 µl of prewarmed SOC medium (26) was added to the cells and incubated for 1 h at 37 °C in a rotary shaker. Then, 600 and 200 µl of the mixture were spread on agar plates containing 30 mg/ml⁻¹ kanamycin. The plates were incubated ON at 37 °C. Grown *E. coli* colonies were tested by colony PCR. Prior to colony PCR, colonies were picked up using a sterile pipette tip and dissolved in 50 µl of double-distilled H₂O (ddH₂O). The mixture was heated up to 100 °C for 5 min to release plasmid DNA, and 2 µl was used for colony PCR with primers amplifying the sense/intron assembly. Positive tested transformants were grown in 5 ml liquid LB medium containing 30 mg/ml⁻¹

kanamycin. Plasmids were isolated from the grown *E. coli* cells following a protocol for extraction referred to as the “rapid boiling method” (42).

Cloning step two

For the second cloning step, we applied the pPK2-vector comprising the sense/intron assembly (pPK2-SI) constructed by cloning step one. An amplified antisense fragment of the candidate gene was double-digested along with pPK2-SI using 5 U of each of the restriction enzymes *AscI* and *BglII*. All the following steps were accomplished as described for cloning step one.

We had very little difficulty achieving positive transformants carrying pPK2 vector with the assembled HP fragment, probably because of the minor transformation efficiency due to the large pPK2-vector. Therefore, we applied *E. coli* strain DH10 β for electroporation, which is described as being optimized for high efficiency transformation with a guaranteed increased efficiency of the accommodation of large plasmids as compared to DH5 α . The success of *E. coli* transformation with pPK2-HP was tested by colony PCR and restriction analysis of the extracted plasmids by cutting out the HP fragments. All vectors used for further experiments showed the calculated lengths of HP fragments for candidate genes on agarose gels after digestion with restriction enzymes *SdaI* and *AscI*. Furthermore, we were able to induce HP structure formation by heating up the digested samples to 100 °C for 5 min and cooling them down before loading them on an agarose gel for electrophoresis. The emerging gel shift demonstrates the ability of the HP fragment to form HP RNA after intracellular expression in *V. longisporum* (see Figure 14).

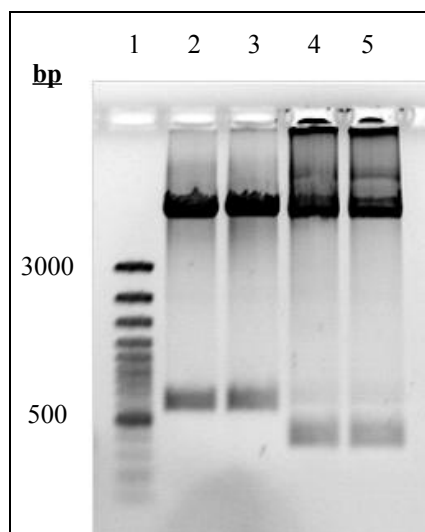


Figure 14: Agarose gel electrophoresis showing insertion of HP fragments into pPK2 by restriction analysis and functionality of HP formation

1 = GeneRuler™ 100 bp Plus DNA Ladder

2 = pPK2-HP for candidate gene VI-12.1 digested with *SdaI* and *AscI*

3 = same as above

4 = pPK2-HP for candidate gene VI-12.1 digested with *SdaI* and *AscI*, heated up to 100 °C before loading

5 = same as above

So far, we have succeeded in constructing several HP constructs cloned in the pPK2-vector for different candidate genes. The pPK2-HP vectors were transformed into *A. thumefaciens* to accomplish AMT of *V. longisporum*. For this we used 1 pg of vector DNA and mixed it along with 50 µl of electrocompetent AGL1 cells, and electroporated them according to the method used for transformation of *E. coli* cells. Deviating from this, the incubation time for the recovery in SOC medium was prolonged to 3 h and the incubation temperature was reduced to 28 °C, which was appropriate for the growth of *A. thumefaciens* strain AGL1. The mixture was spread on agar plates containing 30 mg/ml⁻¹ kanamycin for the selection of pPK2-HP vector and 25 mg/ml⁻¹ carbenicillin and 50 mg/ml⁻¹ rifampicin for the selection of AGL1 carrying Ti-plasmid pTiBo542ΔT. Positive transformants were used for the AMT of *V. longisporum* following the protocol for the transformation of filamentous fungi published by Utermark in 2008 (28). Fungi that grew on the selection media after AMT were tested by PCR with primer for the hygromycin cassette and also by southern hybridization to show if the constructs had been successfully inserted into the genome of *V. longisporum*. Southern

hybridizations show additional signal for the candidate gene on the blot due to the inserted HP fragment (data not shown, see Chapter 3 and 4).

Silencing efficiencies of transformed fungi were assessed by the use of qRT-PCR using cDNA of silencing mutants as a template for primers specific for the candidate genes. Therefore, cDNA was transcribed from extracted RNA which was isolated from fungal cultures grown in liquid SXM (simulating xylem sap) medium (43), which imitates the general nutritional environment existing in the xylem, using Oligo(dT)18 Primer which binds to the poly(A) tail present at the 3'-end of eukaryotic mRNA.

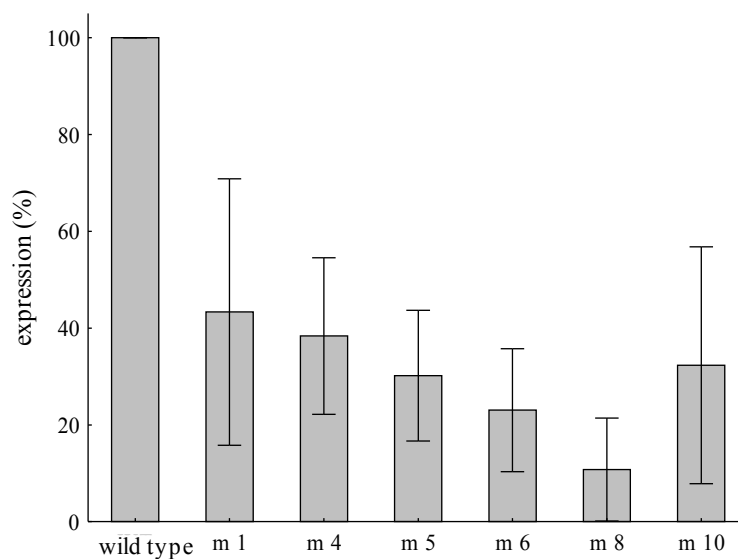


Figure 15: Efficiency of gene silencing triggered by the intracellular expression of a HP cassette for *V. longisporum* candidate gene VI-12.1

For *V. longisporum* mutants carrying HP cassettes for gene-silencing of candidate genes, we could show a reduction in specific gene expression on up to 98 % at best compared to wild type expression (see Chapter 3). Mutants with a silencing efficiency of at least 80 % were used for further characterization of candidates' gene function to evaluate their role in the life cycle of *V. longisporum* (see Chapter 3 and 4).

CONCLUSIONS

Our goal was to establish a method for post-transcriptional silencing by triggering RNAi in *V. longisporum* to decrease the expression of several candidate genes that were found (38) to be putatively involved in the pathogenic life cycle of the phytopathogenic fungus. Different intracellularly-expressed constructs showing the ability to release the production of siRNA have been tested in recent years, working as precursors of RNAi. Plasmid constructs expressing sense, antisense, or hairpin RNAs were reported to be potent triggers for downregulation of corresponding genes. In the plant pathogenic ascomycota fungus *Magnaporthe oryzae*, it was shown that transformants were silenced much more efficiently by HP RNA than by other RNA species (44). Additionally it was shown that the choice of an appropriate spacer, to form the loop of the HP, is of great significance. As reported, spacers are necessary for the stability of the HP structure. However, using a functional intron sequence of the host as spacer for HP fragment constructing, was shown to increase the silencing efficiency from approximately 50 to about 100 % (11). Flanking sense and antisense arms ranging from 98 to 853 bp were reported to be potent triggers for efficient silencing. It was also shown in *M. oryzae* that a silencing vector with a native intron spacer of 147 bp length had a higher silencing efficiency than did those with a longer intron spacer of 850 bp (45). During the research reported in this thesis we designed HP fragments consisting of flanking sense and antisense arms ranging from 180 to 696 bp length and an intervening 125 bp spacer of the native intron from the *V. longisporum* hydrophobin gene *VlHI*. For all generated silencing-mutants of *V. longisporum* candidate genes, we could show a reduction in candidate gene expression of at least 90 %.

In addition to silencing due to HP RNA expression, another method was tested in our lab (46). This relied on the intracellular expression of an antisense RNA (AS-RNA) strand to inhibit gene function on a post-transcriptional level. Constructed AS-RNA-cassettes were designed complementary to the specific mRNA of the candidate gene to inhibit the translation process by expressing an RNA sequence in antisense orientation to the specific target gene. This bound the mRNA of the target gene, forming RNA-RNA-hybrids, thereby causing obstruction of the translation machinery (19). Naturally expressed AS-RNAs were first discovered in 1981 and were reported to control the copy numbers of two *E. coli* plasmids (20, 21). In most cases, AS-RNAs are naturally transcribed by a promoter that is located on the opposite strand

of the DNA molecule coding for the sense mRNA. Therefore, they are completely complementary to the mRNA expressed from the sense strand. To date, AS-RNA has been found to control regulation of gene expression in many other species. In humans, more than 1600 AS-RNAs are known such as the *insulin-like growth factor 2* receptor (22). *V. longisporum* mutants carrying cassettes for the expression of AS-RNAs show a moderate silencing effect on up to 70 % of the corresponding candidate gene.

Our success in achieving HP fragments by the use of OE-PCR was not worth the effort needed to correctly assemble sense and antisense fragments with the spacer. We showed that the assembled HP fragment has a strong tendency to anneal after each denaturation step of the third round of PCR, forming HP structures by pairing of homologous sequences of sense and antisense ssDNA fragments. We made many adjustments to PCR runs to facilitate the amplification of the HP fragments and to suppress the formation of HP structure but could make no improvements. We propose that the amplification of HP fragments during the third round of PCR with end terminal primers may succeed with the use of a larger intervening spacer which would result in spatial separation of the sense and antisense strand and would consequently slow down the formation of the HP structure, allowing the amplification of HP fragments. Pawloski et al. used a 1060 bp β -glucuronidase (GUS) spacer to achieve HP fragments by OE-PCR and still reported “very few difficulties using OE-PCR to assemble RNAi constructs with the desired gene targeting sequence” (34). We decided not to elongate the spacer sequence to achieve better results during amplification of HP fragments, and instead to establish a construction method based on conventional cloning steps to take advantage of higher silencing efficiency due to short spacers.

The use of asymmetric OE-PCR led to one correctly assembled HP fragment out of more than one hundred attempts. We sequenced many putatively positive plasmids showing a signal during analysis of colony PCR with the corresponding *E. coli* cells. As turned out later, all sequenced non-positive fragments showing a variety of unspecific assembled parts of the three fragments that were intended to form the HP fragments. The mass of inserted primers into asymmetric OE-PCR and the resulting amplicons probably lead to a large number of options to assemble to unspecific fragments. Separated samples after asymmetric OE-PCR by agarose gel-electrophoresis show a smeary band pattern, putatively due to the unspecific formation of assemblies. We were able to re-amplify any fragment length which was sliced

out and purified from any position of the smear on the agarose gel, using end terminal primers for the HP fragment. Nevertheless, we used specific HP fragment length, purified from the agarose gel, to perform subcloning into vectors and still succeeded in subcloning for only one sample. It can be assumed that many of the reported problems during construction of HP carrying vectors are due to a hampered DNA replication of plasmids in *E. coli*. It is most likely that a vector which carries an HP fragment has a strong tendency to form the HP structure after winding up of the plasmid DNA to ssDNA during the first step of DNA replication, forming the replication fork by breaking the hydrogen bonds which hold the two DNA strands together. The folded HP structure created during DNA replication would thereby obstruct the replication process by stopping the reading of DNA polymerase. This suggests, and would also explain, our tremendous problems during the second ligation step for conventional cloning of HP fragments. Nevertheless, we established a repeatable method for the conventional cloning of HP vectors by the use of standard molecular techniques.

We could demonstrate in our lab that both the HP RNA and AS-RNA methods are capable of inducing gene silencing in the ascomycota fungus *V. longisporum*. As mentioned in the literature, we could prove that HP RNA triggers RNAi more efficiently as compared to AS-RNA-effected silencing, with a moderate reduction in the expression level of candidate genes. Therefore, we achieved an effective and reliable tool for the characterization of putative pathogenic-related genes of *V. longisporum*.

ACKNOWLEDGMENTS

The author would like to thank the following people for their outstanding assistance with this chapter:

Prof. Petr Karlovsky for his continuous assistance with scientific problems. **Dr. Arne Weiberg** for the remarkable help with work on construction of HP cassettes. **Haiquan Xu** for the construction of *V. longisporum* AS cassettes.

REFERENCES

1. **Crick F.** (1958). On Protein Synthesis. Symp. Soc. Exp. Biol. XII, PMID 13580867.
2. **Terman DS., Ogden D., Petty D.** (1976). Removal of Circulating Antigen and Immune Complexes with Immunoreactive Collodion Membranes, FEBS Letters, vol. 68, No. 1, pp. 89-94.
3. **Capecchi M.** (1989). Altering the genome by homologous recombination, Science, Vol. 244, no. 4910, pp. 1288-1292.
4. **Barbara D.J., Clewes E.** (2003). Plant pathogenic *Verticillium* species: how many of them are there? Mol. Plant Pathol. 4:297-305.
5. **Fahleson J., Lagercrantz U., Hu Q., Steventon L.A., Dixelius C.** (2003). Estimation of genetic variation among *Verticillium* isolates using AFLP analysis. Eur. J. Plant Pathol. 109:361-371.
6. **Fire A, Xu S, Montgomery MK, Kostas SA, Driver SE, Mello CC.** (1998). Potent and specific genetic interference by double-stranded RNA in *Caenorhabditis elegans*. Nature. 1998 Feb 19;391(6669):806-11.
7. **Ratcliff FG, MacFarlane SA, Baulcombe DC.** (1999). Gene silencing without DNA. RNA-mediated cross-protection between viruses Plant Cell 11(7): 1207-16.
8. **Hammond SM, Bernstein E, Beach D, Hannon GJ.** (2000). An RNA-directed nuclease mediates post-transcriptional gene silencing in *Drosophila* cells. Nature. 2000 Mar 16;404 (6775): 293-6.
9. **Hamilton A.J., Baulcombe D.C.** (1999). A species of small antisense RNA in post-transcriptional gene silencing in plants. Science. 286, Nr. 5441 pg. 950–952.
10. **Smith NA, Singh SP, Wang MB, Stoutjesdijk PA, Green AG, Waterhouse PM.** (2000). Total silencing by intron-spliced hairpin RNAs. Nature. 407(6802): 319-20.
11. **Wesley SV, Helliwell CA, Smith NA, Wang MB, Rouse DT, Liu Q, Gooding PS, Singh SP, Abbott D, Stoutjesdijk PA, Robinson SP, Gleave AP, Green AG, Waterhouse PM.** (2001). Construct design for efficient, effective and high-throughput gene silencing in plants. Plant J. Sep;27(6):581-90.
12. **Andrew Eamens, Ming-Bo Wang, Neil A. Smith and Peter M. Waterhouse** (2001). RNA Silencing in Plants: Yesterday, Today, and Tomorrow.

13. **Wang, M.B. and P.M. Waterhouse** (2001). Application of gene silencing in plants. *Curr. Opin. Plant Biol.* 5:146-150.
14. **Miki, D., R. Itoh, and K. Shimamoto** (2005). RNA silencing of single and multiple members in a gene family of rice. *Plant Physiol.* 138:1903-1913.
15. **Liu, Q., S.P. Singh, and A.G. Green** (2002). High-stearic and high-oleic cottonseed oils produced by hairpin RNA-mediated posttranscriptional gene silencing. *Plant Physiol.* 129:1732-1743.
16. **Cejka D, Losert D, Wacheck V.** (2006). Short interfering RNA (siRNA): tool or therapeutic? *Clinical Sciences (London)*. 2006 Jan;110 (1): 47-58.
17. **Singh S.** (2008). Study of genes of the phytopathogenic fungus *Verticillium longisporum* involved in the colonization of xylem vessels of its host *Brassica napus*, Dissertation, Georg-August Universität Göttingen.
18. **Higuchi R, Krummel B, Saiki R** (1988). A general method of *in vitro* preparation and specific mutagenesis of DNA fragments: study of protein and DNA interactions. *Nucleic Acids Res* 16 (15): 7351–67.
19. **Weiss, B., Davidkova, G., and Zhou, L-W.** (1999). Antisense RNA gene therapy for studying and modulating biological processes. *Cell. Mol. Life Sci.* , 55: 334-358.
20. **Tomizawa, J., Itoh, T., Selzer, G., Som, T.** (1981). Inhibition of ColE1 RNA primer formation by a plasmid-specified small RNA. *Proc. Natl. Acad. Sci. U.S.A.* 78: 1421-1425.
21. **Stougaard, P., Molin, S. & Nordström, K.** (1981). RNAs involved in copy-number control and incompatibility of plasmid R1. *Proc. Natl. Acad. Sci. U.S.A.* 78: 6008-6012.
22. **Oshima A, Nolan CM, Kyle JW, Grubb JH, Sly WS** (1988). The human cation-independent mannose 6-phosphate receptor. Cloning and sequence of the full-length cDNA and expression of functional receptor in COS cells. *J. Biol. Chem.* 263 (5): 2553–62.
23. **Koopmann B. and Karlovsky P.** (2001) unpublished.
24. **Yazynin S.A., Deyev S.M., Jucovic M., Hartley R.W.** (1996). A plasmid vector with positive selection and directional cloning based on a conditionally lethal gene. *Gene*, Volume 169, Number 1, 22 February 1996, pp. 131-132.

25. **Kalendar R, Lee D, Schulman AH.** (2009). FastPCR Software for PCR Primer and Probe Design and Repeat Search. *Genes, Genomes and Genomics*, 3(1): 1-14.
26. **Sambrook J., Russell DW.** (1989). *Molecular Cloning: A Laboratory Manual* 2nd Edition, Trade paperback, Cold Spring Harbor Laboratory Press.
27. **Maniatis T., Fritsch EF., Sambrook J.** (1982). *Molecular Cloning: A Laboratory Manual*. Trade paperback, Cold Spring Harbor Laboratory Press.
28. **Utermark J.** (2008). Genetic transformation of filamentous fungi by *Agrobacterium tumefaciens*. *Nature Protocols*, Published online.
29. **Yamamoto I., Numao M., Sakaguchi Y., Tsushima N., Tanaka M.** (2007). Molecular characterization of sequence and expression of chicken GPR39. *General and Comparative Endocrinology* 151:128-134.
30. **Pfaffl, M.W., Horgan, G.W., Dempfle, L.** (2002). Relative expression software tool (REST) for group-wise comparison and statistical analysis of relative expression results in real-time PCR. *NAR* 30, e36.
31. **Baulcombe D.** (2004). RNA silencing in plants. *Nature*, 2004 Sep 16;431 (7006): 356-63.
32. **Wesley, S.V., C.A. Helliwell, Smith NA., Wang M., Rouse DT., Liu Q., Gooding PS., Singh SP., et al.** (2001). Construct design for efficient, effective and high-throughput gene silencing in plants. *Plant J.* 27:581-590.
33. **Miki D, Shimamoto K.** (2004). Simple RNAi vectors for stable and transient suppression of gene function in rice. *Plant Cell Physiol.*; 45(4): 490-5.
34. **Pawloski LC, Deal RB, McKinney EC, Burgos-Rivera B, Meagher RB** (2005). Inverted repeat PCR for the rapid assembly of constructs to induce RNA interference. *Plant Cell Physiol.*; 46(11): 1872-8.
35. **Frey & Suppmann** (1995). *Biochemica* 2, 34-35.
36. **Lawyer FC, Stoffel S, Saiki RK, et al.** (1993). High-level expression, purification, and enzymatic characterization of full-length *Thermus aquaticus* DNA polymerase and a truncated form deficient in 5' to 3' exonuclease activity. *PCR Methods Appl.* 2, Nr. 4, Mai 1993, pg. 275–87.
37. **Lundberg KS, Shoemaker DD, Adams MW, Short JM, Sorge JA, Mathur EJ.** (1991). A High Fidelity Thermostable DNA Polymerase Isolated from *Pyrococcus furiosus*. *Gene*, 12, 108(1): 1-6 .

38. **Weiberg, A.** (2008). Identifizierung von Xylemsaft-induzierten Genen im vaskulären Pathogen *Verticillium longisporum* mittels einer verbesserten cDNA-AFLP Methode für transkriptomweite Expressionsstudien. Dissertation, Georg-August Universität Göttingen.
39. **Yan P, Wang S, Shen W, Gao X, Wu J, Zhou P.** (2010). Simple construction of chimeric hairpin RNA for virus resistance in plants. *J Virol Methods*. 166(1-2): 101-5.
40. **Xiao YH, Yin MH, Hou L, Pei Y.** (2006). Direct amplification of intron-containing hairpin RNA construct from genomic DNA. *Biotechniques*, 41(5): 548, 550, 552.
41. **Hajdukiewicz P., Svab Z., and Maliga P.** (1994). The small, versatile pPZP family of *Agrobacterium* binary vectors for plant transformation. *Plant Molecular Biology*, 25(6):989994.
42. **Riggs MG. and McLachlan A.** (1986). A simple screening procedure for large numbers of plasmid mini-preparations. *Biotechniques*, 4(4):310313.
43. **Neumann M.J., Dobinson K.F.** (2003). Sequence tag analysis of gene expression during pathogenic growth and microsclerotia development in the vascular wilt pathogen *Verticillium dahliae*. *Fung. Genet. Biol.* 38:54-62.
44. **Kadotani N., Nakayashiki H., Tosa Y., Mayama S.** (2003). RNA silencing in the phytopathogenic fungus *Magnaporthe oryzae*. *Mol Plant Microbe Interact.* 2003 Sep;16(9):769-76.
45. **Nakayashiki H., Hanada S., Nguyen BQ., Kadotani N., Tosa Y, Mayama S.** (2005). RNA silencing as a tool for exploring gene function in ascomycete fungi. *Fungal Genet Biol.* 2005 Apr;42(4):275-83.
46. **Xu H.** (2011). Dissertation, Georg-August University of Goettingen.

APPENDIX

VI-12.1

gDNA sequence

```

1  ATGTGCGTGCCAGAACCCTCGCCGCGAGGTCCCCTGTGACCCGCGTCGGCGA
51  CGCTTCCAGCAATGGCCTCACCAGCCTTAAGACCAACATGACCCCTGCGCA
101 AGGGGGCCACCTTCCACTCGCCACCTCTCTCGACTCTTCATCCATCGAC
151 GCCTTCATCCCCCAGCTCTTGGTGTATCTCAGACCAATCTTGAAGACG
201 TGTCGGCGCTCACGTCCGCCGCATGGAGATGATCGTCAGCGGCATCGAGA
251 CATCACTCAATCTGAATGATACCCCAAGGCCGGCCTCCAAGCCTTCGCGT
301 GACGAGTGCCCTGCCCGCACAAACGGCTTCCTCGGCCGCCCTACTGTGCA
351 CCCCGCCATGGCAAAAGACACCAAGACCAGCGGGGAGCGCCGCGTTTTGC
401 GCCAAGACATCGTCGCTCATCGGAGCAGCAGCTTCGGACAGCGGTCTC
451 GGCACCTCTCTGGCCTCTTCCGTCGAGAAGCAAGCCCCAGCATCACCTC
501 CAAGACCAGCAAGGCATCCGCCATTACACGCTCTGCCGCGCTCCTTCCA
551 ACACCATGACCAAGGTCTCTGGCCTGAGCTCCAAGGCGGTGAGCCGTGTT
601 CACGAACACGTTCTTCGCCCCCTTCGTGCCAAGCCTGAGTTGAAGGACTT
651 CGAGCCCATCGTCTGGACATTCCCAGGCGAATCCGTGACAAGGAAATCA
701 TCTGCCCTCAGGGATCTTGAGAAGACTTTGATCTTCATGGCACCGGTAAGT
751 CAACTCTTGTATCAACGCAGCGTTTTGGGGAGATACTTATCGGTGTTGAT
801 GAAGGAGAGGGCCAAGACCGCCGCTTGTACCTCGATTTCTGCCTGACGT
851 CCATTCGATGCATTCGAAGCCACCGTCGAATACCTCAGCGACCGCAACAA
901 ATTAGACCGGCCGACCGACCATAACACTAACGGATACTTCATTGATCTCGT
951 CGAACAGATTGCCAATACGCCGACAAC'TGGCCACTGCCAAGGAAGCCG
1001 GAGTCGAGGGGCGTGAGATGGACGTCGACCCACCGACGAGGTTAAGCTG
1051 TTCGGTGGCATCTCGCAGAACGGCCGCCCGCCGAGCTTGTCCGCGTCAG
1101 AAAGGACGGTCAAGCCATCTCCATGGCCACTGGCCTCCCCGTTGACATGG
1151 ATGAGGACGGCAAGGATTTCCCCAGACTGAAGCGCTCCCTGAGCCAGCAG
1201 CTGGCAGACGACGAGGAGATCATGCGGTCCATGGCTCGCAGGAAGAAGAA
1251 CGCTGCGCCGGAGGAGCTCGCGCCCAAGAAATGCCGCGAGCCTGGCTGCA
1301 ACAAGGAGTTCAAGCGTCCCTGTGACCTGACCAAGCAGAGAAGACTCAC
1351 TCTCGTCCCTGGAAGTGCCCTGTCAAGACGTGCAAGTACCACGAGTACGG
1401 CTGGCCCACCGAGAAGGGGATGGACCGCCATCACAACGACAAGCACTCCT
1451 CAGCGCCCCCATGCACGAGTGCC'TGTTTAAGCCTTGCCCTTACAAGTCG
1501 AAGCGCGAGTCAAGCTGCAAGCAGCACATGGAGAAGGCCACGGATGGCA
1551 GTACGTCCGCACCAAGACCAACGGCGGCAAGAAGGCGCCAGCGTTGCTG
1601 GAAGCTCGGCACAGCCGACCCCTCAGCTTGGCAACATGGCAACGCCCTCG
1651 AGCAGCCACAGTATTGCTACGCCGCCGAGGAGAGCACCAGCCTCTTCCC
1701 GCCTTTTAACCACGATGACTTCCCTACTACGTCCCGGCCGAGGAGTTTG
1751 CTGACACCTGCCTCGGGCCCATGGGACAGCCGCCATGACGCTCGAGGGT
1801 ATCGACTTTAACGACCTTGGCGTGTCTCCCACTGATTACAACACCCCTTC
1851 TACCGACACATCCTACCCATACACCTCTTACCAGGATGGACCCGAGTTTG
1901 TCATCAACAACGATGACATTTACGGCGCCCGTGTCCAGATCCCGACACCG
1951 GCGTGGCCCGAAAAGATGATGGCTGGCATGCAGAACTACGCCCCAGTGTC
2001 TGCATGCCAACCTCAGATGATGCCCGAGCCGCTCGCCCCACACATCTCCC
2051 CGATAGGTCAGGGGAACGCCATGCTCTTACGCCCAACTCGTTGGCCGAG
2101 GTTGACGAAGGCTTTGATGATTTTCGGCGGCTGTGGTGATGATTTACCTT
2151 GTTCCCGTCAACGGGCTCGACAAGGACGCACAATTCAGACTCTGTTTCG
2201 GCAGCGAGATGCCAGCAGCGCCTCGGCTTGTCTCAGGGCGCCTCCCAG
2251 GACTTCTTTGGGAACGGCATGGACTGGTCCAGCATGGAATACCACACCTA
2301 CTCCAGCAGCCCCAGCACCAGCAGTAG

```

amino acid sequence	
1	MSCQNPRRRSPVTRVGDASSNGLTSLKTNMTLRKGATFHSPTSLDSSSID
51	AFIPPALGRISDQSRVGAHVRRMEMIVSGIETSLNLNDTPRPASKPSRD
101	ECLPRTNGFLGRPTVDPAMAKDTKTSGERVLRPRHRSSEQHASDGLG
151	TSLASSVEKQAPSITSKTSKASAITRSAAAPSNMTMKVSGLSKAVSRVH
201	EHVLRPLRAKPELKDFEPIVLDIPRRIRDKEIICLRDLEKTLIFMAPERA
251	KTAALYLDFCLTSIRCIQATVEYLSDREQIRPADRPYTNGYFIDLVEQIR
301	QYAGQLATAKEAGVEGREMDVDPTDEVKLFGGISQNGRPAELVRVRKDGQ
351	AISMATGLPVDMEDEGKDFPRLKRSLSQQLADDEEIMRSMARRKKNAAPE
401	ELAPKKCREPGCNKEFKRPCDLTKHEKTHSRPWKCPVKTCKYHEYGWPT
451	KGMDRHHNDKHSSAPPMECLFKPCPYKSKRESSCKQHMEKAHGQYVRT
501	KTNGGKKAPSVAGSSAQPTPQLGNMATPSSSHSIATPPEESTSLFPPFNH
551	DDFPHYVPAEEFADTCLGPMGQPPMTLEGIDFNDLGVSPDYNTPTDTS
601	YPYTSYQDGPEFVINDDIYGARVQIPTPAWPEKMMAGMQNYAPVSACQP
651	QMMPEPLAPHISPIGQGNAMLF'PNLSLAEVDEGFDDFGGCGDDFTLFPVN
701	GLDKDAQFQTLFGSEMPSSGLGLSQGASQDFFGNGMDWSSMEYHTYSQQP
751	QHQQ

Table 5: gDNA and amino acid sequence of candidate gene VI-12.1

Chapter 3: Characterization of NEP like proteins of *Verticillium longisporum* according to their relevance for pathogenicity in *Brassica napus*

Malte Beinhoff, Arne Weiberg, Mona Quambusch, Haidi Yin*, Ruth Pilot, Haiquan Xu, Christian Loeffke, Richard Splivallo and Petr Karlovsky

Molecular Plant Pathology and Mycotoxin Research Unit, Department for Crop Sciences, Georg-August University of Goettingen, Grisebachstrasse 6, 37077 Goettingen, Germany.

*College of Life Sciences, Peking University, Beijing, China

ABSTRACT

Verticillium longisporum is a soil-borne fungal pathogen showing major yield losses on the rapeseed plant *Brassica napus* in the northern hemisphere. Because of the variety of investigations on the pathosystem of several *Verticillium* spp. to their host plants, the species is on the way to becoming a model system for studying diseases caused by plant pathogenic fungi. Little is known about phytotoxic metabolites of *V. longisporum* which allow the successful host colonization by the induction of plant cell death during the saprophytic phase of the hemi-biotroph fungus to metabolise nutrients released by dead plant tissue. Recently a family of small phytotoxic peptides have been described, referred to as necrosis and ethylene-inducing peptides (NEPs). These have been shown to trigger cell death and the activation of defense signaling reactions in dicotyledonous plants. NEPs are dominantly present in plant pathogenic species with a hemibiotrophic or a necrotrophic life cycle. In this study, five different NEP orthologs from *V. dahliae* were identified in the genome of *V. longisporum* (VI-NEP-1 to 5). Three of them were proved to be strongly upregulated in *V. longisporum*-infected host plant *B. napus* as compared to the expression measured *in vitro*. We functionally analysed the impact of VI-NEP-1 in the pathogenic life-cycle of the fungus. Our findings strongly suggest that VI-NEP-1 is a true virulence factor of *V. longisporum* during infection of *B. napus*.

INTRODUCTION

Plant-pathogenic microbes release a large variety of chemical compounds facilitating their infection of host plants. Some of these compounds are elicitors, whose presence is perceptible by plant cell wall receptor molecules as the first step in pathogen recognition, followed by the activation of innate plant immunity (1). Beside elicitors, disease symptoms can also be caused by cytotoxic compounds (phytotoxins) produced by the pathogen. These can damage and kill plant cells without any activation of programmed cell death (2, 3).

In 1995, Bailey et al. first described a protein purified from culture filtrates of *Fusarium oxysporum* f.sp. *erythroxyli* (4) which is capable of triggering ethylene production and necrosis in numerous dicotyledonous plants and is therefore known as a necrosis and ethylene-inducing protein 1 (NEP-1). This is the first representative of what is currently known to be the large family of NEP-like proteins (NLPs). The predominant presence of NLPs in oomycete, fungal and bacterial species (5), especially for plant pathogenic organisms that have a hemibiotrophic or necrotrophic lifestyle, and the absence in higher eukaryotes including plants and animals, suggests that these proteins are a common feature of microbial organisms and are thus likely to play a role in plant-pathogen interactions (6). The group of NLPs includes small (25-35 kDa), secreted peptides that have the ability to trigger plant responses on host plants (15, 16). In contrast to other known elicitors or phytotoxins, NLPs are taxonomically widespread (16, 17) and are found both in gram-positive and gram-negative bacteria (18) as well in oomycetes (15, 19, 20), ascomycetes (4, 21, 22, 23, 24) and basidiomycetes (25). In spite of the taxonomical prevalence of NLPs, it was shown that functional orthologs, demonstrated by an oomycete NLP, expressed in a NLP-deficient *Pectobacterium carotovorum* mutant, complement partial restoration of virulence (17), suggesting that NLPs of eukaryotic and prokaryotic origins are orthologous proteins. All NLPs share a highly conserved stretch called the necrosis-inducing *Phytophthora* protein 1 (NPP1) domain. This domain comprises the amino acids GHRHDWE (16, 17) in the centre of the peptide and shows no significant similarity to any currently known protein sequence and so provides no reference to NLP function. The conserved domain is supposed to interact with two or four cysteine residues upstream to the domain to execute membrane-disintegrative activity (17, 26, 27). Furthermore, it was shown, that the ability of a NLP from *Phytophthora parasitica* to trigger phytoalexin production and necrotic lesion formation in tobacco leaves

was impaired by site-directed mutagenesis of two conserved cysteine residues to serine. Using the conserved cysteines, NLPs were classified into subgroups comprising Group I, which exhibits two cysteines upstream from the conserved domain, and Group II, which harbours four cysteines (28).

The functionality of NLPs is a controversial issue in that there is still discussion about whether to classify the peptides as functional elicitors (29) or as phytotoxins (5). The elucidation of the crystal structure of a NLP from the phytopathogenic oomycete *Pythium aphanidermatum* shows great similarity to cytolytic toxins produced by marine organisms (30). This report is strengthened by the results of former studies showing cytolytic effects on plants triggered by NLPs expressed by ten different phytopathogenic organisms (5, 28). Immunolocalization results show that NLPs are mainly localized in the plant cell wall and in the cytosol on cellular level (23). Additionally it was shown, that NLP-induced necrosis requires interaction with a target site that is unique to the extracytoplasmic side of dicotyledonous plant plasma membranes. A GFP-fused NLP was found to be associated with the phospholipid bilayers of plasma membrane and the nuclear envelop (26). Additionally, Qutob et al. (5) demonstrated that NLPs have an affinity for lipid bilayers, and their phytotoxic activity and specificity for dicots do not require the presence of a cell wall.

Plant-responses triggered by NLPs are strictly limited to dicotyledonous plants; all monocotyledonous plants or other organisms tested so far are insensitive to NLP exposure (4, 24, 26). Sensitive plants respond with a large variety of modes of action due to NLP exposure such as: up-regulation of defence-related genes (6, 31), transcriptome profiling indicating large-scale reprogramming of plant gene expression (5, 22, 23), the de-novo synthesis of phytoalexins (6, 19) and phenolic compounds (15), production of ethylene (6, 21), initiation of an oxidative burst by nitric oxide and reactive oxygen species (ROS) (5, 18, 30), induction of apoptosis (20, 31), Ca²⁺ influx (6) and callose deposition into plant cell walls (32). All these effects on plants act in a dose-dependent manner (6, 15). NLPs might play dual roles in plant-pathogen interactions as toxin-like virulence factors and as triggers of innate plant immune responses (5). This is supported by the findings that NLP-induced apoptosis was not stopped by specific inhibitors (25). Whether NLPs can act as true virulence factors remains doubtful. Pathogenicity assays with NLP-disfunctional mutants showed no arrest in pathogen spread and limit infection, which was tested in *F. oxysporum* in cocoa (33) and *Erwinia*

carotovora ssp. *carotovora* in different solanaceous plants (16, 18). Although the presence of NLPs has been deeply investigated in the oomycete genera *Phytophthora*, *Pythium* and in the ascomycetes *Fusarium oxysporum* and *Botrytis* spp., nothing is known about the presence and putative contribution of NLPs regarding the pathogenic life cycle of *V. longisporum*. The first representative of an NLP for the genus *Verticillium* was reported by Wang in 2004. He found an NLP in *V. dahliae*, named Vd-NEP, which triggers typical wilting in leaves of the natural host plant, cotton (31).

The soil-borne fungi *Verticillium longisporum*, in contrast to other plant pathogenic *Verticillium* spp. has a limited host range and infects only *Brassica* and other cruciferous plants (7). The pathogenic life cycle of *V. longisporum* starts with the penetration of the host plant via the roots, and proceeds with the colonization of the vascular system (8). During this first stage of infestation, the fungus stays biotrophic and strictly remains in the vessel system of the plant. In a later stage of infection the pathogen changes its life style into that of a necrotrophic-living organism. In this saprophytic stage, the fungus metabolises nutrients released by dead plant tissue. In contrast to other plant-pathogenic *Verticillium* spp., *V. longisporum* is not indicated by wilting of host-plants (9, 10, 11, 12), which is usually a typical feature of the disease, and is known as *Verticillium*-wilt. In addition to this distinctive feature, *V. longisporum* also causes stunting, chlorosis and anthocyanin accumulation, which affects the flowering time and triggers early onset of senescence on host plants (13, 14). In this study we identified five NLP genes from *V. longisporum*, designated as VI-NEP-1 to 5, by molecular techniques.

MATERIALS AND METHODS

Fungal and bacterial strains

V. longisporum VL43 strain was provided by the Department of Crop Sciences, Section Plant Pathology and Crop Protection, (University of Goettingen, Goettingen, Germany) and was used for all experiments in this chapter. The isolate originated from oilseed rape plants

collected in Northern Germany (34). The optimal growth temperature is between 20 and 23 °C and this was therefore used for all experiments using *V. longisporum*.

Agrobacterium tumefaciens strain AGL1 was provided by Dr. Susanne Frick (Leibniz Institute of Plant Biochemistry, Martin-Luther University Halle-Wittenberg, Halle/Saale, Germany) and was used for the transformation of *V. longisporum*.

Protease-deficient *Escherichia coli* strain BL21 (New England Biolabs, Ipswich, United Kingdom) was used for overexpression of VI-NEP-1 protein.

Chemically competent *E. coli* strain DH5 α and electrocompetent DH10 β strains (New England Biolabs, Ipswich, United Kingdom) were used for cloning purposes.

Preparation of spore suspensions

One hundred μ l of a spore solution containing 1×10^6 spores was spread on a potato-dextrose agar (PDA) plate and incubated at 23 °C for 10 days in the dark. The plate was subsequently flooded with 15 % glycerine suspension and the spores were released from the conidiophores by scratching the mycelium with a spatula. The suspension was filtered through a sterile gauze and the spore concentration was estimated using a Thoma hemacytometer with a depth of 0.1 mm (Roth GmbH, Karlsruhe, Germany). The spore suspension was diluted to 1×10^7 spores per ml⁻¹ with a 15 % glycerine solution.

Plant material

The seed material of ‘rapid cycle rape’ (*Brassica napus* var. *napus*, Genom A/Caacc) (35) was provided by the Department of Crop Sciences, Section Plant Pathology and Crop Protection, (University of Goettingen, Goettingen, Germany).

Seeds of *Arabidopsis thaliana* ecotypes Burren (Bur) (36), Columbia (Col-0) (37) and *Landsberg erecta* (Ler) (38) were provided by Prof. Volker Lipka (Department of Plant Cell Biology, Georg-August University of Goettingen, Goettingen, Germany).

Seed material of *Nicotiana tabacum* was provided by the Department of Crop Sciences, Section Plant Pathology and Crop Protection, (University of Goettingen, Goettingen, Germany).

Plasmids

For *A. thumefaciens*-mediated transformation (AMT) of *V. longisporum*, we used the binary vector pPK2 (12) including border sequences for the AMT, and a hygromycin B resistance cassette containing the hygromycin phosphotransferase gene from *E. coli* (hph) for selection of positive transformants.

The plasmid pET21a (MERCK, San Diego, CA, USA) was used for overexpression of VI-NEP-1 protein in *E. coli* strain BL21.

The plasmid pUC57 (Fermentas, St. Leon-Rot, Germany) was used for the construction of a *V. longisporum* genomic library.

Enzymes

For the construction of pPK2 vector containing hairpin (HP)-cassettes, suitable for triggering post-transcriptional gene silencing by RNA interference (RNAi), we used restriction enzymes, ‘T4-DNA Ligase’ and affiliated buffers purchased from Fermentas Inc. (Fermentas, St. Leon-Rot, Germany).

Enzymes and reagents for first strand cDNA synthesis, including ‘Oligo(dT)18 Primer’, ‘RiboLock™ RNase Inhibitor’ and ‘M-MuLV Reverse Transcriptase’ were purchased from Fermentas.

‘Biotaq™ DNA Polymerase’ (Bioline, Luckenwalde, Germany) was used for general amplification of fragments by polymerase chain reaction (PCR) and quantitative real time PCR (qPCR) to assess the amount of fungal DNA in plant tissue

The ‘ABsolute Blue QPCR Fluorescin Mix’ (Fisher Scientific GmbH, Schwerte, Germany) was used for qRT-PCR to assess the silencing efficiency of *V. longisporum* mutants.

The ‘HotStart-IT SYBR Green One-Step qRT-PCR Master Mix Kit’ (Affymetrix UK Ltd., High Wycombe, UK) was used for one-step qRT-PCR for the analysis of the expression of pathogenesis-related genes in *B. napus*.

Genomic library of *V. longisporum*

For the construction of a *V. longisporum* genomic library, 20 µg of isolated gDNA was partially digested with 0.4 U *Bst*143I for 30 minutes. Digested DNA was electrophoretically separated on a 0.6 % agarose gel at 0.5 V/cm overnight. DNA fragments of 8-14 kb were excised and purified from the agarose gel using ‘QIAquick Gel Extraction Kit’ (Qiagen, Hilden, Germany) and ligated into pUC57 vector. For library construction, cloned fragments were transformed into electrocompetent *E. coli* DH5α cells. The library contained a total number of 9600 single clones placed in 100 microtiter plates with a 96 well format. About 50 % of the clones were determined by electrophoresis to contain circularized plasmid without any insert. For the screening of clones comprising full gene sequences (and flanked regions) a stepwise strategy of, in total, 40 PCRs with gene-specific primers was chosen to pinpoint single clones carrying an insert that contained the sought gene sequence. In a first PCR round, pooled clones of ten microtiter plates were used per PCR reaction and subsequently analysed by electrophoresis on a 1.7 % agarose gel. Positive clone pools, which showed a gene-specific PCR product, were used for another round of 10 PCRs, in which pooled clones of single microtiter plates were analysed. A third PCR round of 20 PCRs was performed to dissect the positive tested microtiter plate by analysing pooled clones of each row and each line of the microtiter plate. This resulted in a single positive tested row and a single positive tested line, and the crossing point localized the position of the positive single clone used to sequence the insert.

VI-NEP-1 gene silencing

Construction of pPK2-HP vector, containing a VI-NEP-1 specific HP-cassette, was performed as described in Chapter 2 (Construction of HP-fragments using conventional cloning steps, from page 48). The procedure comprised two cloning steps for the construction of pPK2-HP for the *V. longisporum* candidate gene VI-NEP-1. Fragments for the construction were PCR amplified using primers (see Table 10 in the Appendix) for sense- and antisense-sequences of

the VI-NEP-1 gene and intron-fragments comprising the sequence of a native intron from the *V. longisporum* hydrophobin gene *VlHI*, homologous to *VdHI* from *V. dahliae* (GenBank Accession No. DQ026260.1). All amplicons were associated with suitable restriction sites for directional cloning.

Transformation of *V. longisporum*

Agrobacterium tumefaciens-mediated transformation (AMT) of *V. longisporum* was performed as described in Chapter 2 (see page 31) using a protocol published by Utermark (39).

Southern hybridization

To analyse the number of VI-NEP-1 gene-copies present in the genome of wild type *V. longisporum* and to determine the number of copies in the transformed mutants compared to the wild type, southern hybridization was performed as described in Chapter 2 (see page 30).

Plant pathogenicity assay using VI-NEP-1 silencing mutants

Seeds of ‘rapid cycle rape’ were surface sterilized in 70 % ethanol for 15 sec and rinsed three times in sterile tap water before sowing in sterile silica sand. The silica substrate was carefully rinsed from the rape plants seven days after sowing. The cleaned roots were dip inoculated for 45 min in a spore suspension (1×10^6 spores ml^{-1}) of *V. longisporum* wild type and VI-NEP-1 knock-down mutants. In all experiments, 60 plants were either water inoculated (mock) or inoculated with *V. longisporum* wild type or VI-NEP-1 silencing mutants. Subsequently, plants were transferred into an autoclaved earth/sand mixture (1/1 v/v) and raised under constant conditions in a climatic chamber with a day/night length of 16/8 h, 23° C at daylight and 20° C at night conditions. After 14, 21 and 28 dpi, plant symptoms were evaluated by measuring the plant shoot lengths and by the assessment of a disease score according to Zeise et al. (40). Plants were harvested at different time points depending on the corresponding experiment for measurement of parameters and for extraction of total RNA, gDNA or phytohormones.

Extraction of gDNA and total RNA

Total RNA for qRT-PCR and gDNA for PCR, qPCR, southern hybridization or for the construction of a *V. longisporum* genomic library were extracted from fungal mycelium or plants as described in Chapter 2 (see page 30) using a modified protocol of Maniatis et al. (41).

qRT-PCR

Total RNA from fungal mycelium was used for gene expression analysis. Polyadenylated RNA (mRNA) was purified from total RNA extractions using Oligotex[®] mRNA Mini kit (Qiagen, Hilden, Germany) for analysing fungal transcripts in samples of infected plants. QRT-PCR was performed as described in Chapter 2 (see page 32).

qPCR

QPCR was used to quantify fungal DNA in plant tissue by real-time PCR using SybrGreen. PCR runs were performed using an iCycler detection system (BioRad, Hercules, CA, USA). Approximately 50 ng of extracted gDNA from infected plants was used for qPCR including 0.25 U Taq-polymerase, 3 mM MgCl₂, 200 mM dNTPs and primers OLG 70 and OLG 71 (see Table 11 in the Appendix) to amplify a 261 bp fragment of an ITS region from *V. longisporum*. As a passive reference-dye for well-factor collection with the iCycler detection system, 10 nM fluorescein was used during PCR. SybrGreen I (Invitrogen, Karlsruhe, Germany) diluted 100,000 times, was added to the reaction tube. The qPCR protocol starts with a 2 min step at 95 °C and is followed by 40 cycles including a denaturation step at 95 °C for 20 sec, an annealing step at 59 °C for 30 sec and an elongation step at 72 °C for 40 sec. The detection of fluorescence was automatically measured by the cycler during the elongation step of the PCR. The following melting curve analysis of the amplified fragments was directly carried out after the PCR run by heating the samples to 95°C for 1 min, cooling them to 55°C for 1 min, and carrying out a stepwise increase of the temperature from 65°C to 95°C at the rate of 1 °C/min. The fluorescence was continuously measured by the cycler after each temperature increase. The absolute amount of fungal DNA in the plant matrix was derived from a calibration curve constructed from a dilution series of gDNA from *V. longisporum*.

Measurement of ethylene (C₂H₄)-production of *V. longisporum*

We quantified ethylene concentrations of the wild type and VI-NEP-1 silencing mutants of *V. longisporum*. Therefore, 1×10^4 fungal spores were added to 5 ml liquid potato dextrose broth (PDB) medium (Roth GmbH, Karlsruhe, Germany) in 20 ml solid-phase microextraction (SPME) vials, closed and made airtight with a silicon/polytetrafluoroethylene septum, and grown for 5 days at 23 °C, 16 h photoperiod. The air from the vials including grown fungus in PDB without or with 5 mM L-methionine (added through a sterile filter after autoclaving to the cooled down PDB) was injected into a gas chromatography (GC)-flame ionization detector, and ethylene production was measured and calculated for each treatment using four replicates.

High-performance liquid chromatography-mass spectrometry (HPLC-MS)

For the analysis of the phytohormones salicylic acid (SA), salicylic acid glycoside (SAG), jasmonic acid (JA), abscisic acid (ABA), and auxin (IAA) in *B. napus*, 100 mg of hypocotyl samples were milled in liquid nitrogen. Phytohormones were co-extracted using a modified protocol according to Xiangqing et al. (43) by replacing dichloromethane with 1 Vol. of diethylether as an extraction solvent. After extraction, the organic phase was dried in a speed vacuum centrifuge (Heidolph GmbH, Kelheim, Germany) and the pellet was resolved into 200 µl of H₂O / methanol mixture 1:1 (v/v) and 7 mM acetic acid. Then, 20 µl of the extracts were injected into HPLC-MS for analysis.

Confocal laser scanning microscopy (CLSM)

Seeds of ‘rapid cycle rape’ were double surface sterilized by sequential immersion in 70 % ethanol for 2 min and subsequently in 1 % sodium hypochlorite containing 0.1 % Tween-20 for 15 min (44). The sterilized seeds were rinsed three times in sterile tap water before sowing on water agar in 24 x 24 cm petri dishes. Autoclaved cellophane membranes (Folia Bringmann, Wendelstein, Germany) were previously placed on the agar to prevent roots growing into the medium, and this allowed easy analysis of the interaction between plant roots and the fungus using CLSM. After five days of incubation in a climate cabinet (settings: 14/10 h (light/dark), 23/20 °C (day/night)), germinated seedlings with a well developed branched root system were treated with a spore suspension (1×10^6 spores ml⁻¹) of *V.*

longisporum wild type and VI-NEP-1 knock-down mutants to assess any changes in the ability to enter the roots of *B. napus*. After 12, 24, 36, 48, 72, 96 and 120 h, two roots were harvested from each approach and used for histological staining prior to CLSM. Staining was performed using a protocol published by Eynck et al. (45). Deviating from this protocol, we dispensed with the use of lactophenol due to the toxicity of the substance. This allowed easy handling of the samples. As a result of the treatment with 0.05 % acid fuchsin, a strong staining of all fungal structures and a weaker staining of plant cell walls was achieved. Microscopic analyses were performed using a Leica TCS SP2-CLSM (Leica, Mannheim, Germany). Digital images were acquired by scanning with settings for acid fuchsin fluorescence (absorption: 543 nm, emission: 560-620 nm).

Purification of VI-NEP-1 protein using pET21 system

The VI-NEP-1 gene was amplified by PCR using primers which amplify the complete exon sequence of the gene (see Table 12 in the Appendix) and ligated into *NdeI/BamHI*-digested pET21a, resulting in the VI-NEP-1 expression vector, pET21a-VI-NEP-1 (6.9 kb) including a polyhistidine-tag (his-tag) required for protein-purification. Digestion of vector and insert was performed by incubating the samples along with 5 U *NdeI* and 5 U *BamHI* for 2 h at 37 °C. Ligation was performed in a total volume of 20 µl, containing 5 U of T4-DNA ligase. The reaction mixture was then incubated at 37 °C for approximately 12 h. Ten µl of the mixture was used for transformation of chemically competent *E. coli* BL21 cells and plated on lysogeny broth (LB) agar-media containing 50 mg/ml⁻¹ ampicilin for selection of positive transformants. Transformants that were tested positive in PCR were sequenced by ‘Eurofins MWG Operon’ (Ebersberg, Germany). The protein was over expressed by induction of the lac operon using 1 mM IPTG and subsequently purified. Purification of VI-NEP-1 protein from bacterial cells was performed using TALON His-Tag Purification Resin (Clontech-Takara Bio Europe, Saint-Germain-en-Laye, France) following the manufacturer’s instructions. The protein was concentrated using Sartorius Vivaspin 20 (Sartorius Stedim Biotech GmbH, Göttingen, Germany).

Sodium dodecyl sulfate poly acrylamide gel electrophoresis (SDS page)

Tris SDS gradient gels (12-19 %) with a discontinuous buffer system (46) were poured using SG 15 gradient maker (Hoefer Inc., Holliston, USA), Rotiphorese® Gel A (30 % acrylamide solution) and Rotiphorese® Gel B (2 % bisacrylamide solution) (both: Roth GmbH, Karlsruhe, Germany) and were polymerised by adding 30 µl of a 10 % ammonium persulfate solution and 5 µl TEMED. Gels were cast in the multiple gel caster Hoefer SE 215 (Hoefer Inc., Holliston, USA). The stacking gel contained 4 % acrylamide, 0.125 M Tris-HCL, 0.1 % SDS, 0.1 % APS w/v, and 1 % TEMED v/v. Samples were mixed with loading buffer (12.5 % glycerol, 25 mM Tris, 5 % SDS, 2.5 % Mercaptoethanol and 0.0625 % bromophenol blue) and loaded along with the molecular weight standard Roti®-Mark 10-150 PLUS (Roth GmbH, Karlsruhe, Germany) on the gel. Electrophoresis was conducted at 6 V/cm for 90 min with tris glycine buffer (0.025 M Tris base, 0.192 M glycine, 0.1 % SDS buffer). Gels were stained using silver nitrate according to Blum et al. (47).

Leaf-infiltration assay with VI-NEP-1 protein

Seeds of *B. napus* and *N. tabacum* were surface sterilized in 70 % ethanol for 15 sec and rinsed three times in sterile tap water before being sown in an autoclaved earth/sand mixture (3/1 v/v). The plants were used after approximately 20 days of growth to allow the purified VI-NEP-1 protein to infiltrate the leaves. Different concentrations of the protein, dissolved in 25 mM HEPES, were infiltrated into abaxial leaf tissue by using 1 ml plastic syringes (Roth, Karlsruhe, Germany). A 25 mM Hepes solution was infiltrated as a negative control. Boiled protein (5 min at 95 °C) was used as a second negative control. The leaves were photographed 24 h after infiltration to monitor putative lesion formation.

Seedling growth and root development assay

The seeds of different ecotypes from *A. thaliana* and ‘rapid cycling rape’ were surface sterilized using 70 % ethanol (2 min), 1 % hypochloride and 0.1 % Triton solution (15 min) and subsequently washed twice with sterile tap water before treatment with the purified protein to assess the effects of VI-NEP-1 protein on plant growth. The seeds were then left to grow on 0.8 % agar (1 % Sucrose, 0.5x Murashige and Skoog (MS) basal salts) supplemented with different concentrations of purified VI-NEP-1 protein, and then grown in a growth

chamber at 23 °C on a regular cycle including 18 hours daylight. At different time points, plants were monitored to note any changes compared to non-treated plants.

Western hybridization

Western blotting was used to detect VI-NEP-1 protein in the supernatant of the *V. longisporum* growth medium, mycelium, and also in the protein samples from the infected plants. Both were extracted using a trichloroacetic acid (TCA)/acetone method. Fungi were grown in erlenmeyer flasks with 10 ml liquid PDB medium inside, inoculated with 1×10^4 spores of *V. longisporum* wild type and VI-NEP-1 silencing mutants and incubated at 23 °C for 10 days. Fungal mycelium was harvested and ground to a fine powder using liquid nitrogen. *B. napus* plants were infected with *V. longisporum* as described on page 68. Hypocotyl material was harvested after 28 dpi and ground in liquid nitrogen to a fine powder. Sample powders were added to three volumes of a 10 % TCA/acetone extraction solution and incubated ON at -20 °C. After centrifugation (15000 rpm, 15 min, 4 °C), the precipitate was washed three times with acetone. Subsequently, the pellet was dried and dissolved in a solution containing 7 M Urea, 2 M Thiourea and 2 % CHAPS. Protein concentrations were determined by the method of Bradford et al. (48). Then 10 µg of total protein was loaded per well on the gel for SDS page. Separated proteins were spotted on a polyvinylidene fluoride (PVDF)-membrane (Roth, Karlsruhe, Germany) using Hoefer TE22 mini-gel tank (Hoefer Inc., Holliston, USA) and Towbin Buffer (Serva Electrophoresis GmbH, Heidelberg, Germany) for electrotransfer at 600 mA for 1 h. Western hybridization was performed using VI-NEP-1 polyclonal antiserum (Biogenes GmbH, Berlin, Germany) from rabbit followed by an incubation with goat anti-rabbit IgG horseradish peroxidase conjugate (Sigma-Aldrich Chemie GmbH, Munich, Germany). Immunodetection was performed using CDP-Star from Roche diagnostics (Penzberg, Germany).

Immunofluorescence microscopy

Seeds of ‘rapid cycle rape’ were double surface sterilized by sequential immersion in 70 % ethanol for 2 min, and subsequently washed three times in sterile tap water before being sown in an autoclaved earth/sand mixture (3/1 v/v). Plant parts (root, hypocotyl and stem) were harvested at different time points and fixed using 5 % glutaraldehyde solution. Subsequently,

samples were transferred into a solution of glutaraldehyde and then degassed using a water pump. Fixation using Roti®-Histol and Roti®-Plast (both: Roth, Karlsruhe, Germany) was performed as described in the following table.

step	solution	temperature	treatment
1	PBS	room temperature (RT)	5 min
2	50%EtOH	RT	30 min
3	70%EtOH	RT	30 min
4	90%EtOH	Rt	30 min
5	96%EtOH	RT	30 min
6	EtOH/Roti®-Histol 3:1	RT	30 min
7	EtOH/Roti®-Histol 1:1	RT	30 min
8	EtOH/Roti®-Histol 1:3	RT	30 min
9	Roti®-Histol	RT	45 min
10	Roti®-Histol	RT	45 min
11	Roti®-Histol/Roti®-Plast saturated RT	RT	60 min
12	Roti®-Histol/Roti®-Plast saturated 40°C	40 °C	60 min
13	Pure melted Roti®-Plast	60 °C	ON

Table 1: Fixation procedure of plant samples for immunofluorescence microscopy

Samples were embedded in pure paraffin and stored at 4 °C until use. Prior to microscopy, the embedded samples were cut to 20-30 µm thick slices using microtome HM 335 E (Microm International GmbH, Walldorf, Germany) and placed on a 75 x 25 mm gelatinised microscopy slide at 40 °C. Paraffin was removed from the samples by using Roti®-Histol at RT for 30 min and subsequently washing the samples with different ethanol concentrations (96 %, 90 %, 70 % and 50 %) for 5 min. The samples were rinsed in ddH₂O before the antigen retrieval procedure was carried out. Antigen retrieval was performed following a protocol published by Shi et al. (49) using citrate buffer (0.05 % Tween 20, pH 6.0). Finally the samples were incubated with VI-NEP-1 polyclonal antiserum and fluorescein isothiocyanate (FITC)-labelled antibodies (Sigma-Aldrich Chemie GmbH, Munich, Germany) and trypan blue. We used a laser-scanning microscope Leica DM5000 CS (Leica, Mannheim, Germany) for imaging of the samples (absorption: 488 nm, emission Cy3: 540-590 nm, emission trypan blue: 620-720nm).

Statistical analysis

For statistical analysis and creation of graphs we used the statistical analysis software STATISTICA (StatSoft GmbH, Hamburg, Germany). Data are presented as means \pm standard deviation. Differences of data sets obtained from experiments using *V. longisporum* wild type and silencing mutants were determined using one way analysis of variance (ANOVA) followed by a post hoc test using “Fisher's Least Significant Difference (LSD) test” to show which differences were significant.

RESULTS AND DISCUSSION

NLP orthologs of *V. longisporum*

NLPs are widely distributed among microbes reported to be excreted by diverse pathogens and to induce ethylene production and necrosis in dicot plants. All proteins of this family range from 24-35 kDa in mass and comprise a highly conserved amino acid region, namely a GHRHDWE motif in the centre of the peptide and two to four N-terminal cysteine residues supposed to be relevant for peptide activity. *V. dahliae* and *V. albo-atrum* are closely related species to *V. longisporum*. We inspected the *V. dahliae* genome for NLP genes considering molecular weight, the conserved motif and likelihood of it having a signal peptide. Consequently, we identified eight distinctive sequences (Vd-NEP type A - H) of putative ORFs. Genes were found to be randomly distributed in the *V. dahliae* genome localized on different chromosomes, which makes a co-regulation of the Vd-NEP genes unlikely.

Vd-NEP genes	Database entry	Putative peptide size	Chromosomal locus	Signal peptide	Cleavage site (aa) / p-value
type-A	gb: AY524789.1x*	233 aa / 25,876 Da	Chromosome 3 Chromosome 5	YES	18 / 0.991
type-B	VDAG_01995.1	239 aa / 25,116 Da	Chromosome 7	YES	24 / 0.592
type-C	VDAG_04550.1	256 aa / 27,358 Da	Chromosome 1	YES	20 / 0.962
type-D	VDAG_03497.1	283 aa / 32,384 Da	Chromosome 6	YES	23 / 0.980
type-E	VDAG_09117.1	277 aa / 31,043 Da	Chromosome 4	YES	18 / 0.859
type-F	VDAG_08022.1	308 aa / 35,342 Da	Chromosome 2	YES	20 / 0.783

type-G	VDAG_07972.1	264 aa / 29,420 Da	Chromosome 2	YES	21 / 0.609
type-H	VDAG_02984.1	185 aa / 21,310 Da	Chromosome 3	NO	-

Table 2: Putative NLPs identified in the *V. dahliae* genome

Chromosome locus according to *Verticillium* genome database information (The Broad Institute *Verticillium* group database (50)) and from the *NCBI Genbank (51). Signal peptide and cleavage site was predicted by SignalP 3.0 (52).

Sequence alignment of all identified Vd-NEP genes was done using ClustalW1 (53) to show the conserved GHRHDWE motif and cysteine residues.

Vd-NEP-A	---MLPSAVFSVFA---LVGSALAQPP-----KVNHDSINPVRD--TLGPNGDMIRKF	46
Vd-NEP-B	----MVSKIFSTLALVAAGPVSLRA-----VVPHDSLNPVTQRVQTGAIGDAIAKF	50
Vd-NEP-C	----MQHTLLSTAALLGALSAVNASPAP-----ILRRDIITALP-----GNADEIENKF	45
Vd-NEP-D	-MPSLRITASFSAVAALLLLPAVIATPLPDTPTTKLIRRDLQLPLG-----GSAWSEQEKW	54
Vd-NEP-E	---MLFSVGLLALAALPSSFGAVIQARQDDPEN-PPRDPQPPPPGP--IFGRAPELDKRF	54
Vd-NEP-F	-MLFLQNIHAVVTAMVLSVPSTASVMRRQNNSSRILSESPAEP IVN--GHDFAYYFEVKF	57
Vd-NEP-G	----MYHKILLVGVLATLTGLTSANDAIPGSAFENSGHEAAIAGAPMYHFGRSWDRKPCY	56
Vd-NEP-H	MAHASFSPSLWQPALHRIVLLLVLYLALVHPSNCSVIQRRRAAPPQK--LPKRATENDLRY	58
Vd-NEP-A	QPLLHIAHG-CQPYSAVNTRGEVNAQLQDSGT---TAGGCKETS---KGQTYARSMTLNG	99
Vd-NEP-B	NPLLHIANG-CQPYTAVNDAGDTSGLLQDSGN---ISAGCRDQS---KGQTYARAKVVNG	103
Vd-NEP-C	QPILDFD TDG CYN TAAIDPDGNINPGKATGTP---QGD CRDPPQLENSNVYSRRRCNNG	102
Vd-NEP-D	CPALDYD TDSCYNTVAISPQGLNAGQDETFKSAGEILGWCRKEVRLQQTNIYVRSRCNNG	114
Vd-NEP-E	QPALDFD TDSCYNVPAIGPNDLAI GMFPFEWP--PQAGCRNEEMLDRGNVYSRQRCNNG	112
Vd-NEP-F	QPLVDFD TDSCYSVPAMTMDGTASEGLSPSD---DVGPCRPRSA LDR TNVYVVRGR CNRG	113
Vd-NEP-G	PEAGQTDG VKTDGVSDLCFSSQNGGCADPGP-----WNGVNSPGNPFVYYTVRQCNDN	111
Vd-NEP-H	QPALDFD TDSCYNVPAIGCDGKIAEGLEPDG---TTKDYRDLADLDNTNVYSRQRCNSG	114
Vd-NEP-A	QFGIMYAWYWPKDQPADGN-LASGHRHDWENVVIWFNSNNAN--QA-GILRGAASGHGDY	155
Vd-NEP-B	QLAIMYSFYMPKDQPIAGN-VAGGHRHDWENVVVFVDDPAAN--AAPGLLGGAASGHGEY	160
Vd-NEP-C	VCAIMY EY YFEK DQSVSGSF-AGGHRHDWENVVVFARGDTI-----VRVAPSCHGGYDG-	155
Vd-NEP-D	WCVHMYDY YFEADFGWG-----AHRHDWEHIAVWVQHGL-----KFVSI SQHGKWDIR	163
Vd-NEP-E	YCVIFYAY YFQKDTATP----IDGHRHDWEHIAVWVRQSDS---FVTHVAVSQHKGYEIR	165
Vd-NEP-F	WCAFYAY YFQMDWAWSWPVSGYNHRHDWEHVVVWAKEGKV-----RGVSVSQHGGYESR	168
Vd-NEP-G	EW RVAYS IY YK-----DSGHRHDWENSIVIWNGDGAGGWKRSGTLLGWHSGWDYI	162
Vd-NEP-H	WCA YMYDY YFEKDHAD-----IGAHHRHDWEHIVVVTDDR TK--NKKYACV SQHGEWLCH	167
Vd-NEP-A	KKVNNPQRNN-----NNLHVEYFTSLGKNHELQFKTSPG-----	189
Vd-NEP-B	KKTATPDREG-----DSVKVEYFTTFPTNHELQFTATTG-----	194
Vd-NEP-C	-----ASNEFPADG-----TSPQM VYHKDSAGTHCFRFANDADIGGVENF	195
Vd-NEP-D	ILDGR TAAPRFEHG-----THPKV VYHKDGAL THAFRWANGGDEP-PENH	207
Vd-NEP-E	ENSQVTWTAEN-----GKPAIVYHKDSILTHCFRFNGADAGGPGPE	208
Vd-NEP-F	VAEDQRLRFDYTPKEFPYPAWDPMP TSVAMHPKVVFHKDGARTHC FRFAKDS D-DYEGQE	227
Vd-NEP-G	AWGDIQNTVNNDGD-----LFDQGA KDRNHAKVYQGFYYHATFSTRK TSLNTC	210
Vd-NEP-H	PEDKVLWKDEHP-----KVPIMA-----	185
Vd-NEP-A	-----RTYWIWDWRMDTTVQ GALNRADFGSANC PFNNNNFERNMRAAF-----	233
Vd-NEP-B	-----KTYPI SDWDAMPQAARDALETTDFGSANVPFKDANFDSNLAKAAL-----	239
Vd-NEP-C	SGSFYKSPLVGWL SWP--NEGLRQ TMLGAFSGGVGPKLDD-----EFAGKLGEAAGDAV	247
Vd-NEP-D	WKS WRWGVGAGLIEWERMPDNL RKTLSAKN WGAAEMA VRDKGSDWNFAWYINESQYFCW	267
Vd-NEP-E	NHRNQWITG PLLGYFGWDTVEQRDRMLTHNWEAGAI AIK NENFAENIRKARPAGLVFDEN	268
Vd-NEP-F	NERGIWIRGGLVSM LMP-SDWQDKFRSHGWGSAHMAWANE DFTGHLVKSM PQEARD DG	286
Vd-NEP-G	ANTRDEF RSN DWYFLPDGTW LHNGLDIQDGDWYGSADTNPSSLRNEARWICNRG-----	264
Vd-NEP-H	-----	

```

Vd-NEP-A -----
Vd-NEP-B -----
Vd-NEP-C PEFDENVDE----- 256
Vd-NEP-D ETYCPGFLAPEFKPWG----- 283
Vd-NEP-E IDDEGTNNI----- 277
Vd-NEP-F FDCAYDENPALKGFPMDWKKWD 308
Vd-NEP-G -----
Vd-NEP-H -----

```

Figure 1: Sequence alignment of putative Vd-NEP genes

Black letters indicate the conserved features GHRHDWE and cysteine residues, grey letters indicate amino acid exchanges in the conserved parts.

To check, whether we could find orthologous genes to Vd-NEP type A- H in the genome of *V. longisporum*, we designed primer oligonucleotides (see Table 6 in the Appendix) derived from the putative NLP gene sequences of *V. dahliae*. The forward primers were localized approximately 100 nucleotides upstream of the putative start, and the reverse primers 100 nucleotides downstream of the putative stop codon to obtain the complete open reading frames (ORFs) by direct sequencing of PCR products amplified from gDNA of *V. longisporum*. PCR fragments were sequenced (Eurofins MWG Operon, Ebersberg, Germany) using the amplification primers. We succeeded in amplification of PCR-products either directly using gDNA of *V. longisporum* or by the use of a constructed genomic library of *V. longisporum*. The genomic library of *V. longisporum* was also utilized to identify clones for sequencing that carried a genomic fragment including a NLP gene. It did this by applying the same pairs of primers used for direct amplification. All amplicons were sequenced to prove homology to their corresponding Vd-NEP gene orthologs. Subsequently, specific primers for the VI-NEP genes (VI-NEP-1 -5) were designed. The sequence alignments of all identified VI-NEP genes are given below.

```

V1-NEP-1 ---MLPSTIFSVFALVGSALAQHPKVNHDSINPVRDTLGPNG-----DMIRKFQPL 49
V1-NEP-2 ----MQHTLLSTAALLGALSAVNASP---APILRRDIITALPG-----SADEIENKFQPI 48
V1-NEP-3 --MLFSVGLLALAALPSSFGAVIQARQDDPENPPRDPQPPPPGPI-FGRAPDLDKRFQPA 57
V1-NEP-4 MLSLRNIAVVTAMVLSVPSTASVMRRQSNSSRILSDSQALEPIVGGHDFAYYFEVKFQPL 60
V1-NEP-5 ----MYHKILLVGLATLTGLTSANDAIPGSAFENSHEAAIAGAPMYHFGRSWORDKPCY 56

V1-NEP-1 LHIAHG-CQPYSAVNTRGEVNAGLQ-DSGTTAGGCKETS---KGQTYARSMTLNGQFGIM 104
V1-NEP-2 LDFDTDGCYNTAAIDPDGNINPGKG-ATGTPQGD CRDPPQLENSNVYSRRRCNNGVC AIM 107
V1-NEP-3 LDFDTDSCYNVPAIGPNGDLAIGMYPFEWPPQAGCRNEEMLDRGNVYSRQRCNNGYCVIF 117
V1-NEP-4 VDIIDTDCYSVSPAMTMDGTASEGLS--PSDDVGP CRPRRSALDRSNVYVRGR CNRGWCA FV 118
V1-NEP-5 PEAGQTDG VKTDGVDSDLCFSSQNGGCADPGPWNGVNSPGNPFVYTVRQ CN DNEWRVA 116

V1-NEP-1 YAWYWPKDQPADGNL-ASGHRHDWEN-VVIWFNSNN--ANQAGILRGAASGHG DYK---- 156
V1-NEP-2 YEYYFEKQDSVSGSF-AGGHRHDWEN-VVVFARG----DTIVRVAPSCHGGYGG----- 155
V1-NEP-3 YAYYFQKDTATP----IDGHRHDWEH-IAVWVRQSD--SFVTHVAVSQHKGYDIRENS-- 168
V1-NEP-4 YAYYFQMDWAWSWPVSSYNHRHDWEH-VVWAKE----GKVRGVSVSQHG GYENRVAEDQ 173
V1-NEP-5 YSIYYKGD-----SGHKNWENSIVIWNNGDGAGGWKRS GTLLGWHSGWDYIAWG-- 165

```

V1-NEP-1	--KVNNPQRNN-----NNLHVEYFTSLGKNHELQFKTSP-----GRTY	192
V1-NEP-2	--ALNEFPVDG-----TSPQMVYHKDSAGTHCFRFANDADIGG--VENFSGS	198
V1-NEP-3	--QITWTAAEN-----GKPAIVYHKDSILTHCFRFGSGADAGGPGPENHKNQ	213
V1-NEP-4	RLRFDYTPKEFPYPAPWDPMPTSVAMHPKVVVFKDGDARTHCFRFAKDSDDYE-GQENERGV	232
V1-NEP-5	--DIQNTVNNND-----GDLEFDQGAKDRNHAKVYQGFYYHATFSTRKTSLNTCANTRD	215
V1-NEP-1	WIWD-----WDRMDSTVQGALNRADFGSANCPFNNNN-FERNMRAAF-----	233
V1-NEP-2	FYKSPLVGLSWPNEGLRQTMFG-AFSGGVGPKLDDE-FAGKLGEAAGDAVPE--FDPNV	254
V1-NEP-3	WITGPLLGYFGWDTVEQRDRMLTHNWEAGSIAIKNEN-FAENIRKAR-PAGLV--FDENF	269
V1-NEP-4	WIRGGLISMLLMPS-DWQEKFRSQNWGSAHMAWANEEDFTGHLVKSMPEARDDGFDCAY	291
V1-NEP-5	EFRSNDWYFLPDGTWLHNGDLIQDGWDYGSADTNPSS-LRNEARWICNRG-----	264
V1-NEP-1	-----	
V1-NEP-2	DE-----	256
V1-NEP-3	DDEGTNNI-----	277
V1-NEP-4	DENPALKGFPMDWKKWD	308
V1-NEP-5	-----	

Figure 2: Sequence alignment of VI-NEP orthologs

Black letters indicate the GHRHDWE motif and cysteine residues, grey letters indicate amino acid exchanges in the conserved parts.

The deduced protein sequences were multiply aligned showing the conserved domains of the cysteine residues and the GHRHDWE motif. According to the definition of Gijzen and Nürnberger (54) the identified VI-NEP orthologs can be subdivided into type I NLPs harbouring two conserved C-residues including VI-NEP-1, which is the ortholog of Vd-NEP-A, and type II with 4 C-residues including VI-NEP-2 (ortholog of Vd-NEP-C), VI-NEP-3 (ortholog of Vd-NEP-E), and VI-NEP-4 (ortholog of Vd-NEP-F). Comparable to Vd-NEP-G, which is the ortholog from *V. dahliae*, VI-NEP-5 only harbours one conserved cysteine residue and is therefore not classifiable. Sequence alignments of corresponding orthologs for one NLP gene of *V. dahliae* and *V. longisporum* are given in the following.

Vd-NEP-A	MLPSAVFSVFALVGSALAQQPPKVNHDSINPVRDTLGPNGDMIRKFQPLLHIA	53
V1-NEP-1	MLPSTIFSVFALVGSALAQHPKVNHDSINPVRDTLGPNGDMIRKFQPLLHIA	53
Vd-NEP-A	HGQPYSAVNTRGEVNAQLQDSGTTAGGCKETSKGQTYARSMTLNGQFGIMYA	106
V1-NEP-1	HGQPYSAVNTRGEVNAQLQDSGTTAGGCKETSKGQTYARSMTLNGQFGIMYA	106
Vd-NEP-A	WYWPKDQPADGNLASGHRHDWENVVIWFNSNNANQAGILRGAASGHGDYKKVN	169
V1-NEP-1	WYWPKDQPADGNLASGHRHDWENVVIWFNSNNANQAGILRGAASGHGDYKKVN	169
Vd-NEP-A	NPQRNNNNLHVEYFTSLGKNHELQFKTSPGRTYWIWDWDRMDTTVQGALNRAD	222
V1-NEP-1	NPQRNNNNLHVEYFTSLGKNHELQFKTSPGRTYWIWDWDRMDS TVQGALNRAD	222
Vd-NEP-A	FGSANCPFNNNNFERNMRAAF	233
V1-NEP-1	FGSANCPFNNNNFERNMRAAF	233

Figure 3: Sequence alignment of Vd-NEP-A with VI-NEP ortholog

Black letters indicate the conserved GHRHDWE motif and cysteine residues, grey letters indicate amino acid exchanges in the *V. longisporum* sequence compared to the *V. dahliae* sequence.

The identity of both proteins is equal except for four amino acids. Sequence properties for all identified VI-NEP genes including ORF/protein size, molecular weight of the protein, intron positions and the calculated protein identities to corresponding NLPs of *V. dahliae* and *V. albo-atrum* are given in the following table.

Ortholog	ORF (nt)	Protein size (aa)	Molecular weight (Da)	Intron positions	aa sequence identity to <i>V. dahliae</i>	aa sequence identity to <i>V. albo-atrum</i>
VI-NEP-1	760	233	25,986	207-267	229/233 (98%)*	224/233 (96%)
VI-NEP-2	831	256	27,361	321-380	251/256 (98%)	234/267 (88%)
VI-NEP-3	834	277	31,040	-	262/283 (93%)	269/277 (97%)
VI-NEP-4	927	308	35,327	-	292/308 (95%)	283/296 (96%)
VI-NEP-5	970	264	29,420	92-149 577-631 829-890	264/264 (100%)	185/295 (63%)

Table 3: Sequence properties of VI-NEP orthologs

Protein sequence of *V. dahliae* and *V. albo-atrum* for identity scoring were downloaded from the genome sequence database (The Broad Institute, *Verticillium* group database), except the protein sequence of the *V. dahliae* gene homologous to VI-NEP 1 which was downloaded from the *NCBI database*. Molecular weight was calculated using the Peptide Property Calculator (<http://www.basicnorthwestern.edu/biotools/proteincalc.html>). Introns were determined by sequencing of corresponding cDNA.

We calculated identity scores by pairwise alignments among all VI-NEP types. A redundant gene function of several homologs was not assumed due to the low sequence identities among VI-NEP genes.

	VI-NEP-2	VI-NEP-3	VI-NEP-4	VI-NEP-5
VI-NEP-1	27.8 %	24.0 %	19.9 %	17.5 %
VI-NEP-2	-	35.6 %	32.0 %	20.6 %
VI-NEP-3	-	-	32.2 %	17.6 %
VI-NEP-4	-	-	-	18.8 %

Table 4: Sequence identity among VI-NEP orthologs

Alignment and identity scoring was performed using the Global Pairwise Alignment Algorithm, EMBOSS (55).

The rising numbers for the genome sequence release of microbes revealed a varying number of NLP gene copies in different organisms, a single Mg-NLP copy in *Mycosphaerella graminicola* (56), two copies of NEP-1 and -2 in *Botrytis* spp. (24) and multi-copied NPP genes in the oomycete genera *Pythium* and *Phytophthora* (23). In *Botrytis* spp. the presence of two NLP gene copies may have adaptive significance and some evolutionary changes in NLP genes are presumably driven by positive selection (24). A phylogenetic tree showing the inferred evolutionary relationships among various biological species of protein alignments of all VI-NEPs, including several ascomycetes, five oomycetes and nine bacteria, was created using the bottom-up clustering neighbour-joining method (57).

The phylogram (see page 81) shows that the VI-NEPs are subdivided into four distinctive clades. VI-NEP-1 was found to be clustered in the largest group (C), exclusively representing the oomycete sequences, but also including ascomycota, and bacilli. VI-NEP-2 and VI-NEP-5 were both clustered in small groups (B, E) consisting only of ascomycota representatives. VI-NEP-3 and VI-NEP-4 built up a common cluster (A) including ascomycota and bacteria of the genus *Bacillus*, *Streptomyces* and *Micromonospora*.

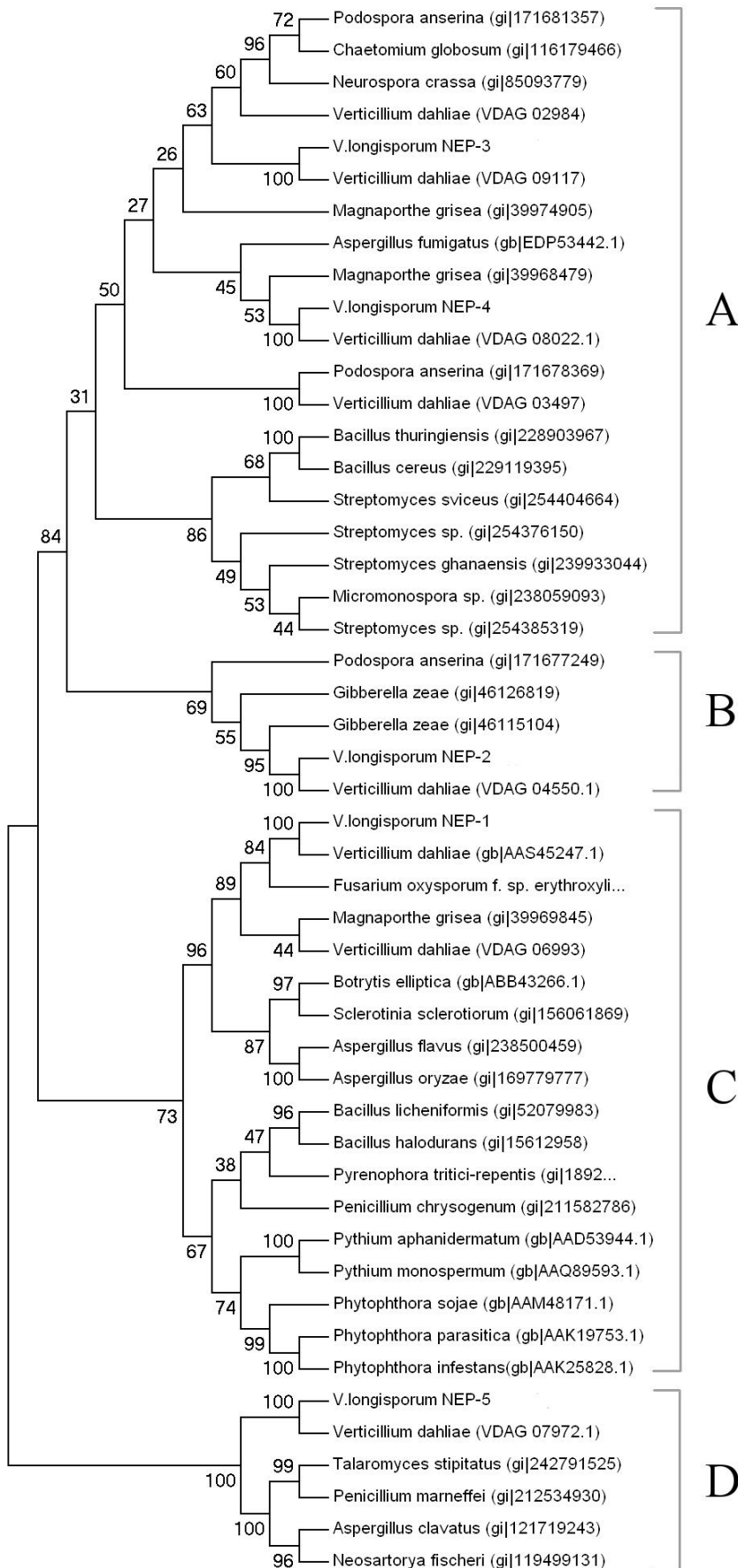


Figure 4: Phylogenetic relationship of microbial NLP orthologs

An evolutionary tree of 49 taxa in NLP orthologs is given. The evolutionary history was inferred using the Neighbour-Joining method. The optimal tree with the sum of branch length = 10.46564852 is shown. The percentage of replicate trees in which the associated taxa clustered together in the bootstrap test (1000 replicates) is shown next to the branches (58). The evolutionary distances were computed using the Poisson correction method (59) and are in the units of the number of amino acid substitutions per site. All positions containing gaps and missing data were eliminated from the dataset (Complete deletion option). There were a total of 100 positions in the final dataset. Phylogenetic analyses were conducted in MEGA4 (60). Four distinct clades of relations (A-D) were identified.

Expression of VI-NEP orthologs

Expression levels of the five identified VI-NEP genes were measured by qRT-PCR using gene specific primers (see Table 7 in the Appendix). For normalization of expression levels, the housekeeping gene β -tubulin was used. We determined the expression of VI-NEP genes under *in vitro* conditions of mycelium grown for 10 days in artificial simulating xylem (SXM) medium in standing cultures with 12 h day/night change. The SXM medium simulated the basic nutritional condition of a xylem environment (61). Secondly we measured the expression levels of these VI-NEP genes in *B. napus* plant samples root-infected with *V. longisporum* and grown under climate chamber conditions. The VI-NEP transcripts were quantified in hypocotyl/root mixed samples at 14, 21, 28 and 35 dpi. Figure 5 shows the time course of \log_2 relative expression values of the VI-NEP genes *in planta* given in relation to the measured *in vitro* expression levels.

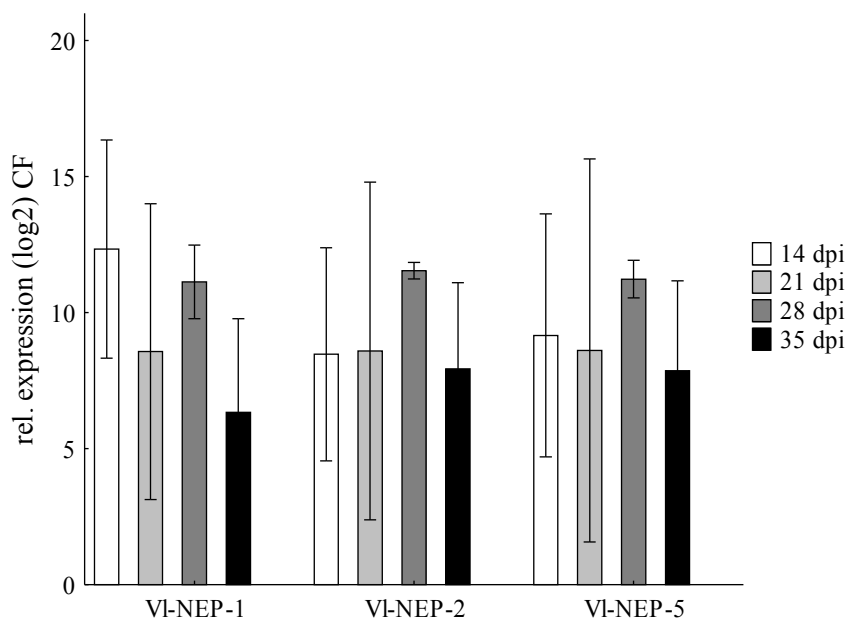


Figure 5: Gene expression analysis of VI-NEP orthologs

Error bars indicate the standard error of 3 biological replicas.

We were able to detect transcripts of VI-NEP-1, VI-NEP-2, and VI-NEP-5 *in vitro* by qRT-PCR as well as in samples of infected plants. VI-NEP-3 and VI-NEP-4 were neither detected *in vitro* nor *in planta*, even with the gene specific primers we used for reverse transcription of RNA prior to qRT-PCR. We postulate that these genes may be pseudogenes, as reported for many other organisms comprising several NLP genes (62, 54, 63). For all three expressed

VI-NEP genes (VI-NEP-1, -2, -5) significant higher expression levels were found in the analysed time points of infection than in SXM cultured *V. longisporum* samples. We have chosen VI-NEP-1 for further analysis because its orthologs from other fungi have been described to show effects of necrosis, cell death and activation of plant defence on hosts (19, 31, 32).

Gene silencing of VI-NEP-1

In general, NEP-encoding genes are found in single copy, and in two and four copies. The highest numbers of copies were identified in *P. aphanidermatum* and in *P. parasitica*, respectively (19, 32). The species *V. longisporum* is described as being near-diploid (64) as a result of a parasexual event of parental *V. dahliae* and *V. albo-atrum* (65); therefore *V. longisporum* probably possesses two copies of the VI-NEP-1 gene in the genome. By southern hybridisation using a PCR amplified digoxigenin-labeled hybridization probe specific for VI-NEP-1 (primers see Table 8 in the Appendix), two copies of the VI-NEP-1 gene were detected in the *V. longisporum* genome which confirmed the diploidy of VI-NEP-1 in the genome of amphihaploid *V. longisporum* (data not shown).

Because phenotypic effects determined by VI-NEP-1 are likely to be genetically dominant and cannot be eliminated by a single mutation event, and the generation of homozygous VI-NEP-1 mutants by crossing of *V. longisporum* is not available, a strategy based on RNAi-mediated post-transcriptional gene silencing was chosen for the inactivation of VI-NEP-1 in *V. longisporum*. For gene silencing, a VI-NEP-1 gene sequence-specific double stranded HP-fragment was constructed because in recent studies its use was demonstrated to be the most effective strategy for triggering RNAi in fungi (66, 67). The fungus was transformed with the pPK2-VI-NEP-1 vector carrying the HP-fragment using AMT to allow intracellular over-expression of a VI-NEP-1 silencing cassette forming an HP-structure triggering RNAi in the fungus.

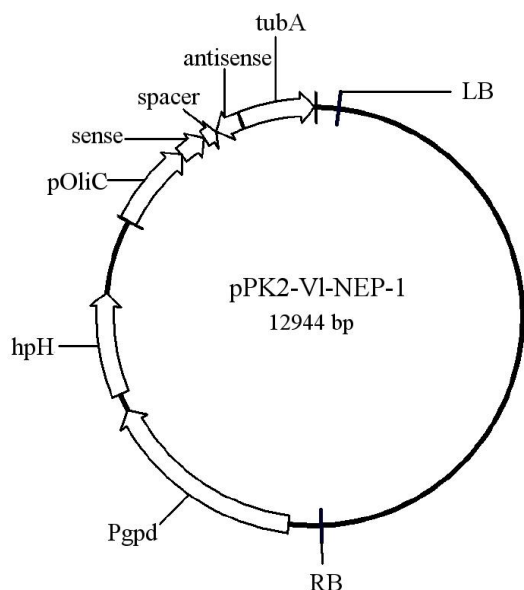


Figure 6: Physical map of binary vector constructed for HP-RNA expression of VI-NEP-1

pPK2-HP vector comprising left (LB) and right border (RB) for the AMT and a hygromycin B resistance cassette (hpH) under the control of constitutive promoter from *A. nidulans* (Pgpd) for the selection of transformants; included HP cassette comprises *oliC* promoter from *A. nidulans* and *tubA* terminator from *B. cinerea*

Seven positive transformants (m4, m9, m10, m11, m16, m19, m23) were identified on a hygromycin-selective medium and checked by PCR and southern hybridization for the success of transformation. PCR analysis was performed using gDNA extracted from *V. longisporum* mutants as a template, and using primers for the amplification of the hygromycin cassette. Additionally, southern hybridisation was performed to determine the number of VI-NEP-1 gene copies in the transformed mutants compared to the wild type *V. longisporum* strain.

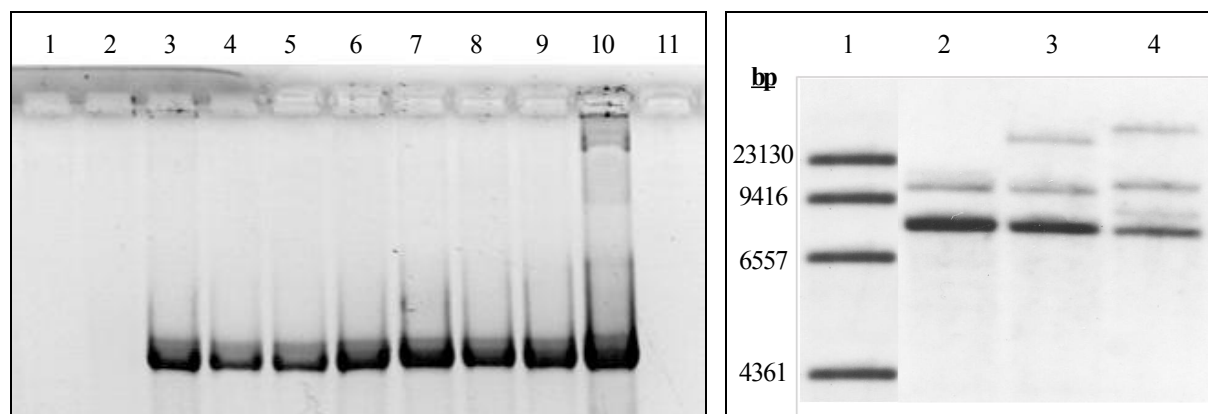


Figure 7-8: Analysis of *V. longisporum* VI-NEP-1 transformants

Figure 7 (left side): PCR analysis using primers for the amplification of the hygromycin cassette.

1-2 = wild type 3-9 = VI-NEP-1 mutants 10 = positive control 11 = negative control

Figure 8 (right side): Southern hybridisation of *V. longisporum* VI-NEP-1 transformants (gDNA cut with *NcoI*)

1 = self-made DNA-ladder comprising incorporated DIG-dUTPs 2 = wild type 3 = VI-NEP mutant 19 4 = m23

All tested mutants showed a positive signal on the agarose gel after electrophoresis. Southern hybridisation of mutants m19 and m23 using a probe, amplified with primers for a VI-NEP-1-fragment, detected an additional third signal accompanying the insertion of the HP-fragment into the genome of the fungus.

To assess the efficiency of silencing, all mutants were cultivated in SXM liquid medium for 10 days. RNA was extracted and used for qRT-PCR to measure the transcript accumulation of VI-NEP-1 mutants in comparison to *V. longisporum* wild types.

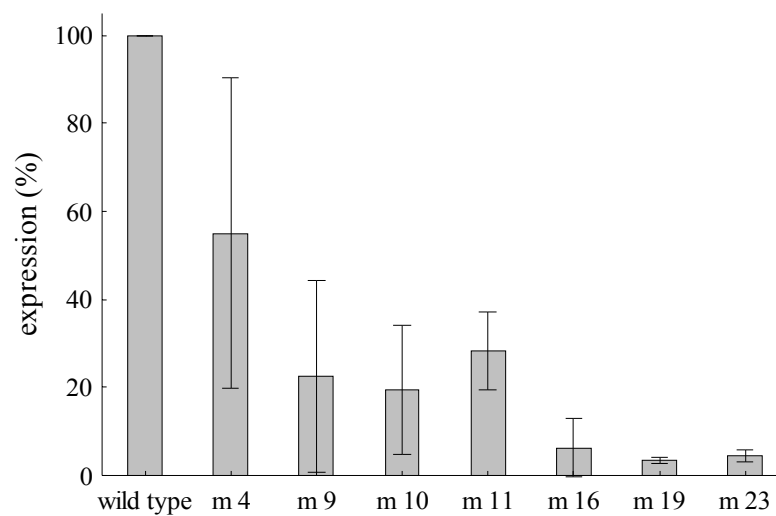


Figure 9: Gene silencing efficiency in VI-NEP-1 transformants

Assessment of silencing efficiency in seven mutants (m4, m9, m10, m11, m16, m19, and m23) were done in reference to wild type *V. longisporum* by qRT-PCR

Expression of the VI-NEP-1 gene was shown to be reduced in a range between 47 to 98 % in VI-NEP-1 silencing mutants as compared to the expression in *V. longisporum* wild type. As proven by qRT-PCR, VI-NEP-2 and 5, which are also expressed by *V. longisporum* wild type in *Brassica* plants, were not silenced by the expression of VI-NEP-1 specific HP cassette in generated mutants (data not shown); therefore all phenotypic effects should be linked to VI-NEP-1 gene suppression.

All transformants were grown *in vitro* on PDA plates to evaluate any ectopic effects on the growth rate and spore germination efficiency in comparison to the wild type by random integration of the silencing cassette into the fungal genome. Single spores of *V. longisporum*

wild type and of each transformant were plated three times, and growth rates were measured every second day for 14 days. For the evaluation of the spore germination rate of *V. longisporum* wild type and the transformants, 50 spores were plated three times, as estimated by a Thoma hemacytometer. The number of fungal colonies was counted after five days of cultivation. For both growth rate and spore germination efficiency, no difference was detected in any transformant regarding the wild type of *V. longisporum* (data not shown), thus we selected two transformants, m19 and m23, which showed strong silencing efficiency, to test for pathogenicity in *B. napus* plants.

Plant pathogenicity assay using VI-NEP-1 silencing mutants

NLPs are known to be involved in infection processes of plant pathogenic microbes supposed to act as elicitors or phytotoxins. In several pathosystems, activation of plant defence mechanisms was shown, while purified NLPs infiltrated into plant tissue can trigger disease-like symptoms. VI-NEP-1 is also supposed to play an active role in the pathogenesis of *V. longisporum* during infection of the host plant *B. napus*, as indicated by strong upregulation of VI-NEP-1 gene expression as shown previously (see Figure 5). To investigate the significance of VI-NEP-1 during the pathogenesis and symptom development we infected rape plants with *V. longisporum* wild type and with the two VI-NEP-1 knock-down mutants, m19 and m23. Symptoms were evaluated by measuring the plant shoot lengths and by the assessment using a disease score according to Zeise et al. (40).

Disease score	Disease symptoms
1	no symptoms
2	slight symptoms on the oldest leaf (yellowing, black veins)
3	slight symptoms on the next youngest leaves
4	about 50 % of the leaves show symptoms
5	more than 50 % of the leaves show symptoms
6	up to 50 % of the leaves are dead
7	more than 50 % of the leaves are dead
8	only apical meristem is still alive
9	the plant is dead

Table 5: Disease score according to Zeise et al.

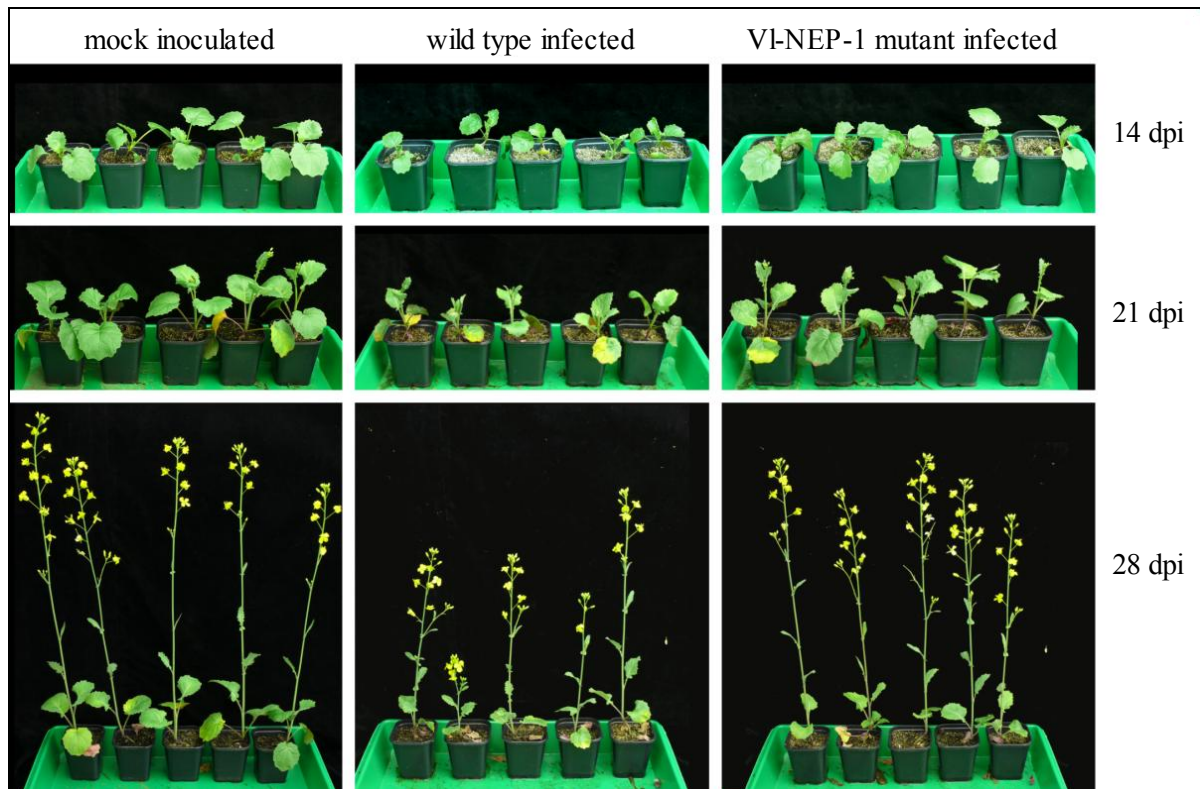


Figure 10: *B. napus* pathogenicity assay with VI-NEP-1 silenced *V. longisporum*

Photography of mock, wild type, and m23 inoculated plants at time points 14, 21, and 28 dpi.

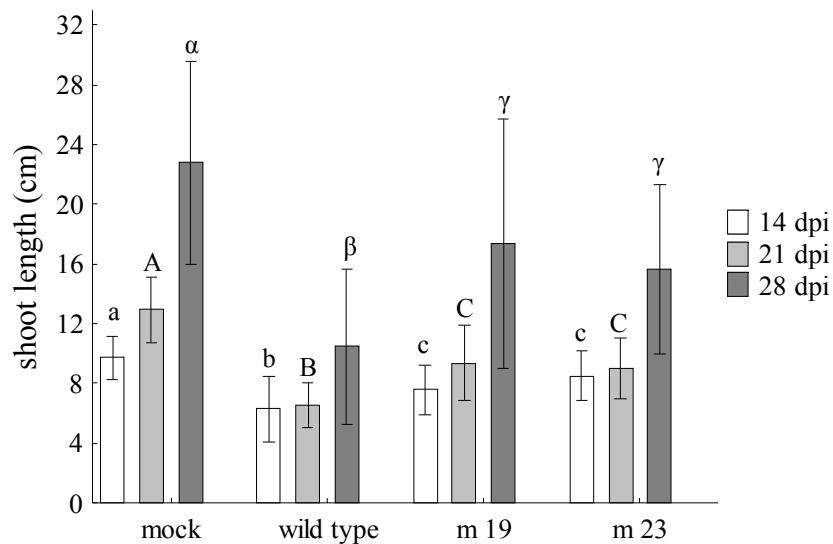


Figure 11: Measured shoot length of *Brassica* plants non-inoculated, wild type inoculated, m19, and m23 inoculated at 14, 21, and 28 dpi.

Applies for all following figures: Values marked by the same letter over the bars do not differ on a significance level of $p \leq 0.05$ (LSD).

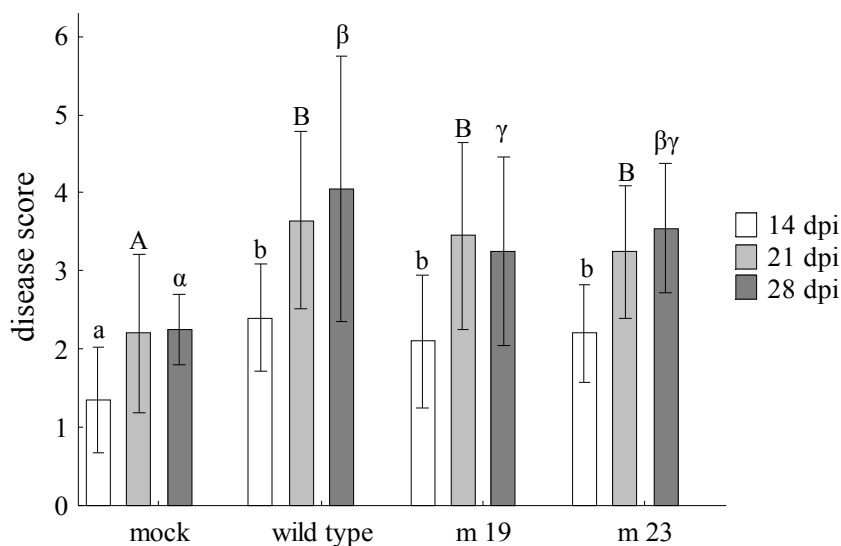


Figure 12: Disease scores of plants according to Zeise.

After 14 dpi a reduction in symptom severity was initially observed regarding the VI-NEP-1 mutants compared to the wild type infected plants. The altered phenotype became significant at 21 dpi and 28 dpi for both VI-NEP-1 mutants m19 and m23. Plants infected with the mutants showed less stunting and lower disease scoring than wild type infected *Brassica* plants. Infection assays were conducted four times, each with the same results. A plant pathogenicity assay on *A. thaliana* using VI-NEP-1 silencing mutants was performed by the ‘Department of General and Developmental Plant Physiology’ (Albrecht von Haller Institute for Plant Sciences, University of Goettingen, Goettingen, Germany). No changes in symptom severity were observed during this experiment. We clearly proved that the inoculum, containing $1 \times 10^6 \text{ ml}^{-1}$ fungal spores for the plant infection, indeed comprises the same number of spores for both wild type and VI-NEP-1 mutants. We obtained this proof by plating the solutions on PDA plates and counting the germinated spores after five days of incubation at $23 \text{ }^\circ\text{C}$. Slight deviations were negligible due to the fact that the symptom severity caused by the infection with *V. longisporum* was consistently in a range between $1 \times 10^5 \text{ ml}^{-1}$ to $1 \times 10^7 \text{ ml}^{-1}$, as proven by plant infection assays using different spore-concentrations (data not shown). We also proved that the reduced symptom severity was not connected to a potential disruption of a non-specific anonymous gene because of the the random insertion of VI-NEP-1 silencing cassettes by AMT. This proof was obtained by using several silencing mutants in a first pathogenicity assay on *B. napus* to exclude any effects not related to VI-NEP-1

disruption. Additionally, mutants did not show any changes in the ability to grow or in the ability to sporulate compared to the wild type

We measured the amount of *Verticillium*-DNA in the infected *Brassica* plants by qPCR to find out if the reduction in symptom development, compared to wild type infection, while undergoing *Brassica*-infection with VI-NEP-1 mutants was due to a reduction of fungal DNA in the plant. Therefore, the biomass of *V. longisporum* wild type strain and VI-NEP-1 silenced mutants m19 and m23 were measured using gDNA extracts from root-inoculated *B. napus* plants by qPCR analysis. The cT values of the qPCR were recorded from 100 mg of hypocotyl tissue and the DNA quantity was derived from a linear correlation curve constructed with a *V. longisporum* DNA concentration series. The fungal biomass was measured at time points 14, 21, and 28 dpi.

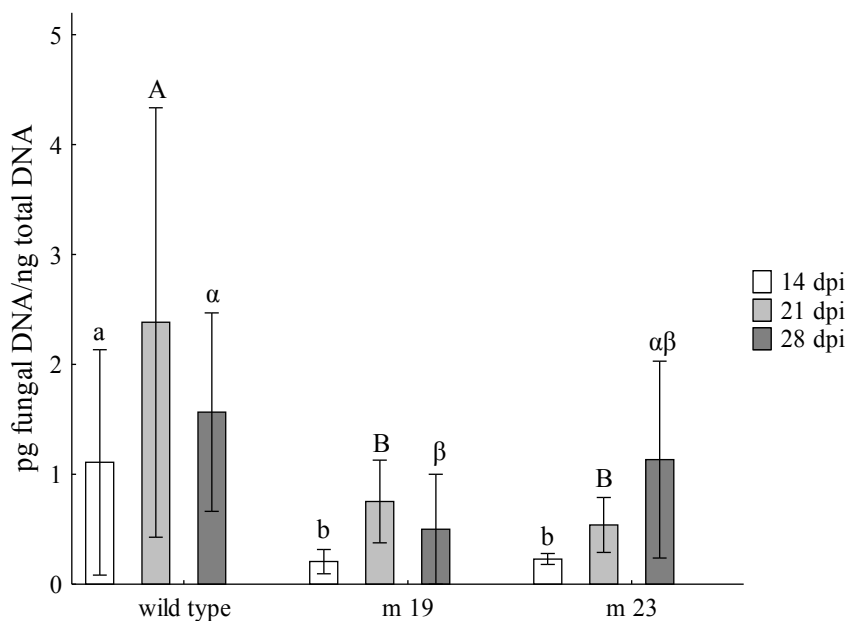


Figure 13: *V. longisporum* biomass in hypocotyl tissue of inoculated *B. napus* plants

Each sample included three biological replicas. Error bars indicate the standard deviation.

The biomass of the VI-NEP-1 mutants m19 and m23 was significantly less than in the wild type infected *Brassica* plants after 14 dpi and 21 dpi in the hypocotyl. At 28 dpi, levels of fungal biomass in the wild type and in the mutant m23 were similar, but for the mutant m19 still lower levels were measured. To investigate whether reduced fungal DNA in the plants infected with silencing mutants compared to wild type infected plants was due to a hampered

ability of VI-NEP-1 silencing mutants to enter the plant over the roots of *B. napus*, we used CLSM using the conventional fluorescence dye acid fuchsin. Infection status was observed every 12 hours for five days.

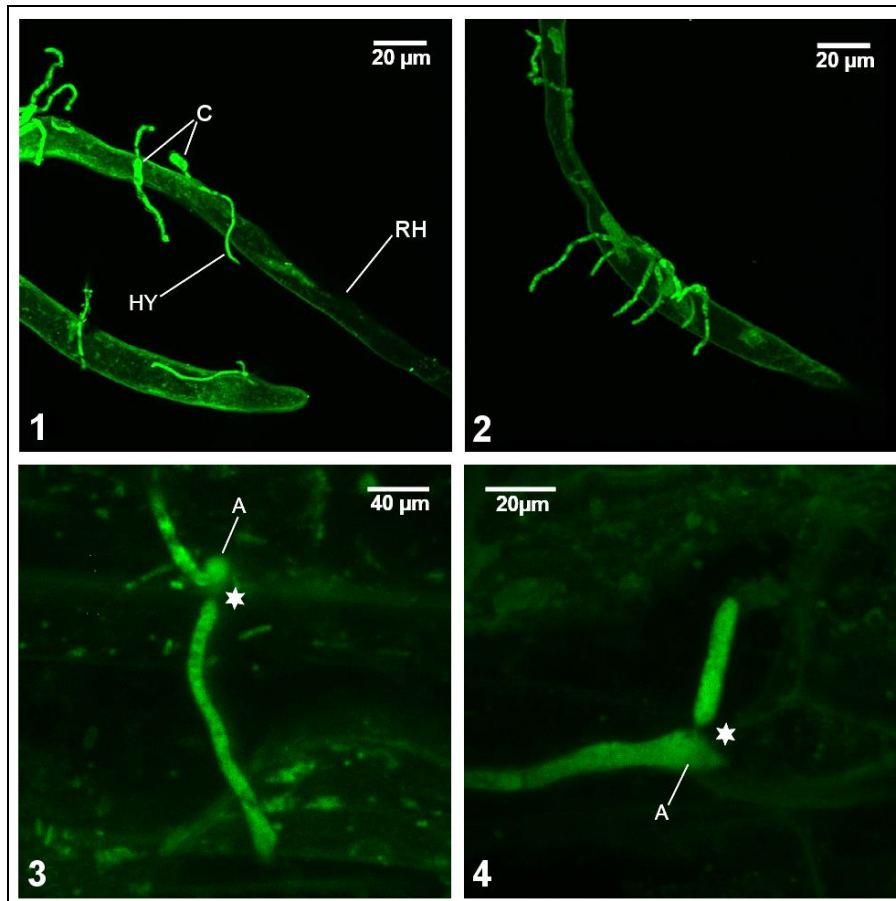


Figure 14: CLSM images of wild type and VI-NEP-1 silencing mutants infected plants

(RH =root hair; C =conidia; HY = hyphae; A = appressoria-like formation; stars = penetration point)

1 = wild type infected, 12 hpi

2 = VI-NEP-1 mutant infected, 12 hpi

3 = wild type infected, 72 hpi

4 = VI-NEP-1 mutant infected, 72 hpi

After 12 hpi, the fungal spores of wild type and silencing mutants had both visibly germinated (see Figure 14-1 and -2). In addition to the primary germination tube with an approximate length of 50 to 200 µm, a secondary tube formed on the opposite side of the spore. After 24 hpi, all grown hyphae expanded in the direction of the lateral roots along the root hairs. After 36 hpi, the hyphae built a dense grid around the root hairs and came into contact with the root cortex but no penetration of the cell wall could be observed. After 72 hpi to 120 hpi, the whole root surface was covered with hyphae (see Figure 15-1 and -2) and first started to

penetrate into the epidermal cells of the root-cortex (see Figure 15-3 and -4). Apressoria-like structures were observed at the penetration points of the hyphae.

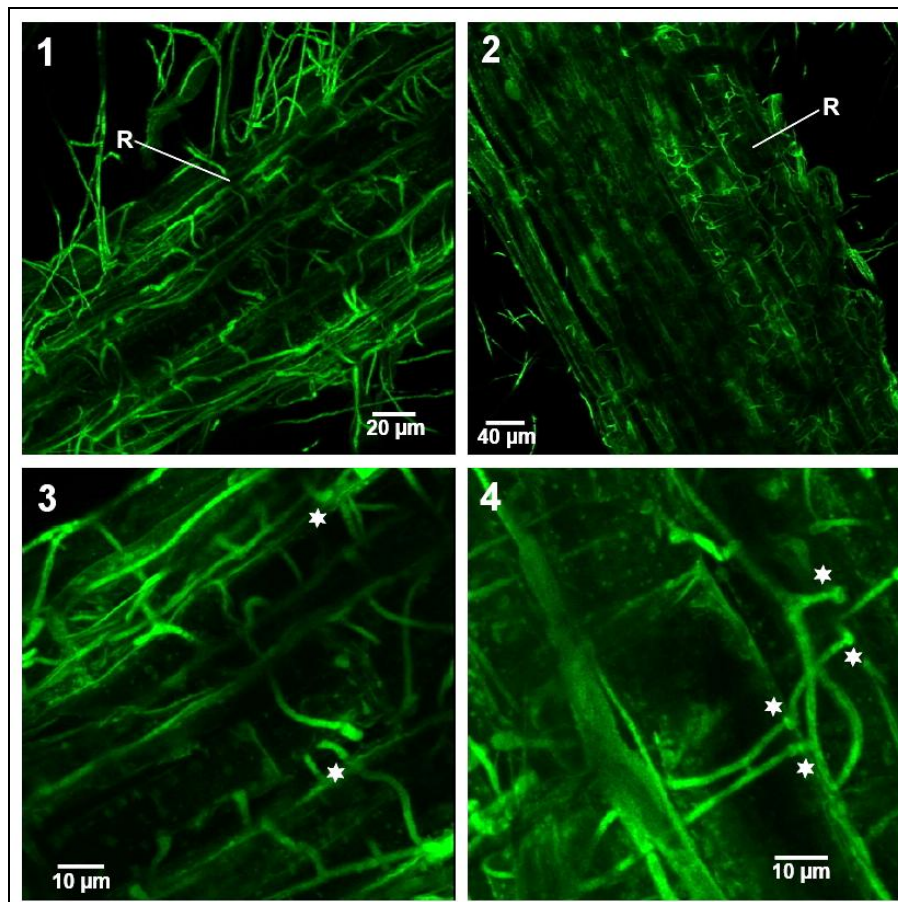


Figure 15: CLSM images of wild type and VI-NEP-1 silencing mutants infected plants

(R = root; stars = penetration point)

1 = wild type infected, 120 hpi

2 = wild type infected, 120 hpi

3 = VI-NEP-1 mutant infected, 120 hpi

4 = VI-NEP-1 mutant infected, 120 hpi

After 120 hpi, hyphae propagated in the epidermal cells by penetrating several cell walls (see Figure 15-3 and -4). The hyphae spread in the direction of the vessel system by wrecking several cell layers. The xylem was not colonized at this stage. For all microscopic examinations, there was no evident difference visible between infection structures or speed of infection in plants infected with wild type strain and the silencing mutants of *V. longisporum*.

Nevertheless, *V. longisporum* mutants m19 and m23 showed high gene silencing efficiency of VI-NEP-1, which correlated with a significant reduction of stunting on *B. napus* plants after root inoculation. Consistent with the reduced stunting effect on *B. napus* plants, the fungal

biomass, quantified by qPCR, was lower in the plants infected with the silencing mutants compared to the wild type infected. This resulted in the hypothesis that VI-NEP-1 must have a influential exercise on the fitness of the fungus in the xylem, and silencing of the gene leads to decreased growth and fungal-spreading in the plant. Therefore, the influence of VI-NEP-1 will be determined by further experiments. In previous studies it was reported that NLPs of different plant pathogens are able to activate patterns of innate plant immunity including defence mechanisms regulated by the phytohormone salicylic acid (SA). To investigate whether the gene silencing of VI-NEP-1 has an impact on phytohormone-regulated plant defence in *B. napus*, we measured the efficiency of the *V. longisporum* wild type strain and the silenced mutants m19 and m23 in inducing hormone signalling pathways.

Effects on phytohormone level

The plant hormones jasmonic acid (JA), SA and ethylene have been implicated in various aspects of plant disease resistance signalling (68). Therefore, we measured the ability of the *V. longisporum* wild type strain and the silencing mutants m19 and m23 to induce the production of the phytohormones JA, SA, salicylic acid glycoside (SAG) and further abscisic acid (ABA), and auxin (IAA) during infection of *B. napus*. Ethylene production after *Verticillium* infection was shown to be associated with the development of disease symptoms in host plants, and was also found to be involved in resistance of *A. thaliana* against the fungus (13, 75, 76). One of the eponymous features of NLPs, its capability to trigger ethylene production due to protein exposure on host plants, was often proved. Therefore, we were very interested in showing any changes, compared to wild type infection, in the ethylene production after infection with the silencing mutants. The extraction from plant material and subsequent detection by HPLC-MS of ethylene is difficult due to the volatile state of the phytohormone, therefore we investigated the expression of the ethylene biosynthesis enzymes 1-aminocyclopropane-1- carboxylate synthase (ACS) and -oxidase (ACO) by qRT-PCR to draw a conclusion on the accumulation of the phytohormone in the plants. Additionally, we determined the expression level of the SA-marker gene PR-1 as well of the JA-marker gene PDF-1.2. We harvested the hypocotyl from infected and mock inoculated plants and extracted phytohormones prior to analysis by HPLC-MS. For measurement of transcripts of phytohormone marker genes we extracted total RNA from the same plants. Both, phytohormone and gene expression analysis included three independent biological replicas.

HPLC-MS and qRT-PCR data were measured using plant material at time points 14, 21, and 28 dpi with *V. longisporum* wild type and VI-NEP-1 silencing mutants. The preliminary results from one measurement are shown in the following. For publishing, the data must be confirmed by two further measurements. IAA was not detectable in any of our samples.

JA is known as a phytohormone regulating plant defence by a pathway antagonistic to SA (69), and ABA is known to communicate with both during the process of activation of the plant defence response. ABA and JA were not significantly affected by *V. longisporum* after root infection of *B. napus*, which is consistent with the findings of Raztinger from 2008 (70), showing that both phytohormones are unaltered due to *V. longisporum* infection measured in both xylem sap and shoot extracts of *B. napus* by HPLC-MS. The amounts of JA in plants infected with the silencing mutants were measured and found to be slightly lower after 28 dpi as compared to wild type and mock infected samples but no significance could be shown.

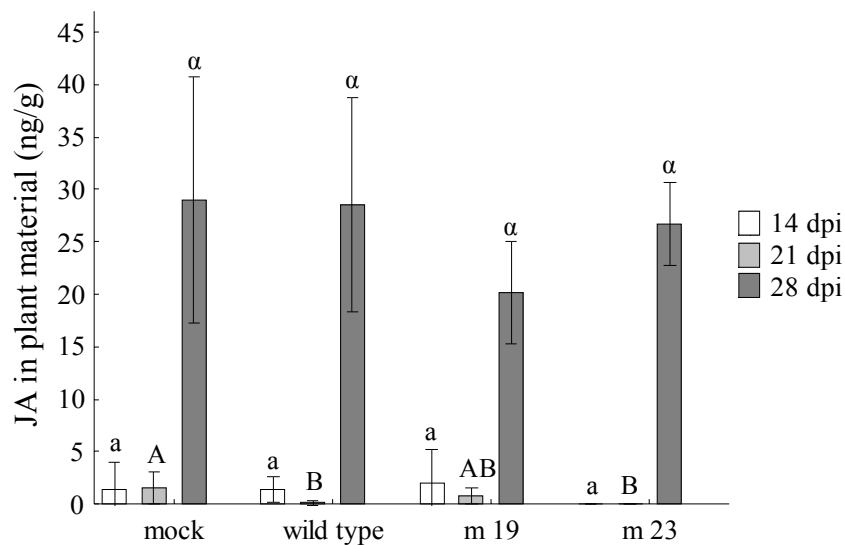


Figure 16: Levels of JA in *B. napus* hypocotyl tissue

Applies for all phytohormon-measurements: Analysis of phytohormons from healthy plants and *V. longisporum*-wild type and VI-NEP-1 mutant-infected plants at different time points after infection is shown. Each data point represents an average of 4 samples (each sample pooled from 5 plants). Error bars indicate standard deviation.

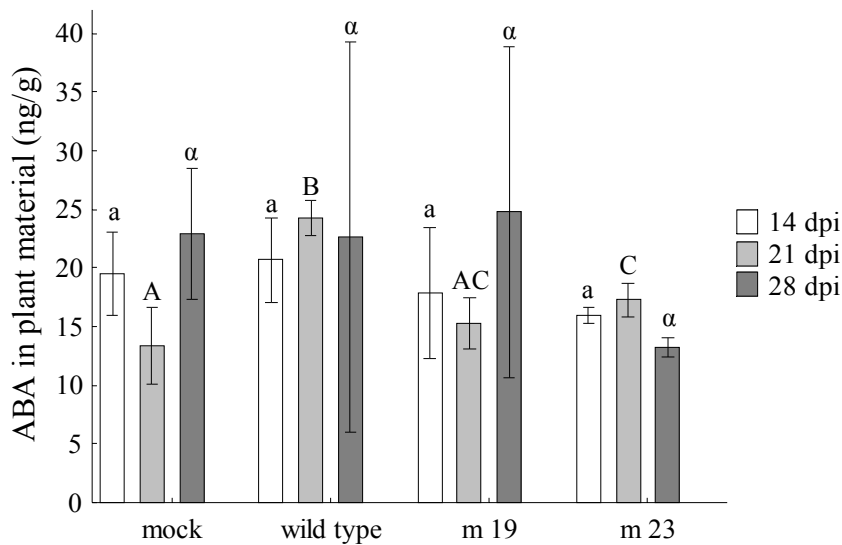


Figure 17: Levels of ABA in *B. napus* hypocotyl tissue

In *Arabidopsis* it was shown that the infection of plants by a biotrophic pathogen results in the activation of SA-mediated defence responses, wherein the infection by a necrotrophic pathogen triggers the JA and ethylene pathway of the plant (69). *V. longisporum* is described as a hemibiotrophic pathogen, which usually shows a biotrophic life style, and in the late stage of infection a necrotrophic life style by decomposing dead plant tissue to release nutrients and spreading of the fungus in the whole plant.

SA as well as SAG were both shown to be up-regulated in *B. napus* upon infection with *V. longisporum*, with a negative correlation to the stunting effect due to infection (70) as described by Ratzinger et al. in 2008. It was also shown that the accumulation of the phytohormone SA and its glucoside (SAG) seem to be unique feature in the response of *B. napus* to infection with *V. longisporum* because no changes in the level of SA and also SAG could be measured after infection with *V. dahliae*.

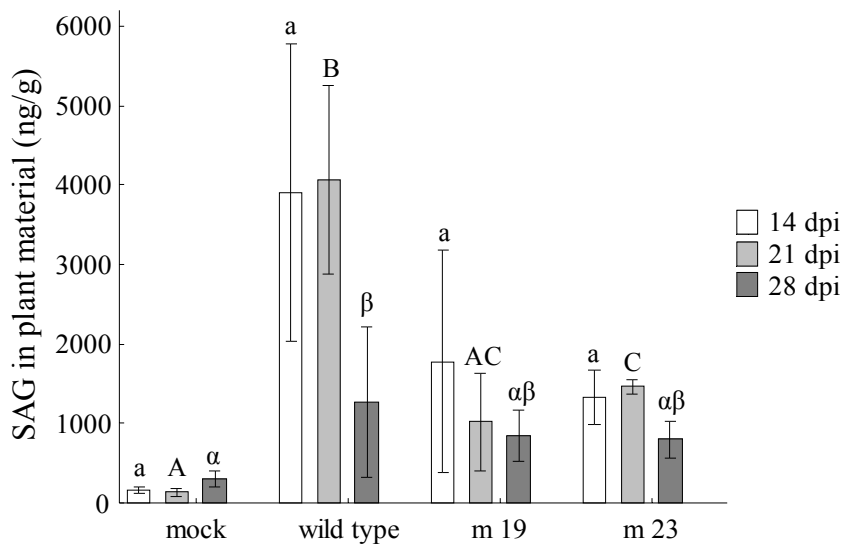


Figure 18: Levels of SAG in *B. napus* hypocotyl tissue

We measured a significant increase of the amount of SAG that is formed from SA by a glucosyl transferase (71) in wild type infected plants, but peculiarly, no changes in the levels of SA (data not shown). In the previous results shown by Ratzinger et al., a strong correlation between SA and SAG both in shoot tissue and xylem sap was measured. The VI-NEP-1 mutants m19 and m23 showed a lower induction potential of SAG but an even higher accumulation of SAG than in the mock inoculated plants. The lower amount of SAG for the mutants probably corresponds to the lower levels of fungal biomass measured for the mutants (see Figure 13) and is therefore connected to the reduced stunting effect shown in the pathogenicity assay on *B. napus*. At 28 dpi the accumulation of SAG and also SA is in both wild type and mutants decreased as compared to the earlier time points, which is believed to be because the fungus enters the saprophytic stage of its pathogenic life cycle showing characteristics of a necrotrophic pathogen and, as shown for *Arabidopsis* responses, triggers the JA and ethylene pathway of the plant to counteract fungal infestation. As shown, we could not show any differences in the induction of JA after 28 dpi, therefore we proceeded with the measurements of ethylene marker-genes to discover if there were any changes in the response to wild type or mutant infection of the plant.

Ethylene production is supposed to play an active role in *Verticillium* pathogenesis and in symptom development. Several ethylene-deficient *Arabidopsis* mutants (e.g. *ein2-1*, *ein4-1*, *ein6-1* or *etr1-1* (Col-0 background)) showed enhanced susceptibility towards *V. longisporum*

infection (13). In higher plants, ethylene is predominantly synthesized via the methionine precursor in the ‘Yang’ cycle (72, 73). S-Adenosyl-L-methionine is transformed to 5`methylthioadenosine and 1-ammino-cyclopropane-carboxylate by ACSs. The latter is transformed into ethylene by ACOs. To confirm that VI-NEP-1 induces the ethylene production in *B. napus* plants and is not synthesized by the fungus itself, we quantified ethylene concentrations of the wild type strain and the two mutants m19 and m23. Ethylene production by the fungal mycelium was measured by a gas chromatography (GC)-flame ionization detector. We ensured that no plants were present in the experimental setup in order to be certain that the ethylene detected was indeed produced by the mycelium. The fungus was grown in liquid PDB medium in SPME vials that were closed and airtight, with and without supplementation of 5 mM methionine, and were pre-cultivated for five days.

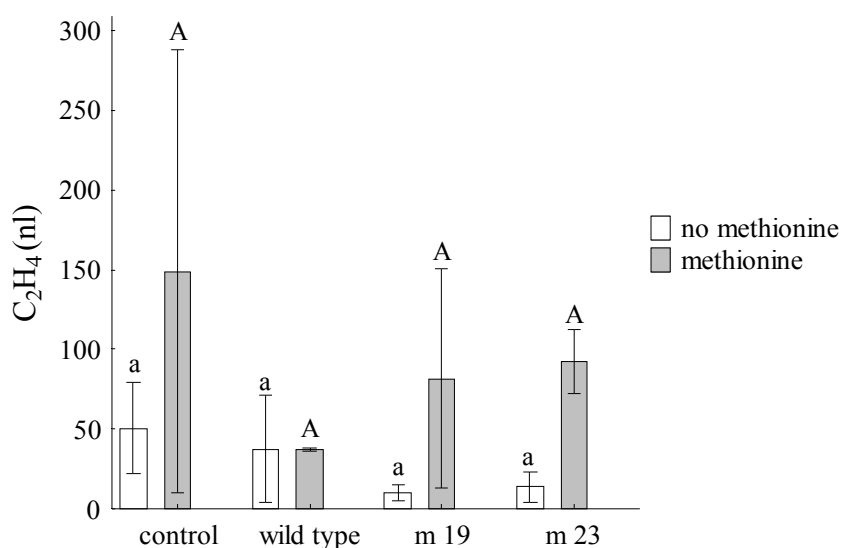


Figure 19: Ethylene production of *V. longisporum*

Results are shown as the average of four replicates (y axis indicates the amount of ethylene in the 20ml vial; Bars indicate standard deviation.) **m 19/23** = VI-NEP-1 mutants m 19 and m 23

The PDB medium itself (control) releases small quantities of ethylene, and neither wild type nor mutants seem to produce more ethylene than the media control ($P > 0.05$, K-Wallis test). No indication for ethylene production of *V. longisporum* was detected. Neither the wild type nor the mutants showed higher concentrations of ethylene compared to the medium control. Slightly lower concentrations were measured for the VI-NEP-1 silencing mutants grown in PDB medium without methionine supplementation.

In order to investigate the influence of VI-NEP-1 expression on the biosynthesis of ethylene in *B. napus*, we measured the expression levels of the ACS-1 gene using primers derived from *B. oleracea* and the ACO-1 gene (gb|L27664.1) in *B. napus* plants infected with the wild type and the VI-NEP-1 mutants m19 and m23 by qRT-PCR. The expression of the genes was calculated relative to the mock inoculated plants. In the literature it was shown that genes encoding ACS and ACO are strongly expressed upon treatment with an NLP from *P. parasitica* (6), but here we could not find any difference in the expression levels of the ACS and ACO in plants treated with *V. longisporum* wild type compared to the VI-NEP-1 silencing mutant. After 28 dpi we measured a rise in the expression of the ACS-1 gene, which could be an indication of the change in the life style of the fungus, as it changed its behaviour to that of a necrotrophic pathogen, triggering ethylene induction as shown for *Arabidopsis* responses.

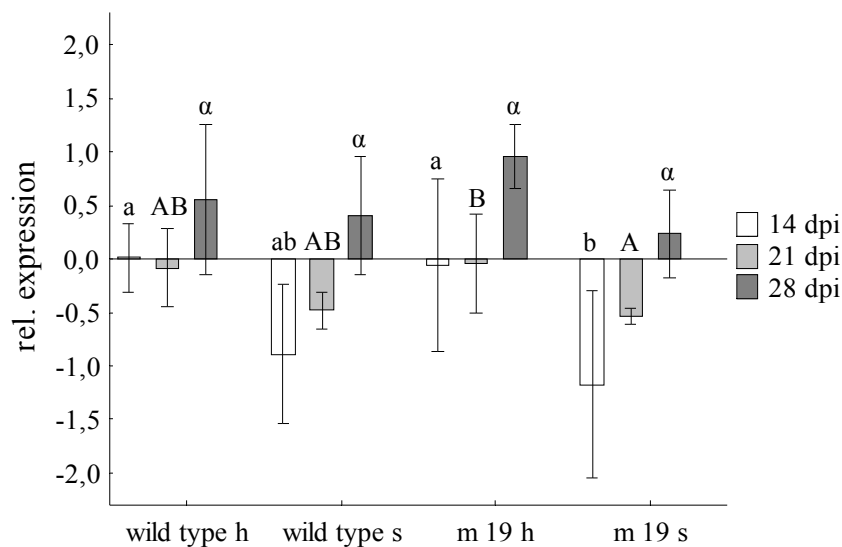


Figure 20: Induction of ACS-1 in hypocotyl and shoot samples of plants infected wild type (WT) and VI-NEP-1 mutant m19 (h = hypocotyl; s = shoot)

Applies for all marker-gene expression-level measurements: Ratios of relative expressions levels to mock inoculated plants were calculated as the mean of $\Delta\Delta\text{Ct}$ values of three biological replicas at each time point. Transcript levels of genes were measured and normalized using two housekeeping genes, actin and histone.

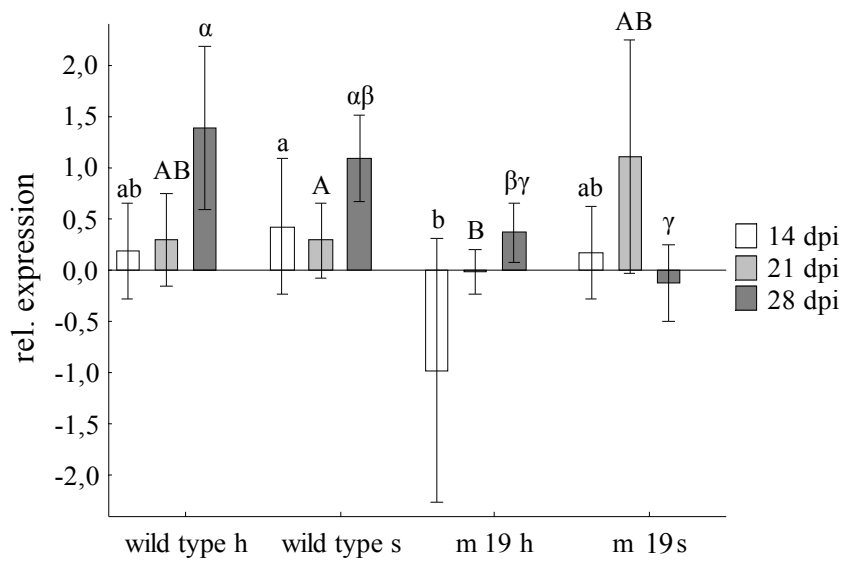


Figure 21: Induction of ACO-1 in hypocotyl and shoot samples of plants infected wild type (WT) and VI-NEP-1 mutant m19

While ethylene has been mainly associated with the development of disease symptoms in *Verticillium* interactions with their host-plants, JA has been shown to be involved in resistance processes. For instance, JA-insensitive *Arabidopsis* plants have been shown to suffer more severely from infection with *Verticillium* (74, 75). Infiltration of the *V. dahlia* orthologous protein of VI-NEP-1 into leaves of *A. thaliana* results in the activation of both SA- and JA-dependent defence pathways. Therefore, we tested the JA-marker gene PDF-1.2 to ascertain whether it was affected by the infection with *V. longisporum* VI-NEP-1 silencing mutants.

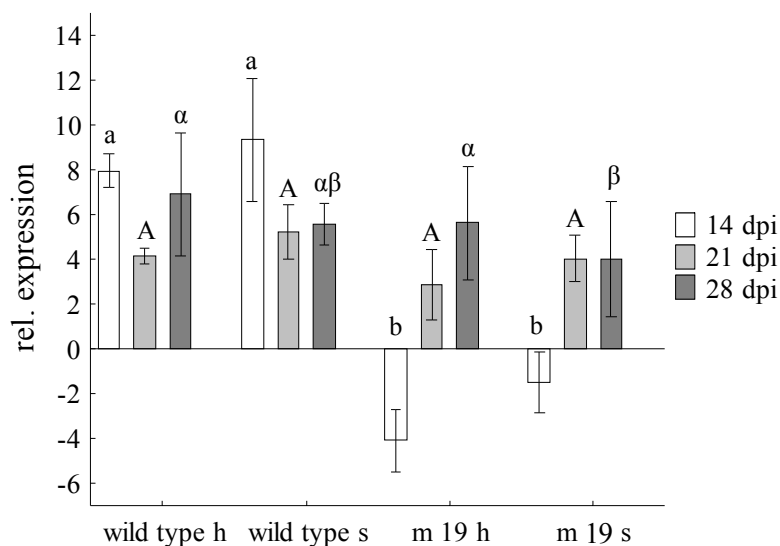


Figure 22: Induction of the JA-marker gene PDF-1.2 in hypocotyl and shoot samples of plants infected with *V. longisporum* wild type and VI-NEP-1 mutant m19

As mentioned before, JA does not seem to be induced by the infection with *V. longisporum*. Nevertheless, we measured a significant upregulation of the expression of PDF-1.2 in wild type infected plants relative to mock inoculated ones, which indicates that the plants probably react to the infection by activating the JA-pathway to accumulate the phytohormone which probably results in the expression of defence-related genes such as pathogenicity-related (PR) genes. The significant downregulation of the PDF-1.2 gene expression that we measured in plants infected with the VI-NEP-1 silencing mutant m19 at 14 dpi could be an indication that the mutant was not well detected by the plant and therefore did not counteract the expression of defence genes. Unfortunately, the expression analysis of the PR-1 gene could not be evaluated during this measurement; therefore further experiments must be performed to strengthen the results and to support this hypothesis.

All documented effects triggered by NLP exposure on plants, such as transcript accumulation of hormone biosynthesis enzyme-encoding genes, production of ROS and ethylene, callose apposition and HR-like cell death, were demonstrated using the purified protein for plant assays. It was reported in literature that using the purified Vd-NEP-A protein, which is the orthologous gene from *V. dahliae* to VI-NEP-1 from *V. longisporum*, for infiltration into leaves of *N. benthamiana* and *A. thaliana* plants, resulted in the formation of necrotic lesions and also resulted in triggering of the production of ROS and the expression of PR genes.

Therefore, we proceeded with the purification of the VI-NEP-1 protein to obtain detailed insights into the mode of action of the protein. This allowed us to draw conclusions on the previous results showing less fungal DNA, even though the plant-infection process by VI-NEP-1 silencing mutants was not impaired compared to that of the wild type fungus, which resulted in less symptom severity of plant infection in the mutants being monitored.

Overexpression and purification of VI-NEP-1 protein and subsequent experiments

RNA was extracted from mycelium of *V. longisporum*, grown in 10 ml of liquid SXM medium (1×10^4 spores, 23 °C, 10 days), for first strand cDNA synthesis to PCR-amplify VI-NEP-1 gene with primers for the complete exon sequence. The amplicon was purified using ‘QIAquick Gel Extraction Kit’ (Qiagen, Hilden, Germany) and ligated into pET21a, resulting in the VI-NEP-1 expression vector pET21a-VI-NEP-1 (6.9 kb) including a polyhistidine-tag (his-tag) required for protein-purification. The plasmid was transformed in *E. coli* BL21 cells, and protein expression of the VI-NEP-1 gene was induced using IPTG. The desired protein was subsequently purified with preparative SDS-PAGE using a chromatography column with nickel beads (Ni^{2+}) and was concentrated, resulting in a purity of >95 % which was good enough for protein-bioassays and polyclonal antibody production for western hybridizations.

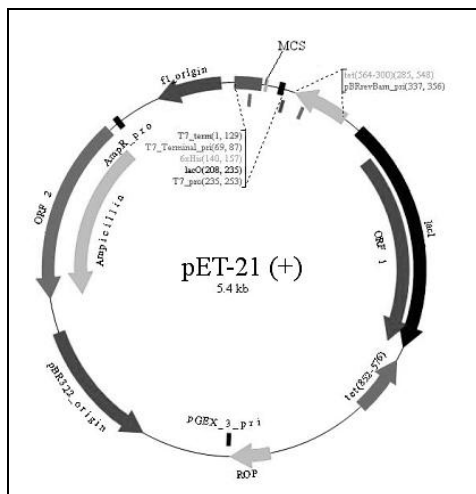


Figure 23: pET-21a expression vector

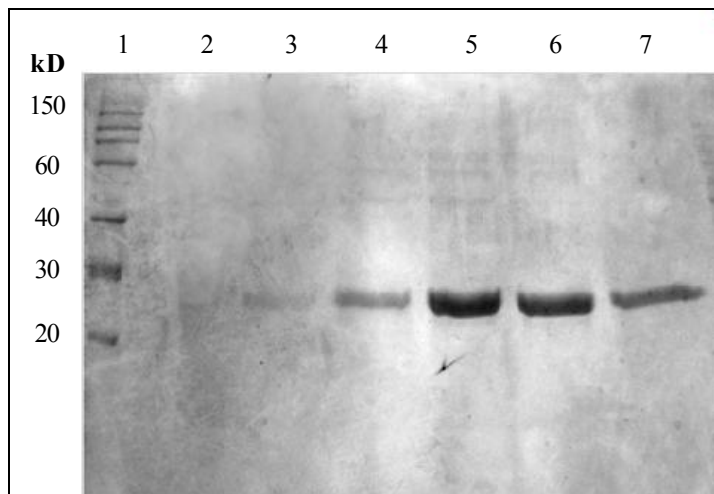


Figure 24: Purification of VI-NEP-1 protein, expression induction using different concentrations of imidazol

1 = Roti®-Mark 10-150 PLUS 2-6 = different imidazol concentrations (5-50 mM)
 7 = crude His-NEP protein

Plants react on NLP exposure with different responses. The way NLPs trigger these is mostly unidentified. NLPs from *P. aphanidermatum*, *F. oxysporum*, *P. parasitica* and *P. sojae* (4, 6, 15, 20) have been shown to induce necrotic responses by infiltrating the purified protein into the leaves of host plants. To study the effects of the pure protein of VI-NEP-1 on plant organs, we infiltrated the protein through the abaxial surface, delivering it by a syringe into the leaves of *B. napus* and *N. tabacum* to visualize putative lesion formation on the leaves. Different concentrations (5 to 0.0005 μg) of the protein were used for infiltration to show if the protein acted in a dose-dependent manner as reported in the literature for other NLPs (6, 15). NLP-induced necrosis is sensitive to changes in protein structure that occur by heating the protein to 65 °C; therefore we used heat-inactivated VI-NEP-1 as a negative control as confirmed by Fellbrich et al., where a reduced activity of up to 92 % (19) was shown.

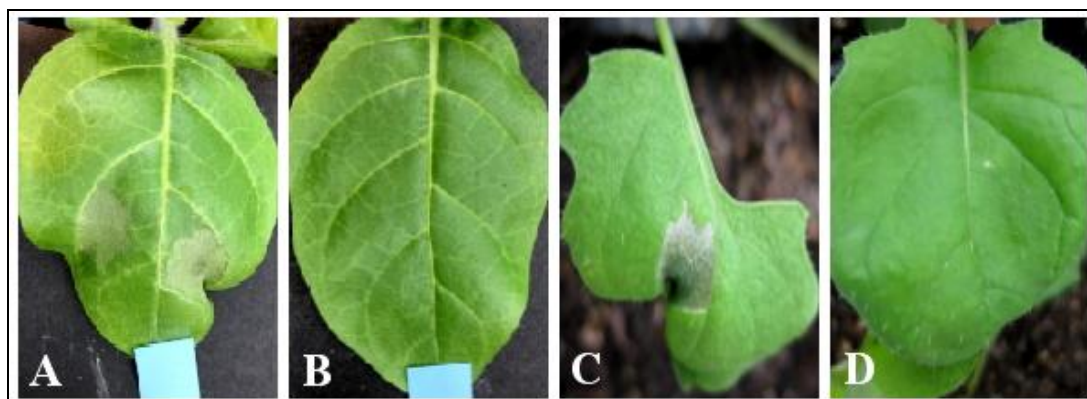


Figure 25: Effects on leaves of *B. napus* and *N. tabacum* infiltrated with VI-NEP-1 protein

A = *N. tabacum* treated with native VI-NEP-1 (5 μg)

B = *N. tabacum* treated with boiled VI-NEP-1

C = *B. napus* treated with native VI-NEP-1 (5 μg)

D = *B. napus* treated with boiled VI-NEP-1

We could demonstrate that VI-NEP-1 protein caused leaf necrosis in both plants. The necrotic lesions were visually apparent within 12 days post-infiltration in a dose-dependent manner. The threshold of necrosis induction is between 0.0005 μg and 0.005 μg . Additionally, we could show that susceptibility to necrosis was also leaf age-dependent after testing on different old leaves (see Figure 26). Younger leaves showed a more severe necrosis formation as compared to older leaves treated with the same concentration of the protein.

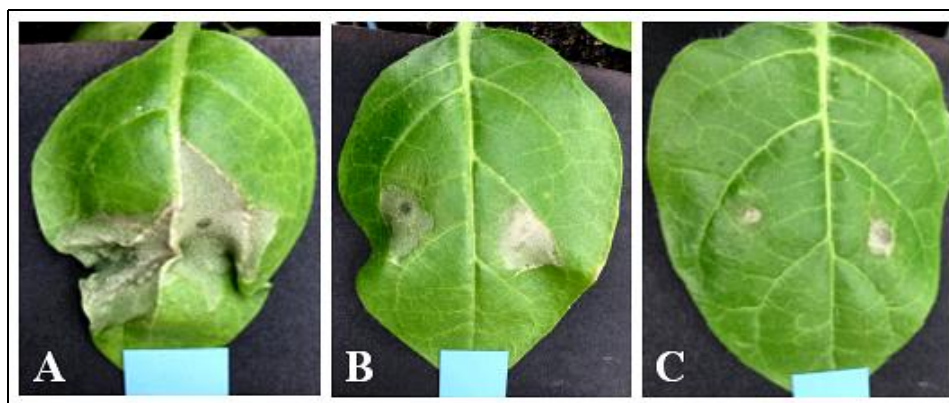


Figure 26: Effects on leaves with different age of *N. tabacum* infiltrated with VI-NEP-1 protein

A = third leaf of *N. tabacum* plant treated with native VI-NEP-1 (2,5 μg)

B = fourth leaf of *N. tabacum* plant treated with native VI-NEP-1 (2,5 μg)

C = fifth leaf of *N. tabacum* plant treated with native VI-NEP-1 (2,5 μg)

To assess the effects of VI-NEP-1 protein on plant growth, seedlings of ‘rapid cycling rape’ and *Arabidopsis* ecotypes Bur, Col-0 and Ler were treated with the purified protein. It is known from literature that an ecotype-specific genetic variability exists in *Arabidopsis* (77, 78). Ecotype Bur is known to be more resistant to *V. longisporum* infection as compared to Ler or Col-0 (79). For protein treatment, seedlings were grown on agar plates supplemented with increasing concentrations (50 to 5 $\mu\text{g/ml}$) of purified VI-NEP-1. Exposure of purified NLPs from *P. sojae* to *Arabidopsis* ecotype Col-0 (23) and a NLP from *F. oxysporum* tested on 17 different ecotypes (5) was shown to result in a significant reduction of root growth. Here we tested for the first time the effect of an NLP from *V. longisporum* to show the effects of natural host plant *B. napus*.

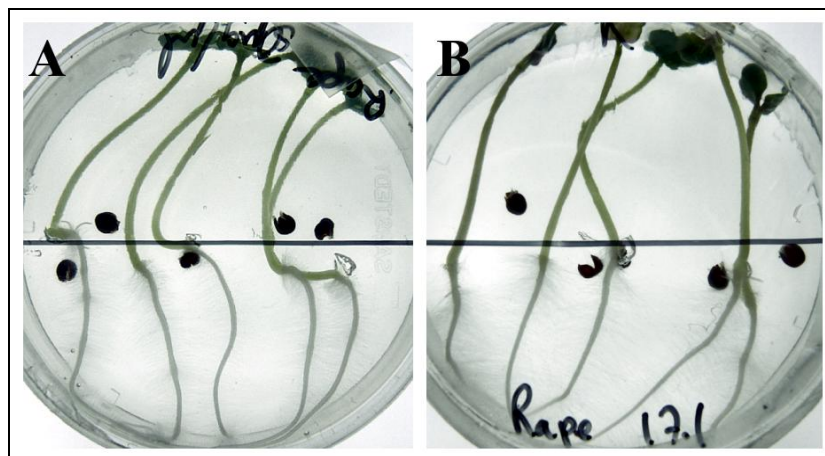


Figure 27: Effects on seedlings of *B. napus* treated with VI-NEP-1 protein

A = seedlings grown for 4 days in agar supplemented with 50 $\mu\text{g/ml}$ VI-NEP-1 protein

B = seedlings grown for 4 days in agar without the protein

When *Brassica* seedlings were treated with VI-NEP-1, the growth of roots and cotyledons were not inhibited for any of the tested protein concentrations. The plants showed no disease symptoms as reported for NLP exposure on *Arabidopsis*. We could also prove that VI-NEP shows effects on the growth of *Arabidopsis* roots. The inhibition-effect on the root-length was severe and showed a significant reduction for all tested concentrations on all tested ecotypes. The *Arabidopsis* ecotype Bur seemed to recover after approximately 8 dpi, showing similar root length compared to non-treated control plants.

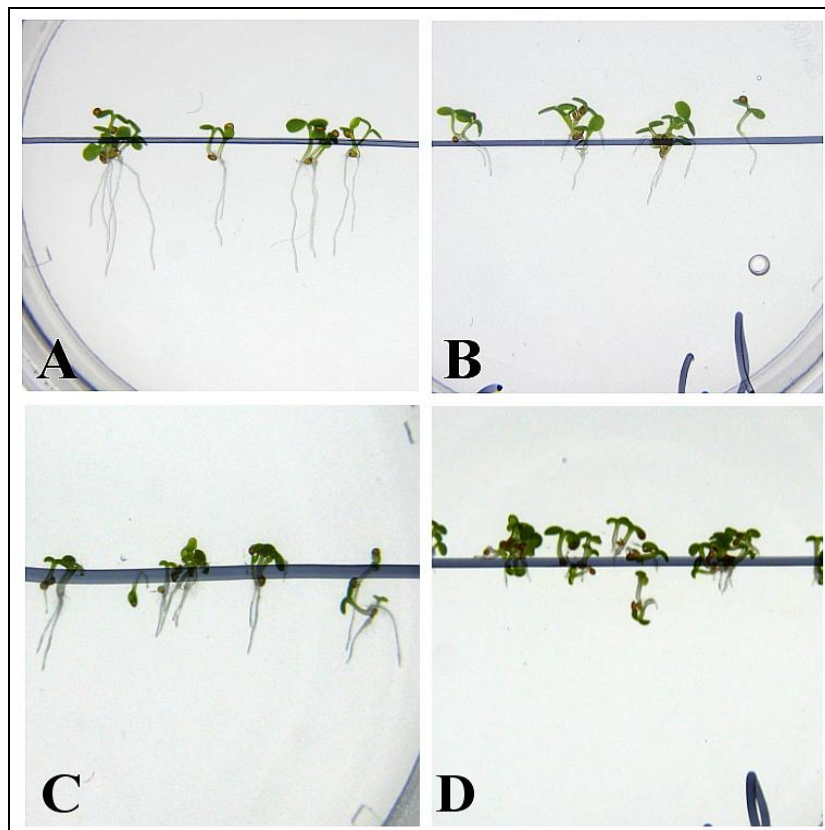


Figure 28: Effects on seedlings of *Arabidopsis* ecotypes Ler and Bur treated with VI-NEP-1 protein

A = seedlings (Ler) grown for 4 days in agar without the protein

B = seedlings (Ler) grown for 4 days in agar supplemented with 50 µg/ml VI-NEP-1 protein

C = seedlings (Bur) grown for 4 days in agar without the protein

D = seedlings (Bur) grown for 4 days in agar supplemented with 50 µg/ml VI-NEP-1 protein

In 2006, Bae et al. reported on the further effects on *Arabidopsis* plants as a result of treatment with an NLP from *F. oxysporum*. Besides the already mentioned inhibition effect on the root growth, he showed necrotic lesion formation on cotyledons, inhibition of the formation of root hairs, and damaged root tips due to protein exposure. Interestingly, VI-NEP-

1 treatment resulted in the induction of the formation of root hairs of *Arabidopsis* ecotypes Bur, Ler and Col-0, which stands in complete contradiction to the observations shown for the NLP of *F. oxysporum* (23).

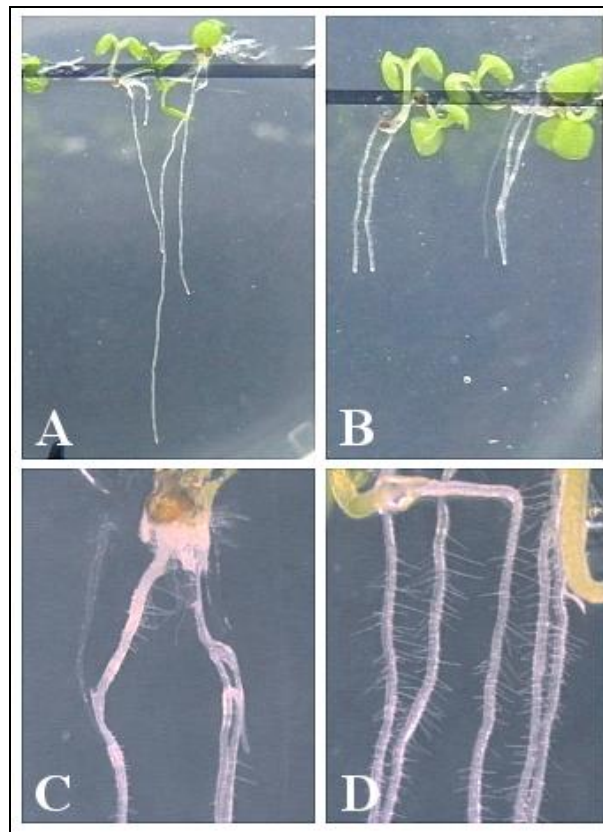


Figure 29: Effects on seedlings of *Arabidopsis* ecotypes Ler and Bur treated with VI-NEP-1 protein

A = seedlings (Ler) grown for 4 days in agar without the protein

B = seedlings (Ler) grown for 4 days in agar supplemented with 50 µg/ml VI-NEP-1 protein

C = seedlings (Bur) grown for 4 days in agar without the protein

D = seedlings (Bur) grown for 4 days in agar supplemented with 50 µg/ml VI-NEP-1 protein

The plant material was collected from both experiments for further phytohormone measurements by HPLC-MS and expression analysis of hormone biosynthesis enzyme-encoding genes for different plant defence pathways by qRT-PCR to prove the influence of VI-NEP-1 on the phytohormone level during infection with the fungus.

To ensure that the VI-NEP-1 protein is synthesized and secreted in the plant by *V. longisporum* wild type and repressed in the VI-NEP-1 knock-down mutants, we analysed the expression of the protein by western hybridization using VI-NEP-1 polyclonal antiserum.

Therefore, we grew wild type and VI-NEP-1 mutants in the sugar rich complete PDB medium and in artificial synthetic SXM medium which simulates the basic nutritional condition of a xylem environment. Both the mycelium and supernatant of the cultures were used for western blotting.

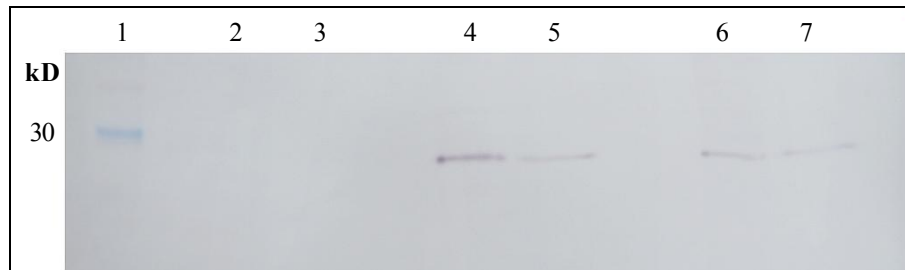


Figure 30: Detection of VI-NEP-1 protein in fungal mycelium and culture supernatant by western hybridization

- 1 = Marker
- 2 = mycelium of wild type fungus grown in PDB medium
- 3 = culture supernatant of wild type fungus grown in PDB medium
- 4 = mycelium of wild type grown fungus in SXM medium
- 5 = culture supernatant of wild type grown fungus in SXM medium
- 6 = mycelium of VI-NEP-1 mutant m19 grown in SXM medium
- 7 = culture supernatant of VI-NEP-1 mutant m19 grown in SXM medium

We could only detect signals representing the expressed VI-NEP-1 protein in extracts of *V. longisporum* grown in SXM medium, which suggests that the expression of VI-NEP-1 is induced by the presence of conditions imitating the xylem sap environment. Additionally, the culture supernatant also showed signals for VI-NEP-1, which indicated that this was a secretory protein, which, as shown in the literature, is a typical feature of different NLPs (15, 16). The band intensity displaying the protein expression of VI-NEP-1 silencing mutant m19 grown in mycelium was slightly lower compared to wild type expression as a result of post-transcriptional silencing by RNAi.

As mentioned, the pathogenic life cycle of *V. longisporum* is characterized by the biotrophic growth of the fungus staying in the vascular system up to a late stage of *B. napus* infestation. After approximately 28 dpi, the fungus enters the saprophytic phase and starts spreading into the upper parts of the plant. A recent study showed that the amount of fungal DNA increases up to five times after 35 dpi as compared to the amount after 28 dpi (45) indicating that the

fungus does not leave the hypocotyl until this time. To find if VI-NEP-1 can act as a signalling molecule during infection by *B. napus*, we harvested plant tissue from the root and the upper part of the stem after 28 dpi to see if we could detect signals for VI-NEP-1 expression by western hybridization in the stem, although the fungus was absent in this part of the plant.

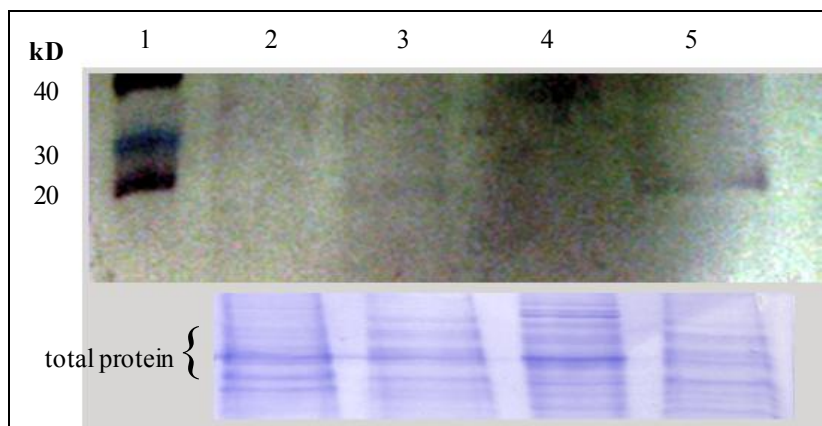


Figure 31: Detection of VI-NEP-1 protein in infected plant tissue by western hybridization

1 = Marker

2 = stem tissue of non-infected plants after 28 dpi

3 = stem tissue of infected plants after 28 dpi

4 = hypocotyl tissue of non-infected plants after 28 dpi

5 = hypocotyl tissue of infected plants after 28 dpi

The blot showed a strong signal for VI-NEP-1 expression in protein extracts of the hypocotyl tissue of infected plants, and furthermore a slighter signal in the lane using stem tissue of infected plants after 28 dpi. This may indicate that the protein is transported upwards in infected plants even though the fungus is still not present. This gives us a hint to an elicitor-like mode of action of VI-NEP-1, but still the specific function of the protein remains unclear.

Recently we have started to use immunofluorescence microscopy with the aid of FITC-labelled antibodies of VI-NEP-1 to investigate the distribution of the protein in terms of expression time and site of action, in order to clarify the putative effects of VI-NEP-1. Therefore, 20-30 μm thick samples from different plant parts were examined using a laser scanning fluorescence microscope. Preliminary results are highlighted by two digital images showing *V. longisporum* growing in the root after 28 dpi (see Figure 32) and a cross-section

of the stem showing direct immunofluorescence due to antibody deposition mainly in the vascular system of *B. napus* (see Figure 33).

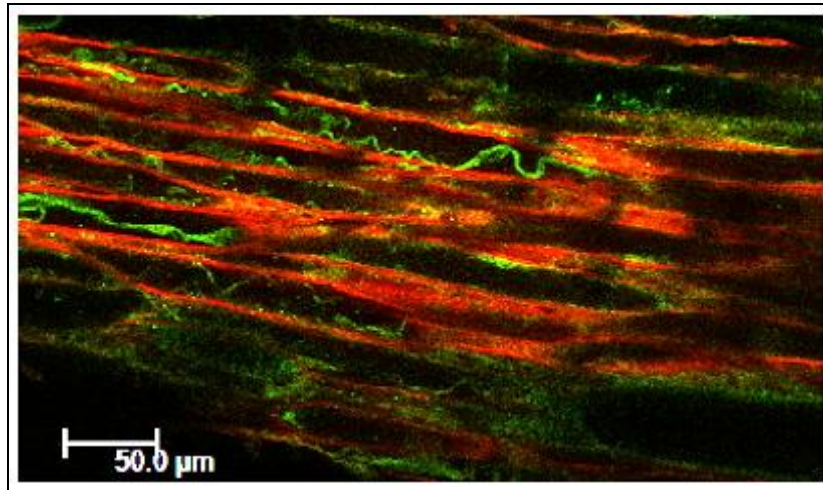


Figure 32: Digital image of a longitudinal section of a root sample after 28 dpi

During this experiment, we could only detect fungal hyphae in the root and rarely in hypocotyl samples of *V. longisporum*-infected plants, but we have never seen growing fungus in the stem even after 35 dpi. Nevertheless, a clear immunofluorescence could be observed after 28 dpi in both stem and leaf tissues in contrast to non-infected plant samples. The protein seems to accumulate in and around the central cylinder of the plants, which gives a further indication that VI-NEP-1 is transported upstream to the upper parts of the plant.

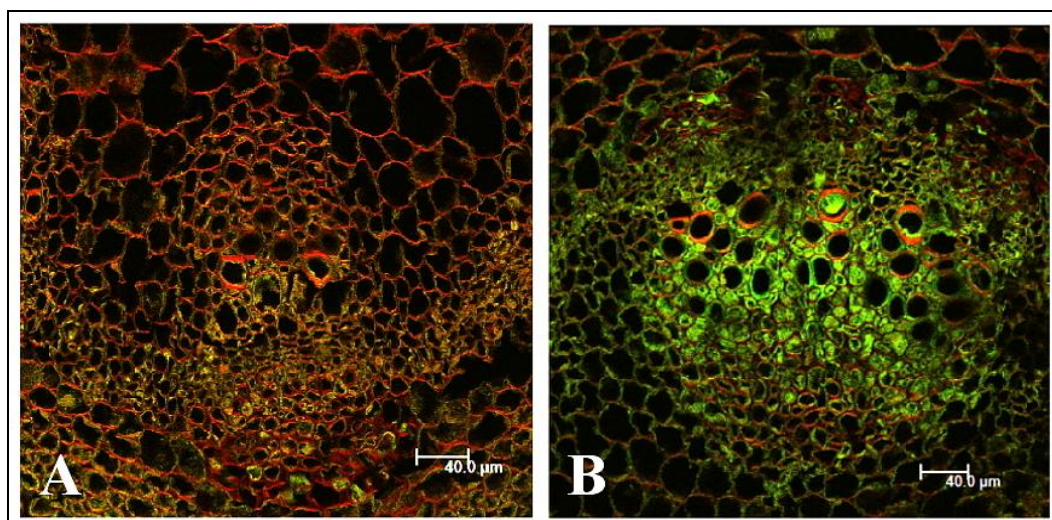


Figure 33: Digital image of a cross-section of a stem sample after 35 dpi

A = control (uninfected plant) **B** = infected plant

The restricted localization of the VI-NEP-1 protein to the vascular system during the whole infection cycle of *V. longisporum* makes a function at this location likely. The hydrophilic property shown for NLPs (6) probably prevents the protein passing through the plasma membranes into the plant cells. Therefore it is most likely that NLPs act as signal molecules identified by receptors attached to the cell walls of plants. The identification of the putative receptor of the protein is closely connected with the identification of the function of VI-NEP-1 of clarifying the impact of these protein in the plant-pathogen interaction of *V. longisporum* and *B. napus*.

CONCLUSIONS

In this chapter, we have reported on the identification of five NLPs of *V. longisporum* (see Figure 3 and Table 3) and the characterization of one of them named VI-NEP-1, which is the orthologous gene of Vd-NEP-A. This is found in the parental *V. dahliae* genome and has been proven in literature to have the ability to trigger plant responses such as wilting as a result of protein infiltration of natural host plant cotton. In 2002, Bailey demonstrated that a disruption or overexpression of an NLP gene from *F. oxysporum* had no impact on the ability of the fungus to exert an influence on the host plant *Erythroxylum coca* (4). However, that study was unable to detect any transcripts in the plant of these NLPs, even in the overexpressed mutants. In 2004, Pemberton et al. postulated that the nutritional limitations of the xylem sap result in the absence of any expression of NLPs *in planta* for pathogens mainly located in the xylem. Additionally, they mentioned that NLPs that are expressed *in planta* probably alert plants to the presence of pathogens and subsequently trigger plant defences that bring any infection to a sudden end (16). Nevertheless, due to the fact that *V. longisporum* is known to stay in the xylem up to a late stage of infection, living as a biotroph organism undetected by the plant, we could measure strong expression levels of three NLP genes (VI-NEP-1, -2, -5) *in planta* by qRT-PCR. This finding makes acceptable a contribution in the pathogenic life cycle of *V. longisporum* while infecting *B. napus* as compared to non-expressed NLPs from other pathogens. VI-NEP genes with higher homology to *V. dahliae* (VI-NEP-1, -2, -5) were shown to be expressed; those to *V. albo-atrum* were not (compare Table 3 with Figure 5). Therefore,

it must be assumed that *V. dahliae* genes in the *V. longisporum* genome express the virulence/pathogenicity of the fungus in *B. napus*.

Pathogenicity assays using ‘rapid cycle rape’ infected with generated VI-NEP-1 mutants with a silencing efficiency of protein expression of over 90 % show a significant reduction in symptom severity, indicated by reduced stunting and a lower disease score on plants infected with silencing mutants compared to wild type infection (Figure 10-12). The reproducibility of the effects on plants was proved by four independent experiments showing the same results as before. We are firmly convinced that the lower symptom severity was caused by a reduced presence of the fungus in the plants infected with the mutants as proven by the lower amount of fungal DNA we measured by qPCR (Figure 13). At this stage we believe that the VI-NEP-1 silencing mutants may have partly lost their ability to enter the plant via the roots due to an up to date, unknown function of the VI-NEP-1 protein. However, this assumption was rejected because of the results of CLSM studies on the infection of plants with both wild type and VI-NEP-1 mutants, which showed no difference in the ability to enter the roots of the plants or in the speed of infection (Figure 14-15).

The recognition of pathogens by infected plants and the subsequent initiation of defence strategies and conversely the overcoming of these plant defences by the invader are of crucial importance in plant pathogen interactions and are significant features in the classification of the interaction between the pathogen and the host-plant into that of compatible or a incompatible interaction. Researchers have found over the past decades that plants have evolved manifold recognition strategies to counteract an imminent infection by expression of different classes of resistance genes (R-genes) such as NBS-LRR genes (80) or the cell surface pattern recognition receptors (PRR) (81). The gene products of R-genes can recognize certain AVR gene products expressed by the pathogen and therefore respond to the attack by triggering the hypersensitive response (HR) or the systemic acquired resistance (SAR) for example. All these responses involve the accumulation of chemical messengers, such as SA or JA. These phytohormones can therefore be used as distinctive indicators to prove a reaction by measuring them and comparing them to the accumulated phytohormones of non-infected plants. In contrast to JA, it was shown that SA plays an important role in the response of *B. napus* to the infection with *V. longisporum*. We could not detect any significant change in the production of JA due to *V. longisporum* wild type nor to VI-NEP-1 silencing mutant infection

of *B. napus* as compared to un-infected plants (69). These results did not match our finding for the expression analysis of the JA-marker gene PDF-1.2 showing an upregulation in wild type infected and a downregulation in VI-NEP-1 silencing mutant infected plants, 14 dpi, in relation to the mock inoculated plants. Further measurements must be done to examine the impact of VI-NEP-1 on the plant defence driven by JA accumulation to prove the hypothesis that VI-NEP-1 mutants are not detected as well as the wild type fungus. The lower levels of SAG measured for the mutants are explainable by the lower levels of fungal biomass measured for the mutants by qPCR as revealed by Ratziger in 2008 (70). In the near future we will also perform phytohormone- and marker-gene measurements using plant material harvested from plants we use for infiltration assays with the purified protein. This will provide a more detailed look at the impact of VI-NEP-1 on the phytohormone balance of the plant infected with *V. longisporum* wild type and the silencing mutants, and will allow us to learn more about the role of VI-NEP-1 in fungus during an infestation of *B. napus*.

We were able to prove the distinctive features mentioned for NLPs by using the purified protein for plant assays during this work. Necrotic lesion formation through NLPs was shown in literature not to be host-specific, to be artificially inducible by leaf infiltration of the protein, to act in a dose-dependent manner and to be restricted to dicots, as no effect was detectable in monocotyl plants (32, 56, 62), moss, nor in any animal cell types (5). Here we have shown that the necrosis effect of VI-NEP-1 is inducible on leaves of *Brassica* and *Tobacco* after infiltration of the protein, showing both a leaf age and a dose-dependent impact on the severity of necrosis symptom characteristics. In field trials and greenhouse experiments, *B. napus* does not show any necrosis during infection with *V. longisporum* as compared to infection of host plants by other plant pathogenic *Verticillium* spp.; therefore we postulate that the concentration of VI-NEP-1 in the plant is apparently too low to induce necrosis *in vivo* and does not reach the phytotoxic threshold during natural infestation. Besides necrosis, the inhibition of root and cotyledon growth in *Arabidopsis* was reported (5, 23). However, we showed that VI-NEP-1 negatively affects the root growth of *Arabidopsis* seedlings but enhances the development of root hairs on all tested ecotypes when treated with the protein. In contrast to this, we were able to show that the growth of natural host plant *B. napus* is not affected at all by the treatment with the protein. As we showed by CLSM studies with VI-NEP-1 silencing mutants, the protein does not seem to be involved in the ability of the fungus to penetrate the root to get into the plant. There seems to be a crucial role for VI-

NEP-1 to infest the plant by giving the fungus the ability to spread in the plant but live undetected as a biotroph organism, as shown by pathogenicity assays using VL-NEP-1 silencing mutants and subsequent quantification of fungal DNA in the plant by qPCR. Pathogenicity assays using *A. thaliana* for inoculation showed no difference in symptom severity using VI-NEP-1 silencing mutants compared to wild type infected plants, which suggests that VI-NEP-1 does not play a crucial role during the infestation of *Arabidopsis*. This hypothesis seems to be supported by the fact that plants of *A. thaliana* react to morphological changes like inhibition of root length upon treatment with purified VI-NEP-1, whereas *B. napus* shows no changes, and therefore these plants probably differ in their defence reaction to infection. Furthermore, the reaction of *Arabidopsis* to *V. longisporum* does not lead to a drastic increase of SA compared to infection of *B. napus*, as proved by Ratzinger et al. in 2008 (70) and by our experiments, which leads to the assumption that the ways plants attempt to counteract fungal infestation vary.

Regarding our results from western hybridizations, showing the ability of VI-NEP-1 to secrete out of the fungus (see Figure 30) and to be transported upwards in the plant (see Figure 31) which was strengthened by immunofluorescence microscopy analysis showing a clear immunofluorescence in stem tissue in the absence of any fungal hyphae, we concluded our observations during this work by showing that the protein probably had a function in the xylem vessels of allowing the fungus to grow and spread into the plant. By accepting the recent characterization of NLPs as showing phytotoxic activity (5), structural high similarity to cytolytic toxins (30) and plasma membrane permeabilization activity, we end up with the hypothesis that VINEP-1 is secreted in the xylem by the fungus and permeabilizes the surrounding cell-membranes of the xylem cylinder and causes leakage of nutrients from adjacent tissue into the xylem sap, thereby increasing the fitness of *V. longisporum* in the xylem.

ACKNOWLEDGMENTS

The author would like to thank the following people for their outstanding assistance with this chapter:

Prof. Petr Karlovsky for giving me the opportunity to work on NLPs of *V. longisporum*, and his continuous assistance with scientific problems. **Dr. Arne Weiberg** for the excellent cooperation and the remarkable help with work on NLPs and with writing this chapter. **Mona Quambusch** for her assistance during *B. napus* pathogenicity assays, measuring phytohormone marker genes, and also for her work on CLSM studies. **Haidi Yin** and **Ruth Pilot** for working on the protein purification and subsequent related experiments. **Dr. Richard Splivallo** for measuring ethylene production of *V. longisporum*. **Haiquan Xu** for the construction of a *V. longisporum* genomic library and subsequent identification of VI-NEP genes.

REFERENCES

1. **Nürnberg T.** (1999). Signal perception in plant pathogen defence. *Cell. Mol. Life Sci.* 55:167-182.
2. **Luke H.H., Wheeler H.E.** (1955). Toxin production by *Helminthosporium victoriae*. *Phytopathol.* 45:453-458.
3. **Agrios G.N.** (2005). *Plant Pathology*. Elsevier Academic Press, London.
4. **Bailey B.A.** (1995). Purification of a protein from cultures filtrates of *Fusarium oxysporum* that induces ethylene and necrosis in leaves of *Erythroxylum coca*. *Phytopathol.* 85:1250-1255.
5. **Qutob D., Kemmerling B., Brunner F., Kufner I., Engelhardt S., Gust A.A., Luberacki B., et al.** (2006). Phytotoxicity and Innate Immune Responses Induced by Nep1-Like Proteins. *The Plant Cell* 18:3721-3744.
6. **Fellbrich G., Romanski A., Varet A., Blume B., Brunner F., Engelhardt S., Felix G., Kemmerling B., Krzymowska M., Nürnberg T.** (2002). NPP1, a *Phytophthora*-associated trigger of plant defence in parsley and *Arabidopsis*. *Plant J.* 32:375-390.
7. **Karapapa et al.** (1997). *Advances in Verticillium research and disease management*. St. Paul, Minnesota, APS Press, 196-203.
8. **Beckmann C.H.** (1987). *The nature of wilt disease of plants*. St. Paul, MN, USA, APS Press.

9. **Pullman, G. S., De Vay, J. E.** (1982). Epidemiology of *Verticillium* wilt of cotton: A relationship between inoculum density and disease progression. *Phytopathology* 72: 549-554.
10. **Koike M., Fujita M., Nagoa H., Ohshima S.** (1996): Random amplified polymorphic DNA analysis of Japanese isolates of *Verticillium dahliae* and *V. albo atrum*. *Plant Disease* 80: 1224-1227.
11. **Xiao C. L., Subbaro K. V.** (1998). Relationship between *Verticillium dahliae* inoculum density and wilt incidence, severity, and growth of cauliflower. *Phytopathology* 88: 1108-1115.
12. **Debode, J., Claeys, D. & Höfte, M.** (2004). Control of *Verticillium* wilt of cauliflower with crop residues, lignin and microbial antagonists. *IOBC WPRS Bull* 27, 41–45.
13. **Veronese P., Narasimhan M.L., Stevenson R.A., Zhu J.K., Weller S.C., Subbarao K.V., Bressan R.A.** (2003). Identification of a locus controlling *Verticillium* disease symptom response in *Arabidopsis thaliana*. *Plant J.* 35:574-587.
14. **Eynck C., Koopmann B., Grunewalt-Stocker G., Karlovsky P., von Tiedemann A.** (2007). Differential interactions of *Verticillium longisporum* and *V. dahliae* with *Brassica napus* detected with molecular and histological techniques. *Eur. J. Plant Pathol.* 118:259-274.
15. **Koch W., Wagner C., Seitz H.U.** (1998). Elicitor-induced cell death and phytoalexin synthesis in *Daucus carota* L. *Planta* 206:523-532.
16. **Pemberton C.L., Salmond G.P.C.** (2004). The Nep1-like proteins – a growing family of microbial elicitors of plant necrosis. *Mol. Plant Pathol.* 5:353-359.
17. **Ottmann C., Lubracki B., Kufner I., Koch W., Brunner F., Weyand M., Mattinen L., Pirhonen M., Anderluh G., Seitz H.U., Nürnberger T., Oecking C.** (2009). A common toxin fold mediates microbial attack and plant defence. *PNAS* 106 (25):10359-10364.
18. **Mattinen L., Tshuikina M., Mäe A., Pirhonen M.** (2004). Identification and Characterization of Nip, Necrosis-Inducing Virulence Protein of *Erwinia carotovora* subsp. *carotovora*. *MPMI* 17 (12):1366-1375.

19. **Fellbrich G., Blume B., Brunner F., Hirt H., Kroj T., Ligterink W., Romanski A., Nürnberger T.** (2000). *Phytophthora parasitica* Elicitor-Induced Reactions in Cells of *Petroselinum crispum*. *Plant Cell Physiol.* 41 (6):692-701.
20. **Qutob D., Kemmerling B., Brunner F., Kufner I., Engelhardt S., Gust A.A., Luberacki B., Seitz H.U., Stahl D., Rauhut T., Glawischnig E., Schween G., Lacombe B., Watanabe N., Lam E., Schlichting R., Scheel D., Nau K., Dodt G., Hubert D., Gijzen M., Nürnberger T.** (2002). Phytotoxicity and innate immune responses induced by Nep1-like proteins. *Plant Cell* 18:3721-3744.
21. **Jennings J.C., Apel-Birkhold P.C., Bailey B.A., Anderson J.D.** (2000). Induction of ethylene biosynthesis and necrosis in weed leaves by a *Fusarium oxysporum* protein. *Weed Sci.* 48:7-14.
22. **Keates S.E., Kostman T.A., Anderson J.D., Bailey B.A.** (2003). Altered gene expression in three plant species in response to treatment with Nep1, a fungal protein that causes necrosis. *Plant Physiol.* 132:1610-1622.
23. **Bae H., Kim M.S., Sicher R.C., Bae H.-J., Bailey B.A.** (2006). Necrosis- and ethylene inducing peptide from *Fusarium oxysporum* induces a complex cascade of transcripts associated with signal transduction and cell death in Arabidopsis. *Plant Physiol.* 141:1056-1067.
24. **Staats M., van Baarlem P., Schouten A., van Kan J.A.L., Bakker F.T.** (2007). Positive selection in phytotoxic protein-encoding genes of *Botrytis* species. *Fung. Genet. Biol.* 44:52-63.
25. **Garcia O., Macedo J.A., Tibúrcio R., Zaparoli G., Rincones J., Bittencourt L.M., Ceita G.O., Micheli F., Gesteira A., Mariano A.C., Schiavinato M.A., Medrano F.J., Meinhardt L.W., Pereira G.A., Cascardo J.C.** (2007). Characterization of necrosis and ethylene-inducing proteins (NEP) in the basidiomycete *Moniliophthora perniciosa*, the causal agent of witches' broom in *Theobroma cacao*. *Mycol. Res.* 111 (4):443-455.
26. **Schouten A., van Baarlen P., van Kan J.A.L.** (2008). Phytotoxic Nep1-like proteins from the necrotrophic fungus *Botrytis cinerea* associate with membranes and the nucleus of plant cells *New Phytologist* 177:493-505.

27. **Cechin A.L., Sinigaglia M., Lemke N., Echeverrigaray S., Cabrera O.G., Pereira G.A.G., Mombach J.C.M.** (2008). Cupin: A candidate molecular structure for the Nep1-like protein family. *BMC Plant Biol.* 8:50.
28. **Gijzen M., Nürnberger T.** (2006). Nep1-like proteins from plant pathogens: Recruitment and diversification of the NPP1 domain across taxa. *Phytochem.* 67:1800-1807.
29. **Fradin E.F., Thomma B.P.H.J.** (2006). Physiology and molecular aspects of *Verticillium* wilt diseases caused by *V. dahliae* and *V. albo-atrum*. *Mol. Plant Pathol.* 7:71-88.
30. **Küfner I, Ottmann C, Oecking C, Nürnberger T.** (2009). Cytolytic toxins as triggers of plant immune response. *Plant Signal Behav.* 2009 Oct;4(10):977-9.
31. **Wang J., Cai Y., Gou J., Mao Y., Xu Y., Jiang W., Chen X.** (2004). Vd-NEP, an elicitor from *Verticillium dahliae*, induces cotton plant wilting. *Appl. Environ. Microbiol.* 70:4989-4995.
32. **Veit S., Wörle J.M., Nürnberger T., Koch W., Seitz H.U.** (2001). A novel protein elicitor (PaNie) from *Pythium aphanidermatum* induces multiple defence responses in carrot, *Arabidopsis*, and tobacco. *Plant Physiol.* 127:832-841.
33. **Bailey B.A., Apel-Birkhold P.C, Luster D.G.** (2002). Expression of NEP1 by *Fusarium oxysporum* f. sp. *erythroxyli* After Gene Replacement and Overexpression Using Polyethylene Glycol-Mediated Transformation. *Phytopathol.* 92 (8):833-841.
34. **Zeise K., von Tiedemann A.** (2001) Morphological and physiological differentiation among vegetative compatibility groups of *Verticillium dahliae* in relation to *V. longisporum*. *Journal of Phytopathology* 149: 469-475.
35. **Williams PH. & Hill C. B.** (1986). Rapid-cycling populations of *Brassica*. *Science* 232, 1385-1389.
36. **NASC ID: N1029**, The European Arabidopsis Stock Centre, Loughborough, United Kingdom.
37. **NASC ID: N1092**, The European Arabidopsis Stock Centre, Loughborough, United Kingdom.
38. **NASC ID: N1686**, The European Arabidopsis Stock Centre, Loughborough, United Kingdom.

39. **Utermark J.** (2008). Genetic transformation of filamentous fungi by *Agrobacterium tumefaciens*. Nature Protocols, Published online 20 March 2008.
40. **Zeise, K.** (1992). Gewächshaustest zur Resistenzprüfung von Winterraps (*Brassica napus* L. var. *oleifera* Metzger) gegen den Erreger der Rapswelke *Verticillium dahliae* Kleb. Nachrichtenblatt Deutscher Pflanzenschutzdienst 44:125-128.
41. **Maniatis T., Fritsch EF., Sambrook J.** (1982). Molecular Cloning: A Laboratory Manual. Trade paperback, Cold Spring Harbor Laboratory Press.
42. **Xu H.** (2011). Dissertation, Georg-August University of Goettingen.
43. **Xiangqing Pan, Ruth Welti, Xuemin Wang** (2010). Quantitative analysis of major plant hormones in crude plant extracts by high-performance liquid chromatography-mass spectrometry. Nat Protoc. 2010 ;5 (6):986-92.
44. **Zou WJ, Yoneyama K, Takeuchi Y, Iso S, Rugmekarat S, Chae SH, Sato D, Joel DM** (2004) *In vitro* infection of host roots by differentiated calli of the parasitic plant *Orobanchae*. Journal of Experimental Botany 55: 899-907.
45. **Eynck C, Koopmann B., Grunewaldt-Stoecker G., Karlovsky P. and von Tiedemann A.** (2007). Differential interactions of *Verticillium longisporum* and *V. dahliae* with *Brassica napus* detected with molecular and histological techniques. European Journal of Plant Pathology, 118(3):259-274.
46. **Laemmli UK.** (1970). Cleavage of structural proteins during the assembly of the head of bacteriophage T4. Nature 227 (5259): 680–685.
47. **Blum H., Beier H., Gross HJ.** (1987). Improved silver staining of plant-proteins, RNA and DNA in polyacrylamide gels. Electrophoresis 8, p. 93–99.
48. **Bradford MM** (1976) A rapid and sensitive method for the quantitation of microgram quantities of protein utilizing the principle of protein-dye binding. Annu Rev Biochem 72 248–254.
49. **Shi SR, Key ME, Kalra KL.** (1991). Antigen retrieval in formalin-fixed, paraffin-embedded tissues: an enhancement method for immunohistochemical staining based on microwave oven heating of tissue sections. J Histochem Cytochem.; 39(6):741-8.
50. **The Broad Institute**, homepage *Verticillium* group database (<http://www.broad.mit.edu/annotation/genome/verticilliumdahliae/MultiHome.html>).
51. **National Center for Biotechnology Information**, homepage (<http://www.ncbi.nlm.nih.gov/>).

52. **Emanuelsson O., Brunak S., von Heijne G., Nielsen H.** (2007). Locating proteins in the cell using TargetP, SignalP, and related tools. *Nature Protocols* 2:953-971.
53. **Larkin M.A., Blackshields G., Brown N.P., Chenna R., McGettigan P.A., McWilliam H., Valentin F., Wallace I.M., Wilm A., Lopez R., Thompson J.D., Gibson T.J., Higgins D.G.** (2007). Clustal W and Clustal X version 2.0. *Bioinformatics* 23 (21):2947-2948.
54. **Gijzen, M. and Nürnberger, T.** (2006). Nep1-like proteins from plant pathogens: recruitment and diversification of the NPP1 domain across taxa. *Phytochemistry* 67(16): 1800-1807.
55. **Rice P., Longden I., Bleasby A.** (2000). EMBOSS: the European Molecular Biology Open Software Suite. *Trends Genet.* 16 (6):276-277.
56. **Motteram J., Kufner I., Deller S., Brunner F., Hammond-Kosack K.E., Nürnberger T., Rudd J.J.** (2009). Molecular Characterization and Functional Analysis of MgNLP, the Sole NPP1 Domain-Containing Protein, from the Fungal Wheat Leaf Pathogen *Mycosphaerella graminicola*. *MPMI* 22 (7):790-799.
57. **Saitou N., Nei M.** (1987). The neighbor-joining method: A new method for reconstructing phylogenetic trees. *Mol. Biol. Evol.* 4:406-425.
58. **Felsenstein J.** (1985). Confidence limits on phylogenies: An approach using the bootstrap. *Evolution* 39:783-791.
59. **Zuckerandl E., Pauling L.** (1965). Evolutionary divergence and convergence in proteins, pp. 97-166 in *Evolving Genes and Proteins*, edited by V. Bryson and H.J. Vogel. Academic Press, New York.
60. **Tamura K., Dudley J., Nei M., Kumar S.** (2007). MEGA4: Molecular Evolutionary Genetics Analysis (MEGA) software version 4.0. *Mol. Biol. Evol.* 24:1596-1599.
61. **Neumann M.J., Dobinson K.F.** (2003). Sequence tag analysis of gene expression during pathogenic growth and microsclerotia development in the vascular wilt pathogen *Verticillium dahliae*. *Fung. Genet. Biol.* 38:54-62.
62. **Staats M., Van Baarlen P., Schouten A., Van Kan J.A.L.** (2007). Functional analysis of NLP genes from *Botrytis elliptica*. *Mol. Plant Pathol.* 8 (2):209-214.
63. **Tyler BM, Tripathy S, Zhang X, Dehal P, Jiang RH, Aerts A, Arredondo FD, Baxter L, Bensasson D, Beynon JL, Chapman J, Damasceno CMB, Dorrance AE, Dou D, Dickerman AW, Dubchak IL, Garbelotto M, Gijzen M, Gordon SC,**

- Govers F, Grunwald NJ, Huang W, Ivors KL, Jones RW, Kamoun S, Krampis K, Lamour KH, Lee MK, McDonald WH, Medina M, Meijer HJG, Nordberg EK, Maclean DJ, Ospina- Giraldo MD, Morris PF, Phuntumart V, Putnam NH, Rash S, Rose JKC, Sakihama Y, Salamov AA, Savidor A, Scheuring CF, Smith BM, Sobral BWS, Terry A, Torto-Alalibo TA, Win J, Xu Z, Zhang H, Grigoriev IV, Rokhsar DS, Boore JL. (2006). *Phytophthora* genome sequences uncover evolutionary origins and mechanisms of pathogenesis. Science 313:1261-1266.**
64. **Barbara D.J., Clewes E. (2003).** Plant pathogenic *Verticillium* species: how many of them are there? Mol. Plant Pathol. 4:297-305.
65. **Fahleson J., Lagercrantz U., Hu Q., Steventon L.A., Dixelius C. (2003).** Estimation of genetic variation among *Verticillium* isolates using AFLP analysis. Eur. J. Plant Pathol. 109:361-371.
66. **Kadotani N., Nakayashiki H., Tosa Y., Mayama S. (2003).** RNA Silencing in the Phytopathogenic Fungus *Magnaporthe oryzae*. MPMI 16 (9):769-776.
67. **Nakayashiki H., Hanada S., Quoc N.B., Kadotani N., Tosa Y., Mayama S. (2005).** RNA silencing as a tool for exploring gene function in ascomycete fungi. Fung. Genet. Biol. 42:275-283.
68. **Pieterse CM, Van Loon LC. (2004).** NPR1: the spider in the web of induced resistance signaling pathways. Curr Opin Plant Biol. 2004 Aug;7(4):456-64.
69. **Glazebrook J. (2005).** Contrasting mechanisms of defence against biotrophic and necrotrophic pathogens. Annu Rev Phytopathol. 2005;43:205-27.
70. **Ratzinger A. (2008).** Development and application of LC-MS-based differential metabolic profiling in plant systems. Dissertation, Georg-August Universität Göttingen.
71. **Yalpani N, Balke NE, Schulz M (1992).** Induction of UDP-glucose: salicylic acid glucosyltransferase in oat roots. Plant Physiol 100:1114-1119.
72. **Buchanan B.B., Gruissem W., Jones R.L. (2002).** Biochemistry and Molecular Biology of Plants. Am Soc Plant Phys (Rockville).
73. **Wang K.C.L., Li H., Ecker J.R. (2002).** Ethylene Biosynthesis and Signaling Networks. Plant Cell (Supplement) S131-S151.

74. **Thaler, J.S., Owen, B. and Higgins, V.J.** (2004). The role of the jasmonate response in plant susceptibility to diverse pathogens with a range of lifestyles. *Plant Physiol.* 135, 530–538.
75. **Tjamos, S.E., Flemetakis, E., Paplomatas, E.J. and Katinakis, P.** (2005). Induction of resistance to *Verticillium dahliae* in *Arabidopsis thaliana* by biocontrol agent K-165 and pathogenesis-related proteins gene expression. *Mol. Plant–Microbe. Interact.* 18, 555–561.
76. **Johansson A, Staal J, Dixelius C** (2006). Early responses in the *Arabidopsis-Verticillium longisporum* pathosystem are dependent on NDR1, JA- and ET-associated signals via cytosolic NPR1 and RFO1. *Mol Plant Microbe Interact* 19:958-969
77. **Narang, R.A., Bruene, A., and Altmann, T.** (2000). Analysis of phosphate acquisition efficiency in different *Arabidopsis* accessions. *Plant Physiol* 124, 1786-1799.
78. **Meyer, R.C., Torjek, O., Becher, M., and Altmann, T.** (2004). Heterosis of biomass production in *Arabidopsis*. Establishment during early development. *Plant Physiol* 134, 1813-1823.
79. **Tappe H.** (2008). *Verticillium longisporum* induced gene expression in *Arabidopsis thaliana*. Dissertation, Georg-August University of Goettingen.
80. **McHale L, Tan X, Koehl P, Michelmore RW** (2006). Plant NBS-LRR proteins: adaptable guards. *Genome Biol* 7 (4): 212.
81. **Song W-Y Wang G-L, Zhu L-H Fauquet C, Ronald P** (1995). A receptor kinase-like protein encoded by the rice disease resistance gene Xa21. *Science* 270: 1804–1806.

APPENDIX

Primer name	Primer sequences
NEP-type A	F A TGCTTCCCTCCACAATC R AAACGCGGCGCGCATGTTTC
NEP-type B	F TGCCACGAGATTTCTCTCCA R CTGACATGCGGCGCACGTG
NEP-type C	F CAATTCGTATCAAGATCCAACACAG R CACCCGTCGGTCCATTGCT
NEP-type D	F ATAGCATGCCAGCTGCACTC R CGACTGCCAGAGCAGCTTGA
NEP-type E	F GCAACAGCCTCATCAGCCTCA R TCCGTATCTTGAGCACCGGA
NEP-type F	F ATCTCACTAGCCTTGTCTTC R CTGGGTCTGGCTTCCATTGT
NEP-type G	F ATCGGAAACATCTTCACTTGGC R TGGGTCTGATTTCGCAGTATC
NEP-type H	F AGATGGCGACTCGGTTCTGGT R TCATCTTCCGCATTAGCAAAGC

Table 6: *V. dahliae* NLP primers

Primer name	Primer sequences
VI-NEP-1	F CCAGCCTCTGCTTCACATTGCCACG R GGCCTGGTTTTCGTTGTTCGAGTTGA
VI-NEP-2	F ACGTAGTCGTCTTCGCACGCGGA R CGGGCTCTTGTAGAACGAGCCTG
VI-NEP-3	F GCGATTGTCTACCACAAGGACAGCA R GCCTAGCCTTGCGAATGTTCTCAG
VI-NEP-4	F TGCCGACGAGCGTAGCCATGCA R TCCTCATTAGCCCATGCCATGTGA
VI-NEP-5	F GTACGCTGCTTGGCTGGCACA R GTTGTGAAGCCACGTGCCGTCA
VI-tubulin	F GTTCATCTTCAGACCGGTCAGT R CGATCTCGTTTCGGAGTACCAGC
VI-rps17	F GCATCTGCGATGAGATCGCCA R TCGGAGTTCTGGGTAAAGTCGAGA

Table 7: *V. longisporum* qRT-PCR primers

Primer name	Primer sequences
VI-NEP-1-SB	F TGACGACATTCTCCCAGTCG
	R CGGTGAGGTCAAGTAAGACACGC

Table 8: VI-NEP-1 specific primers for southern hybridization

Primer name	Primer sequences
Bn-PR-1*	F AGTCACTAACTGTTCTCGAC
	R CGATTACACGTCCACATAATT
Bn-PDF-1.2*	F GAAGCACCAACAATGGTG
	R GTGACACAGACTTATTGAACG
Bn-aco-1	F CTCTCGAGACCGAAGTGGAAGA
	R CTGTGTGAGCCCTAAGCCCTTTG
Bn-acs-1	F ATCGATGACGTGTCAGTCAAGGAA
	R CATCCGACAACATGGAAGCCAA
Bn-act	F AAGAGCAGTTCTTCGGTGA
	R GCGACCACCTTGATCTTCAT
Bn-his	F AAAGGTCGTTACGCGATCAG
	R TTTGGCAGCTTTAGCAGCTT

*primer sequence published by Kamble et al. 2007.

Table 9: *B. napus* qRT-PCR primers

Primer name	Primer sequence
VI-NEP-1-sense- <i>SdaI</i> -F	TAGTGACCTGCAGGTGACGACATTCTCCCAGTCG
VI-NEP-1-sense- <i>NdeI</i> -R	GATATGCATATGCGGTGAGGTCAAGTAAGACACGC
VI-NEP-1-antisense- <i>AscI</i> -F	GAGCTCGGCGCGCCTGACGACATTCTCCCAGTCG
VI-NEP-1-antisense- <i>BglII</i> -R	GATATGAGATCTCGGTGAGGTCAAGTAAGACACGC
intron- <i>NdeI</i> -F	CTATACCATATGACTGCTCTACCCGTACGTTG
intron- <i>BglII</i> -R	GATATGAGATCTCCTGGCACTCTTTGCTATTGTTGG

Table 10: Primer sequences to construct a HP-fragment of VI-NEP-1

(bold: cloning sites; italic: gene-specific sequence)

Primer name	Primer sequence
OLG-70	CAGCGAAACGCGATATGTAG
OLG-71	GGCTTGTAGGGGGTTTAGA

Table 11: Primer sequences to amplify a fragment of an ITS region from *V. longisporum*

Primer name	Primer sequence
VL-NEP-1-cDNA-compl	F AGAGACATATGCAGCATCCCCCAAGGTTA
	R AGAGAGGATCCAGAAACGCGGCGCGCATGTTC

Table 12: Primer sequences to amplify complete cDNA of VI-NEP-1**Complete gDNA and cDNA sequences and alignments of VI-NEP genes**

VI-NEP-1	
gDNA sequence	
1 51 101 151 201 251 301 351 401 451 501 551 601 651 701 751	ATGCTTCCCTCCACAATCTTCTCGGTCTTTGCCCTCGTCGGCAGCGCCTT GGCTCAGCATCCCCCAAGGTTAACCACGACAGTATCAACCCCGTCCGCG ATACTCTGGGGCCCAACGGCGACATGATCAGGAAGTTCAGCCTCTGCTT CACATTGCCACGGTTGCCAGCCTTACTCCGCTGTCAACACCCGCGGTGA GGTCAAGTAAGACACGCAGCACTCCCTTCAGCTTACACAAAGCTCCACGC TAACACATATTCTGCAGCGCCGGTCTCCAAGACAGCGGTACCACCGCAGG CGGCTGCAAGGAAACCAGCAAGGGCCAGACCTACGCCCGCTCCATGACCC TGAACGGCCAGTTCGGCATCATGTACGCCCTGGTACTGGCCCAAGGACCAG CCCGCCGACGGCAACCTCGCCAGCGGCCACCGCCACGACTGGGAGAACGT CGTCATCTGGTTCAACTCGAACAACGCAAACCAGGCCGGCATCCTGCGCG GCGCCGCTCGGGCCACGGCGACTACAAGAAGGTCAACAACCCCCAGCGC AACAAACAACCTCCACGTCGAGTACTTCACCAGCCTCGGCAAGAACCA CGAGCTGCAGTTCAAGACGTCGCCCCGGCCGACCTACTGGATCTGGGACT GGGACAGGATGGACAGCACCGTCCAGGGCGCCCTCAACCGCGCCGACTTT GGCAGCGCAACTGCCCTTCAACAACAACAACCTTTGAGAGGAACATGCG CGCCGCTTTTAA
cDNA sequence	
1 51 101 151 201 251 301 351 401 451 501 551 601 651 701	ATGCTTCCCTCCACAATCTTCTCGGTTTTTGTCTCGTCGGCAGCGCCTT GGCTCAGCATCCCCCAAGGTTAACCACGACAGTATCAACCCCGTCCGCG ATACTCTGGGGCCCAACGGCGACATGATCAGGAAGTTCAGCCTCTGCTT CACATTGCCACGGTTGCCAGCCTTACTCCGCTGTCAACACCCGCGGTGA GGTCAACGCCGGTCTCCAAGACAGCGGTACCACCGCAGGCGGTGCAAGG AAACCAGCAAGGGCCAGACCTACGCCCGCTCCATGACCCTGAACGGCCAG TTCGGCATCATGTACGCCCTGGTACTGGCCCAAGGACCAGCCCGCCGACGG CAACCTCGCCAGCGGCCACCGCCACGACTGGGAGAACGTCTGTCATCTGGT TCAACTCGAACAACGCAAACCAGGCCGGCATCCTGCGCGGCGCCGCTCG GGCCAGGCGACTACAAGAAGGTCAACAACCCCCAGCGCAACAACAACA CCTCCAGTCGAGTACTTCACCAGCCTCGGCAAGAACCACGAGCTGCAGT TCAAGACGTCGCCCCGGCCGACCTACTGGATCTGGGACTGGGACAGGATG GACAGCACCGTCCAGGGCGCCCTCAACCGCGCCGACTTTGGCAGCGCCAA CTGCCCTTCAACAACAACAACCTTTGAGAGGAACATGCGCGCCGCTTTT AA
Alignment	

gDNA	1	ATGCTTCCCTCCACAATCTTCTCGGTCTTTGCTCTCGTCGGCAGCGCCTT	50
cDNA	1	ATGCTTCCCTCCACAATCTTCTCGGTCTTTGCTCTCGTCGGCAGCGCCTT	50
gDNA	51	GGCTCAGCATCCCCCAAGGTTAACCACGACAGTATCAACCCCGTCCGCG	100
cDNA	51	GGCTCAGCATCCCCCAAGGTTAACCACGACAGTATCAACCCCGTCCGCG	100
gDNA	101	ATACTCTGGGGCCCAACGGCGACATGATCAGGAAGTTCCAGCCTCTGCTT	150
cDNA	101	ATACTCTGGGGCCCAACGGCGACATGATCAGGAAGTTCCAGCCTCTGCTT	150
gDNA	151	CACATTGCCACGGTTGCCAGCCTTACTCCGCTGTCAACACCCGCGGTGA	200
cDNA	151	CACATTGCCACGGTTGCCAGCCTTACTCCGCTGTCAACACCCGCGGTGA	200
gDNA	201	GGTCAAGTAAGACACGCAGCACTCCCTTCAGCTTACACAAAGCTCCACGC	250
cDNA	201	GGTCAA-----	206
gDNA	251	TAACACATATTCTGCAGCGCCGGTCTCCAAGACAGCGGTACCACCGCAGG	300
cDNA	207	-----CGCCGGTCTCCAAGACAGCGGTACCACCGCAGG	239
gDNA	301	CGGCTGCAAGGAAACCAGCAAGGGCCAGACCTACGCCCGCTCCATGACCC	350
cDNA	240	CGGCTGCAAGGAAACCAGCAAGGGCCAGACCTACGCCCGCTCCATGACCC	289
gDNA	351	TGAACGGCCAGTTCGGCATCATGTACGCCTGGTACTGGCCCAAGGACCAG	400
cDNA	290	TGAACGGCCAGTTCGGCATCATGTACGCCTGGTACTGGCCCAAGGACCAG	339
gDNA	401	CCCGCCGACGGCAACCTCGCCAGCGGCCACCGCCACGACTGGGAGAACGT	450
cDNA	340	CCCGCCGACGGCAACCTCGCCAGCGGCCACCGCCACGACTGGGAGAACGT	389
gDNA	451	CGTCATCTGGTTCAACTCGAACAACGCAAACCAGGCCGGCATCTCTGCGCG	500
cDNA	390	CGTCATCTGGTTCAACTCGAACAACGCAAACCAGGCCGGCATCTCTGCGCG	439
gDNA	501	GCGCCGCCTCGGGCCACGGCGACTACAAGAAGGTCAACAACCCCCAGCGC	550
cDNA	440	GCGCCGCCTCGGGCCACGGCGACTACAAGAAGGTCAACAACCCCCAGCGC	489
gDNA	551	AACAACAACAACCTCCACGTCGAGTACTTCACCAGCCTCGGCAAGAACCA	600
cDNA	490	AACAACAACAACCTCCACGTCGAGTACTTCACCAGCCTCGGCAAGAACCA	539
gDNA	601	CGAGCTGCAGTTCAAGACGTCGCCCCGGCCGACCTACTGGATCTGGGACT	650
cDNA	540	CGAGCTGCAGTTCAAGACGTCGCCCCGGCCGACCTACTGGATCTGGGACT	589
gDNA	651	GGGACAGGATGGACAGCACCGTCCAGGGCGCCCTCAACCGCGCCGACTTT	700
cDNA	590	GGGACAGGATGGACAGCACCGTCCAGGGCGCCCTCAACCGCGCCGACTTT	639
cDNA	701	GGCAGCGCCAAC TGCCCTTCAACAACAACAAC TTTGAGAGGAACATGCG	750
gDNA	640	GGCAGCGCCAAC TGCCCTTCAACAACAACAAC TTTGAGAGGAACATGCG	689
gDNA	751	CGCCGCGTTTTAA	763
cDNA	690	CGCCGCGTTTTAA	702

VI-NEP-2

gDNA sequence

1 ATGCAGCATACTCTCTCTCTCAACCGCCCGCCCTGCTTGGCGCCCTGTCA
 51 GCCGTCAATGCTTCTCTCTGCGGCCATTTTGAGGCGTGATATTATCACCG

101	GCCTTCCCAGAAACGCCGACGAGATTGAGAACCAGTTCAGCCCATTTTT	
151	GACTTTGATACAGACGGGTGGTACAACACAGCTGCCCATGATCCTGACGG	
201	CAACACTAACCCTGGCAAGGGCGCCCCGGCCCTTCTCAGGGGGGCTGCC	
251	CCGATTCTCCTTAACTTGAGAACAACCATGTTTACTTCCGGTGCCGGTGC	
301	AACAACGGCGTCTGCGCTATTATGTAAGGCCACCACATTTTTTTCAGGAAG	
351	<u>GTGCCCTTTTTGAAACACATCTGACAATAATAGGTACGAGTATTATTTT</u>	
401	GAAAAGGACCAGTCGGTCAGCAGCTCGTTTGCGGGGCGCCACCGTCACGA	
451	CTGGGAAAACGTAGTCGTCTTCGCACGCGGAGACACTATTGTACGTGTTG	
501	CGCCATCTTGCCACGGCGGCTACGGCGGTGCATTGAATGAGTTCCTGTG	
551	GACGGCACGAGCCCGCAGATGGTCTACCACAAGGACAGTGCCGGCACTCA	
601	CTGCTTTCGCTTCGCCAACGACGCCGACATTGGCGGCGTCGAGAACTTCT	
651	CAGGCTCGTTCTACAAGAGCCCGCTCGTCGGATGGCTCAGCTGGCCCAAC	
701	GAGGGGTTGCGCCAAACCATGTTTGGAGCTTTCAGCGGGGAGTTGGGCC	
751	AAAGTTGGACGATGAGTTTGCGGGCAAGCTTGGTGAGGCAGCTGTGATGC	
801	TGTCGGAGTTTGACCCGAATGTTGACGAGTAG	
cDNA sequence		
1	ATGCAGCATACTCTCTCTCTCAACCGCCCCGCCCTGCTTGGCGCCCTGTCA	
51	GCCGTCAATGCTTCTCCTGCGCCATTCTGAGGCGTGATATTATCACCGC	
101	CCTCCCAGGAAACGCCGACGAGATCGAGAACAAGTTCAGCCAATTCTTG	
151	ACTTCGATACAGACGGCTGCTACAACACAGCTGCCATTGATCCTGACGGC	
201	AACACAAAACCCTGGCAAGGGCGCCACCGGCACTCCTCAGGGCGACTGCCG	
251	CGATCCTCCTCAGCTCGAGAACAGCAATGTTTACTCCCGGCGCCGCTGCA	
301	ACAACGGCGTCTGCGCTATTATGTACGAGTATTATTTTAAAAGGACCAG	
351	TCGGTCAGCAGCTCGTTTGCGGGGCGCCACCGTCACGACTGGGAAAACGT	
401	AGTCGTCTTCGCACGCGGCGACACTATTGTACGTGTTGCGCCATCTTGCC	
451	ACGGTGGCTACGGCGGCGCATCGAATGAGTTCCTGCCGACGGCACGAGC	
501	CCGAGATGGTCTACCACAAGGACAGTGCCGGCACTCACTGCTTCCGCTT	
551	CGCCAACGACGCCGACATTGGCGGCGTCGAGAACTTCTCAGGCTCGTTCT	
601	ACAAGAGCCCGCTCGTCGGATGGCTCAGCTGGCCTAACGAGGGGTTGCGC	
651	CAAACCATGCTTGGAGCTTTCAGCGGGGAGTTGGGCCAAAGTTGGACGA	
701	CGAGTTTGACAGGAAGCTTGGTGAGGCACCTGGTGATGCTGTCCCAGTT	
751	TGACCCGAATGTTGACGAGTAG	
Alignment		
gDNA	1 ATGCAGCATACTCTCTCTCTCAACCGCCCCGCCCTGCTTGGCGCCCTGTCA	50
cDNA	1 ATGCAGCATACTCTCTCTCTCAACCGCCCCGCCCTGCTTGGCGCCCTGTCA	50
gDNA	51 GCCGTCAATGCTTCTCCTGCGCGCCATTTTGGAGGCGTGATATTATCACCG	100
cDNA	51 GCCGTCAATGCTTCTCCTGCGC-CCATTCTGAGGCGTGATATTATCACCG	99
gDNA	101 GCCTTCCCAGAAACGCCGACGAGATTGAGAACCAGTTCAGCCCATTTTTT	150
cDNA	100 CCCTCCCAGGAAACGCCGACGAGATCGAGAACAAGTTCAGCCAATTCTT	149
gDNA	151 GACTTTGATACAGACGGGTGGTACAACACAGCTGCCCATGATCCTGACGG	200
cDNA	150 GACTTCGATACAGACGGCTGCTACAACACAGCTGCCATTGATCCTGACGG	199
gDNA	201 CAACACTAACCCTGGCAAGGGCGCCCCGGCCCTTCTCAGGGGGGCTGCC	250
cDNA	200 CAACACAAAACCCTGGCAAGGGCGCCACCGGCACTCCTCAGGGCGACTGCC	249
gDNA	251 CCGATTCTCCTTAACTTGAGAACAACCATGTTTACTTCCGGTGCCGGTGC	300
cDNA	250 GCGATCCTCCTCAGCTCGAGAACAGCAATGTTTACTCCCGGCGCCGCTGC	299
gDNA	301 AACAACGGCGTCTGCGCTATTATGTAAGGCCACCACATTTTTTTCAGGAAG	350

cDNA	300	AACAACGGCGTCTGCGCTATTATGTA-----	325
gDNA	351	GTGCCCTTTTTGAAACACATCTGACAATAATAGGTACGAGTATTATTTT	400
cDNA	326	-----CGAGTATTATTTT	338
gDNA	401	GAAAAGGACCAGTCGGTCAGCAGCTCGTTTGC GGCGGCCACCGTCACGA	450
cDNA	339	GAAAAGGACCAGTCGGTCAGCAGCTCGTTTGC GGCGGCCACCGTCACGA	388
gDNA	451	CTGGGAAAACGTAGTCGTCTTCGCACGCGGAGACACTATTGTACGTGTTG	500
cDNA	389	CTGGGAAAACGTAGTCGTCTTCGCACGCGGCGACACTATTGTACGTGTTG	438
gDNA	501	CGCCATCTTGCCACGGCGGCTACGGCGGTGCATTGAATGAGTTCCCTGTC	550
cDNA	439	CGCCATCTTGCCACGGTGGCTACGGCGGCGCATCGAATGAGTTCCCTGCC	488
gDNA	551	GACGGCACGAGCCCGCAGATGGTCTACCACAAGGACAGTGCCGGCACTCA	600
cDNA	489	GACGGCACGAGCCCGCAGATGGTCTACCACAAGGACAGTGCCGGCACTCA	538
gDNA	601	CTGCTTTCGCTTCGCCAACGACGCCGACATTGGCGGCGTCGAGAACTTCT	650
cDNA	539	CTGCTTTCGCTTCGCCAACGACGCCGACATTGGCGGCGTCGAGAACTTCT	588
gDNA	651	CAGGCTCGTTCCTACAAGAGCCCGCTCGTCCGATGGCTCAGCTGGCCCAAC	700
cDNA	589	CAGGCTCGTTCCTACAAGAGCCCGCTCGTCCGATGGCTCAGCTGGCCCAAC	638
gDNA	701	GAGGGTTGCGCCAAACCATGTTTGGAGCTTTCAGCGGGGAGTTGGGCC	750
cDNA	639	GAGGGTTGCGCCAAACCATGCTTGGAGCTTTCAGCGGGGAGTTGGGCC	688
gDNA	751	AAAGTTGGACGATGAGTTTGC GGCAAGCTTGGTGAGGCAGCTGGTGATG	799
cDNA	689	AAAGTTGGACGACGAGTTTGCAGGCAAGCTTGGTGAGGCACCTGGTGATG	738
gDNA	800	CTGTCCCGAGTTTGACCCGAATGTTGACGAGTAG	833
cDNA	739	CTGTCCCGAGTTTGACCCGAATGTTGACGAGTAG	773

VI-NEP-3

gDNA sequence

```

1  ATGCTTTTCAGTGTCGGACTCCTCGCCCTTGCGGCTTTGCCTACGTCTTT
51  CGGAGCTGTCATTCAGGCGCGCCAGGACGACCCCGAGAACCCTCCCGTG
101  AACCCAGCCTCCTCCTCCCGGCCCATCTTCGGACGGGCACCCGACCTC
151  GACAAGCGCTCCAGCCTGCTCTTGACTTTGACACGGACAGCTGTACAA
201  TGCACCAGCAATCGGCCCAACGGCGACCTCGCCATTGGCATGTATCCCT
251  TCGAGTGGCCGCTCAAGCGGGCTGCCGCAACGAAGAGATGCTGGACAGA
301  GGCAATGTCTACTCCCAGCAGCTGTAACAACGGCTATTGCGTCATCTT
351  TTACGCCTACTACTTCCAGAAGGATACGGCGACGCCATTGACGGGCACC
401  GCCACGACTGGGAGCACATTGCCGTGTGGGTGCGCCAGAGCGACAGCTTC
451  GTCACGCACGTTGCCGTAGCCAGCACAAGGGCTACGACATTTCGTGAAAA
501  CTCCCAGATCACCTGGACTGCGGGCGGAGAATGGAAAGCCGGCGATTGTCT
551  ACCACAAGGACAGCATTCAGACACACTGCTTCCGGTTCGGCAGTGGTGCC
601  GACGCCGGCGGTCCCGGGCCGGAGAACCACAGGAACCAGTGGATCACGGG
651  CCCGCTTCTGGGGTACTTCGGTTGGGACACTGTCGAGCAGAGGGACAGGA
701  TGCTGACGCACAACCTGGGAGGCTGGCTCTATCGCCATCAAGAATGAGAAC
751  TTTGCTGAGAACATTCGCAAGGCTAGGCCTGCTGGGCTGGTCTCTGACGA
801  CAACTTGACGACGAGGGCAGCACAACATCTGA
    
```

VI-NEP-4

gDNA sequence

```

1  ATGGTGCTGTCAGTGCCATCGACCGCTCAGTCATGCGGGGCCAGAGCAA
51  CTCGAGTCGGATCCTCAGCGATAGTCAAGCGCTCGAACCCATCGTGGGCG
101  GCCACGACTTCGCCTACTATTTTGAAGTGAAGTTCCAGCCATTGGTGGAC
151  ATCGACACCGACAGCTGCTACAGCGTGCCCGCCATGACCATGGACGGAAC
201  CGCATCCGAGGGCCTTTCACCCCTCCGACGATGTCGGTCCGTGCCGTCCCC
251  GCTCCGCCCTTGACCGGTCCAACGTGTATGTCAGGGGCCGCTGCAACCGC
301  GGATGGTGCGCATTCGTCTACGCCATTACTTCCAGATGGACTGGGCTG
351  GTCGTGGCCCCGTGAGCAGCTACAACCACCGCCACGACTGGGAGCACGTG
401  TCGTCTGGGCCAAGGAGGGCAAAGTCCGCGGCGTTTCCGTCTCGCAACAC
451  GGCGGCTACGAGAACCAGCGTCCGCGAAGACCAGAGGCTTCGCTTCGACTA
501  CACACCAAAGGAGTTTCCGTATCCTGCGTGGGATCCCATGCCGACGAGCG
551  TAGCCATGCACCCCAAGGTCGTCTTTCACAAGGACGGTGCCCGCACGCAC
601  TGCTTCCGCTTCGCCAAGGACAGCGACGACTATGAGGGCCAGGAGAATGA
651  GAGAGGCGTTTGGATTTCGTGGCGGTCTCATCAGTATGCTGCTCATGCCGA
701  GCGACTGGCAGGAGAAGTTCAGATCTCAGAATTGGGGGAGTGCTCACATG
751  GCATGGGCTAATGAGGAGGACTTTACCGGGCATCTCGTCAAGTCCATGCC
801  GCAGGAAGCCAGAGACGACGGGTTTACTGTGCCTACGACGAGAATCCAG
851  CTCTCAAAGGCTTTCCTATGGACTGGAAGAAGTGGGGACTGA

```

VI-NEP-5

gDNA sequence

```

1  ATGTATCACAAAATCCTTCTCGTCGGCGTGCTAGCCACCCTTACTGGGTT
51  GACTTCCGCCAATGACGCGATCCCAGGCAGTGCTTTCGAAAAGTGAGCCAA
101  CCCAAGAACACAATTACAACACAGATCGCAGTCAACTAACGATCTATAGA
151  CAGCGGACAAGAAGCAGCCATCGCCGGTGCTCCCATGTATCACTTTGGTC
201  GCTCGTGGGACCGCAAGCCATGCTACCCAGAGGCCGGTCAGACTGACGGC
251  GTCAAGACGGACGGCGTTGACTCGGACCTGTGCTTCAGCAGTCAGAATGG
301  CGGTTGTGCCGATCCCGGACCCTGGAACGGCGTCAACTCTCCCGGAAACC
351  CGTTTCCGGTGTATTACACCGTTCGGCAGTGCAACGACAATGAGTGGCGC
401  GTTGCTACAGCATCTACTATAAGAAGGATTCTGGCCATAAGAACGACTG
451  GGAGAACAGCATTTGTCATCTGGAACGGAGACGGTGCTGGCGGCTGGAAGC
501  GGAGCGGTACGCTGCTTGGCTGGCACAGCGGTGGGATTACATTGCTTGG
551  GGCGACATCCAGAACACTGTGAACAAGTAAGCAAAATCCAGGAGATGCAG
601  CTTTTCAAAGCGTCTTTGCTGACAAACGTAGCGACGGCGATCTTTTCGAC
651  CAGGGCGCCAAGGATCGAAACCATGCCAAGGCTTATCAGGGATTCTACTA
701  CCATGCCACGTTCTCGACTCGCAAGACGTCCCTCAACACCTGCGCCAACA
751  CTACGGACGAGTTCCGATCGAACGACTGGTACTTCCCTCCCTGACGGCAG
801  TGGCTTCAACACGGAGATCTCATCCAAGGTAGGCTGGTAACGGAAAGAGT
851  AATACGTTGAGCATCAAACACTAACTCTGACTCCATCCAGATGGCTGGGA
901  TTAGGGCTCTGCCGACACAAACCCGTCTTCTCTGCCAAATGAGCGCGCTG
951  GATCTGCAACCGAGGCTGA

```

cDNA sequence

```

1  ATGTATCACAAAATCCTTCTCGTCGGCGTGCTAGCCACCCTTACTGGGTT
51  GACTTCCGCCAATGACGCGATCCCAGGCAGTGCTTTCGAAAACAGCGGAC

```

101	ATGAAGCAGCCATCGCCGGTGTCTCCCATGTATCACTTTGGTCGCTCGTGG	
151	GACCGCAAGCCATGCTACCCAGAGGCTGGTCAGACTGACGGCGTCAAGAC	
201	GGACGGCGTTGACTCGGACCTTTGCTTCAGCAGTCAGAATGGCGGTTGTG	
251	CCGATCCCGGACCCGGAACGGCGTCAACTCTCCCGGAAACCCGTTTCCG	
301	GTGTATTACACCGTTCGGCAGTGCAACGACAATGAGTGGCGCGTTGCGTA	
351	CAGCATCTACTATAAGAAGGATTCTGGCCATAAGAACGACTGGGAGAACA	
401	GCATTGTCATCTGGAACGGAGACGGTGTCTGGCGGCTGGAAGCGGAGCGGT	
451	ACGCTGCTTGGCTGGCACAGCGGTTGGGATTACATTGCTTGGGGCGACAT	
501	CCAGAACACTGTGAACAACGACGGCGATCTTTTCGACCAGGGCGCCAAGG	
551	ATCGAAACCATGCCAAGGTTTATCAGGGATTCTACTACCATGCCACGTTT	
601	TCGACTCGCAAGACGTCCCTCAACACCTGCGCCAACACTAGGGACGAGTT	
651	CCGATCGAACGACTGGTACTTCCCTCCCTGACGGCAGTGGCTTCACAACG	
701	GAGATCTCATCCAAGATGGCTGGGATTATGGCTCTGCCGACACGAACCCG	
751	TCTTCTCTGCGAAATGAAGCACGCTGGATCTGCAACCGAGGCTGA	
Alignment		
gDNA	1 ATGTATCACAAAATCCTTCTCGTCGGCGTGCTAGCCACCCTTACTGGGTT	50
cDNA	1 ATGTATCACAAAATCCTTCTCGTCGGCGTGCTAGCCACCCTTACTGGGTT	50
gDNA	51 GACTTCCGCCAATGACGCGATCCCAGGCAGTGCTTTCGAAAGTGAGCCAA	100
cDNA	51 GACTTCCGCCAATGACGCGATCCCAGGCAGTGCTTTCGAAA-----	91
gDNA	101 CCCAAGAACACAATTACAACACAGATCGCAGTCAACTAACGATCTATAGA	150
cDNA	92 -----A	92
gDNA	151 CAGCGGACAAGAAGCAGCCATCGCCGGTGTCTCCCATGTATCACTTTGGTC	200
cDNA	93 CAGCGGACATGAAGCAGCCATCGCCGGTGTCTCCCATGTATCACTTTGGTC	142
gDNA	201 GCTCGTGGGACCGCAAGCCATGCTACCCAGAGGCCGGTCAGACTGACGGC	250
cDNA	143 GCTCGTGGGACCGCAAGCCATGCTACCCAGAGGCTGGTCAGACTGACGGC	192
gDNA	251 GTCAAGACGGACGGCGTTGACTCGGACCTGTGCTTCAGCAGTCAGAATGG	300
cDNA	193 GTCAAGACGGACGGCGTTGACTCGGACCTTTGCTTCAGCAGTCAGAATGG	242
gDNA	301 CGGTTGTGCCGATCCCGGACCCGGAACGGCGTCAACTCTCCCGGAAACC	350
cDNA	243 CGGTTGTGCCGATCCCGGACCCGGAACGGCGTCAACTCTCCCGGAAACC	292
gDNA	351 CGTTTCCGGTGTATTACACCGTTTCGGCAGTGCAACGACAATGAGTGGCGC	400
cDNA	293 CGTTTCCGGTGTATTACACCGTTTCGGCAGTGCAACGACAATGAGTGGCGC	342
gDNA	401 GTTGCGTACAGCATCTACTATAAGAAGGATTCTGGCCATAAGAACGACTG	450
cDNA	343 GTTGCGTACAGCATCTACTATAAGAAGGATTCTGGCCATAAGAACGACTG	392
gDNA	451 GGAGAACAGCATTGTCATCTGGAACGGAGACGGTGTCTGGCGGCTGGAAGC	500
cDNA	393 GGAGAACAGCATTGTCATCTGGAACGGAGACGGTGTCTGGCGGCTGGAAGC	442
gDNA	501 GGAGCGGTACGCTGCTTGGCTGGCACAGCGGTTGGGATTACATTGCTTGG	550
cDNA	443 GGAGCGGTACGCTGCTTGGCTGGCACAGCGGTTGGGATTACATTGCTTGG	492
gDNA	551 GGCGACATCCAGAACACTGTGAACAAGTAAGCAAAATCCAGGAGATGCAG	600
cDNA	493 GGCGACATCCAGAACACTGTGAACAA-----	518
gDNA	601 CTTTTCAAAGCGTCTTTGCTGACAAACGTAGCGACGGCGATCTTTTCGAC	650
cDNA	519 -----CGACGGCGATCTTTTCGAC	537
gDNA	651 CAGGGCGCCAAGGATCGAAACCATGCCAAGGCTTATCAGGGATTCTACTA	700

cDNA	538	CAGGGCGCCAAGGATCGAAACCATGCCAAGGTTTATCAGGGATTCTACTA	587
gDNA	701	CCATGCCACGTTCTCGACTCGCAAGACGTCCCTCAACACCTGCGCCAACA	750
cDNA	588	CCATGCCACGTTCTCGACTCGCAAGACGTCCCTCAACACCTGCGCCAACA	637
gDNA	751	CTACGGACGAGTTCCGATCGAACGACTGGTACTTCCTCCCTGACGGCACG	800
cDNA	638	CTAGGGACGAGTTCCGATCGAACGACTGGTACTTCCTCCCTGACGGCACG	687
gDNA	801	TGGCTTCACAACGGAGATCTCATCCAAGGTAGGCTGGTAACGAAAGAGT	850
cDNA	688	TGGCTTCACAACGGAGATCTCATCCAAG-----	715
gDNA	851	AATACGTTGAGCATCAAACACTAACTCTGACTCCATCCAGATGGCTGGGA	900
cDNA	716	-----ATGGCTGGGA	725
gDNA	901	TTAGGGCTCTGCCGACACAAACCCGTCTTCTCTGCCAAATGA-GCGCGCT	949
cDNA	726	TTATGGCTCTGCCGACACGAACCCGTCTTCTCTGCCAAATGAAGCACGCT	775
gDNA	950	GGATCTGCAACCGAGGCTGA	970
cDNA	776	GGATCTGCAACCGAGGCTGA	795

Chapter 4: Detection and functional analysis of a polyketide synthase gene of *Verticillium longisporum*

Malte Beinhoff, Arne Weiberg, Haiquan Xu, Hanno Wolf, Wolfgang Hiegl and Petr Karlovsky

Molecular Plant Pathology and Mycotoxin Research Unit, Department for Crop Sciences, Georg-August University of Goettingen, Grisebachstrasse 6, 37077 Goettingen, Germany.

ABSTRACT

Polyketides from phytopathogenic fungi are known to often play a role during the host-pathogen interaction as toxins, or as pathogenicity or virulence factors. Here we report our results on a polyketide synthase (PKS) gene of *Verticillium longisporum*, named as VI-PKS-1, which we detected in the genome of the *V. longisporum* isolate VL43 using degenerated primers based on a fungal L-ketoacylsynthase (KS)-domain. The detected fragment shows high homology to other fungal PKS genes of the *wA*-type. Strongly enhanced transcript levels of VI-PKS-1 in hypocotyl tissue of *V. longisporum* infected *Brassica napus* plants compared to the expression in grown mycelium implies the role of the gene in the interaction with the host plant, and this motivated us to construct knock down mutants to switch off the gene function in *V. longisporum* to elucidate the role of VI-PKS-1 in the pathogenic life cycle of the fungus.

INTRODUCTION

Fungal polyketides (PK) belong to a large group of well-characterized secondary metabolites with diverse biological functions (1) such as toxins (mycotoxin) like fumonisins, aflatoxins or zearalenones (2, 3, 4), or as pigments such as melanin, which is known from literature to play an important role in appressoria-mediated infection processes of plant pathogens (2, 5). PKs

have been deeply investigated in both prokaryotic and eukaryotic organisms, and it has been shown that despite the structural diversity of PKs these secondary metabolites are all derived from highly functionalized carbon chains assembled by a mechanism close to the fatty acid synthetic pathway (6). The biosynthesis of PKs is carried out by enzymes called polyketide synthases (PKSs). The large family of PKSs can be subdivided into three classes according to their functionality, and these are referred to as type I, type II and type III PKSs (7, 8). Type I PKSs are large multifunctional enzymes (9) that are encoded by a single gene, similar to the type I fatty acid synthases (FAS) of fungi and animals with up to 350 kDa (10). These characteristic PKSs of fungi and vertebrates form reduced PKs such as erythromycin. The biosynthesis of the PKs is thereby derived by catalyzing the transfer of acetyl units from malonyl-coenzyme A (CoA) to the active site thiol of the β -ketoacyl synthase (KS) by an acetyl carrier protein (ACP) as a starting point for the elongation of the PK chain. These chains include several domains with defined function such as keto-reductase (KR) domains or dehydratase (DH) domains, and this gives rise to the structural diversity of PKs and their manifold biological activities. Type II PKSs are characteristic of FAS II found in bacteria and plants, and form mostly aromatic PKs such as tetracycline by the use of only a single domain. Type III PKSs are only present in plants and show major differences compared to the other classes of PKSs. Type III PKSs are 80-85 kDa large enzymes which execute a direct condensation of malonyl-CoA and therefore lack the presence of an ACP domain which is a key enzyme in the fatty acid and PK biosynthesis.

The first fungal PKS gene was discovered in 1990 by Beck et al. in the filamentous fungus *Penicillium patulum* (11). The isolated type I PKS gene comprises five catalytic domains identified as KS, KR, DH, AT and ACP, and was characterized to synthesize the antibiotic 6-methylsalicylic acid. Since then, many PKS genes that synthesize PKs with characteristics of mycotoxins or fungal pigments that are essential for the pathogenic life style of fungi have been detected in various plant pathogenic species (3, 12, 13, 14). PKs are primarily responsible for the colouring of fungal organs by pigments such as melanin, which have a great functional significance in appressoria or microsclerotia of fungi, giving these organs protection and stability against external influences such as micro-organism competitors or abiotic factors such as UV irradiation due to their toxic ability and their phenolic-like chemical structure. The essential function of melanins in the appressorial turgor generation and subsequent penetration of plant cell walls by fungal pathogens was first shown in

Pyricularia oryzae (2, 5). In *Colletotrichum lagenarium* knock-down mutants of a type I PKS change to an albino phenotype with non-melanized appressoria showing a reduced ability to penetrate the cell wall of host plants (15). In fungi, the best researched melanin is produced by a pathway that forms 1,8-dihydroxynaphthalene (DHN), which is polymerized to so-called DHN melanin. This type of melanin is widely distributed among ascomycota fungi.

Here we report on the identification of a PKS from the ascomycota fungus *V. longisporum* named as VI-PKS-1. This has high homology to other fungal PKS genes of the *wA*-type, which are known to be involved in pigment and aflatoxin biosynthetic pathways. *V. longisporum* is a soil-borne plant pathogen that infects only *Brassica* and other cruciferous plants (16). The fungus has the characteristics of a hemibiotrophic pathogen, starting its pathogenic life cycle living as a biotroph organism undetected by the plant, and strictly restricted to the xylem vessels of host plants. Only at late stages of infection does *V. longisporum* switch its life style to that of a necrotrophic organism and release nutrients from dying plant tissue. During this stage of plant infestation, the fungus forms dark melanized resting structures that are released to the soil by dead plant tissue. Because of the protective and stabilizing features of melanins, these so-called microsclerotia can remain in the soil for many years and stay capable to germinate until the environmental conditions are suitable to start a new infection cycle. As known from study of other phytopathogenic fungi, *V. longisporum* does not show any melanized appressoria during infection of host plants; therefore the contribution of melanins in this infection process should not be assumed. During this report we give notes about a putative contribution of VI-PKS-1 in the life cycle of *V. longisporum*.

MATERIALS AND METHODS

Fungal and bacterial strains

V. longisporum VL43 strain was provided by the Department of Crop Sciences, Section Plant Pathology and Crop Protection, (University of Goettingen, Goettingen, Germany) and was used for all experiments in this chapter. The isolate originates from oilseed rape plants

collected in Northern Germany (17). Optimal growth temperature is between 20 and 23 °C and this was therefore used for all experiments using *V. longisporum*.

Gliocladium roseum (DSMZ 62726), *Fusarium culmorum* strain Fc3-8F (DSMZ 62223), *F. verticilloides* strain TR3 and *F. proliferatum* strain 3 was provided by Dr. Evelyn Möller (State Plant Breeding Institute, University of Hohenheim, Hohenheim, Germany (emeritus state)) and were used for a fungal interaction assay.

Trichoderma harzianum (DSMZ 63323) was provided by the Department of Crop Sciences, Section Plant Pathology and Crop Protection (University of Goettingen, Goettingen, Germany) and was also used for a fungal interaction assay.

Agrobacterium tumefaciens strain AGL1 was provided by Dr. Susanne Frick (Leibniz Institute of Plant Biochemistry, Martin-Luther University Halle-Wittenberg, Halle/Saale, Germany) and was used for the transformation of *V. longisporum*.

Electrocompetent *Escherichia coli* DH10 β strain (New England Biolabs, Ipswich, United Kingdom) was used for cloning purposes.

Preparation of spore suspensions

Approximately 1×10^4 spores were spread on a PDA plate and incubated at 23 °C for 10 days in the dark. The plates were subsequently flooded with 15 % glycerine suspension and the spores were released from the conidiophores by scratching the mycelium with a spatula. The suspension was filtered through a sterile gauze and the spore concentration was estimated using a Thoma hemacytometer with a depth of 0.1 mm (Roth GmbH, Karlsruhe, Germany). Spore suspension was diluted to 1×10^7 spores per ml⁻¹ with a 15 % glycerine solution and immediately stored in a -80 °C freezer.

Plant material

The seed material of “rapid cycle rape” (*Brassica napus* var. *napus*, Genom A Caacc) (18) was provided by the Department of Crop Sciences, Section Plant Pathology and Crop Protection (University of Goettingen, Goettingen, Germany).

Plasmids

For *A. thumefaciens*-mediated transformation (AMT) of *V. longisporum*, we used the binary vector pPK2 (19) including boarder sequences for the AMT and a hygromycin B resistance cassette containing the hygromycin phosphotransferase gene from *E. coli* (hph) for selection of positive transformants.

Enzymes

For the construction of a pPK2 vector containing a hairpin (HP)-cassette and a antisense (AS)-RNA cassette to knock down the function of VI-PKS-1 gene, we used restriction enzymes, “T4-DNA Ligase” and affiliated buffers purchased from Fermentas Inc. (Fermentas, St. Leon-Rot, Germany).

Enzymes and reagents for first strand cDNA synthesis, including “Oligo(dT)18 Primer”, “RiboLock™ RNase Inhibitor” and “M-MuLV Reverse Transcriptase” were also purchased from Fermentas Inc..

“Biotaq™ DNA Polymerase” (Bioline, Luckenwalde, Germany) was used for general amplification of fragments by polymerase chain reaction (PCR).

The “Absolute Blue QPCR Fluorescin Mix“ (Fisher Scientific GmbH, Schwerte, Germany) was used for quantitative reverse transcriptase real time PCR (qRT-PCR) to assess the silencing efficiency of *V. longisporum* mutants.

Primer walking

Starting from a known DNA sequence of the candidate gene VI-PKS-1, which we obtained by sequencing of fragments we amplified using degenerated primers of conserved domains from other fungal PKSs for PCR, we searched for homologous sequences by comparing our sequence with a database of known sequences from other organisms to find homologies among these (23). Using an alignment of VI-PKS-1 and highly homologous sequences, we designed deduced degenerated primer sequences to amplify new sequence-information of VI-PKS-1 using gDNA of *V. longisporum* as a template for PCR. Amplification was performed using one primer as a starting point for DNA synthesis derived from specific sequence-

information of VI-PKS-1 and a degenerated primer derived from VI-PKS-1 homologous sequences from other organisms, including several universal nucleotides. Amplification was performed starting from both the *downstream* and *upstream* end of the VI-PKS-1 fragment to obtain new sequence information from both directions of the gene. Primers we used for primer walking are listed in Table 5 in the appendix.

VI-PKS-1 gene silencing

Construction of pPK2-HP vector, containing a VI-PKS-1 specific HP- or AS RNA cassette, was performed as described in Chapter 2 (Construction of HP-fragments using conventional cloning steps, from page 48).

Transformation of *V. longisporum*

Agrobacterium tumefaciens-mediated transformation (AMT) of *V. longisporum* was performed as described in Chapter 2 (see page 31) using a protocol published by Utermark (20).

Southern hybridization

To analyse the number of VI-PKS-1 gene-copies present in the genome of wild type *V. longisporum* and to determine the number of copies in the transformed VI-PKS-1 mutants compared to the wild type, southern hybridization was performed as described in Chapter 2 (see page 30).

Plant pathogenicity assay using VI-PKS-1 silencing mutants

To assess any changes in the ability of *V. longisporum* wild type compared to VI-PKS-1 silencing mutants to infest *B. napus* plants we performed a pathogenicity assay as described in Chapter 3 (see page 68).

Extraction of gDNA and total RNA

Total RNA for qRT-PCR and gDNA for PCR and southern hybridization were extracted from fungal mycelium or plants as described in Chapter 2 (see page 30) using a modified protocol of Maniatis et al. (21).

qRT-PCR

Total RNA from fungal mycelium was used for gene expression analysis. QRT-PCR was performed as described in Chapter 2 (see page 32).

Fungal interaction assay

A variety of other soil-borne fungi (*G. roseum*, *F. culmorum*, *F. proliferatum*, *F. verticilloides*, *T. harzianum*) were selected for co-inoculation along with *V. longisporum* wild type and VI-PKS-1 silencing mutants. Therefore, 5 µl of a spore suspension with a defined concentration (1×10^6 spores/ml⁻¹) of both *V. longisporum* wild type or VI-PKS-1 mutants and the fungal interactor was dropped on opposite sites of a PDA plate and was then grown at 23 °C in the dark. Because of its slow growth rate as compared to some tested fungi, *V. longisporum* was in some cases pre-grown for 7 days before inoculating the other fungi. Every day we observed the plates to find any notable changes in the interaction of *V. longisporum* wild type or VI-PKS-1 silencing mutants on the growth of the fungal interactors.

Statistical analysis

For statistical analysis and creation of graphs we used the statistical analysis software STATISTICA (StatSoft GmbH, Hamburg, Germany). Data are presented as means ± standard deviation. Differences of data sets obtained from experiments using *V. longisporum* wild type and silencing mutants were determined using one way analysis of variance (ANOVA) followed by a post hoc test using “Fisher's Least Significant Difference (LSD) test” to show which differences were significant.

RESULTS AND DISCUSSION

Highly conserved domains that are present in members of the PK family can be used to target PKSs in diverse organisms without having knowledge of any specific gene-sequences of the organism. We used degenerate primers (see Table 4 in the Appendix) based on a fungal L-KS-domain (22) to amplify putative PKS genes by using gDNA of *V. longisporum* isolate VL43 as a template for PCR. The amplified gene fragments were sequenced (Eurofins MWG Operon, Ebersberg, Germany) and compared with a database of known sequences to find homologies (23). From the amplified fragments, we detected an alignment that showed high homology to other fungal L-KS domains. The sequence of the putative PKS gene of *V. longisporum* was extended using the “Primer walking” technique. The extended fragment with a length of 1986 bp showed high homology to fungal PKS genes of the *wA*-type, especially those involved in the biosynthesis of 1,8-dihydroxynaphthalene (DHN)-melanin. We designated the detected gene as VI-PKS-1. The translated cDNA sequence of the gene has high sequence homology (76 % identity, GenBank Accession No. D83643.1) to a PKS type I gene of *Colletotrichum lagenarium*, which is a fungal pathogen causing anthracnose on host plants. PKS-1 knock-down mutants of *C. lagenarium* morphologically changed to albinos (15). Therefore, the involvement of VI-PKS-1 in the biosynthesis of melanin in the life cycle of *V. longisporum* is assumable. Among many sequence homologies to other PKSs from diverse fungi, we could also match a hit with a significantly high similarity (96 % identity, GenBank Accession No. XM_003008852.1) to the extended VI-PKS-1 sequence to a conidial yellow pigment synthase from *V. dahliae*, which is reported to be a parental strain of amphihaploid *V. longisporum* (24, 25).

<i>V. longisporum</i>	DPRFFNMSPREAYQTDPMQRMALTTAYEALEMSGYVPNRTASTRLDRIGTFYGQTSDDWR	60
<i>V. dahliae</i>	DPRFFNMSPREAYQTDPMQRMALTTAYEALEMSGYVPNRTASTRLDRIGTFYGQTSDDWR	60
<i>C. lagenarium</i>	DPRFFNMSPREAFQTDPMQRMALTTAYEALEMCGYVPNRTASTRLDRIGTFYGQTSDDWR	60
	*****;*****;*****;*****;*****;*****;*****;*****;*****;*****	
<i>V. longisporum</i>	EINAAQEVDTYFITGGVRAFGPGRINYHFGFSGPSLNIDTACSSSAAALQIACTSLWAKD	120
<i>V. dahliae</i>	EINAAQEVDTYFITGGVRAFGPGRINYHFGFSGPSLNIDTACSSSAAALQIACTSLWAKD	120
<i>C. lagenarium</i>	EINAAQEVDTYYITGGVRAFGPGRINYHFGFSGPSLNVDTACSSSAAALNVACNSLWQKD	120
	*****;*****;*****;*****;*****;*****;*****;*****;*****;*****	
<i>V. longisporum</i>	CDTAVVGGLSMTPDIFSGLSRGQFLSKTGPCATFDNGADGYCRADGCASVIVKRLDDA	180
<i>V. dahliae</i>	CDTAVVGGLSMTPDIFSGLSRGQFLSKTGPCATFDNGADGYCRADGCASVIVKRLDDA	180
<i>C. lagenarium</i>	CDTAIVGGLSMTPDIFAGLSRGQFLSKTGPCATFDNGADGYCRADGCASVIVKRLDDA	180
	****;*****;*****;*****;*****;*****;*****;*****;*****;*****	

tetrahydroxynaphthalene (T4HN) and produces its pigment without the use of the DHN pentaketide pathway (30), the enzyme produced by PKS-1, which was found in *C. lagenarium*, was identified to be a pentaketide synthase which synthesizes the pentaketide precursor TH4N directly for DHN melanin (14, 31). It is not known how *A. nidulans* uses a heptaketide synthase to initiate the biosynthesis of a pentaketide melanin but recent studies show that the heptaketide YWA1 is converted to the pentaketide 1,3,6,8 TH4N through a novel PK shortening mechanism (32).

Expression levels of VI-PKS-1 transcripts were measured by qRT-PCR in hypocotyl samples of *V. longisporum* infected *B. napus* plants and in *in vitro* samples of 10-day-old mycelium grown in artificial simulating xylem (SXM) medium in standing cultures with 12 h day/night change. Both were used to calculate a changefold factor describing the *in planta* vs. *in vitro* expression ratio.

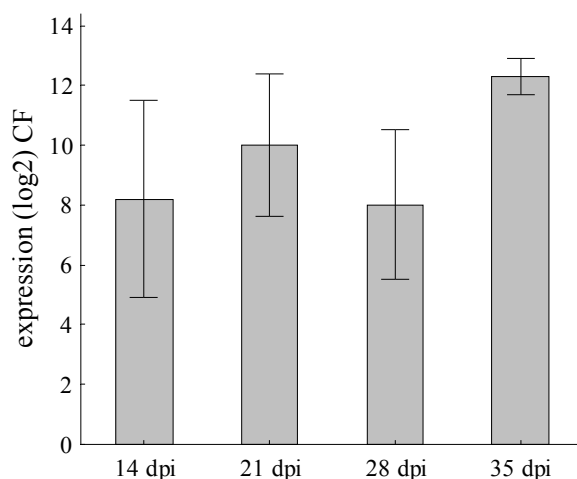


Figure 2: Gene expression analysis of VI-PKS-1

Error bars indicate the standard error of three biological replicas.

Highly upregulated gene expression of VI-PKS-1 *in planta* makes a contribution to the pathogenic life cycle of *V. longisporum* assumable, and this motivated us to construct knock-down mutants for post-transcriptional inhibition of the candidate gene by intracellular expression of an HP-construct and also by expression of AS-RNA suitable to trigger RNA-mediated gene silencing in *V. longisporum*. Transformation vectors VI-PKS-1-pPK2 carrying HP- or AS-cassettes were transformed into *V. longisporum* using *Agrobacterium thumefaciens* mediated transformation (AMT). Mutants were tested by PCR with primers for

the hygromycin-cassette that was used for selection of positive transformants (data not shown) and also by southern hybridization. Four VI-PKS-1 (m2, 4, 9 and 10) mutants were generated by the intracellular expression of an HP cassette triggering RNAi in the fungus with a silencing efficiency up to 90 %. Transformants of *V. longisporum* that express an AS-RNA cassette for post-transcriptional silencing of VI-PKS-1 show a moderate silencing efficiency of 70 % at best (data not shown).

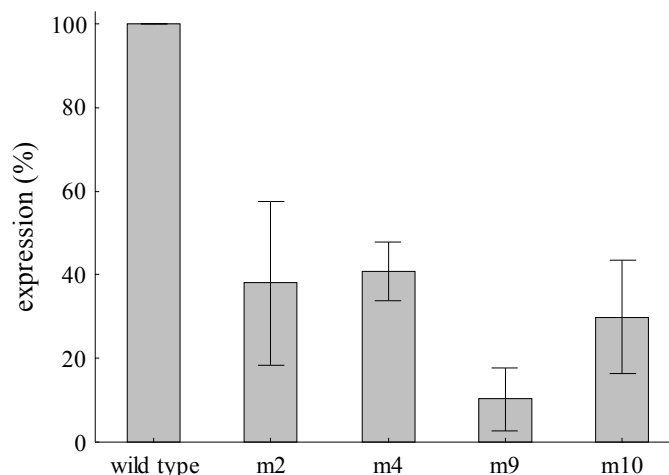


Figure 3: Gene silencing efficiency in VI-PKS-1 transformants

Assessment of silencing efficiency triggered by the intracellular expression of an HP cassette in four mutants (m2, m4, m9, m10) was done in reference to wild type *V. longisporum* by qRT-PCR

Unexpectedly, the southern hybridization we performed using gDNA of *V. longisporum* and VI-PKS-1 silencing mutants m9 and m10 for hybridization with a VI-PKS-1 specific 683 bp PCR-amplified probe, only showed a single native gene copy present in the genome of *V. longisporum*. Because the fungus is described as an interspecific hybrid of parental haploid *V. dahliae* and *V. albo-atrum* strains (16, 17) and in both parental strains the homologous PKS to VI-PKS-1 named as conidial yellow pigment synthase could be detected by comparison with a *Verticillium* comparative genomics database (33), we expected that the VI-PKS-1 gene would be present twice in the genome of *V. longisporum*. For the VI-PKS-1 mutants, additional signals could be detected on the blot accompanying the insertion of the HP-fragment into the genome of the fungus.

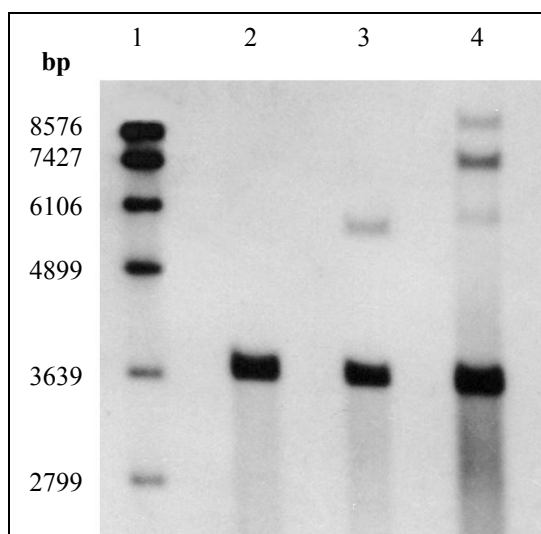


Figure 4: Southern-hybridization for candidate gene VI-PKS-1

1 = DNA Molecular Weight Marker VII, DIG-labelled (Roche Diagnostics GmbH, Penzberg, Germany)

2 = gDNA from *V. longisporum* wild type cut with *NcoI*

3 = gDNA from VI-PKS-1 silencing mutant m9 cut with *NcoI*

4 = gDNA from VI-PKS-1 silencing mutant m10 cut with *NcoI*

To evaluate any ectopic effects caused by the random integration of the silencing cassette into the fungal genome, we assessed the growth rate and germination efficiency of the mutants compared to the wild type of *V. longisporum*. For the evaluation of the spore germination rate of *V. longisporum* wild-type and the transformants, 50 spores were plated three-times and counted after 5 days of cultivation at 22 °C in the dark. No difference in the ability to germinate of the wild type fungus as compared to the silencing mutants could be detected. To assess the growth rate, single spores of wild-type and each transformant were plated three-times and growth rates were measured every second day for 14 days. We observed an increased growth rate of the VI-PKS-1 silencing mutants as compared to the wild type fungus. This growth rate became significant after 10 dpi.

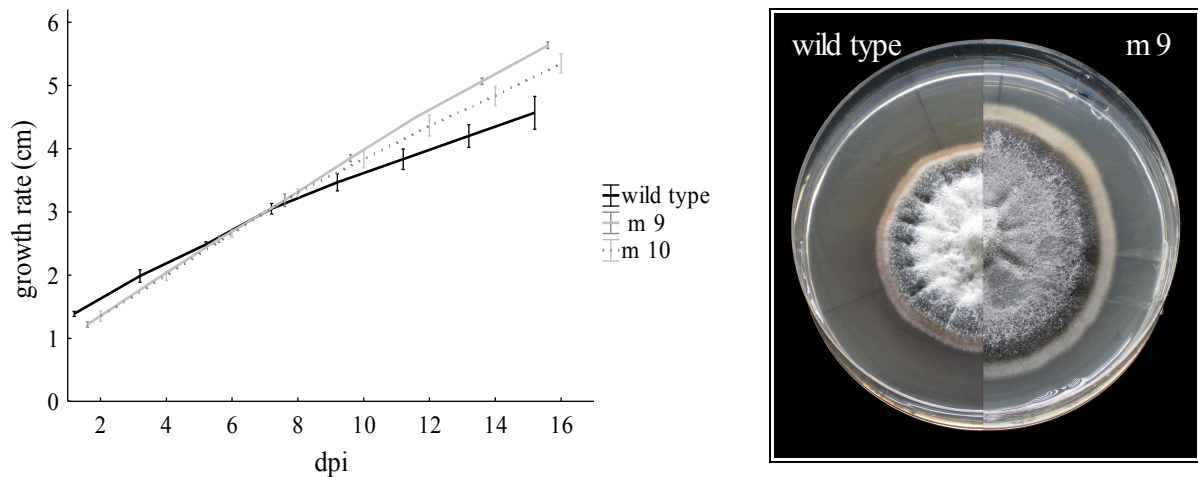


Figure 5: Growth rate of VI-PKS-1 silencing mutants compared to *V. longisporum* wild types

left side = radial growth was measured on four sides of the colonies, the graph shows the means of the calculated diameter with the standard deviation

right side = single colonies of *V. longisporum* wild type and VI-PKS-1 mutant m9 (20 dpi)

As reported in literature, PKS-1 knock-down-mutants of *C. lagenarium* and also YWA1 knock-out mutants of *A. nidulans* morphologically changed to albinos. We could demonstrate that VI-PKS-1 mutants show a delayed pigmentation of the mycelium when grown as a single colony on potato dextrose agar (PDA) medium. Pigmentation of *V. longisporum* wild type started at about 10 dpi when grown in the dark at 23 °C. VI-PKS-1 mutant pigmentation started at about 14 dpi. This effect was also observed for VI-PKS-1 mutants that were generated using the AS-RNA technique for the post-transcriptional downregulation of the candidate gene (data not shown). Therefore, it is most likely that VI-PKS-1 is involved in the biosynthesis of a pigment such as melanin.

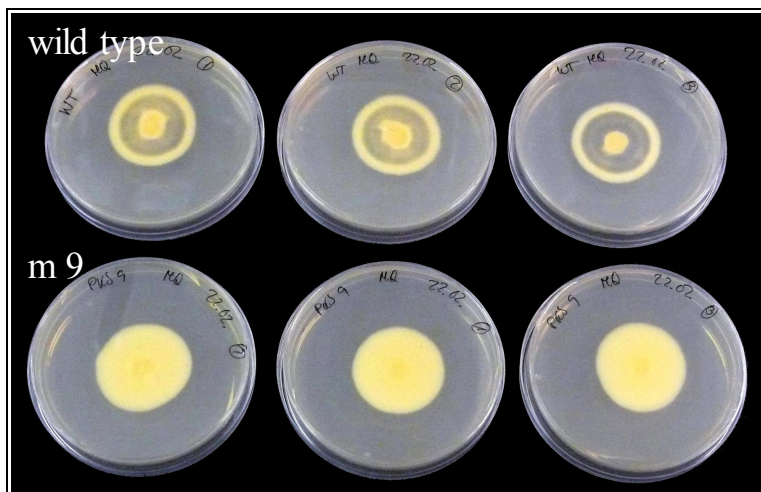


Figure 6: Phenotypic effect on the colonies of VI-PKS-1 silencing mutant m9 grown on PDA plates compared to wild type fungus (12 dpi)

We performed *B. napus* pathogenicity assays using “rapid cycle rape” to discover if VI-PKS-1 is involved in the melanization process of microsclerotia of *V. longisporum* (a process which is initiated *in planta* at the end of the parasitic life cycle) or if it has any other impact on the pathogenic life style of the fungus while infecting *B. napus*. No significant changes could be observed by assessing using the disease score of Zeise et al. (34) or in the shoot length of *V. longisporum* wild type or VI-PKS-1 mutant-infected plants. Microsclerotia-formation, which started at about 50 dpi showed no differences in microsclerotia-pigmentation of VI-PKS-1 mutants compared to the wild types. In summary we can say that the reduced ability of *V. longisporum*-mutants to produce VI-PKS-1 did not affect the pathogenicity to the natural host plant *B. napus*; therefore it is most likely that VI-PKS-1 is not a virulence or pathogenicity factor of the fungus in the interaction with *B. napus*.

Nevertheless, to understand the role of VI-PKS-1 in the *V. longisporum* life cycle, we tested whether VI-PKS-1 mutants have a different behaviour in their interaction with other soil-borne fungi as compared to *V. longisporum* wild type. Putatively, VI-PKS-1 helps the fungus to compete with other fungi in the soil because of the potential toxic ability of the PK synthesized by VI-PKS-1. We tested five different soil-borne ascomycota fungi by co-inoculating them along with *V. longisporum* wild type or VI-PKS-1 mutants. Then we plated both putative competitive fungi on opposite sides of a PDA plate and let them grow at 22 °C in the dark. We observed the fungal growth to detect if there were any changes in the interaction of the fungi. No changes in the interaction of *V. longisporum* wild type compared to VI-PKS-1 mutants could be observed while using *F. verticilloides*, *F. proliferatum* and *T. harzianum* for co-inoculation.

We observed notable changes in the interaction of *V. longisporum* wild type with *G. roseum*, which is known to be a natural competitor of different *Verticillium* species, as compared to the interaction while using VI-PKS-1 mutants for co-inoculation with *G. roseum*. We were able to show a slight inhibition zone between *V. longisporum* wild type and *G. roseum* after 16 dpi which could not be observed between the VI-PKS-1 mutants and the competitor. At this time point, *G. roseum* was only able to overgrow the VI-PKS-1 mutants but not the wild type. At later time points *G. roseum* also started to overgrow the surface of *V. longisporum* wild type but the mycelium of the competitor looked unhealthy and weak compared to that grown on the surface of VI-PKS-1 mutants.

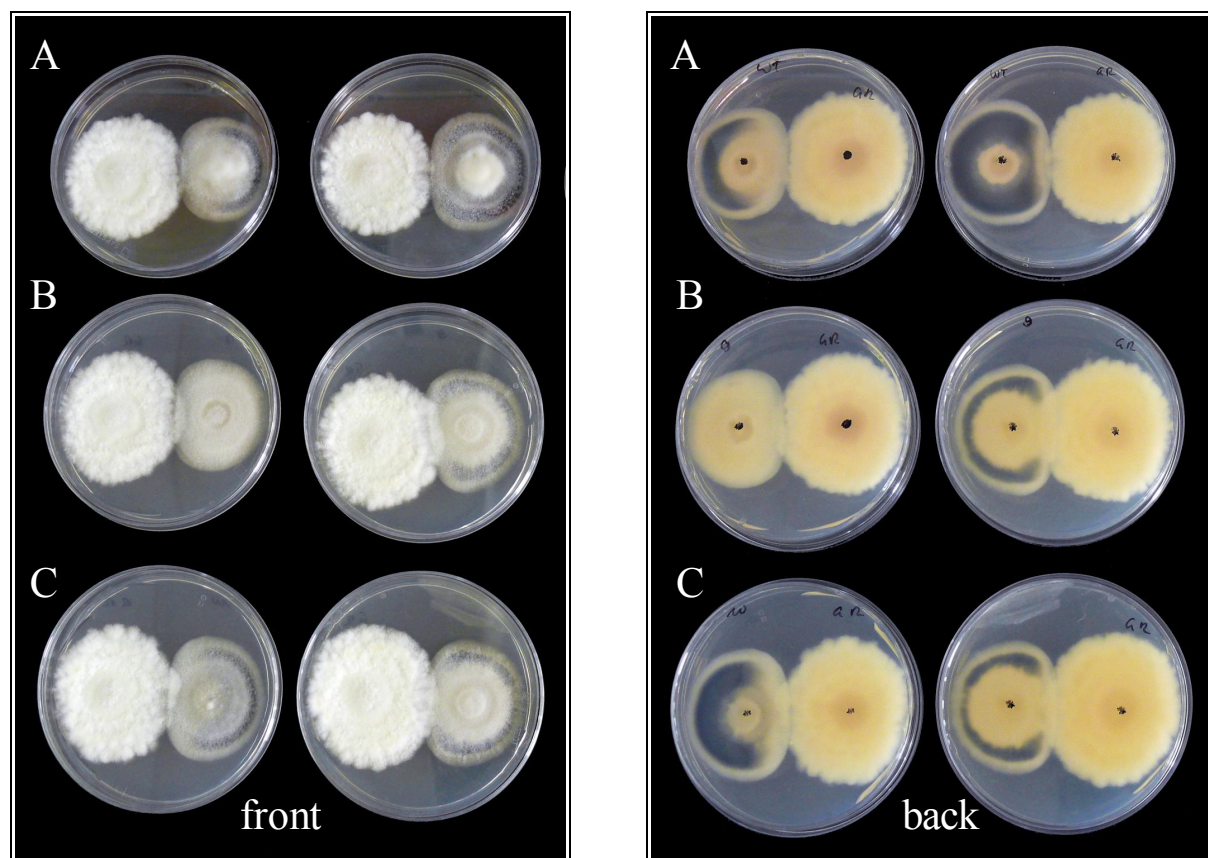


Figure 7: Fungal interaction assay using *V. longisporum* wild type and VI-PKS-1 silencing mutants to display any changes in the growth against *G. roseum*

A = *V. longisporum* wild type co-inoculated with *G. roseum* (both 16 dpi)

B = VI-PKS-1 mutant m9 co-inoculated with *G. roseum* (both 16 dpi)

C = VI-PKS-1 mutant m10 co-inoculated with *G. roseum* (both 16 dpi)

We noted another notable change in the growth of VI-PKS-1 mutants as compared to that of *V. longisporum* wild type while co-inoculating them along with *F. culmorum*. We observed the simultaneous inoculated fungi for 16 days without seeing any changes in the interaction of the fungi, but after 20 dpi we observed a significant change in the pigmentation of the grown mycelium of *F. culmorum* which was co-inoculated along with *V. longisporum* wild type. The mycelium of *G. roseum* which was co-inoculated along with VI-PKS-1 mutants stayed naturally orange (Figure 8 A-C). Because of the comparable fast growth rate, *F. culmorum* was able to completely overgrow both *V. longisporum* wild type and VI-PKS-1 mutants, but only showed a dark red pigmentation while growing along with the wild type fungus. In a repetition of the interaction assay, we inoculated *F. culmorum* only after 7 days of pre-incubation of *V. longisporum* on PDA plates to ensure that both fungi had the same size when

they came into contact with each other. After a total of 14 dpi we observed that in the area where *V. longisporum* and *F. culmorum* touched each other, again, a dark red pigmentation of the mycelium of *G. roseum* appeared (Figure 8 D). When growing *F. culmorum* along with VI-PKS-1 mutants, again, the mycelium stayed naturally orange as be observed when growing *F. culmorum* as a single colony on a PDA plate without any other fungi (Figure 8 E-F).

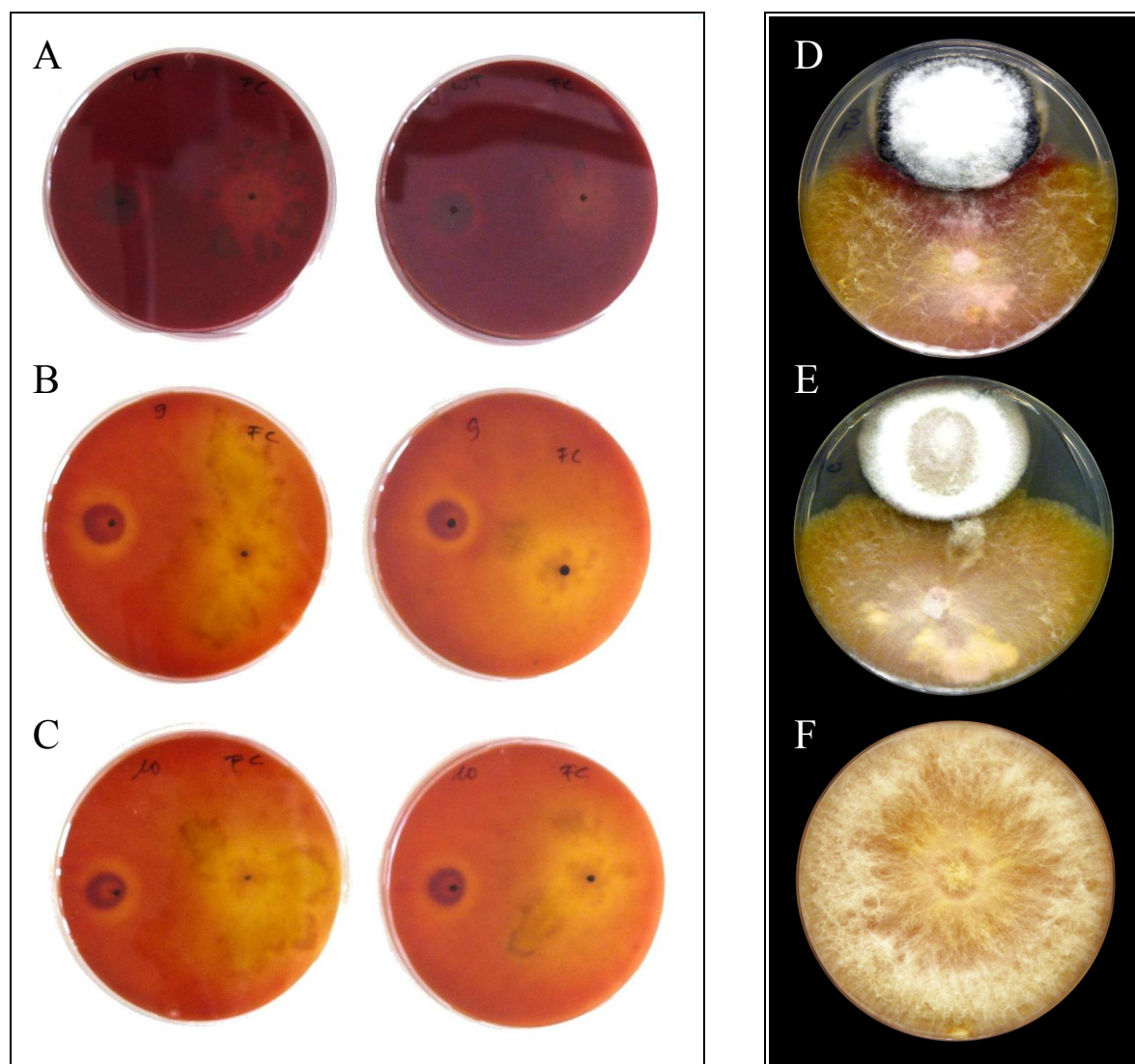


Figure 8: Fungal interaction assay using *V. longisporum* wild type and VI-PKS-1 silencing mutants to display any changes in the growth against *F. culmorum*

A = *V. longisporum* wild type co-inoculated with *F. culmorum* (both 20 dpi)

B = VI-PKS-1 mutant m9 co-inoculated with *F. culmorum* (both 20 dpi)

C = VI-PKS-1 mutant m10 co-inoculated with *F. culmorum* (both 20 dpi)

D = *V. longisporum* wild type co-inoculated with *F. culmorum* (*F. culmorum* 7 dpi, *V. longisporum* 14 dpi)

E = VI-PKS-1 mutant m9 co-inoculated with *F. culmorum* (*F. culmorum* 7 dpi, *V. longisporum* 14 dpi)

F = *F. culmorum* grown without *V. longisporum* (7 dpi)

A similar effect was described by Schlegel et al. in 2001, showing that colonies of *F. culmorum* responded to an extract of *Ulucladium* by enhanced production of a darker orange-red pigment as compared to the pigmentation which can be observed for the untreated fungus (35). The active compound of these extracts was identified as L-tenuazonic acid by using fractions of a column chromatography experiment from *Ulucladium* extract to test for their ability to induce the production of the orange-red pigment in the mycelium of *F. culmorum*. L-tenuazonic acid was first found in the fungus *Alternaria tenuis* and is described as a metabolite with antibiotic properties and that is believed to act as a mycotoxin. Schlegel postulated that L-tenuazonic acid strongly induces the production of a reddish PK such as fusarubin, which was reported to be expressed by *F. culmorum* (36). In our experiment the previously unknown PK, which is synthesized by VI-PKS-1, seemed to have a comparable ability to induce the production of a reddish pigment in *F. culmorum*.

When growing *V. longisporum* wild type at 22 °C in the dark, we observed that the PDA medium changed its typical yellow colour to a slight redder colouring after approximately 16 dpi. We could show that VI-PKS-1 silencing mutants did not show any change in the colour of the media. The same effect could be observed when growing the fungi in liquid potato dextrose broth (PDB) medium.

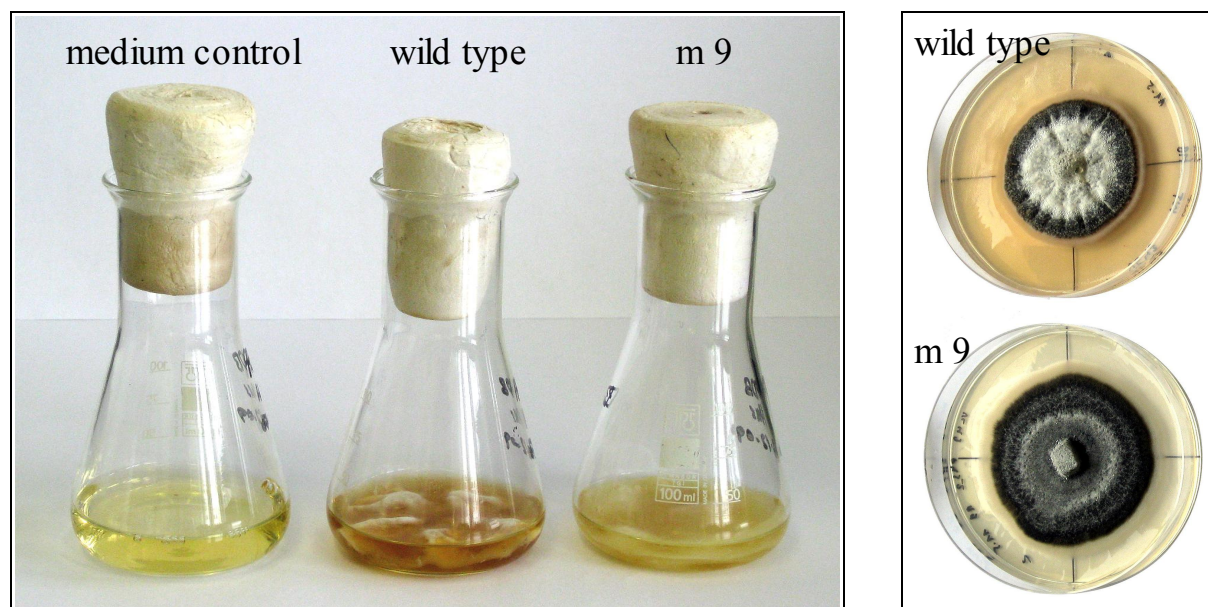


Figure 9: Colour change within the PDA medium caused by the growth of *V. longisporum* wild type
left side = *V. longisporum* grown in liquid PDB medium (16 dpi)
right side = *V. longisporum* grown on PDA plates (16 dpi)

Starting at a pH value of approximately 4, PDA and also PDB medium change colour, without any grown fungus inside, to a redder colour as compared to a medium with a pH above 4. The growth of *V. longisporum* typically decreases the pH value of culture media from the starting pH of 6 to a pH value of about 4.5-5, which is also present in the xylem sap of plants where the fungus mostly stays during its pathogenic life cycle and to which it is therefore adapted. We never measured any deviations in the pH value of the growth media of *V. longisporum* wild type as compared to the pH value measured in the growth media from VI-PKS-1 mutants which could be linked to the previously mentioned absence of the reddish colour media of the VI-PKS-1 mutant. To distinguish whether the reddish colouring we observed during co-inoculation using *V. longisporum* wild type and *F. culmorum* is caused by the reddish colour we observed in growing cultures of *V. longisporum*, we have recently started to investigate the metabolic profiles of VI-PKS-1 mutants and wild type cultures grown in PDB medium to identify the VI-PKS-1 synthesized PK. Therefore, culture media will be extracted using ethyl acetate, and changes in the metabolic profiles will be investigated using HPLC-MS with an RP-C18 column with a gradient of 10 % to 90 % methanol. Further experiments using the isolated compound should clarify the role of this PK in the life cycle of *V. longisporum*.

CONCLUSION

Among the multitude of PKS domains, the KS domain is the most highly conserved one and is therefore a suitable target to screen for PKS genes in various organisms. We used degenerated primers LC1 and LC2 described by Bingle et al. for amplification of KS domain fragments using *V. longisporum* for PCR (22). We identified a gene showing high homology to other fungal PKS genes that are known to be involved in pigment and aflatoxin biosynthetic pathways referred to as PKSs of the *wA*-type. By the use of the “Primer walking” technique, we were able to extend the gene-sequence of the putative PKS of *V. longisporum*, which we named as VI-PKS-1, to 1986 bp. Sequence alignment using the known VI-PKS-1 sequence as a query to compare with a library of sequences from a comparative database, enlightened the conserved KS domain in the VI-PKS-1 sequence and thereby showed high sequence-homology to several PKS type I genes of diverse fungi. The highest homology we found was with a conidial yellow pigment synthase of both parental *V. dahliae* and *V. albo-*

atrum strains, which is known to synthesize a heptaketide naphthopyrene YWA1. YWA1 is a yellow pigment found in the conidia of different *Aspergillus* species. At the moment we are working on the elucidation of the complete genomic sequence of VI-PKS-1 to show all included conserved PKS domains to allow a more precise forecast of the function of the PKS that is encoded by the gene.

Despite the highly upregulated gene expression of VI-PKS-1 during all stages of the pathogenic life cycle of *V. longisporum* as shown by qRT-PCR analysis, we did not observe that silencing of the gene expression led to any alteration on the phenotype of the infected host plant *B. napus*. Nevertheless, we could show that VI-PKS-1 silencing mutants exhibited major differences regarding the growth rate, the pigmentation of the mycelium and the interaction with other fungi as compared to the wild type of *V. longisporum*.

The delayed pigmentation of the mycelium of VI-PKS-1 mutants as compared to the wild type fungus, when grown on PDA plates as a single colony, implies the involvement of the synthesized PK in the biosynthesis of a pigment like melanin. However, older cultures of VI-PKS-1 mutants still show a strong pigmentation of the mycelium comparable to that we observed when growing *V. longisporum* wild type cultures. Up to now, we could not say with absolute certainty if the VI-PKS-1 mutants show a delayed, but finally existing pigmentation, because the gene-function of VI-PKS-1 was not fully switched off by RNAi in the mutants, or because of a homologous gene with a redundant function which is expressed by the fungus taking over the function of VI-PKS-1 and thereby synthesizing the related PK. Finally, it can be speculated that the first assumption is correct because of the knowledge gained about post-transcriptional downregulation of genes, triggered by the intracellular expression of an HP cassette by the release of a mechanism referred to as RNAi. It has often been reported that specific HP RNA of a candidate gene also executes downregulation of gene-function for redundant genes with high homology to the candidate gene (37).

In consideration of the enhanced growth rate of VI-PKS-1 mutants and the ability of *G. roseum* to overgrow the mycelium of VI-PKS-1 mutants as compared to that of *V. longisporum* wild type, we postulate that the synthesized PK by VI-PKS-1 seems to act in a toxic manner, which leads to a low dimensional self-toxicity and thereby a slight suppression of fungal growth. Therefore, it can be explained that *V. longisporum* wild type showed a protective ability against competitive fungi like *G. roseum* due to assumed secretion of the PK

into the surrounding growth medium. This assumption was supported by our observation of a reddish colouring of the medium of *V. longisporum* wild type when grown on PDA plates and even in liquid PDB medium. This colouring of the media is absent when growing the VI-PKS-1 mutants under the same conditions. Therefore, we postulate that the PK which is synthesized by VI-PKS-1 is probably secreted into the medium. To investigate whether the dark-red colouring of the mycelium of *F. culmorum* that we observed during co-inoculation along with *V. longisporum* wild type is actually caused by the reddish colour we observed while growing *V. longisporum* wild type on PDA plates or liquid PDB medium without any other fungi, or is caused by an induction of an reddish PK such as fusarubin by the PK synthesized by VI-PKS-1, our focus is on the identification of the active compound that is synthesized by VI-PKS-1. Thereby we hope to prove the hypotheses we formulated based on the results of the experiments in this chapter.

ACKNOWLEDGMENTS

The author would like to thank the following people for their outstanding assistance during this chapter:

Prof. Petr Karlovsky for giving me the opportunity to work on VI-PKS-1 of *V. longisporum* and the continuous assistance regarding scientific problems. **Dr. Hanno Wolf** for the detection of VI-PKS-1 using degenerated primers for PCR. **Wolfgang Hiegl** for sequence extension of VI-PKS-1 gene using the “Primer walking” technique. **Dr. Arne Weiberg** for measuring VI-PKS-1 expression ratios *in vitro* and *in planta* and further, for the excellent cooperation and the remarkable help working on VI-PKS-1. **Mona Quambusch** for her assistance during *B. napus* pathogenicity assays. **Haiquan Xu** for the construction the AS-RNA expression vector and the subsequent transformation of *V. longisporum*.

REFERENCES

1. **O'Hagan D.** (1995). Biosynthesis of fatty acid and polyketide metabolites. *Nat Prod Rep* 12:1–32.
2. **Kim Y.T., Lee Y.R., Jin J., Han K.H., Kim H., Kim J.C., Lee T., Yun S.H., Lee Y.W.** (2005). Two different polyketide synthase genes are required for zearalenone in *Gibberellazeae*. *Mol. Microbiol.* 58:1102-1113.
3. **Proctor R.H., Desjardins A.E., Plattner R.D., Hohn T.M.** (1999). A polyketide synthase gene required for biosynthesis of fumonisin mycotoxins in *Gibberella fujikuroi* mating population A. *Fung. Genet. Biol.* 27:100-112.
4. **Watanabe C.M., Wilson D., Linz J.E., Townsend C.A.** (1996). Demonstration of the catalytic roles and evidence for the physical association of type I fatty acid synthases and a polyketide synthase in the biosynthesis of aflatoxin B1. *Chem. Biol.* 3:463-469.
5. **Howard R.J., Ferrari M.A., Roach D.H., Money N.P.** (1991). Penetration of hard substrates by a fungus employing enormous turgor pressures. *PNAS* 88:11281-11284.
6. **O'Hagan D.** (1991). Biosynthesis of polyketide metabolites. *Nat. Prod. Rep.*, 9, 447-479.
7. **Hopwood DA.** (1997). Genetic contributions to understanding polyketide synthases. *Chem Rev* 97:2465–2497.
8. **Khosla C, Gokhale RS, Jacobsen JR, Cane DE** (1999). Tolerance and specificity of polyketide synthases. *Annu Rev Biochem* 68:219–253.
9. **Simpson T.J.** (1995). *Chemistry and Industry. Polyketide biosynthesis*, 407-413.
10. **Pieper, R., Luo, G. L., Cane, D. E. & Khosla, C.** (1995). Cell-free synthesis of polyketides by recombinant erythromycin polyketide synthases. *Nature* 378, 1995, 263-266.
11. **Beck, J., Ripka, S., Siegner, A., Schiltz, E., and Schweizer, E.** (1990) The Multifunctional 6- Methylsalicylic Acid Synthase Gene of *Penicillium patulum* - Its Gene Structure Relative to That of Other Polyketide Synthases. *European Journal of Biochemistry* 192: 487-498.
12. **Brown DW, Yu J-H, Kelnar HS, Fernandes M, Nesbitt TC, Keller NP, Adams TH, Leonard TJ** (1996). Twenty-five co-regulated transcripts define a

- sterigmatocystin gene cluster in *Aspergillus nidulans*. Proc Natl Acad Sci USA 93:1418–1422.
13. **Chang PK, Cary JW, Yu J, Bhatnagar D, Cleveland TE** (1995). The *Aspergillus parasiticus* polyketide synthase gene *pkA*, a homolog of *Aspergillus nidulans wA*, is required for aflatoxin B-1 biosynthesis. Mol Gen Genet 248:270–277.
 14. **Watanabe A, Fujii I, Sankawa U, Mayorga ME, Timberlake WE, Ebizuka Y** (1999). Re-identification of *Aspergillus wA* gene to code for a polyketide synthase of naphthopyrone. Tetrahedron Lett 40:91–94.
 15. **Takano Y., Kubo Y., Shimizu K., Mise K., Okuno T., Furusawa I.** (1995). Structural analysis of PKS1, a polyketide synthase gene involved in melanin biosynthesis in *Colletotrichum lagenarium*. Mol. Gen. Genet. 249:162-167.
 16. **Reinke, J.; Berthold, G.** (1879). Die Zersetzung der Kartoffel durch Pilze: 63.
 17. **Zeise K., von Tiedemann A.** (2001) Morphological and physiological differentiation among vegetative compatibility groups of *Verticillium dahliae* in relation to *V. longisporum*. Journal of Phytopathology 149: 469-475.
 18. **Williams PH. & Hill C. B.** (1986). Rapid-cycling populations of *Brassica*. Science 232, 1385-1389.
 19. **Debode, J., Claeys, D. & Höfte, M.** (2004). Control of *Verticillium* wilt of cauliflower with crop residues, lignin and microbial antagonists. IOBC WPRS Bull 27, 41–45.
 20. **Utermark J.** (2008). Genetic transformation of filamentous fungi by *Agrobacterium tumefaciens*. Nature Protocols, Published online 20 March 2008.
 21. **Maniatis T., Fritsch EF., Sambrook J.** (1982). Molecular Cloning: A Laboratory Manual. Trade paperback, Cold Spring Harbor Laboratory Press.
 22. **Bingle, L.E.H., Simpson, T.J. & Lazarus, C.M.** (1999). Ketosynthase Domain Probes Identify Two Subclasses of Fungal Polyketide Synthase Genes. Fungal Genetics and Biology 26: 209-223.
 23. **National Center for Biotechnology Information**, homepage (<http://www.ncbi.nlm.nih.gov/>).
 24. **Barbara D.J., Clewes E.** (2003). Plant pathogenic *Verticillium* species: how many of them are there? Mol. Plant Pathol. 4:297-305.

25. **Collins A., Okoli C.A.N., Morton A., Parry D., Edwards S.G., Barbara D.J.** (2003). Isolates of *Verticillium dahliae* pathogenic to crucifers are of at least three distinct molecular types. *Phytopathol.* 93:364-376.
26. **Dixon DM, Polak A, Szaniszlo PJ.** (1987). Pathogenicity and virulence of wild-type and melanin-deficient *Wangiella dermatitidis*. *J Med Vet Mycol.*; 25(2):97-106.
27. **Lundqvist, T.; Rice, J.; Hodge, C.N.; Basarab, G.; Pierce, J.; Lindqvist, Y.** (1994). Crystal Structure of Scytalone Dehydratase: a Disease determinant of the Rice Pathogen *Magnaporthe grisea*. *Structure* 2, 937-944.
28. **Perpetua NS, Kubo Y, Yasuda N, Takano Y, Furusawa I.** (1996). Cloning and characterization of a melanin biosynthetic THR1 reductase gene essential for appressorial penetration of *Colletotrichum lagenarium*. *Mol Plant Microbe Interact.*; 9(5):323-9.
29. **Mayorga ME, Timberlake WE.** (1992). The developmentally regulated *Aspergillus nidulans wa* gene encodes a polypeptide homologous to polyketide and fatty acid synthases. *Mol Gen Genet.* Nov;235(2-3):205-12.
30. **Fujii I, Mori Y, Watanabe A, Kubo Y, Tsuji G, Ebizuka Y** (2000). Enzymatic synthesis of 1,3,6,8-tetrahydroxynaphthalene solely from malonyl coenzyme A by a fungal iterative type tsI polyketide synthase PKS1. *Biochemistry* 39:8853–8858.
31. **Fujii I, Mori Y, Watanabe A, Kubo Y, Tsuji G, Ebizuka Y.** (1999). Heterologous expression and product identification of *Colletotrichum lagenarium* polyketide synthase encoded by the PKS1 gene involved in melanin biosynthesis. *Biosci Biotechnol Biochem.* 1999 Aug;63(8):1445-52.
32. **Tsai HF, Fujii I, Watanabe A, Wheeler MH, Chang YC, Yasuoka Y, Ebizuka Y, Kwon-Chung KJ.** (2001). Pentaketide melanin biosynthesis in *Aspergillus fumigatus* requires chain-length shortening of a heptaketide precursor. *J Biol Chem.*; 276(31): 29292-8.
33. **The Broad Institute,** homepage *Verticillium* group database (<http://www.broad.mit.edu/annotation/genome/verticilliumdahliae/MultiHome.html>).
34. **Zeise, K.** (1992). Gewächshaustest zur Resistenzprüfung von Winterraps (*Brassica napus* L. var. *oleifera* Metzger) gegen den Erreger der Rapswelke *Verticillium dahliae* Kleb. *Nachrichtenblatt Deutscher Pflanzenschutzdienst* 44:125-128.

35. **Schlegel B, Schmidtke M, Dörfelt H, Kleinwächter P, Gräfe U.** (2001). (-)-Terpestacin and L-tenuazonic acid, inducers of pigment and aerial mycelium formation by *Fusarium culmorum* JP 15. *J Basic Microbiol.*;41(3-4):179-83.
36. **Laatsch, H.** (1999). *Antibase*. Database of microbial metabolites. Chemical Concepts, Heidelberg.
37. **C Napoli, C Lemieux, and R Jorgensen** (1990). Introduction of a Chimeric Chalcone Synthase Gene into *Petunia* Results in Reversible Co-Suppression of Homologous Genes in trans. *Plant Cell.*; 2(4): 279–289.

APPENDIX

primer name	sequence (5' → 3')
sense- <i>SdaI</i> -F	TAGTGACCTGCAGGACATCGAGAGGATCGACGCCAGC
sense- <i>NdeI</i> -R	GATATGCATATGACATGTCGCCGCGCGAGCCTAC
antisense- <i>AscI</i> -F	GAGCTCGGCGCGCCACATCGAGAGGATCGACGCCAGC
antisense- <i>BglII</i> -R	GATATGAGATCTACATGTCGCCGCGCGAGCCTAC
spacer- <i>NdeI</i> -F	CTATACCATATGACTGCTCTACCCGTACGTTG
spacer- <i>BglII</i> -R	GATATGAGATCTCCTGGCACTCTTTGCTATTGTTGG

Table 1: Primer sequences for the amplification of fragments possess restriction sites suitable for the construction of an HP fragment using conventional cloning steps

primer name	sequence (5' → 3')
VI-PKS-1-SB-sense-F	ACATCGAGAGGATCGACGCCAGC
VI-PKS-1-SB-sense-R	ACATGTCGCCGCGCGAGCCTAC

Table 2: Primer sequences for the amplification of probes for southern hybridization

primer name	sequence (5' → 3')
VI-PKS-1-RT-sense-F	AGCGTCCTGCAAACAGACC
VI-PKS-1-RT-sense-R	TGTCAGTGGGAAAGCGATG
tubulin-F	GTTTCATCTTCAGACCGGTCAGT
tubulin-R	CCAGACTGGCCGAAAACGAAGT
rps17-F	GCATCTGCGATGAGATCGCCA
rps17-R	TCGGAGTTCTGGGTAAAGTCGAGA

Table 3: Primer sequences to measure silencing efficiency of silencing mutants by qRT-PCR

primer name	sequence (5' → 3')
LC1	GTGTTGTGTTGCGGCCGCGAYCCNMGNTTYTTAAAYATG
LC2	GTNCCNGTNC CRTGCATYTC

Table 4: Degenerated primers according to Bingle et al.

primer name	sequence (5' → 3')
VI-PKS-1 W1-F	CTACCAACCATTCTGCCGACGCC
VI-PKS-1 W1-R	CCYTGNCNGTRAANATRAANGC
VI-PKS-1 W2-F	ATCCCGAAACCCCGCTTGCTG
VI-PKS-1 W2-R	ACYTGNGCNGARTGRAANGC
VI-PKS-1 W3-F	GTNTAYGGNTCNTAYCAYGC
VI-PKS-1 W3-R	TCATCGGAGGTCTGACCGTAA

Table 5: Primers used for “primer walking” to extend the VI-PKS-1 sequence

VI-PKS-1	
gDNA sequence (incomplete)	
1	GATCCGAGGTTTTTTAAACATGTCGCCGCGGAAGCCTACCAGACCGACCC
51	CATGCAACGCATGGCCCTGACCACGGCTTATGAAGCCTTGGAATGTCTG
101	GGTATGTCCCGAATAGGACAGCCTCTACCAGGCTTGACCGGATTGGTACA
151	TTTTACGGTCAGACCTCCGATGATTGGCGAGAGATCAATGCCGCACAGGA
201	AGTCGACACATACTTCATCACCAGGGGAGTACGCGCCTTTGGCCCTGGCA
251	GAATCAACTACCACTTCGGTTTTAGTGGACCTAGTCTGAACATCGATACA
301	GCCTGTTCTTCCAGTGCCGCAGCTCTGCAAATCGCATGCACCTCGCTCTG
351	GGCCAAGGACTGTGACACGGCAGTCGTTGGCGGCTTGTCTTGCATGACCA
401	ACCCGATATTTTCTCAGGACTCAGCCGTGGCCAGTTCCTTGTCCAAGACT
451	GGTCCCTGTGCTACGTTTGACAATGGAGCTGATGGTTACTGCCGAGCTGA
501	TGGCTGCGCCTCCGTCATTGTGAAGCGTCTGGATGATGCCATTGCCGACA
551	AGGACAATGTCTGGCGGTCATCCTGGGCACGGCTACCAACCATTCTGCC
601	GACGCCATATCGATTACCCATCCTCATGGACCTACGCAGTCGATCCTATC
651	ATCAGCCATTCTCGATGAGGCTGGCGTCGATCCTCTCGATGTTGACTACG
701	TCGAGATGCATGGGACAGGCACTCAGGCCGGTGTGGCACGGAAATGGTC
751	TCTGTACAGACGTATTCGCACCTGCCAACCGCAAGCGTCTTGC AAACAG
801	ACCTCTGTATCTCGGCGCTGTGAAATCTAACATCGGCCACGGTGAGGCTG
851	CTTCAGGCGTGACAGCTCTCTGCAAGGTTCTCATGATGTTGCAAAAAAAC
901	GCCATCCCTCCTCAGTCGGCATAAAAAAGGATATCAACAAGACCTTCC
951	TAAGGATCTTGCGGAGCGAAACGTCAACATCGCTTTCCACATGACACCTC
1001	TCAAAAAGGCATGATGGGAAACCCAGGAGAATCTTCATCAACAACCTCAGC
1051	GCCGCCGGTGGTAATACCGGTCTCCTCCTTGAGGATGGTCCCAGCCAGAC
1101	GCCCACACAGGCGGACCCTCGCAGTGCTCAAGTCATTACTATCACGGCCA
1151	AGTCCAAGACGGCCATGATTAAGAATGCTGAACAATTGGTGACGTGGATG
1201	GAGAAGAAATCCCGAAACCCCGCTTGCTGATGTTGCTTACACCACAACGGC
1251	CCGTCGCATGCAACACTACTGGCGCCTGAATGTCGCCGCCTCCACCTTGT
1301	CTGAAGCCATGTCAGCCATCAAGGAGAGGCTCACTCAAACTTTGTGCC
1351	ATCTCGACTGAGCAGCCAAAGGTGGCCTTCATCTTACAGGCCAAGGCTC
1401	TCACTATGCTGGTCTTGGAAGGACCTTACGCCACTACGCTGTCTTCA
1451	GAGACAGCATCAATGAGTTCAATCATATCGCCGAAGTCCATGGCTTCCCG
1501	TCTTTTGTGCCATTGATTGATGGCAGCGAACCTGACGTCTCCAAGCTATC
1551	ACCCGTGGTTGTGCAGCTTGGCCTCTGCTGCTTCGAGATGGCTCTAGCCA
1601	GACTGTGGGCTGCATGGGGTATCAGGCCCGCTGTGGTTCTGGGGCACTCT

1651	CTCGGAGAATATGCTGCTCTGAACGCCGCCGGCGTACTGTCCGCAAGCGA
1701	CACCATCTATCTCGTCGGCAGTCGCGCTCAGCTTCTCGTCGACAGGTGCA
1751	CTGCTGGTACCCATGCCATGCTTGCTGTGCAGGGCCCCGGTTGGGACTGTC
1801	AACGAGGCTCTCGGATCCGAATTCGCCTCAGTCAACATCGCCTGCATCAA
1851	CGGGCCTCGTGAGACCGTTCTCAGTGGTGAAACTGACCACATGATGAAGA
1901	TTGCCACGCAATTGGGCGCGTCTGGATTCAAGTGCACCCAGCTGAATGTT
1951	CCCTATGCCTTCCACTCC

Table 6: gDNA sequence of VI-PKS-1 obtained by „Primer walking“

Chapter 5: Final discussion

This thesis was realized during participation in the DFG research unit FOR 546, whose task was to identify and elucidate signals which shape the interaction between the plant-pathogenic fungus *V. longisporum* and its host plants (1). The genus *Verticillium* includes many plant pathogenic species that cause serious economic losses through the infection of host plants, and it belongs to one of the most widespread groups of plant pathogens in the world (2). The species with the highest impact on yield loss on important agricultural crops, including e.g. cotton, strawberry, tomato and potato (3, 4), are *V. dahliae* and *V. albo-atrum*, which are present in temperate and subtropical regions (5) and cause diverse symptoms that vary among host plants. *V. longisporum* is described as an amphihaploid interspecific hybrid of parental *V. dahliae* and *V. albo-atrum* strains (6, 7), and therefore shares many characteristics with these strains. Like *V. dahliae* and *V. albo-atrum*, *V. longisporum* is a soil-borne vascular pathogen with a hemibiotrophic lifestyle, but notwithstanding, the host range is strictly limited to the family of *Brassicaceae* (8). The fungus also did not show any wilting symptoms after infection of hosts in the field nor in the greenhouse (9, 10, 11, 12), which is described to be a typical symptom on host plants with *Verticillium* infection. The basis of the infection of *V. longisporum* on plants is mostly unknown and, therefore, studying the host-pathogen interaction using molecular-genetic and chemical-analytical methods provides the opportunity for a better understanding of the disease caused by the fungus, and thereby helps in finding new strategies for the prevention or the control of infection. Comparative studies were done by other members of the DFG research unit FOR 546, using liquid chromatography mass spectrometry (HPLC-MS)-derived metabolic profiles and cDNA-amplified fragment-length polymorphism (AFLP)-derived transcriptome profiles of xylem sap from uninfected plants. These were compared to *V. longisporum*-infected plants and the result revealed 19 metabolites and 8 transcript-derived fragments (TDFs) to be accumulated or expressed differently upon *V. longisporum* infection (13, 14). Metabolites, including salicylic acid (SA) and its glucoside (SAG), and TDFs, including a water-soluble carbohydrate binding protein and a zinc finger transcription factor, are putatively involved in the host-pathogen interaction upon infection. Selected TDFs with an upregulated expression during plant-infestation were tested for having a role in the pathogenic-life cycle of the fungus by switching of the candidate gene function (15). Because of its amphihaploid genome, which comprises two almost complete sets of haploid genomes derived from parental strains in one single nucleus, it is most likely that *V.*

longisporum often carries more than one gene-copy of specific candidate genes, and therefore the production of knock-out mutants using homologous recombination to switch off specific gene functions is hampered.

Gene silencing in *V. longisporum*

HP expression of candidate genes has been reported in the literature to be the most potent trigger for post-transcriptional downregulation in ascomycota fungi (16), and it was recently shown, by another member of the DFG research unit, that RNA interference (RNAi) could be released by intracellular expression of hairpin (HP)-constructs in *V. longisporum* (17). Our attempts to use the overlap-extension (OE)-PCR technique for the construction of HP-fragments without the use of any conventional cloning steps was impaired by the strong tendency of the HP-fragments to anneal after each denaturation step of PCR, forming HP structures by pairing of homologous sequences of sense and antisense ssDNA fragments (see Chapter 2). The use of asymmetric OE-PCR led to only one correctly assembled HP fragment out of more than one hundred attempts, and was therefore not worth the effort needed to correctly assemble sense and antisense fragments with the spacer. By using a method based on conventional cloning steps, we succeeded in HP fragment construction. We assembled flanking sense and antisense arms ranging from 180 to 696 bp length and an intervening 125 bp spacer of a native intron from the *V. longisporum* hydrophobin gene *VlHI*. We created several *V. longisporum* mutants by *Agrobacterium thumefaciens* mediated transformation (AMT) (18) by integrating HP expression-cassettes of different candidate genes suitable for triggering RNAi in the fungus. The generated mutants showed silencing efficiency of candidate genes of 98 % at best as compared to *V. longisporum* wild type gene expression. Additionally we were able to show that intracellular expression of an antisense RNA (AS-RNA), which was designed complementary to the specific mRNA of the candidate gene, was a potent trigger for triggering postranscriptional downregulation of gene-function in *V. longisporum*. AS- RNA expression results in a moderate silencing-efficiency of candidate genes of up to 70 % compared to wild type gene expression (15).

Both, HP RNA and AS-RNA, were used during the research of this thesis for functional characterization of pathogenicity-related genes of the ascomycota fungus *V. longisporum*. Many candidate genes were efficiently silenced in the “Molecular phytopathology and

mycotoxin research” laboratory, including the upregulated TDFs displayed by cDNA-AFLP (14), and also genes which were reported in literature to be potential virulence or pathogenicity factors of ascomycetes during infection of host plants. During the research reported in this thesis we gave preference to the results for two genes that showed notable changes due to silencing of specific gene-functions.

The impact of VI-NEP-1 on the pathogenicity to *B. napus*

Previous studies regarding pathogenicity factors expressed by *Verticillium* species during the host-pathogen interaction showed that mostly polysaccharolytic active peptides, such as pectinases, which have a degradative feature on plant cell walls, are linked to a successful infestation of the plant by the pathogen. Nevertheless, pectinase-deficient mutants of *V. longisporum* show interfered symptom development in the plant but finally no change in the degree of colonization compared to wild type infected plants. Accordingly, pectinases have been classified as virulence factors and not as pathogenicity factors (19, 20). During our research, we demonstrated that downregulation of a gene with a high homology to the necrosis and ethylene inducing peptide (NEP)- family, which we therefore designated as VI-NEP-1, was connected to symptom severity caused by *V. longisporum* on the natural host plant *B. napus*, and thereby indicated a reduced ability of the fungus to spread into the plant. In summary, we detected five NEP genes, designated as VI-NEP-1 to 5, in the genome of *V. longisporum* from which we could measure strong expression levels of three NEP genes (VI-NEP-1, -2, -5) *in planta* by qRT-PCR. This makes a contribution of these genes to the pathogenic life cycle of *V. longisporum* while infecting *B. napus* acceptable.

Our results for VI-NEP-1 suggest that the related gene product is secreted in the xylem by the fungus and permeabilizes the surrounding cell membranes of the xylem cylinder, causing leakage of monomers from adjacent tissue into the xylem sap. These monomers are putatively used as nutrients by the fungus and thereby increase the fitness of *V. longisporum* in the xylem. Distinctive features of NEP-like proteins (NLPs) could be proved while using the purified VI-NEP-1 protein to test for plant reactions after treatment. Consistent with previous reports which showed that necrotic lesion formation is artificially inducible by leaf infiltration of the protein (21), we were able to induce lesions on leaves of *Brassica* and *Tobacco*. Thereby, lesion formation was proved to be both leaf age and dose dependent after infiltration

of the protein. Necrosis on host plants was never observed as a symptom after natural infection of host-plants with *V. longisporum*, or on artificially infected plants in the laboratory. Therefore, we believe that the concentration of VI-NEP-1 in the plant is apparently too low to induce necrosis and does not reach the phytotoxic threshold that is required to induce necrosis in the plant. Recently conducted pathogenicity-assays on *B. napus* using spore solutions with 1×10^7 to 1×10^9 spores/ml⁻¹ for root-dip inoculation revealed that infected plants show serious symptoms, including necrotic lesion formation.

Besides necrosis, the inhibition of root growth in *Arabidopsis* was reported as a result of treatment of NLPs (22, 23). We also showed that VI-NEP-1 treatment results in reduced root length while adding the protein to the growth medium of *Arabidopsis* seedlings from different ecotypes. In contrast, we showed that *B. napus* plants were not affected at all by the treatment with the purified protein. This could be an indication that VI-NEP-1 silencing mutants showed reduced symptom development on *B. napus* plants; however *A. thaliana* did not show any change as a result of inoculation with VI-NEP-1 mutants as compared to *V. longisporum* wild type infection. This finding suggests that VI-NEP-1 seems to have a crucial role in the infection-process of the natural host plant *B. napus* but not in *A. thaliana*. Further tests must be performed to show if the expression of VI-NEP-1 in *A. thaliana*-infected plants is not as strong as in *B. napus*-infected plants or if an assumed receptor of the protein is not present in the xylem-cylinders of *A. thaliana* plants. We are firmly convinced that the identification of a VI-NEP-1 related receptor in *B. napus* is linked with functional understanding of the protein.

The role of VI-PKS-1 in the life cycle of *V. longisporum*

Another candidate gene shows notable effects as a result of post-transcriptional downregulation of gene function using RNAi, and has high homology to fungal type I polyketide synthase (PKS) genes of the *wA* type, and we therefore named this gene VI-PKS-1. PKS catalyze the series of small carboxylic acids into polyketides (PK) which belong to a large group of fungal secondary metabolites that are described as compounds not primarily needed for essential processes concerning the survival and the reproduction of the fungus (24). PKS includes several highly conserved domains, each of which has a defined function. Type I PKS consists of starting modules referred to as acyltransferase (AT) and an acyl carrier protein (ACP) which executes the synthesizing of the growing PK chain. A keto synthase

(KS) initiates the elongation of the PK chain. Several elongation modules, such as keto-reductase (KR) domains or dehydratase (DH) domains, which give rise to the structural diversity of PKs and their manifold biological activities, are stepwise added to the chain. The thio esterase (TE) domain acts as a termination module hydrolyzing the completed polyketide from the ACP.

We used degenerate primers based on fungal KS-domains (25) to amplify putative PKS genes from the gDNA of *V. longisporum* by PCR. We were able to detect a gene, which we named VI-PKS-1, that has a highly upregulated gene expression *in planta* as compared to *in vitro*, and this makes a contribution in the pathogenic life cycle of *V. longisporum* assumable. VI-PKS-1 show high homology to a conidial yellow pigment synthase gene from *V. dahliae*, which is reported to be a parental strain of amphihaploid *V. longisporum* (26, 27). The conidial yellow pigment synthase is known to be involved in a process that forms the heptaketide naphthopyrene YWA1, which is a yellow pigment first found in mature asexual spores (conidia) of *Aspergillus nidulans* (28). Gene silencing mutants of VI-PKS-1 show major differences in their growth characteristics as compared to those of *V. longisporum* wild type. As compared to the wild type of *V. longisporum*, a significant increased growth rate of VI-PKS-1 mutants and their partial loss of competitive capacity, which we demonstrated by an fungal-interaction assay using *G. roseum* for co-inoculation with *V. longisporum*, both plated on PDA agar, suggests that the metabolite synthesized by VI-PKS-1 has a toxic ability, as mentioned in literature for different PKs known from other fungi (29, 30, 31). Additionally we could show that, when growing *V. longisporum* wild type both in liquid potato dextrose broth (PDB) and on solid potato dextrose agar (PDA), the medium changed its colour from typical yellow to a redder colour, which we could not observe when growing the VI-PKS-1 mutants in the same way. A similar effect was shown during the fungal-interaction assay while growing *V. longisporum* along with *Fusarium culmorum*. Thereby, *V. longisporum* wild type seems to induce a reddish colouring of the mycelium of *F. culmorum*, which we never observed when using the VI-PKS-1 mutants for co-inoculation with *F. culmorum*. It was not clear whether the colour change was indeed caused by the induction-ability of the metabolite synthesized by VI-PKS-1 or was due to the secretion of a reddish compound by the fungus we observed in the PDB medium. Therefore, we recently started to identify the metabolite synthesized by VI-PKS-1 using HPLC-MS to get a closer look at its function.

As compared to type I PKS knock out mutants from *Colletotrichum lagenarium* and *A. nidulans*, which shows an albino phenotype, we were able to observe a delayed pigmentation on VI-PKS-1 mutants. The albino phenotype, which was apparent on VI-PKS-1 mutants after 12 dpi as compared to the strong pigmentation of *V. longisporum* wild type fungus at the same time, was most likely revoked due to the gene function of VI-PKS-1 not being fully switched off by RNAi. In 2005, Kehr et al. postulated that defence-related proteins with capacities to degrade fungal cell walls (32) are present in the xylem sap. When growing *V. longisporum* in simulated xylem medium (SXM), which simulates the basic nutritional condition of a xylem environment (33), the fungus showed a much stronger and earlier pigmentation as compared to the growth in other media. This could be an indication for that *V. longisporum* melanization is a response to these defence-related proteins in the xylem sap (17). It was also mentioned in literature that strong melanized fungi are less susceptible to host-plant defence mechanisms (34), but we could not show any reduction in the symptom severity on *B. napus* plants infected with VI-PKS-1 mutants as compared to *V. longisporum* wild type-infected plants.

Outlook

For the results presented in this thesis on two candidate genes, we were able to demonstrate, firstly, a reduction in symptom severity on the natural host plant *B. napus* (VI-NEP-1), and secondly, a phenotypic change in the growth-characteristics of *V. longisporum* (VI-PKS-1). These were both a result of downregulation of specific gene functions. Further experiments to identify the putative receptor molecule of VI-NEP-1 present in *B. napus* should elucidate the role of the protein in the pathogenicity and thereby enlighten the function of the protein while infecting *B. napus*. We recently began the construction of HP constructs suitable for triggering RNAi for the other VI-NEP genes that were shown to be upregulated upon infection. The purpose is to prove that they also have a role in the pathogenic life cycle of *V. longisporum* while infecting the natural host plant *B. napus*. The identification of the VI-PKS-1-synthesized PK is connected to understanding the protein-function in the life cycle of *V. longisporum*, and should help us to elucidate the role of this metabolite and its impact on the *V. longisporum* life cycle. It is intended that both VI-NEP-1 and VI-PKS-1 will be subject to further study in the “Molecular phytopathology and mycotoxin research” laboratory headed by Prof. Petr Karlovsky.

REFERENCES

1. **Research Unit DFG 546** homepage (<http://www.ubpb.gwdg.de/~forschergruppe/index.html>).
2. **Pegg, G.F., Brady, B.L.** (2002). *Verticillium* Wilts. Wallingford, UK: CAB Publishing
3. **Gordon, T.R., Kirkpatrick, S.C., Hansen, J., Shaw, D.V.** (2006). Response of strawberry genotypes to inoculation with isolates of *Verticillium dahliae* differing in host origin. *Plant Pathology* 55, 766-769.
4. **Heale, J.B.** (2000). Diversification and speciation in *Verticillium* - An overview. In: *Advances in Verticillium research and disease management*. Tjamos, E.C., Rowe, R.C., Heale, J.B., Fravel, D.R. (eds.), St. Paul, Minnesota, APS Press, 175-177.
5. **Schwantes, H.O.** (1996). *Biologie der Pilze*. Verlag Eugen Ulmer, Stuttgart 6.
6. **Barbara D.J., Clewes E.** (2003). Plant pathogenic *Verticillium* species: how many of them are there? *Mol. Plant Pathol.* 4:297-305.
7. **Fahleson J., Lagercrantz U., Hu Q., Steventon L.A., Dixelius C.** (2003). Estimation of genetic variation among *Verticillium* isolates using AFLP analysis. *Eur. J. Plant Pathol.* 109:361-371.
8. **Fire A, Xu S, Montgomery MK, Kostas SA, Driver SE, Mello CC.** (1989). Potent and specific genetic interference by double-stranded RNA in *Caenorhabditis elegans*. *Nature*. 1998 Feb 19;391(6669): 806-11.
9. **Pullman, G. S., De Vay, J. E.** (1982). Epidemiology of *Verticillium* wilt of cotton: A relationship between inoculum density and disease progression. *Phytopathology* 72: 549-554.
10. **Koike M., Fujita M., Nagoa H., Ohshima S.** (1996): Random amplified polymorphic DNA analysis of Japanese isolates of *Verticillium dahliae* and *V. albo-atrum*. *Plant Disease* 80: 1224-1227.
11. **Xiao C. L., Subbaro K. V.** (1998). Relationship between *Verticillium dahliae* inoculum density and wilt incidence, severity, and growth of cauliflower. *Phytopathology* 88: 1108-1115.

12. **Debode, J., Claeys, D. & Höfte, M.** (2004). Control of *Verticillium* wilt of cauliflower with crop residues, lignin and microbial antagonists. *IOBC WPRS Bull* 27, 41–45.
13. **Ratzinger A.** (2008). Development and application of LC-MS-based differential metabolic profiling in plant systems. Dissertation, Georg-August Universität Göttingen.
14. **Weiberg, A.** (2008). Identifizierung von Xylemsaft-induzierten Genen im vaskulären Pathogen *Verticillium longisporum* mittels einer verbesserten cDNA-AFLP Methode für transkriptomweite Expressionsstudien. Dissertation, Georg-August Universität Göttingen.
15. **Xu H.** (2011). Dissertation, Georg-August Universität Göttingen.
16. **Kadotani N., Nakayashiki H., Tosa Y., Mayama S.** (2003). RNA silencing in the phytopathogenic fungus *Magnaporthe oryzae*. *Mol Plant Microbe Interact.* 2003 Sep;16(9):769-76.
17. **Singh S.** (2008). Study of genes of the phytopathogenic fungus *Verticillium longisporum* involved in the colonization of xylem vessels of its host *Brassica napus*. Dissertation, Universität Göttingen.
18. **Utermark J.** (2008). Genetic transformation of filamentous fungi by *Agrobacterium tumefaciens*. *Nature Protocols*, Published online.
19. **Durrands P.K., Cooper R.M.** (1988). Selection and characterization of pectinase deficient mutants of the vascular pathogen *Verticillium dahliae*. *Physiol. Mol. Plant Pathol.* 32:343-362.
20. **Durrands P.K., Cooper R.M.** (1988). The role of pectinases in vascular wilt disease as determined by defined mutants of *Verticillium albo-atrum*. *Physiol. Mol. Plant Pathol.* 32:363-371.
21. **Veit S., Wörle J.M., Nürnberger T., Koch W., Seitz H.U.** (2001). A novel protein elicitor (PaNie) from *Pythium aphanidermatum* induces multiple defence responses in carrot, *Arabidopsis*, and tobacco. *Plant Physiol.* 127:832-841.
22. **Qutob D., Kemmerling B., Brunner F., Kufner I., Engelhardt S., Gust A.A., Luberacki B.** (2006). Phytotoxicity and Innate Immune Responses Induced by Nep1-like Proteins. *The Plant Cell* 18:3721-3744.

23. **Bae H., Kim M.S., Sicher R.C., Bae H.-J., Bailey B.A.** (2006). Necrosis- and ethylene inducing peptide from *Fusarium oxysporum* induces a complex cascade of transcripts associated with signal transduction and cell death in *Arabidopsis*. *Plant Physiol.* 141:1056-1067.
24. **Karlovsky P.** (2008). Secondary metabolites in soil ecology. Springer Verlag, Berlin.
25. **Bingle, L.E.H., Simpson, T.J. & Lazarus, C.M.** (1999). Ketosynthase Domain Probes Identify Two Subclasses of Fungal Polyketide Synthase Genes. *Fungal Genetics and Biology* 26: 209-223.
26. **Barbara D.J., Clewes E.** (2003). Plant pathogenic *Verticillium* species: how many of them are there? *Mol. Plant Pathol.* 4:297-305.
27. **Collins A., Okoli C.A.N., Morton A., Parry D., Edwards S.G., Barbara D.J.** (2003). Isolates of *Verticillium dahliae* pathogenic to crucifers are of at least three distinct molecular types. *Phytopathol.* 93:364-376.
28. **Mayorga ME, Timberlake WE.** (1992). The developmentally regulated *Aspergillus nidulans wa* gene encodes a polypeptide homologous to polyketide and fatty acid synthases. *Mol Gen Genet.* Nov;235(2-3): 205-12.
29. **Kim Y.T., Lee Y.R., Jin J., Han K.H., Kim H., Kim J.C., Lee T., Yun S.H., Lee Y.W.** (2005). Two different polyketide synthase genes are required for zearalenone in *Gibberellazeae*. *Mol. Microbiol.* 58: 1102-1113.
30. **Proctor R.H., Desjardins A.E., Plattner R.D., Hohn T.M.** (1999). A polyketide synthase gene required for biosynthesis of fumonisin mycotoxins in *Gibberella fujikuroi* mating population A. *Fung. Genet. Biol.* 27:100-112.
31. **Watanabe C.M., Wilson D., Linz J.E., Townsend C.A.** (1996). Demonstration of the catalytic roles and evidence for the physical association of type I fatty acid synthases and a polyketide synthase in the biosynthesis of aflatoxin B1. *Chem. Biol.* 3:463-469.
32. **Mauch F, Staehelin LA** (1989). Functional implications of the subcellular localization of ethylene-induced chitinase and beta 1,3-glucanase in bean leaves. *The Plant Cell* 1:447-457.
33. **Neumann M.J., Dobinson K.F.** (2003). Sequence tag analysis of gene expression during pathogenic growth and microsclerotia development in the vascular wilt pathogen *Verticillium dahliae*. *Fung. Genet. Biol.* 38:54-62.

34. **Taborda, C.P., da Silva, M.B., Nosanchuk, J.D., and Travassos, L.R.** (2008). Melanin as a virulence factor of *Paracoccidioides brasiliensis* and other dimorphic pathogenic fungi: a minireview. *Mycopathologia* 165: 331-339.

Danksagung

Zu allererst möchte ich mich ganz herzlich bei **Prof. Petr Karlovsky** für die Bereitstellung des Themas der vorliegenden Dissertationsschrift sowie für die allumfassende Hilfe in wissenschaftlichen Fragestellungen bedanken. Die mir von ihm gewährten Freiheiten während der Erstellung meiner Arbeit und sein stets freundschaftlicher Umgang mit mir werden mir in guter Erinnerung bleiben.

Bei **Prof. Andrea Polle** bedanke ich mich für die bereitwillige Übernahme des Korreferats meiner Dissertation. Ebenso gilt mein Dank **Prof. Heiko Becker**, der als dritter Gutachter fungiert hat.

Ein großer Dank gilt den **Mitarbeitern der Abteilung „Molecular Phytopathology and Mycotoxin Research“** der Universität Göttingen, die durch das Schaffen einer freundschaftlichen Atmosphäre und durch den stetigen Austausch von wissenschaftlichen Themen maßgeblich an dem Gelingen der Experimente meiner Dissertation Anteil hatten. Ein besonderer Dank gilt dabei **Dr. Arne Weiberg**, **Dr. Jan Utermark** und **Björn** die mir zu Beginn meiner Promotion, aufgrund ihrer Laborerfahrung, den Einstieg in die experimentelle Arbeit sehr erleichtert haben. Hervorheben möchte ich ebenso **Heike Rollwage**, die mir bei der Durchführung der Experimente sehr geholfen hat. Ebenso danke ich **Mona Quambusch** für ihre hervorragende Mitarbeit an verschiedenen Experimenten meiner Arbeit. Bei **Haidi Yin** (Peking University, Beijing, China) und **Ruth Pilot** bedanke ich mich für die Arbeit bezüglich der Proteinaufreinigung von VI-NEP-1 und den darauf aufbauenden Experimenten.

Darüber hinaus bedanke ich mich bei allen **Mitarbeitern des Departments für Nutzpflanzenwissenschaften** der Universität Göttingen für die gute Arbeitsatmosphäre. Ein besonderer Dank gilt dabei **Tobias Wulf**, der mir bei der statistischen Auswertung meiner Daten geholfen hat.

Bei der **Deutschen Forschungsgemeinschaft (DFG)** möchte ich mich für die finanzielle Unterstützung meiner Promotion bedanken.

Ebenso möchte ich mich bei allen **Mitgliedern der DFG Forschergruppe FOR 543** (“Signalling between the soil-borne fungus *Verticillium longisporum* and its host plants”) für die Einsichten in die experimentelle Arbeit der interdisziplinären Arbeitsgruppen bedanken. Die

gehaltenen wissenschaftlichen Vorträge und die anschließenden Diskussionen in der Forscherguppe haben mir dabei geholfen, die Gesamtheit des Pathosystems *V. longisporum* besser zu verstehen und angewandte Methoden aus den verschiedenen Bereichen der Forschung kennenzulernen.

Mein größter Dank gilt jedoch meiner Mutter, meinem Bruder und meinem Vater, die mir mit ihrer finanziellen und besonders psychologischen Unterstützung ermöglicht haben, meine Promotion durchzuführen. Einen großen Anteil am Gelingen meiner Promotion haben auch meine hoffentlich zukünftigen Schwiegereltern. Mein abschließender Dank gilt meiner Freundin, die mir in den vergangenen Jahren immer zur Seite gestanden hat.

Herzlichen Dank

CURRICULUM VITAE

PERSÖNLICHE DATEN

Name: **Malte Matthias Beinhoff**
Geburtsdatum: 7. März 1981
Geburtsort: Hannover
Familienstand: ledig
Staatsangehörigkeit: deutsch



BERUFSPRAXIS

seit 02/2007 **wissenschaftlicher Mitarbeiter**
Abteilung „Molecular Phytopathology and Mycotoxin
Research“ ([Link](#))
Georg-August-Universität Göttingen

DFG-Forschergruppe:
Mitglied in der Research Unit FOR 546
Thematik: „Signalling between the soil-borne plant pathogen
Verticillium longisporum and its host plants“ ([Link](#))

Tagungen/Kongresse:
"From Foliar to Root-Interacting Pathogens and Symbionts"
Göttingen (Februar 2011) ([Link](#))

10th International Verticillium Symposium
Korfu, Griechenland (Mai 2009) ([Link](#))

VAAM-Tagung „Molekularbiologie der Pilze“
Hamburg (September 2008)

STUDIUM

07/2011 Abschluss als **promovierter Agrarwissenschaftler**
(Note: magna cum laude)

12/2007 - 07/2011 Promotionsstudiengang für Agrarwissenschaften
Georg-August-Universität Göttingen
Thematik: „Molecular and functional characterization of
potential pathogenicity related genes from *Verticillium*
longisporum“
(Betreuer: Prof. Dr. Petr Karlovsky, Prof. Dr. Andrea Polle)

- 12/2007 Abschluss als Diplom-Biologe
(Note: befriedigend)
- 12/2006 - 12/2007 Diplomarbeit
Thematik: „Identifikation und Charakterisierung von pathogenitätsrelevanten Genen des Rapspathogens *Verticillium longisporum*“
(Betreuer: Prof. Dr. Christiane Gatz, Prof. Dr. Petr Karlovsky)
- 10/2001 - 12/2007 Studium der Biologie
Georg-August-Universität Göttingen
Hauptfach: Botanik
Nebenfächer: Genetik, Mikrobiologie
- ZIVILDIENT/SCHULBILDUNG**
- 08/2000 - 06/2001 Zivildienst in der Alten- und Behindertenpflege
Diakoniestation Sarstedt
- 06/2000 **Allgemeine Hochschulreife**
Robert-Bosch-Gesamtschule Hildesheim

Eidesstattliche Erklärung

Hiermit erkläre ich eidestattlich, dass diese Dissertation selbständig und ohne unerlaubte Hilfe angefertigt wurde.

Göttingen, im Juni 2011